ÇUKUROVA UNIVERSITY

INSTITUTE OF BASIC AND APPLIED SCIENCES

Ph.D. THESIS

Rifat REŞATOĞLU

THREE DIMENSIONAL ANALYSIS OF NON-PLANAR COUPLED SHEAR WALLS SUBJECT TO LATERAL FORCES

DEPARTMENT OF CIVIL ENGINEERING

ADANA, 2005

ÇUKUROVA UNIVERSITY
INSTITUTE OF BASIC AND APPLIED SCIENCES

THREE DIMENSIONAL ANALYSIS OF NON-PLANAR COUPLED SHEAR WALLS SUBJECT TO LATERAL FORCES

Rifat REŞATOĞLU

Ph.D. THESIS

DEPARTMENT OF CIVIL ENGINEERING

Bu tez / / 2005 Tarihinde Aşağıdaki Jüri Üyeleri Tarafından Oybirliği İle Kabul Edilmiştir.

İmza:....................................	**İmza:..**	**İmza:...................................**
Prof. Dr. Orhan AKSOĞAN	**Prof. Dr. Ragıp ERDÖL**	**Prof. Dr. Vebil YILDIRIM**
DANIŞMAN	**ÜYE**	**ÜYE**

İmza:...	**İmza:..**
Asst. Prof. Dr. H. M. ARSLAN	**Asst. Prof. Dr. Seren (AKAVCI) GÜVEN**
ÜYE	**ÜYE**

Bu tez Enstitümüz İnşaat Mühendisliği Anabilim Dalında hazırlanmıştır.

Kod No:

Prof. Dr. Aziz ERTUNÇ
Enstitü Müdürü

Bu Çalışma Çukurova Üniversitesi Bilimsel Araştırma Projeleri Birimi Tarafından Desteklenmiştir.
Proje No: MMF-2003-D10

Dedicated to my father, Aziz Reşatoğlu

ABSTRACT

Ph.D. THESIS

THREE DIMENSIONAL ANALYSIS OF NON-PLANAR COUPLED SHEAR WALLS SUBJECT TO LATERAL FORCES

Rifat REŞATOĞLU

DEPARTMENT OF CIVIL ENGINEERING
INSTITUTE OF BASIC AND APPLIED SCIENCES
UNIVERSITY OF ÇUKUROVA

Supervisor: Prof. Dr. Orhan AKSOĞAN

Year: 2005**, Pages:** 275

Jury : Prof. Dr. Orhan AKSOĞAN
: Prof. Dr. Ragıp ERDÖL
: Prof. Dr. Vebil YILDIRIM
: Asst. Prof. Dr. H. Murat ARSLAN
: Asst. Prof. Dr. Seren (AKAVCI) GÜVEN

In this study, a static analysis has been carried out for non-planar coupled shear walls on rigid foundation, with the properties of the connecting beams and the rotational stiffnesses of their end connections, varying from region to region in the vertical direction, considering the effect of shear deformations in the beams. Continuous Connection Method (CCM) has been employed in the analysis and the compatibility equation has been written at the midpoints of the connecting beams. For this purpose, the connecting beams have been replaced by an equivalent layered medium. The warping of the sections of the piers due to their twist, as well as their bending, has been considered in obtaining the displacements. Vlasov's thin walled beam theory has been used for this purpose. After obtaining the axial force in the piers from the differential equation obtained using the expressions for the lateral displacements and the rotation in terms of the axial forces, all relevant quantities of the problem are determined. Finally, a general purpose computer program has been prepared in Fortran language and examples have been solved. The results found are compared with the results present in the literature and for further verification, some problems are solved both by the present method and the SAP2000 structural analysis program which are observed to be in perfect agreement.

Key Words: Continuous Connection Method, Non-planar Coupled Shear Wall, Static Analysis, Thin-Walled Beams, Vlasov's Theory.

ÖZ

DOKTORA TEZİ

DÜZLEMSEL OLMAYAN BOŞLUKLU DEPREM PERDELERİNİN YATAY YÜKLERE GÖRE ÜÇ BOYUTLU ANALİZİ

Rifat REŞATOĞLU

ÇUKUROVA ÜNİVERSİTESİ
FEN BİLİMLERİ ENSTİTÜSÜ
İNŞAAT MÜHENDİSLİĞİ ANABİLİM DALI

Danışman: Prof. Dr. Orhan AKSOĞAN

Yıl: 2005, **Sayfa:** 275

Jüri **:** Prof. Dr. Orhan AKSOĞAN
: Prof. Dr. Ragıp ERDÖL
: Prof. Dr. Vebil YILDIRIM
: Asst. Prof. Dr. H. Murat ARSLAN
: Asst. Prof. Dr. Seren (AKAVCI) GÜVEN

Bu çalışmada, rijit temel üzerine oturan, bağlantı kirişlerinin özellikleri ve uçlarındaki dönel rijitlikler düşey doğrultuda bölgeden bölgeye değişebilen, düzlemsel olmayan simetrik ve asimetrik boşluklu deprem perdelerinin, kirişlerindeki kayma etkileri hesaba katılarak, statik analizi yapılmıştır. Analizde, sürekli bağlantı yöntemi (SBY) kullanılmış olup, bağlantı kirişlerinin orta noktalarında uygunluk denklemi yazılmıştır. Bu amaçla bağlantı kirişleri sürekli bir ortama dönüştürülmüştür. Yerdeğiştirme ifadeleri elde edilirken duvarların eğilmelerine ek olarak burulmadan dolayı kesitlerin çarpılması da göz önüne alınmıştır. Bu amaçla Vlasov'un ince cidarlı kiriş teorisi kullanılmıştır. Elde edilen diferansiyel denklemden perdenin eksenel kuvvet ifadesi bulunduktan sonra, eksenel kuvvet cinsinden yatay yerdeğiştirmeler ve dönme ifadeleri kullanılarak, problem için önem taşıyan büyüklükler elde edilmiştir. Son olarak, Fortran dilinde genel amaçlı bir bilgisayar programı hazırlanıp, bu programla literatürde var olan sonuçlarla karşılaştırma ve SAP2000 yapı analizi programı ile doğrulama yapmak için örnekler çözülmüştür.

Anahtar Kelimeler: Sürekli Bağlantı Yöntemi, Düzlemsel Olmayan Boşluklu Deprem Perdeleri, Statik Analiz, İnce Cidarlı Kiriş, Vlasov Teorisi.

ACKNOWLEDGEMENT

First of all I would like to thank Prof. Dr. Orhan AKSOĞAN for his supervision and encouragement that enabled me to complete my research satisfactorily. It has been a great pleasure for me to work with him. My special thanks also go to Mr. Engin EMSEN, for his beneficial discussions, valuable comments and encouragement and his close friendship.

I should be most thankful to my girlfriend Miss Seval Bolat for her continuous support and patience. I would also like to thank all the people in the Department of Civil Engineering at Çukurova University for their valuable friendship and support during my stay in the computer laboratory of the department.

I am also most thankful to Prof.Dr. Wai K. Tso, Prof. Emeritus in McMaster University in Canada, for his responses to our demands about their previous work on our subject.

Finally, I wish to thank my family for their support, care, encouragement and belief in my success in my education life.

CONTENTS **Page Number**

LIST OF TABLES **Page Number**

LIST OF FIGURES **Page Number**

NOMENCLATURE

a	:	distance between the centroids of the piers in X-direction,
(a_x,a_y)	:	linear coordinates of principal pole,
A_{ji}	:	cross sectional area of the j^{th} pier in region i,
A_{ci}	:	cross sectional area of connecting beams in region i,
A^*_{ci}	:	effective cross-sectional area in shear for rectangular sections in region i,
b	:	distance between the centroids of the piers in Y-direction,
b_k	:	width of k^{th} section in a thin-walled beam (defined in (3.1)),
(b_x,b_y)	:	linear coordinates of an arbitrarily placed pole,
B_z	:	bimoment,
B_{zj}	:	bimoment value of the j^{th} pier,
c	:	clear span of connecting beam,
C_{cbi}	:	rotational stiffness of connecting beam-pier connections in region i,
d	:	a geometric property (defined in (5.29)),
D	:	displacement vector of shear wall in local axes,
D_j	:	displacement vector of shear wall in principal axes,
d_{px} , d_{py}	:	moment arms of the components of the concentrated force,
d_{wx} , d_{wy}	:	moment arms of the distributed force components,
e	:	distance of bimoment from shear center,
E	:	modulus of elasticity,
E_{ci}	:	elasticity modulus of connecting beams in region i,
G	:	shear modulus,
G_{Xj} , G_{Yj}	:	coordinates of centroid of jth pier in section i, referring to global axes, X and Y, respectively,
$\overline{G_{Xj}}$, $\overline{G_{Yj}}$	:	coordinates of centroid of jth pier in section i, referring to principal axes, $\overline{X}$ and $\overline{Y}$, respectively,
H	:	total height of shear wall,

h_i	:	storey height in region i,
h_s	:	distance of a pole from the tangent line at a point on the contour line,
i	:	region number,
I_{ci}	:	moment of inertia of connecting beams in region i,
I_{xj} , I_{yj}	:	moments of inertia of a section w.r.t. global X and Y axes, respectively,
I_{xyj}	:	product of inertia of pier j w.r.t. axes passing through the centroid parallel to global axes,
$\overline{I_{xj}}$, $\overline{I_{yj}}$	:	moments of inertia of the section of a thin-walled beam w.r.t. principal $\overline{X}$ and $\overline{Y}$ axes,
$\overline{I_{xyj}}$	:	product of inertia of pier j w.r.t. axes passing through the centroid parallel to principal axes,
$I_{\omega j}$	:	sectorial moment of inertia of pier j,
I_{ω}	:	sum of the sectorial moments of inertia of the two piers at point O,
$\overline{I_{\omega}}$	:	a constant (see App. 1),
$I_{\theta x}$, $I_{\theta y}$	:	sectional properties (defined in (5.55-56)),
j	:	pier number,
J_j	:	St. Venant torsional constant (moment of inertia) of pier j,
J	:	sum of the St. Venant torsional constants of the two piers,
J_o	:	polar moment of inertia of a circular cross-section,
K1	:	a geometrical quantity related to moments of inertia, (see App.1)
K2	:	a geometrical quantity related to moments of inertia, (see App.1)
K3	:	a geometrical quantity related to moments of inertia, (see App.1)
K4	:	a geometrical quantity related to moments of inertia, (see App.1)

k^2	:	a constant (defined in (3.65)),
m	:	external twisting moment per unit length,
m_{sv}	:	total torsional moment of the shear stress distribution per unit length along the contour line,
M	:	bending moment in an arbitrary plane,
M_{exi} , M_{eyi}	:	external bending moments in region i about the respective axes due to the loading above the cross-section considered,
M_{eti}	:	external twisting moment in region i due to the loading above the cross-section considered,
M_{mp}	:	bending moment at the mid-points of the connecting beams,
$\overline{M}_{eti}$	:	resultant torque about point O, due to resistance offered by piers, in region i,
$\overline{\overline{M}}_{eti}$	:	resultant torque, about the vertical axis through O, due to component shears and torques, in region i,
M_{tot}	:	total twisting moment in a thin-walled beam,
M_{sv}	:	St. Venant twisting moment,
M_{ω}	:	flexural twisting moment,
n	:	number of regions in vertical direction,
O(X,Y,Z)	:	orthogonal system of global axes,
P_x , P_y	:	concentrated forces in X and Y directions, respectively,
Q_{xj} , Q_{yj}	:	shear forces developed in a region due to shear force, q, in the laminae,
q_i	:	shear force in laminae per unit length in region i,
R_j	:	rotation matrix (defined in (5.2)),
r	:	a constant (see App. 1)
ρ	:	radial distance from the shear center S,
S	:	shear center (principal pole),
S_j	:	shear center of j^{th} pier,
S_{Xj}, S_{Yj}	:	coordinates of shear center of jth pier, referring to global axes, X and Y, respectively,

S_x , S_y : statical moments of an area with respect to principal X and Y axes, respectively,

$S_{\omega x}$, $S_{\omega y}$: sectorial statical moments of a section about global axes X and Y, respectively,

S_{ω} : sectorial statical moment of a section from its center of twist,

T_i : axial force in region i,

t : thickness of a thin-walled beam,

t_k : thickness of k^{th} section in a thin-walled beam (defined in (3.1)),

u_x , u_y , u_z : displacement components in the directions of orthogonal global system of axes O(X,Y,Z),

u_s : displacement component in the tangential direction to the contour line,

u_i : horizontal global displacement of j^{th} pier in X direction in region i,

$\bar{u}_j$: horizontal principal displacement of j^{th} pier in $\bar{X}$ direction,

v_i : horizontal global displacement of j^{th} pier in Y direction in region i,

$\bar{v}_j$: horizontal principal displacement of j^{th} pier in $\bar{Y}$ direction,

V_x , V_y : components of shear force along the global X and Y axes,

$\overline{V_x}$, $\overline{V_y}$: components of shear force along the principal $\bar{X}$ and $\bar{Y}$ axes,

z : spatial coordinate measured along the height of the structure,

w_x : uniform load in X direction,

w_y : uniform load in Y direction,

β_{1i} , β_{2i} , β_{3i} : constants (see App.1)

δ_{1i} : the relative vertical displacement due to the bending of the piers in $\bar{X}$ and $\bar{Y}$ directions and due to the twisting of the piers,

δ_{2i} : the relative vertical displacement due to the bending of the connecting beams,

δ_{3i} : the relative vertical displacement due to axial deformation of the piers caused by the induced axial forces arising from the shear flow q in connecting medium,

δ_{4i} : the relative vertical displacement due to shear deformations in the laminae,

δ_{5i} : the relative vertical displacement due to relative rotation of the ends of connecting beams w.r.t. piers,

θ_i : rotational global displacement in region i,

θ'_z : angle of twist per unit length,

ω_s : sectorial area,

ω_j : sectorial area of pier j at point O,

ϕ_j : angle between the global axes and the principal axes of j^{th} pier,

γ_{ci} : a constant property of connecting beams (defined in (5.47)),

Δ : a constant (see App. 1).

1. INTRODUCTION

The growth in modern tall building construction, which began in the 1880s, has been largely for commercial and residential purposes. Tall commercial buildings are often developed in city centers as prestige symbols. The rapid growth of the urban population forces people to use the existing areas in the most economic way and also aim to be close to each other to avoid a continuous urban sprawl. For this purpose architects and engineers have to participate in the stages of the project in order to come up with an economical building. However, the higher the buildings get, the more increased are the lateral loads, in addition to vertical loads. For this reason, especially in earthquake regions, shear walls are preferred instead of columns.

In multistory buildings made of reinforced concrete, the lateral loads are often resisted by specially arranged shear walls. The most elementary shape in which a shear wall is employed in a tall building is a planar shear wall without openings. The behaviour of a shear wall is essentially similar to a deep, slender cantilever beam. Shear wall components may be planar, are usually located at the sides of the building or in the form of a core which houses staircases or elevator shafts. When one or more rows of openings divide the shear wall into solid walls connected by lintel beams, the resulting structural system is called a coupled shear wall. ‘‘Planar coupled shear wall’’, ‘‘pierced shear wall’’ and ‘‘shear wall with openings’’ are other commonly used terminologies for such structural elements in civil engineering practice. Weakening of shear walls in tall buildings by doors, windows and corridor openings is one of the most frequently encountered problems of structural engineering. When the coupling action between the walls separated by openings becomes important, some of the external moment is resisted by the couple formed by the axial forces in the walls due to the increase in the stiffness of the coupled system by the connecting beams. In planar coupled shear wall analyses, the lateral loads are applied in such a way that the deformation of the shear wall is confined within its own plane.

Actually, the deformation of a coupled shear wall subjected to lateral loading is not confined to its plane. In other words, either applied loading is not confined to the plane of the wall or the cross-sections of the piers are not planar. Studies considering in-plane, out-of-plane and torsional deformations in the investigation of coupled shear walls are called non-planar coupled shear wall analyses. In non-planar coupled shear walls, both the flexural and torsional behaviours under external loading have to be taken into account in the analysis. The bending analysis of the structure is rather simple. However, its torsional analysis is rather difficult and needs to be explained in detail.

In this study, the Continuous Connection Method (CCM) is used in conjuction with Vlasov’s theory of thin-walled beams, for the three dimensional analysis of non-planar coupled shear walls subjected to lateral loads which produce combined flexural and torsional deformations.

One method for the analysis of coupled shear walls is the CCM, which replaces the discrete connecting beams between the piers by an equivalent continuous system of laminae (Rosman, 1964). Based on this method, a host of investigations have been made about the static and dynamic analyses of plane coupled shear walls. However, the studies about non-planar coupled shear walls is far from being adequate.

In the theory of flexure, the assumption of plane sections remaining plane during bending, is usually referred to as the Bernoulli-Navier hypothesis. Torsion was considered to be completely determined by St.Venant’s theory in 1850s. The crucial point in St.Venant’s theory, is that the cross-section is free to deform out of its plane during torsion. This is called ‘free warping’ of the cross-section. St. Venant’s theory was applied to uniform, as well as non-uniform, sections. A general theory of non-uniform torsion came in 1905, when Timoshenko considered the effect of restraining the warping of a beam at its ends. The coupling of flexure and torsion was explained in 1921, when Maillart introduced the concept of the shear center and showed that the transverse loads and supports must act through this center, if no torsion is to result.

A comprehensive theory of combined torsion and flexure of open thin-walled bars was developed by Vlasov in 1940s. However, his work had not become generally known, until his book was translated into English in 1961. This theory is generally called Vlasov's theory. Vlasov's theory for thin-walled open-section beams points out the fact that the sections cannot warp freely as assumed in the St. Venant solutions. This theory is an approximate theory developed for engineering purposes and it is based on certain simplifying assumptions.

When thin-walled structures are twisted, there is a so-called ‘‘warping’’ of the cross-section and the Bernoulli-Navier hypothesis is violated. Warping is defined as the out-of-plane distortion of the cross-section of a beam in the direction of the longitudinal axis. The warping of shear walls is greatly restrained by the floor slabs and the foundations. As a result of this interaction, two types of warping stresses, namely direct stresses in the longitudinal direction and shear stresses in the tangential direction of the piers are introduced. A classical analysis of warping torsion requires the prior evaluation of the shear center location, the principal sectorial area diagram, the warping moment of inertia and the torsion constant. In this study, the top, bottom and each height at which there is a change of storey height, beam height and/or connection stiffness will be called ‘‘ends’’ and the section between any two consecutive ends will be called a ‘‘region’’.

In the present study, at first, the general analytical treatment of the static analysis of non-planar coupled shear walls, is studied, based on Vlasov's theory of thin-walled beams and the CCM with flexible connection on rigid foundation, with the properties of the connecting beams and the rotational stiffnesses of their end connections, varying from region to region in the vertical direction. Then, using those analytical results, a computer program in Fortran language has been prepared for the solution of the set of equations, thus obtained, and various examples have been solved. The results have been compared with those obtained by the SAP2000 structural analysis program to support the validity of the present method.

2. PREVIOUS STUDIES

Continuous Connection Method was originated by Chitty in 1940s, and developed by Beck (1962), Rosman (1964) and Coull (1966). It has been extended by Glück (1970) and Tso and Biswas (1973) to deal with three dimensional shear/core wall assemblies.

Vlasov (1961) presented a comprehensive theory of combined torsion and flexure of open thin-walled bars. The theory stipulated that, Bernoulli-Navier hypothesis of the bending of beams was not applicable to thin-walled beams, because of the distortion (warping) of the section.

Beck (1962) presented an approximate method of analysis where a continuous system replaces the discontinuous frame system which allows a simple calculation in high multistory buildings.

Clough et al. (1964) presented a method based on the wide-column frame analogy for the analysis of planar coupled shear wall structures. Both vertical and lateral loading of structures with an arbitrary system of shear walls were considered in this study.

Rosman (1964) has used the CCM to solve a two bay symmetrical coupled shear wall on rigid foundation. In his analysis, he kept the number of unknown functions to a minimum, to solve the static problem.

Coull and Smith (1966) presented a method based on the continuous connection method.

Soane (1967) analyzed high multi-bay shear walls in complex buildings using analog computers.

Coull and Puri (1968) found the solution for a shear wall with variations in the cross-sectional area and compared their analytical results with those of experimental works.

Glück (1970) presented a study on the three dimensional application of the continuous connection method to solve the problem of a structure consisting of coupled, prismatic or non-prismatic shear walls and frames arranged asymmetrically in the horizontal plane.

Macleod (1970) published an article regarding different aspects of shear-wall frame interaction. In this study, it was stated that the finite element method would give, the most accurate results for shear walls.

Heidebrecht and Swift (1971) proposed a method to analyze coupled asymmetric shear walls, considering the warping of the shear wall piers and the coupling of the piers by floor beams and slabs.

Smith and Taranath (1972) carried out a study on the open section shear cores subjected to torsional loads. Experimental results for a model core structure with and without floor slabs are shown to compare loosely with the theoretical results.

Coull and Subedi (1972) treated the case of shear walls with two rows of non-symmetrical and three rows of symmetrical openings by the CCM. They also compared their results with those of their experimental work on models.

Tso and Biswas (1973) presented the analysis of a coupled non-planar wall structure based on the CCM and Vlasov's theory. In their analysis, rotation is taken as the main unknown. They plotted their analytical and experimental results for comparison.

Khan and Smith (1975) proposed a method for thin-walled open section beams with bracings across the openings to restrain warping. However, their analysis was not widely accepted because it ended up with negative moments of inertia in some cases.

Macleod and Hosny (1977) employed a method for analyzing shear wall cores and proposed two types of elements that comprise a generalized column element and a solid wall element for modelling planar wall units.

Sümer and Aşkar (1992) carried out a study on an open mono-symmetric core wall coupled with connecting beams considering cases where shear deformation of the walls is significant.

Kwan (1993), in his article, investigated the erroneous results in the wide-column frame analogy when shear deformation of the walls is significant. He suggested the use of beam elements with vertical rigid arms for the coupling beams together with solid wall elements with no rotational degree of freedom to eliminate the underestimation of the beam end rotation due to shear strain in the walls.

Doğan (1995) analyzed coupled shear walls by using different finite element types and compared the results with those of the CCM and wide-column-frame analogy.

Arviddson (1997) proposed a method for the analysis of three dimensional structures consisting of non-planar coupled shear walls. The theory of analysis is based on the CCM by taking into account both flexural and torsional behaviour of such walls. To simplify the analysis, he ignored the effect of St. Venant's torsion in his work.

Arslan (1999) presented a study on the dynamic analysis of stiffened coupled shear walls with variable cross-sections on flexible foundations, considering the effects of shear deformations in the walls and beams.

Mendis (2001) published an article on an open section thin-walled beam with connecting beams for estimating the longitudinal stresses on the piers. The study employed the CCM and expressed the relevance of warping stresses in a torsionally loaded concrete core. The cases with and without connecting beams were analyzed to study the effect of their presence.

Bikçe (2002) carried out a study on the static and dynamic analyses of multi-bay planar coupled shear walls on elastic foundation, with finite number of stiffening beams based on the CCM. He prepared two computer programs in the Mathematica programming language for the static and dynamic analyses, separately.

Aksogan, Arslan and Akavcı (2003) published an article about the stiffening of coupled shear walls on elastic foundation with flexible connections and stepwise changes in width.

Arslan, Aksogan and Choo (2004) presented an article about free vibrations of flexibly connected elastically supported stiffened coupled shear walls with stepwise changes in width.

3. TORSIONAL BEHAVIOUR AND THEORY OF OPEN SECTION THIN-WALLED BEAMS

3.1. Introduction

The behaviour of a one dimensional structure can be investigated for two cases, torsion and flexure, as stated in Chapter 1. The bending analysis of a beam is rather simple. However, the torsional analysis of it is rather complex and needs to be studied in detail.

The elementary theory of extension or compression, flexure and pure torsion is included in the general engineering theory of solid beams, which is based on the application of St.Venant's principle. St.Venant's theory is based on the hypothesis that the twisting of any cross-section will produce only shear stresses. St.Venant's theory is suitable only for thick walled beams. The theory of flexure is based on the assumption of plane sections remaining plane during bending, usually referred to as the Bernoulli-Navier hypothesis.

The high-rise buildings with wide spans and reduced self weight encouraged the application of thin-walled beams in design. It is known that, the behaviour of a thin-walled beam in bending and axial loading is very similar to that of a solid beam. However, under torsional loading, relative axial displacements of the beam complicates the behaviour. Thin-walled beams must be given special consideration in their analysis and design. The main feature of thin-walled beams is that they can undergo longitudinal extension as a result of torsion. Consequently, longitudinal normal stresses proportional to strains are created, which lead to an internal equilibrium of the longitudinal forces in each cross-section. These stresses, which arise as a result of the relative warping of the section and which are not examined in the theory of pure torsion, can attain very large values in thin-walled beams. When a thin-walled beam of an open section is subjected to simultaneous bending and torsion, it is necessary to calculate some new geometrical properties of the cross-section called sectorial properties. The main principles of the theory of thin-walled beams was developed by Vlasov (1961) and, therefore, it is generally called Vlasov's theory.

Warping is defined as the out-of-plane distortion of the cross-section of a beam in the direction of the longitudinal axis, which violates the Bernoulli-Navier hypothesis. Structural engineers, generally, are not familiar with the concepts of warping behaviour and its methods of analysis. Engineers should be able to appreciate whether an open section is liable to twist and warp. The aim of this chapter is to establish an understanding of the influence of certain structural parameters related to warping.

3.2. Cross-Sectional Properties of an Open Section Thin-Walled Beam

3.2.1 Dimensional Properties

A thin-walled member is one of the basic elements in structural engineering which is made from thin plates joined along their edges. Thin-walled structures are the most modern and optimal structures designed for minimum weight and maximum stiffness. They are used extensively in long span bridges and other structures where weight and cost are prime considerations. They are not always made of steel. For example, a box girder can be constructed as a reinforced concrete structure, known as thin-walled tube.

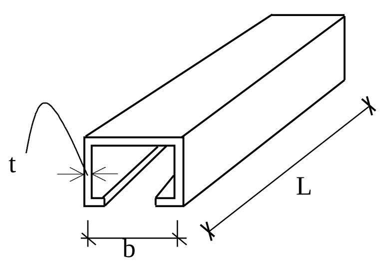

To classify a given structure as thin-walled beam, the proportions must satisfy the relations :

$$\frac{t}{b} \leq 0.1 \text{ and } \frac{b}{L} \leq 0.1$$

Figure 3.1 Geometrical dimensions of a thin–walled beam

Thin-walled beams are characterized by the fact that their three dimensions (t, b, L) are all of different orders of magnitude as shown in Fig. 3.1. The thickness of a beam is small compared with any characteristic dimension of the cross-section, and the cross-sectional dimensions are small compared with the length of the beam.

3.2.2 Coordinate System

In order to show the development of Vlasov's basic theory, the general form of an open tube and an open bar can be considered as shown in Fig. 3.2 and in Fig. 3.3, respectively, and they are, generally, called thin-walled open section beams. An axis in the middle surface parallel to the beam axis is called the generator and the intersection of the middle surface with a plane perpendicular to the generator is called the contour line. An orthogonal system of coordinates (z,s) is chosen, the first being in the direction of the longitudinal generators and the second tangent to a contour line. The coordinate z starts from one end and the coordinate s from any generator. P(z,s) is an arbitrary point on the middle surface and its displacements in the coordinate directions are called u_z and u_s.

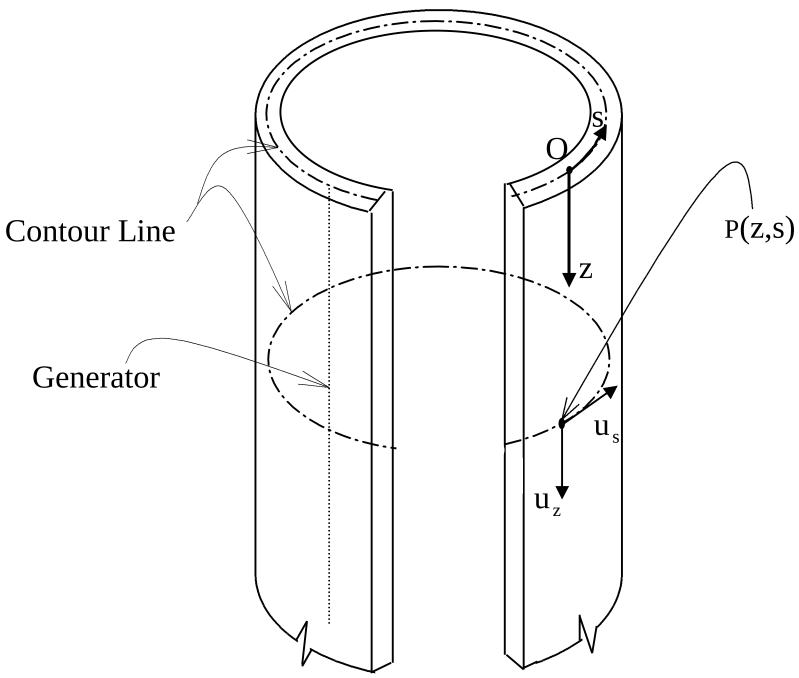

Figure 3.2. General form of an open tube

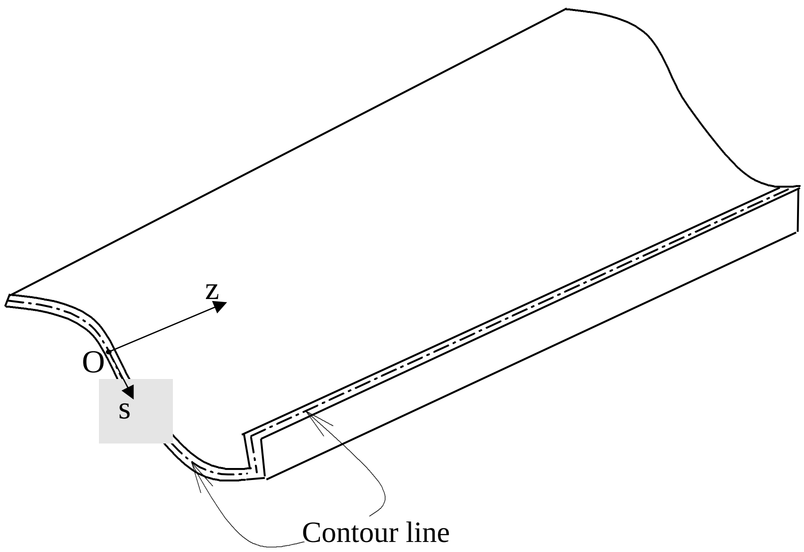

Figure 3.3. General form of an open bar

3.2.3. Torsion Constant

St. Venant's theory is based on the hypothesis that the twisting of a shaft of any cross-section will produce only shear stresses. This theory will be explained in detail in section (3.4). When an open section is subjected to a torque, it twists, producing shear stresses of the type as shown in Fig. 3.4. The stresses are distributed linearly across the thickness of the wall, acting in opposite directions. As the effective lever arm of these stresses is equal to only two-thirds of the wall thickness, the torsional resistance of these stresses is very low for an open section. The torsion constant for this twisting action can be written as

$$J = \frac{1}{3}\sum_{k=1}^{n} b_k\, t_k^{\,3} \tag{3.1}$$

where b_k is the width of section k and t_k is its thickness and n is the number of sections in the cross-section (n=3 in Fig. 3.4). It must be noted that J is not the polar moment of inertia when the section is non-circular as in Fig. 3.4. The twisting rigidity of a section is given by GJ. G is known as the shear modulus of the material.

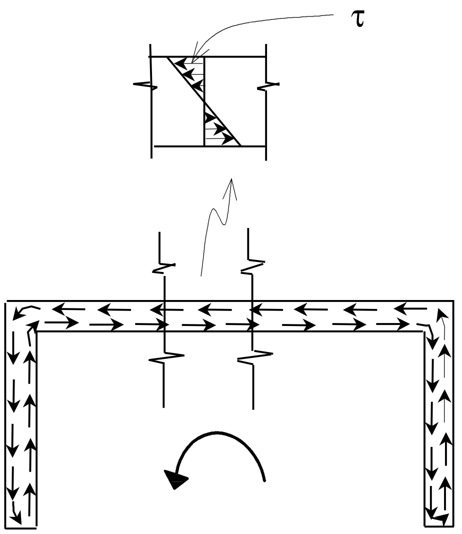

Figure 3.4. Stress distribution in a twisted open section beam

3.2.4. Sectorial Area

In addition to the familiar flexural properties of cross-sections, such as centroid, static moments, moments of inertia, etc., there are some other properties which are used in the analysis of thin-walled beams. For this purpose, a new coordinate called the sectorial area is introduced. The diagram of an element of the sectorial area of the cross-section of a beam is shown in Fig. 3.5.

$$dA = \frac{ds \cdot h_s}{2} = \frac{d\omega_s}{2}$$

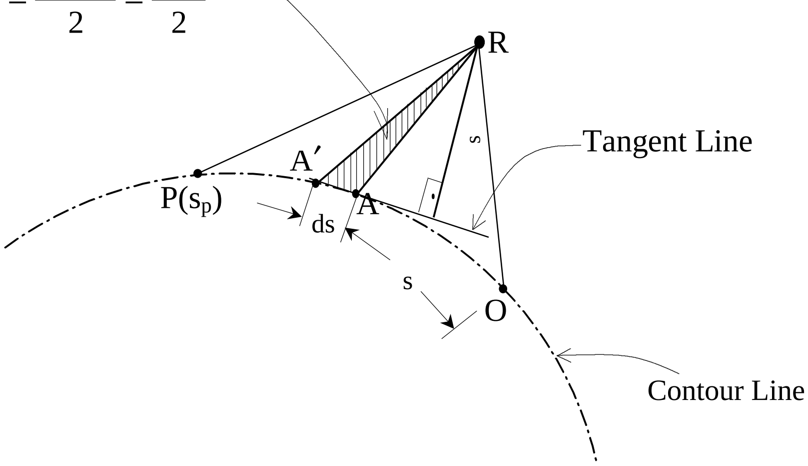

Figure 3.5. Computation of sectorial area

The sectorial area of a point on a section is computed using the median line of the outline of the section. ω_s is the sectorial area for a point, P, with coordinate s_p and is equal to twice the area swept by the line connecting R, an arbitrary center of rotation (initial pole), to the points on the contour line, starting from O and ending at P, as shown in Fig. 3.5. It's mathematical definition is:

$$\omega_s = \int_0^{s_p} h_s \, ds \tag{3.2}$$

where

ω_s : sectorial area,

h_s : distance from point R to the line tangent to the contour line at point A,

s : coordinate of a point on the contour line.

The parameter ω_s is used in the warping of the section. The sectorial area corresponding to the shear center (principal pole) as the pole, is called the principal sectorial area, and it's plot for the section is the principal sectorial area diagram. The process of calculating the sectorial areas of a section is laborious and time consuming. Therefore, to speed up these calculations, a program in Fortran language is written in this thesis. The program is given in Appendix 3 and a worked example is given in Appendix 4.

The sign of the increment of sectorial area is positive if the sliding radius, $\overrightarrow{RA}$, rotates in the counter-clockwise direction and negative if clockwise (as in Fig. 3.5).

3.2.5. Shear Center

3.2.5.1. Introduction

There is a special point in the cross-section of a thin walled beam, called the shear center, S, of the cross-section, which is defined to be the point where a shear force, when applied to the cross-section, will produce bending only (no twisting).

The following points constitute simple rules for the determination of the shear center location for some typical cross-sections:

1. The shear center always falls on a cross-sectional axis of symmetry (two sections on the left in Fig. 3.6).
2. If the cross-section contains two perpendicular axes of symmetry, or a symmetry center, then the shear center is located at the intersection of the symmetry axes and the symmetry center, respectively (two sections on the right in Fig. 3.6). It should be noted that, this is the only case where shear center and centroid coincide.

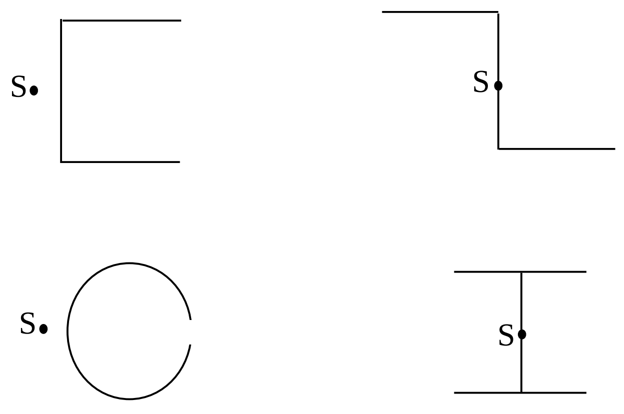

Figure 3.6. Shear centers of typical cross-sectional shapes due to symmetry

Shear center is also the point, to which warping properties of a section are related, in the way that the bending properties of a section are related to the centroid (through which the neutral axis passes). If the cross-section contains no axis of symmetry or only one axis of symmetry, the determination of the exact location of shear center requires a more detailed analysis.

3.2.5.2. Determination of the Shear Center Using Sectorial Area

In the calculation of the shear and bending stresses in a section, linear coordinates (x,y) of a section are used for finding the five flexural properties which are S_x, S_y, I_{xy}, I_x and I_y. The position of the origin and the direction of the principal axes are defined by the conditions, S_x=S_y=0 and I_{xy}=0. The first two of these are used for locating the origin of the principal linear axes called the centroid of the section or simply G and the third gives the direction of the principal linear axes. These values are not sufficient for the analysis of a thin walled beam. There are some other properties of sections which are defined on the basis of sectorial area and named as sectorial properties of a section. For the analysis of internal stresses, these properties must be known to determine the location of the shear center through the use of the sectorial area. Fig. 3.7 shows the procedure for the determination of the location of the shear center based on the sectorial area. The moment of the shear stresses in the cross-section with respect to a certain point D is:

$$M_D = \int_A \tau \, t \, h_s \, ds = \int_{s_1}^{s_2} \tau \, t \, h_s \, ds \tag{3.3}$$

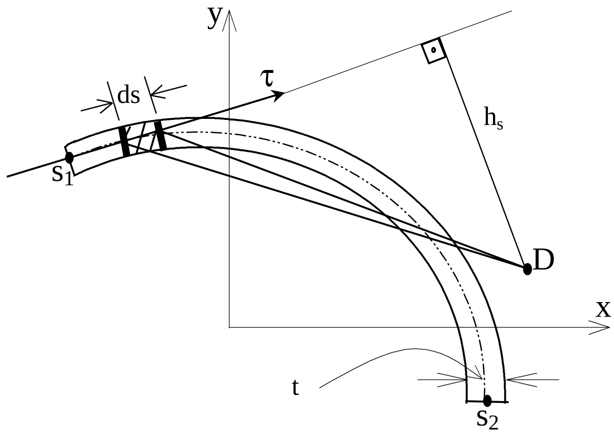

Figure 3.7. Determination of the shear center

Since $d\omega_s = h_s\, ds$

$$M_D = \int_A \tau\, t\, d\omega_s \tag{3.4}$$

If τ is eliminated using

$$\tau = \frac{V_x\, S_y}{\overline{I_y}\, t} + \frac{V_y\, S_x}{\overline{I_y}\;\, t} \tag{3.5}$$

where

V_x and V_y : components of the shear force along the principal x, y axes,

S_x and S_y : statical moment of the cross-section with respect to the principal x, y axes,

$\overline{I_x}, \overline{I_y}$: moment of inertia of the cross-section with respect to the principal x, y axes,

t : thickness of the cross-section where the shearing stress is to be determined.

Substituting equation (3.5) into equation (3.3), moment about point D is found as follows:

$$M_D = \frac{V_y}{\overline{I_x}} \int_A S_x \frac{d\omega_s}{dA}\, dA + \frac{V_x}{\overline{I_y}} \int_A S_y \frac{d\omega_s}{dA}\, dA \tag{3.6}$$

Using integration by parts technique, the first integral in (3.6) can be evaluated in the following form:

$$\int_A S_x \frac{d\omega_s}{dA}\, dA = S_x\, \omega_s \Big|_{s_1}^{s_2} - \int_A \frac{dS_x}{dA}\, \omega_s\, dA \tag{3.7}$$

where the limits s_1 and s_2 signify the end points of the cross-section (see Fig. 3.7).

It is known that the statical moment about x axis is

$$S_x = \int_A y\, dA \tag{3.8}$$

and S_x is zero for points 1 and 2. Hence,

$$S_x\, \omega_s \Big|_{s_1}^{s_2} = 0 \tag{3.9}$$

and

$$\frac{dS_x}{dA} = y \tag{3.10}$$

Thus, the integral under consideration becomes

$$\int_A S_x \frac{d\omega_s}{dA} dA = \int_A y\, \omega_s dA \tag{3.11}$$

The second integral appearing in equation (3.6) is transformed in a similar way. Finally, the moment of the shear stresses about point D is found as

$$M_D = -\frac{V_y}{\overline{I}_x} \int_A y\, \omega_s dA - \frac{V_x}{\overline{I}_y} \int_A x\, \omega_s dA \tag{3.12}$$

If the point D coincides with the shear center, the moment M_D is zero regardless of the values V_x and V_y. Therefore, the entities called the sectorial statical moments of a section about axes x and y can be written, respectively, as

$$S_{\omega x} = \int_A y\,\omega_s\,dA \tag{3.13}$$

and

$$S_{\omega y} = \int_A x\,\omega_s\,dA \tag{3.14}$$

The principal pole (shear center) of a section can be defined by equating the expressions (3.13) and (3.14) to zero. The line segment connecting the shear center and the point on the contour line at which the sectorial area is zero is called the principal radius. Hence, to locate the principal radius, the sectorial statical moment of the section is set equal to zero (see Appendix 4),

$$S_{\omega} = \int_A \omega_s\,dA = 0 \tag{3.15}$$

The method of finding the position of the shear center of a section resembles that of finding the principal radius. Let us assume an arbitrarily placed initial pole and an initial radius. The theoretical formulas for calculating the location of the shear center and evaluating the coordinates for the shear center are given in the following equations (see Appendix 5):

$$a_x = b_x + \frac{1}{I_x}\int_A \omega_s y\,dA = b_x + \frac{S_{\omega x}}{I_x} \tag{3.16}$$

$$a_y = b_y - \frac{1}{I_y}\int_A \omega_s x\,dA = b_y - \frac{S_{\omega y}}{I_y} \tag{3.17}$$

where a_x and a_y are linear coordinates of a principal pole, b_x and b_y are linear coordinates of an arbitrarily placed pole (see Fig. 3.8).

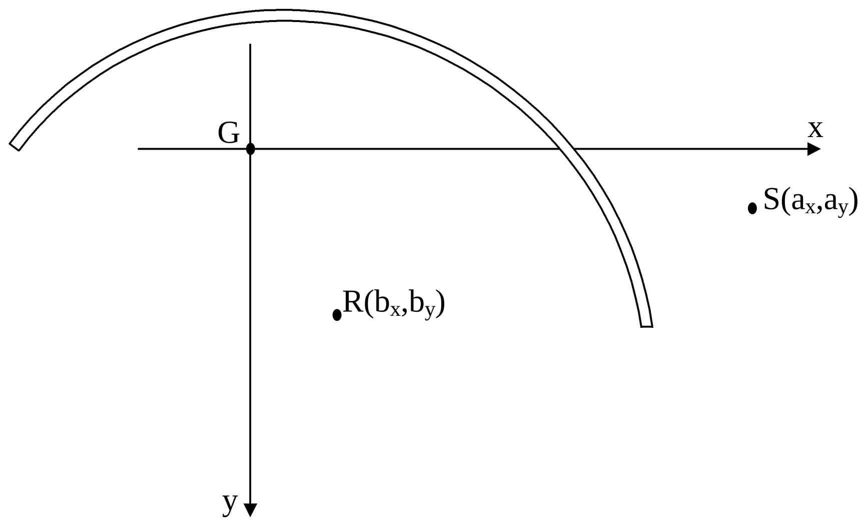

Figure 3.8. Arbitrarily placed pole R and principal pole S

These formulas are valid only if axes x and y are identical with the principal axes of a section, in other words, only if $I_{xy}=0$. In the case where the given axes x and y do not coincide with the principal axes of a section ($I_{xy} \neq 0$), but pass through the center of gravity, the following equations must be used:

$$a_x = b_x + \frac{I_y S_{\omega x} - I_{xy} S_{\omega y}}{I_x I_y - I_{xy}^2} \tag{3.18}$$

$$a_y = b_y - \frac{I_x S_{\omega y} - I_{xy} S_{\omega x}}{I_x I_y - I_{xy}^2} \tag{3.19}$$

The derivation of the formulas for the position of a shear center (3.18 and 3.19) and the location of principal radius are given in Appendix 5.

3.2.6. Warping Moment of Inertia (Sectorial Moment of Inertia)

Warping moment of inertia expresses the warping torsional resistance of a section, or in other words, the capacity of the section to resist warping torsion. It is analogous to the moment of inertia in bending. The warping moment of inertia is derived from the sectorial area distribution, and can be written as

$$I_\omega = \int_A \omega_s^2 \, dA \qquad (3.20)$$

Similar to flexural rigidity EI, EI_ω is the warping rigidity of a section. The integral expression in (3.20) shows up in section 3.5 in Vlasov's theory.

All the star sections (including all angle-sections and T-sections) shown in Fig. 3.9, have their shear centers at the intersection of their branches. Since all shear force increments pass through the shear centers, the sectorial areas are equal to zero at all points of the cross-sections. Therefore, the warping moments of inertia are all equal to zero for star sections.

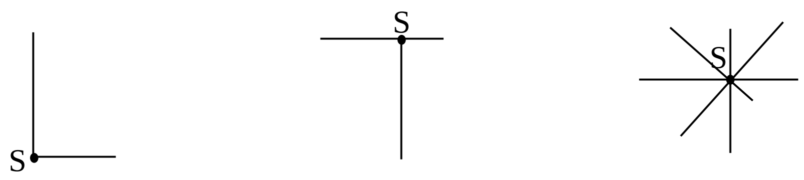

Figure 3.9. Some star sections for which $\omega_s = I_\omega = 0$

3.3. Physical Meanings of St.Venant Twist and Flexural Twist

3.3.1. St. Venant Twist

A thin walled beam of open section is liable to warp when subject to a twisting moment. For two beams of identical material and cross-sectional shape, the warping effect is much greater for the open section. The fact is that the open section does not have high warping resistance because of the continuity of its contour line and also does not allow the St. Venant torsional stresses to circulate around the contour and thereby not develop a high internal torsional resistance.

The theory of the twisting moment acting on a thick walled beam was developed by St.Venant and is a generalization of the problem of the twisting of a circular shaft as shown in Fig. 3.10. St. Venant's theory is perfectly valid for a circular cross-section and remains practically valid for any thick walled beam.

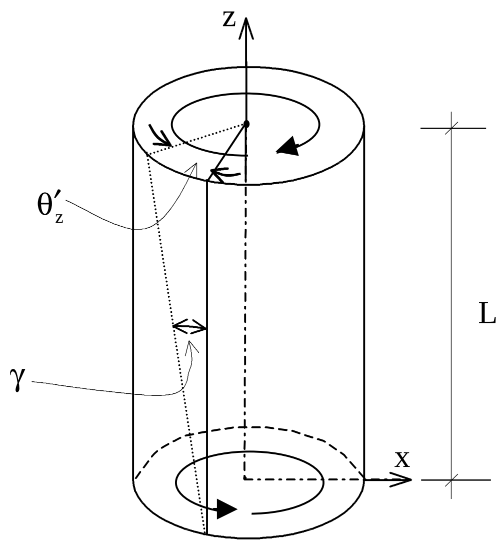

Figure 3.10. Twisting of a circular shaft (no warping)

The twisting of a circular shaft does not produce any longitudinal stresses, but only shear stresses. St.Venant's theory is based on the hypothesis that the twisting of a shaft of any cross-section produces only shear stresses. The warping effect of a twisting moment can be seen clearly in Fig. 3.11(a) and (b). (Although the displacements due to warping are not very large in magnitude and do not have a major significance, they gain importance when warping is prevented). It is apparent in Fig. 3.10 that the deformation is equal to γL where γ is the shear strain.

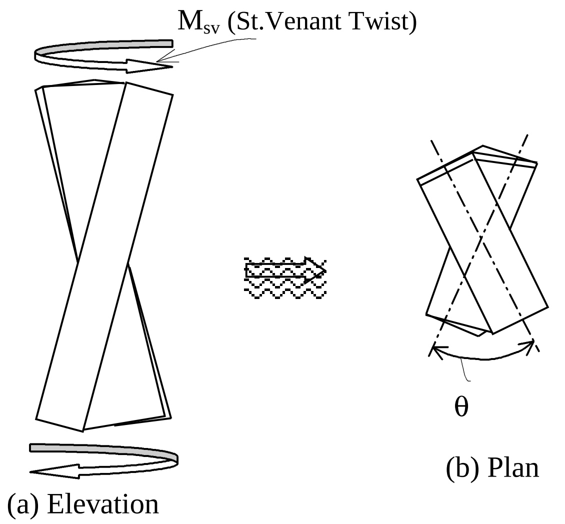

Figure 3.11. Twisting of a rectangular beam (warping not restrained)

3.3.2. Flexural Twist and Bimoment

The same beam is shown with one end rigidly fixed (restrained) in Fig. 3.12. The warping of the bottom surface of this beam is restrained. When a thin-walled beam is constrained against warping, a distribution of longitudinal stresses develop to eliminate the warping displacements at the constrained section. These normal stresses vary along the member. If an imaginary elemental beam is separated as shown in Fig. 3.12(b), its deflected shape represents a cantilever deformed by forces acting between this cantilever and the remaining portion of the beam. This deflection will cause an internal bending moment in the cantilever, which in turn will cause longitudinal stresses.

The presence of longitudinal stresses infers that part of the work done by the twisting moment is used up in developing them, and only the remainder will develop shear stresses associated with the St.Venant twist. These longitudinal stresses can become more important to the safety of a structure than shears caused by a St.Venant twist.

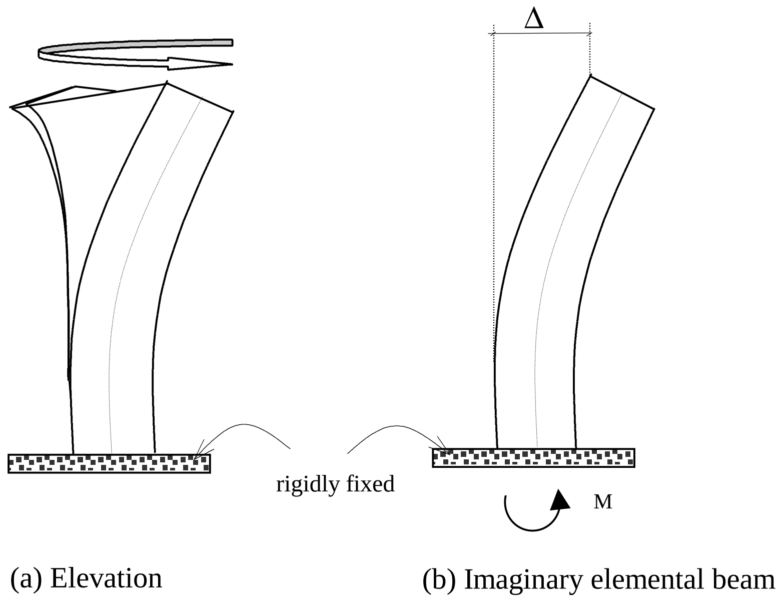

Figure 3.12. Twisting of a rectangular beam (warping restrained)

Considering an I-section beam loaded by a twisting moment at its unrestrained end as shown in Fig. 3.13(a). The final distortion of this beam takes place as the summation of the distortions shown in Fig. 3.13(b,c). The first distortion in Fig. 3.13(b) is due to the action of the St. Venant twist and the second is caused by a twisting moment resulting from the bending of the rectangular components of the beam. The second distortion caused by a bending twist (flexural twist) or flexural torsional moment is denoted by M_{ω}. Because of the considerable rigidity of flanges, the twisting moments producing deflection (Δ) is greater than the component producing a rotation (angle θ). It can be concluded from Fig. 3.13 that a twisting moment acting on a thin walled beam is composed of flexural and pure twisting moments. Therefore, the total twisting moment acting on a thin-walled beam can be written as follows:

$$M_{tot} = M_{\omega} + M_{sv} \tag{3.21}$$

where

M_{tot} : Twisting moment acting on a thin-walled beam

M_{ω} : Flexural twisting moment (warping torque)

M_{sv} : St.Venant (pure) twisting moment

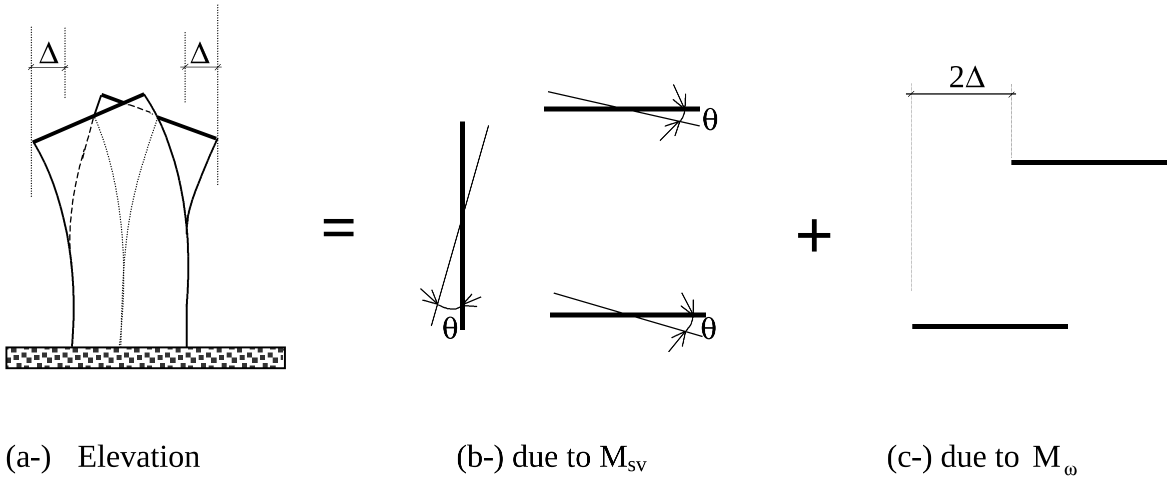

Figure 3.13. A twisting moment and resulting distortions

It is clear that flexural twist always causes some bending moments in a structure. This assumption is too general since it is known that a flexural twist evokes a pair of bending moments. Such a pair of bending moments is called a '***Bimoment***' and represented by B_z. A bimoment is a mathematical function introduced by Vlasov(1961). The general definition of bimoment is a pair of equal but opposite bending moments acting in two parallel planes as shown in Fig. 3.14.

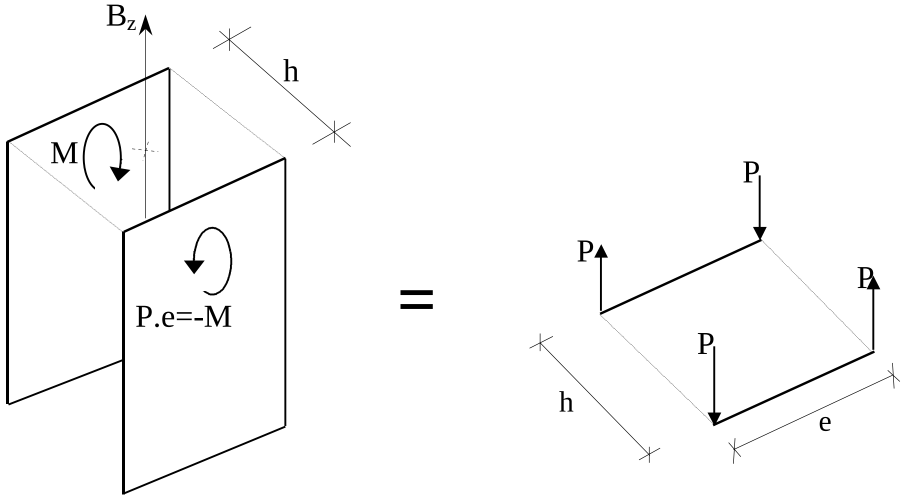

Figure 3.14. Representation of a bimoment

A bimoment can be either positive or negative and has a direction in the same manner as a bending moment. It is a vector not a scalar quantity. In this study, a bimoment is assumed to be positive when the direction of one moment seen from the plane of the other moment is clockwise (as in Fig. 3.14). Bimoment has units of force times the square of the length (lb-in^2, kip-ft^2, kN-m^2, t-m^2, etc.). The magnitude of a bimoment is given by the product of the distance of these parallel planes and the moment on one of them.

$$B_z = M\,h \tag{3.22}$$

As mentioned earlier, a flexural twist acting on a thin-walled beam is accompanied by a bimoment. An example of bimoment caused by a twisting moment is shown in Fig. 3.13(a). The flexural twist at the top of this column produces bending moments in both flanges. These bending moments are equal and opposite in the opposite flanges.

Now let us consider an I-shaped shear wall which is loaded at one corner by a load P as an external force parallel to the longitudinal axis as shown in Fig. 3.15. In the cases of the first three loadings on the right side, which represent the axial loading and the bending moments about x and y axes, the Bernoulli-Navier hypothesis is valid. In the last loading case, it is obvious that the cross-section does not remain plane. The flanges which are bending in opposite directions, produce significant warping stresses as shown in Fig. 3.15(e).

As defined by St. Venant, uniform torsion component of shear stresses is not dependent on s, the coordinate variable along the contour line. Warping stresses, however, vary with s, since they result from a non-uniform distribution of axial stresses over the contour.

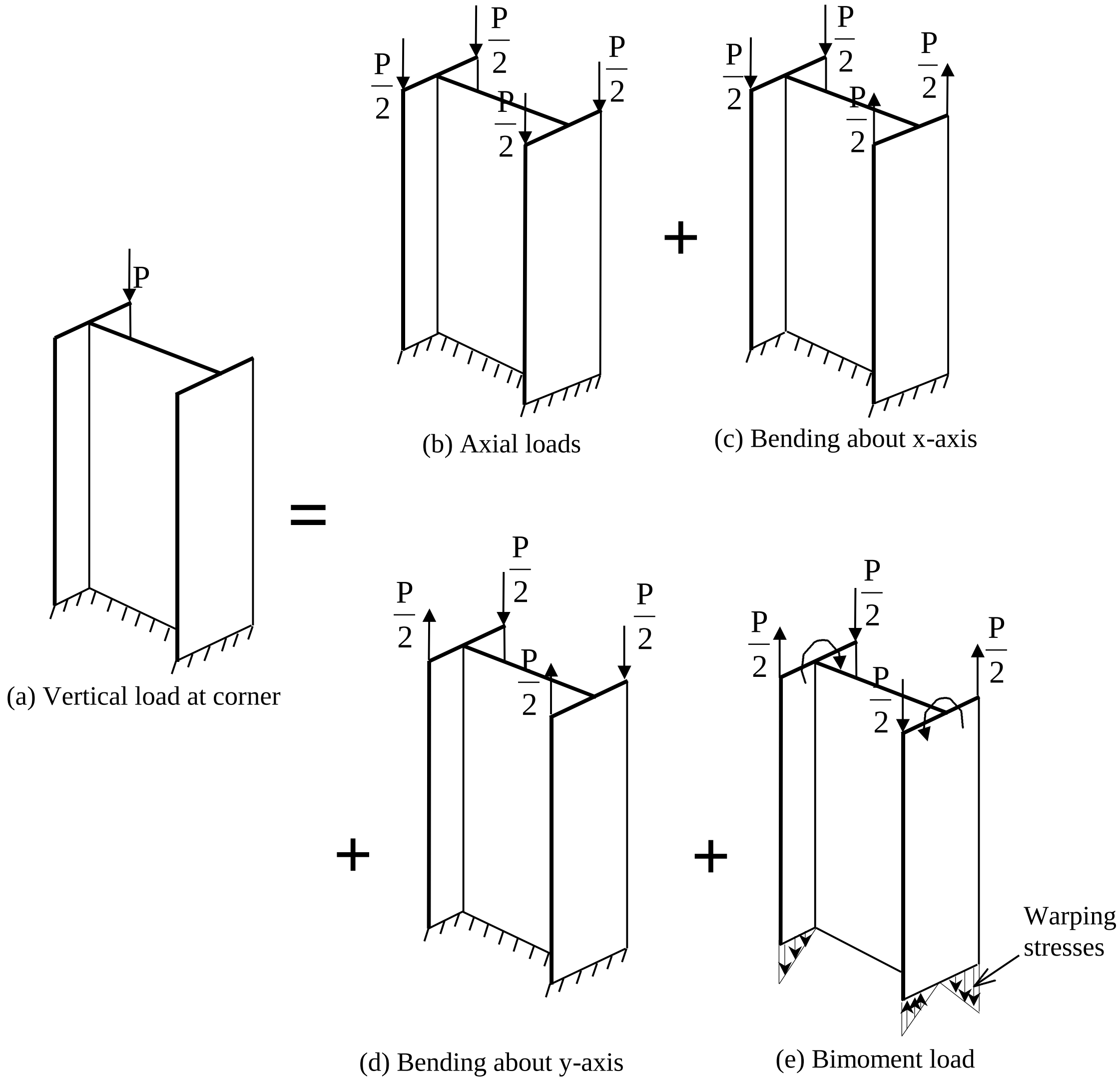

Figure 3.15. A thin-walled I-shaped cantilever column subjected to an eccentric load

The resistance offered by the interconnecting web is not strong enough. The bending action of the flanges can be thought of as being brought about by equal and opposite horizontal forces parallel to the flanges. The compatibility condition between the web and flanges results in a rotation of the cross-section as shown in Fig. 3.16.

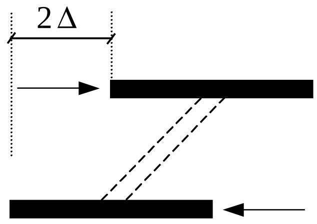

(a) Displacement of flanges due to bimoment load

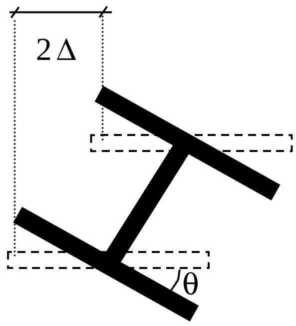

(b) Rotation with geometric compatibility between flanges and web

Figure 3.16. Plan section of an I-shaped column

In Fig. 3.17, the two external forces P are producing equal and opposite moments acting on the opposite flanges of a beam. The deformation of this column is practically same as the deformation caused by the twisting moment previously shown in Fig. 3.13(a). In this case, there is no external twist. Therefore, total twisting moment acting on a thin-walled beam is equal to zero ($M_{tot} = M_{\omega} + M_{sv} = 0$) or ($M_{\omega} = -M_{sv} \neq 0$). Although there is no external twist, shearing stresses exist.

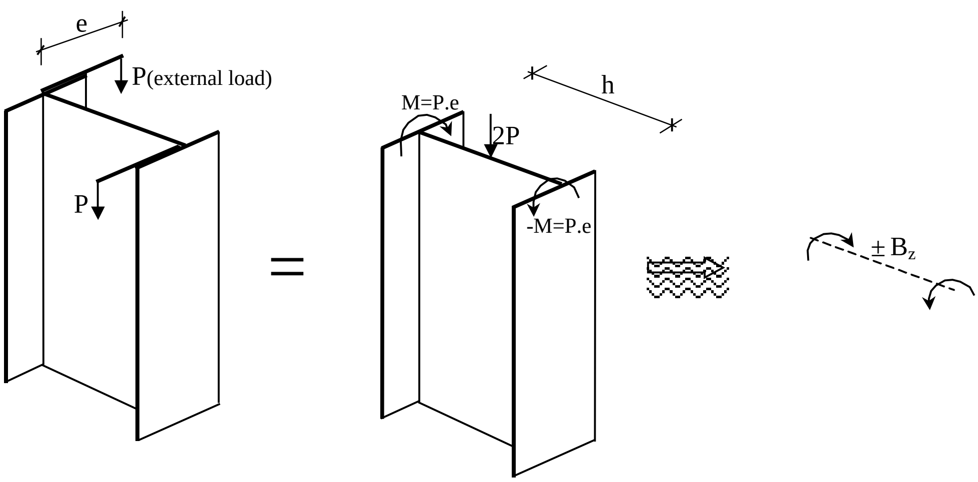

Figure 3.17. Bimoment creating a twist

Hence, an internal flexural twist is created by an external bimoment. The relation between bimoment and flexural twist will be explained in detail in section 3.5 in which the Vlasov's theorems will be given. These theorems enable us to determine the internal stresses and strains as simple as the ones in a thick walled beam due to bending moments and shear forces.

3.4. St. Venant's Theory (Uniform Torsion)

3.4.1. Torsion of a Bar with Circular Cross-Section

A cylinder of a circular cross-section being twisted by couples applied at the end planes was given before in Fig. 3.10. The behaviour of a circular cylinder under torsion is such that all cross-sections normal to the axis remain plane after deformation. The shearing stress in a cylider of circular cross-section under torsion is known from the strength of materials. It is well known that these stresses satisfy the boundary conditions, therefore, they represent the exact solution for a circular cylinder. The exact solution for that problem was first formulated by St. Venant and is generally called St. Venant's theory. St. Venant assumed that the projection of any deformed cross-section on the x-y plane (see Fig. 3.10) rotates as a rigid body, the angle of twist per unit length being constant.

The displacement of any point P due to rotation is shown in Fig. 3.18. The line SP which is equal to ρ (radial distance), rotates through a small angle θ_z about S, which is called the center of twist and its displacement in the horizontal plane is zero. Since the angle of rotation θ_z is small, arc PP^* is assumed to be a straight line normal to SP. The x and y components of the displacement of P, then, are given by

$$\begin{aligned} u_z &= 0 \\ u_x &= -\rho\ \theta_z \sin\beta = -\,y\ \theta_z \qquad (3.23a) \\ u_y &= \rho\ \theta_z \cos\beta = x\ \theta_z \end{aligned}$$

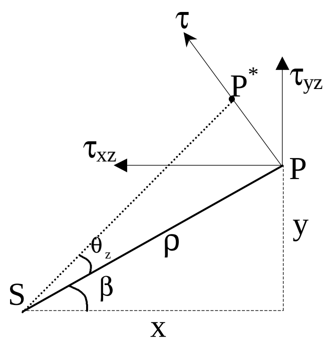

Figure 3.18. Shear stresses in uniform torsion

If normal cross-sections remain plane after deformation, one might assume that the deformation in the longitudinal direction is zero. If the cross-section is at a distance z from the origin, the angle of rotation is given by ($\theta_z = \theta_z^{'} z$), where $\theta_z^{'}$ is the angle of twist per unit length along the z-direction. Then, the displacements are

$$u_z = 0$$
$$u_x = - \theta_z^{'} y z \tag{3.23b}$$
$$u_y = \theta_z^{'} x z$$

These displacements produce only shear strains in the bar so that by generalized Hooke's law the only non-zero stresses in the bar are the shear stresses, i.e.,

$$\varepsilon_z = 0,\ \varepsilon_x = 0,\ \varepsilon_y = 0$$
$$\gamma_{xz} = -\theta_z^{'} y,\ \gamma_{yz} = \theta_z^{'} x,\ \gamma_{xy} = 0$$
$$\tau_{xz} = G\gamma_{xz} = -G\theta_z^{'} y \tag{3.24}$$
$$\tau_{yz} = G\gamma_{yz} = G\theta_z^{'} x$$

From Fig. 3.18, these shear stresses can be used to relate the internal torque, M_{sv}, to the twist per unit length as follows:

$$M_{sv}=\int_A \left(x\tau_{yz} - y\tau_{xz}\right)dA$$

$$M_{sv}=G\theta_z' \int_A \left(x^2 + y^2\right)dA$$

$$M_{sv}=G\theta_z' J_o \tag{3.25}$$

J_o is the polar moment of inertia of the cross-section given by

$$J_o = \int_A \left(x^2 + y^2\right)dA = \int_A \rho^2 dA \tag{3.26}$$

3.4.2. Torsion of a Bar with Non-Circular Cross-Section

In the previous section it was assumed that each planar cross-section of a circular bar remained planar and merely rotated about the central axis of the bar. When a torque is applied to a non-circular cross-section, the cross-section again rotates about the central axis but there is also a significant distortion of the cross-section in z-direction, i.e. the cross-sections both rotate and warp as shown in Fig. 3.19(b).

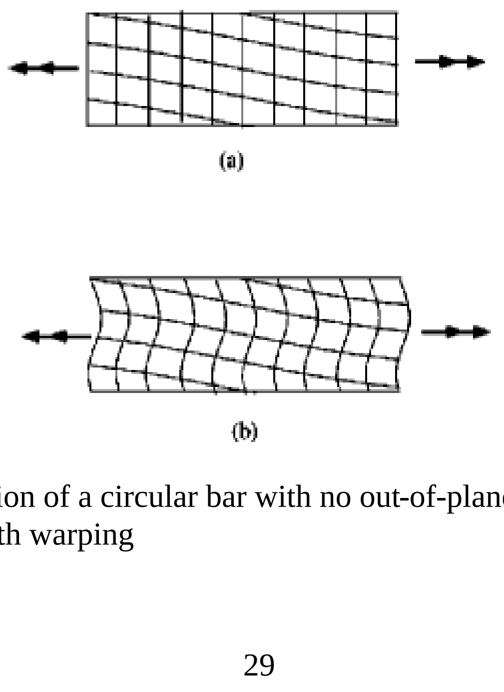

Figure 3.19. (a) Torsion of a circular bar with no out-of-plane warping (b) Torsion of a non-circular bar with warping

For a circular cross-section, the displacements are assumed to be due to a pure rotation of each cross-section with no displacement in the axial direction. On the other hand, for a non-circular cross-section there are axial displacements. However, since the warping of each cross-section is assumed to be the same, all points on a line parallel to the z-axis move through the same distance in the z-direction. The displacement of any point P due to rotation is shown in Fig. 3.20.

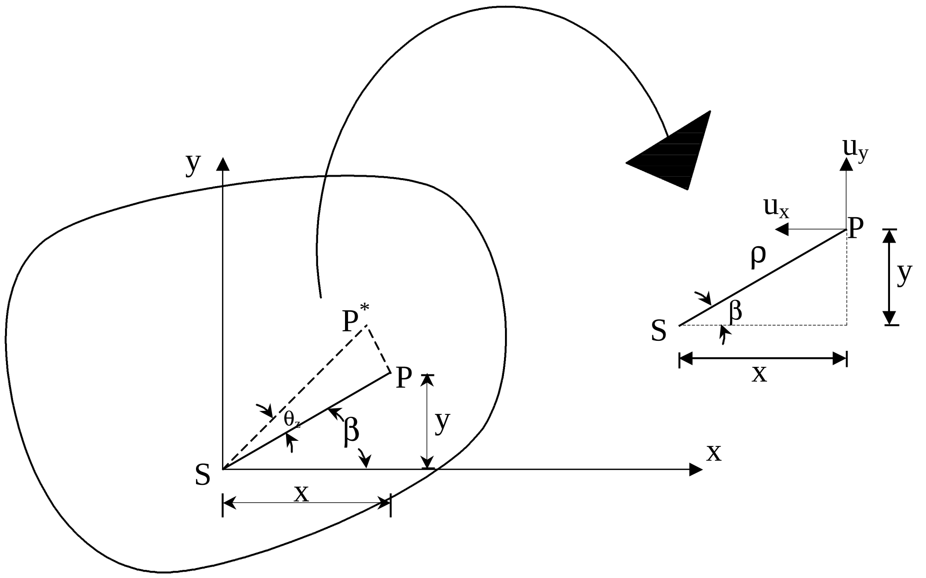

Figure 3.20. Displacements of a non-circular bar due to rotation

Incorporating the warping action into our previous description of the displacements of the bar mentioned in equations (3.23.a and b), the following relations can be written:

$$
\begin{aligned}
u_z &= \theta_z' f(x,y) \\
u_x &= -\theta_z' y \\
u_y &= \theta_z' x
\end{aligned}
\tag{3.27}
$$

where f(x,y) represents the warping function (describing the z displacement of each section independent of position along the axis). These displacements produce strains in the bar so that by generalized Hooke’s law the only non-zero stresses in the bar are the shear stresses. Within the elastic limit, shear strain is proportional to the shear stress $\left(\gamma = \frac{\tau}{G}\right)$.

$$\begin{aligned}
&\varepsilon_z = 0, \varepsilon_x = 0, \varepsilon_y = 0 \\
&\gamma_{xz} = -\theta_z'\left(\frac{\partial f}{\partial x} - y\right), \ \gamma_{yz} = \theta_z'\left(\frac{\partial f}{\partial y} + x\right), \ \gamma_{xy} = 0 \\
&\tau_{xz} = G\theta_z'\left(\frac{\partial f}{\partial x} - y\right) \\
&\tau_{yz} = G\theta_z'\left(\frac{\partial f}{\partial y} + x\right)
\end{aligned} \tag{3.28}$$

The internal torque M_{sv} is a constant since the only loading is a pair of twisting moments at the ends of the bar. From Fig. 3.20, these shear stresses can be used to relate the internal torque, M_{sv}, to the twist per unit length as follows:

$$M_{sv} = \int_A \left(x\tau_{yz} - y\tau_{xz}\right) dA \tag{3.29}$$

Substituting the shear stress components from equation (3.28) into (3.29), the following expression is found:

$$M_{sv} = GJ\theta_z' \tag{3.30}$$

where J is a torsional constant and G is the shear modulus of the material.

3.5. Vlasov's Theory (Non-Uniform Torsion)

The cross-sections of shear walls used for bracing tall buildings are frequently open and are characterized by the fact that their three dimensions, height, width and thickness, are all of different orders of magnitude. When such a system is subjected to torsion, it suffers warping displacements and may develop axial stresses due to the restraint at the foundation.

When the sections are free to warp, a beam responds in uniform torsion (St.Venant torsion). This behaviour was given in section 3.4. On the contrary, if warping is prevented, due to the complex distribution of longitudinal stresses, shear stresses in the cross-section can be related to two different modes of torsional behaviour. One is due to the uniform torsional behaviour of the structure, therefore, varying linearly over the thickness of the beam and does not change with sectorial areas. The other is due to the warping torsion, coupled with transverse bending and axial loading of the beam, uniform over the thickness of the beam and changes with s.

Vlasov's theory explains the difference of behaviour between thin-walled and thick-walled beams under the same loading. Furthermore, it not only explains but renders it possible to calculate stresses and distortions of a thin-walled beam which cannot be explained by the classic thick-walled beam theory. Only open section thin-walled beams are considered and analyzed in this study. Vlasov introduced two new types of effects which are called Flexural Twist (M_{ω}) and Bimoment (B_z). Furthermore, additional properties of a section called sectorial properties are introduced. According to Vlasov's theory of thin-walled beams, the following assumptions are made:

Assumption 1 : The cross-section is completely rigid in its own plane.

Assumption 2 : The shear strain of the middle surface is negligible (s direction is perpendicular to z direction after deformation).

The first assumption depicts that the shape of the outline of a cross-section remains unchanged under loading. It means that, under external loading, the profile of a section may be translated or rotated from its initial position, but the relative position of points on the profile will remain unchanged in x-y plane not along longitudinal axis z as shown in Fig. 3.21.

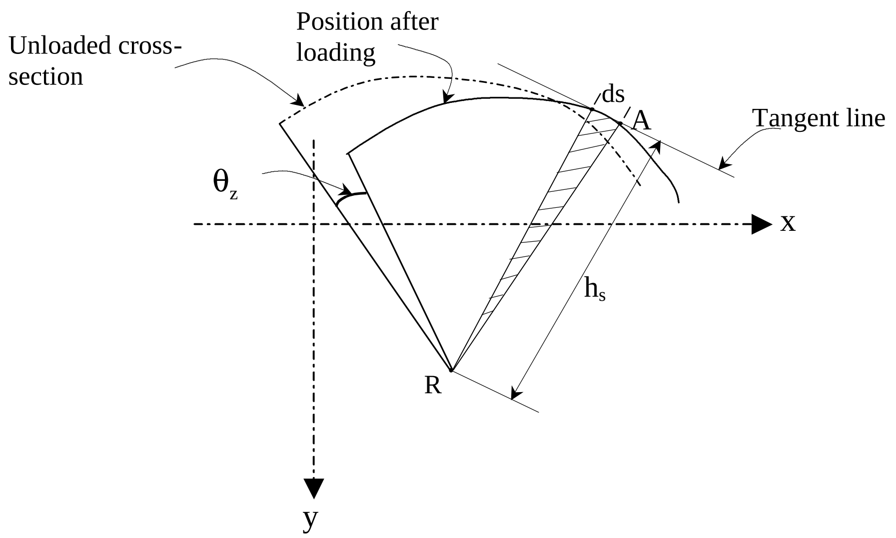

Figure 3.21. Displacement of a section in non-uniform torsion

The transverse displacement u_s in the direction of the tangent to the contour line is given by:

$$u_s(z,s) = \theta_z \cdot h_s \qquad (3.31)$$

where

$u_s(z,s)$: displacement of point A measured along curve s of the profile of a section

θ_z : angle of rotation of the profile at a distance z from the base

The other assumption is similar to that made in the normal theory of bending of a beam. It states that the contour of the section remains perpendicular to the longitudinal axis after deformation, meaning that shear deflections are equal to zero. Hence , according to Vlasov’s second assumption:

$$\gamma = \frac{\partial u_z(z,s)}{\partial s} + \frac{\partial u_s(z,s)}{\partial z} = 0 \tag{3.32}$$

Substituting equation (3.31) into equation (3.32),

$$\frac{\partial u_z(z,s)}{\partial s} + h_s \cdot \frac{d\theta_z}{dz} = 0 \tag{3.33}$$

Integrating this equation with respect to s, the longitudinal displacement of point A along z-axis, is found as

$$u_z(z,s) = -\int_0^s h_s \, ds \frac{d\theta_z}{dz} \tag{3.34}$$

where $u_z(z,s)$ is the longitudinal displacement along the generator and θ'_z is the relative angle of torsion (also referred to as torsional warping). The product $h_s.ds$ is equal to twice the area of the triangle whose base and height are equal to ds and h_s, respectively, and is usually given the symbol $d\omega_s$. Hence,

$$u_z(z,s) = -\int_0^s d\omega_s \frac{d\theta_z}{dz} \tag{3.35}$$

After some necessary arrangements, equation (3.35) can be written as

$$u_z(z,s) = -\frac{d\theta_z}{dz}\omega_s \tag{3.36}$$

where ω_s is as defined in section 3.2.4. Equation (3.36) determines the longitudinal displacement that does not obey the law of plane sections and arises as a result of torsion. This is the sectorial warping of the section. Warping is defined as the out-of-plane distortion of the cross-section of a beam in the direction of the longitudinal axis. This warping is given by the law of sectorial areas. Since the displacement $u_z(z,s)$ changes along the distance z, the longitudinal strain of a point measured along z can be written as follows:

$$\varepsilon(z,s) = \frac{\partial u_z(z,s)}{\partial z} \tag{3.37}$$

$$\varepsilon(z,s) = -\theta_z'' \omega_s \tag{3.38}$$

Considering the in plane rigidity of the section contour and considering the shearing strain to be zero (i.e. the section will remain orthogonal after deformation), equation (3.38) can be obtained as for longitudinal deformation.

In this study, the warping stress expression is given by Vlasov's theory of thin-walled beams of open section. Vlasov's first theorem is as follows:

Theorem 1 : *The stress in a longitudinal fibre of a thin walled beam due to a bimoment is equal to the product of this bimoment and the principal sectorial area divided by the principal sectorial moment of inertia of the cross-section.*

Vlasov's theory, which concerns beams consisting of thin plates, considers only the normal stresses in the direction of the generator of the middle surface and the shear stresses in the direction of the tangent to the contour line. Using the physical relations between the stresses and strains in the beam, normal stresses $\sigma(z,s)$, and shear stresses $\tau(z,s)$ can be found. Equation (3.38) does not determine the strain explicitly yet, since the function θ_z is still unknown. When the beam is deformed, internal elastic forces arise in it. These forces represent normal and shear stresses in the cross-section. According to Vlasov's theory, the shear stresses, which are directed along the normal to the contour line, are assumed to vanish.

In Vlasov's theory it is assumed that the normal stresses are constant over the thickness of the beam wall and that the shear stresses in the thickness direction vary according to a linear law as shown in Fig. 3.22(c). The shear stresses lead to a force , τt , per unit length of the cross-section acting along the tangent to the contour as shown in Fig. 3.22(a). On the other hand, the total torsional moment M_{sv} in the whole cross-section can be assumed to be the sum of the torsional moments $m_{sv}(z,s)$ per unit length of the cross-section (along the contour line) as shown in Fig. 3.22(b).

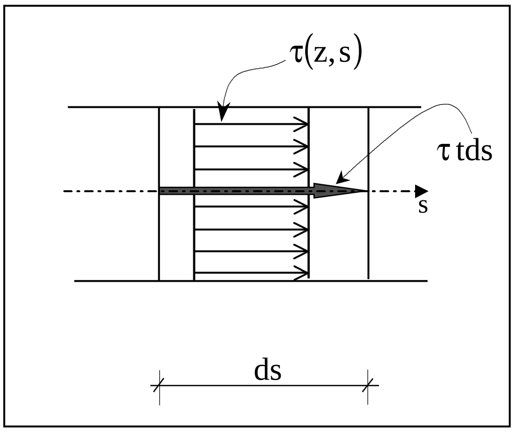

(a) Flexure without torsion

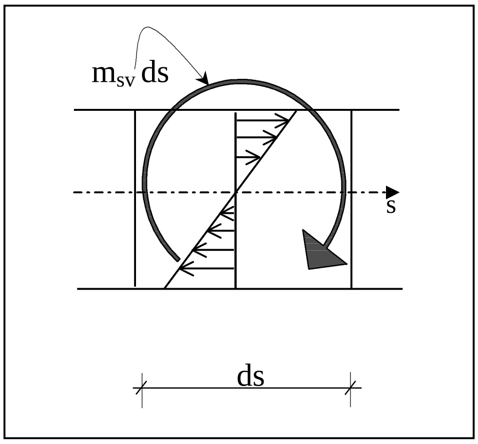

(b) Torsional moments

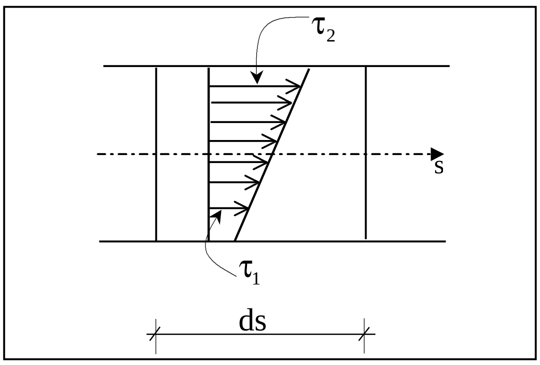

(c) Flexure with torsion

Figure 3.22. Effect of shear stresses in an open section thin-walled beam

The state of stress in the cross-sectional plane can be expressed by the normal stresses $\sigma(z,s)$, the average shear stresses $\tau(z,s)$ and the torsional moments. The shear and normal stresses are considered as functions of the two variables z and s. The torsional moment which depends on the difference of the shear stresses at the extreme points of the wall are shown in Fig. 3.22(b). The torsional moment (M_{sv}) in the whole cross-section is a function of the variable z only.

By using the physical relations between the stresses and strains in the beam, it is possible to find the stresses (σ, τ) and the moments M_{sv} from the strains. According to Hooke's law

$$\sigma(z,s) = E\,\varepsilon(z,s) \tag{3.39}$$

Substituting equation (3.38) into equation (3.39), the normal stress is found as follows:

$$\sigma(z,s) = -E\,\theta_z''\,\omega_s \tag{3.40}$$

The difference between Vlasov's and St. Venant's theories is the inclusion of sectorial properties in the former, as it is seen from equation (3.40). Multiplying both sides of this equation by $\omega_s\, t$ and integrating over the whole contour line yields

$$B_z = \int_0^s \sigma(z,s)\,\omega_s\, t\, ds = -E\theta_z'' \int_0^s \omega_s^2\, t\, ds \tag{3.41}$$

The integral on the right was defined as the warping moment of inertia, I_ω, which expresses the warping torsional resistance of the cross-section (see section 3.2.6). Hence,

$$B_z = -E\theta_z'' I_\omega \tag{3.42}$$

Dividing both sides by EI_ω

$$\theta_z'' = -\frac{B_z}{EI_\omega} \tag{3.43}$$

Substituting expression (3.43) into (3.40), longitudinal normal stresses can be obtained as

$$\sigma(z,s) = \frac{B_z}{I_\omega}\omega_s \tag{3.44}$$

Equation (3.44) is the mathematical definition of the first theorem. It determines the normal stresses which arise because the cross-sections do not remain plane under torsion.

Vlasov's second theorem is as follows:

Theorem 2 : *A shear stress in a fibre of a thin walled beam caused by a flexural twist is equal to the product of this flexural twist and the sectorial statical moment of this point divided by the wall thickness (at this point) and the principal sectorial moment of inertia.*

Normal stresses described by equation (3.44) were determined by using the relation between stress and strain for the elastic beam. However, the analogous of elastic equation cannot be used to determine the average shear stresses $\tau(z,s)$ shown in Fig. 3.22(b), since the shearing strains caused by the shear stresses are taken to be zero in Vlasov's theory.

To determine the shear stresses, the condition of equilibrium of the vertical forces acting on an infinitesimal beam element with the sides dz and ds as shown in Fig. 3.23, is set equal to zero,

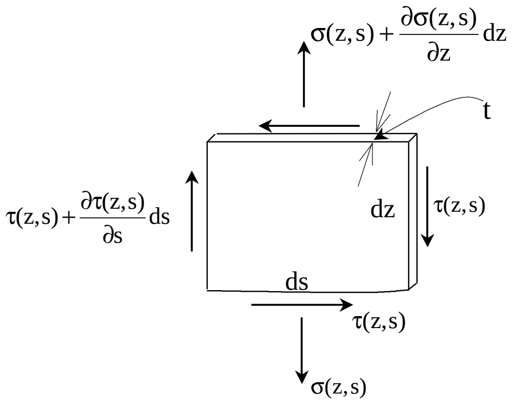

Figure 3.23. Free body diagram of an element (t dz ds) of a thin-walled beam

$$t\,\frac{\partial\sigma(z,s)}{\partial z}\,dz\,ds + t\,\frac{\partial\tau(z,s)}{\partial s}\,dz\,ds = 0 \tag{3.45}$$

Hence,

$$\frac{\partial\sigma(z,s)}{\partial z} + \frac{\partial\tau(z,s)}{\partial s} = 0 \tag{3.46}$$

Differentiating the normal stress expression (3.40) with respect to z, substituting it into equation (3.46) and integrating

$$\tau(z,s) = E\theta_z''' \int_0^s \omega_s\,ds \tag{3.47}$$

The value of shear stress at a point A in Fig. 3.21 can be obtained by integrating the shear stress expression (3.47) from a free edge (s=0) to s. Denoting (t ds) by (dA), the shear stress is found as

$$\tau(z,s) = \frac{1}{t} E\theta_z''' \int_A \omega_s dA \tag{3.48}$$

The integral on the right side of (3.48) was defined, in section 3.2.5.2, as the sectorial or warping statical moment, S_ω, of the cross-section.

Hence,

$$\tau(z,s) = E\theta_z''' \frac{S_\omega}{t} \tag{3.49}$$

Equation (3.49), infers the shear stresses in s direction which appear in the restrained torsion of a thin-walled beam and are distributed uniformly across the wall as shown in Fig. 3.22(a).

The flexural torsional moment (flexural twist) carried by membrane shear stresses as shown in Fig. 3.22(a) can be obtained as follows:

$$M_\omega = \int_0^s \tau(z,s)\, t\, h_s\, ds = \int_0^s \tau(z,s)\, t\, d\omega_s \tag{3.50}$$

Substituting the stresses $\tau(z,s)$, found as in equation (3.47) into (3.50), and remembering the definition of sectorial warping moment of inertia (see equation (3.20)),

$$M_\omega = -EI_\omega \theta_z''' \tag{3.51}$$

Rearranging equation (3.51)

$$\theta_z''' = -\frac{M_\omega}{EI_\omega} \tag{3.52}$$

By substituting the value found in (3.52) into equation (3.49), the shear stress component parallel to the z axis can be obtained expressing the mathematical definition of Vlasov's second theorem

$$\tau(z,s) = -\frac{1}{t}\left(\frac{M_\omega}{I_\omega} S_\omega\right) \tag{3.53}$$

Therefore, from relations obtained in equation (3.43) and (3.52),

$$M_\omega = B_z' \tag{3.54}$$

The sum of the moments (M_{sv}) and (M_ω) gives the total torsional moment, that is denoted by (M_{tot}). Hence,

$$M_{tot} = M_{sv} + M_\omega = -EI_\omega\theta_z''' + GJ\theta_z' \tag{3.55}$$

3.6. Internal Bimoment and Flexural Twist due to External Loading

In the previous sections, it was mentioned that it would not be simple to find the relationship between the external loading and the internal forces which were in our case bimoment and flexural twist. This relationship is given by a differential equation which will be studied in the following sections. Before dealing with that differential equation, it is useful in practice to know two theorems which will enable us to recognize the presence of an internal bimoment.

3.6.1. Bimoment caused by a Force Parallel to the Longitudinal Axis of a Thin-walled Beam

The relationship between an internal bimoment and an external force is given by the first theorem as follows:

Theorem 1 : *A bimoment caused by an external force parallel to the longitudinal axis of a beam is equal to the product of this force and the principal sectorial co-ordinate of the point of its application.*
This theorem can be expressed mathematically as shown below:

$$B_z = P \times \omega_p \tag{3.56}$$

This equation, actually, is the other mathematical definition of bimoment given in equation (3.41) which is

$$B_z = \int_A \sigma(z,s)\,\omega_s \, dA \tag{3.57}$$

or

$$B_z = \sum_{k=1}^{n} P_k \times \omega_k \tag{3.58}$$

3.6.2. Bimoment caused by an External Bending Moment Acting in a Plane Parallel to the Longitudinal Axis of a Beam

The relation between an external bending moment and its internal bimoment is defined by the second theorem as follows:

Theorem 2 : *A bimoment caused by a bending moment acting in a plane parallel to the longitudinal axis of a beam is equal to the product of the value of this bending moment and the distance of its plane from the shear center of that beam.*
This theorem can be expressed mathematically by the formula:

$$B_z = M \times e \tag{3.59}$$

The validity of this theorem becomes apparent from the definition of a bimoment as a pair of parallel bending moments as shown in Fig.3.24.

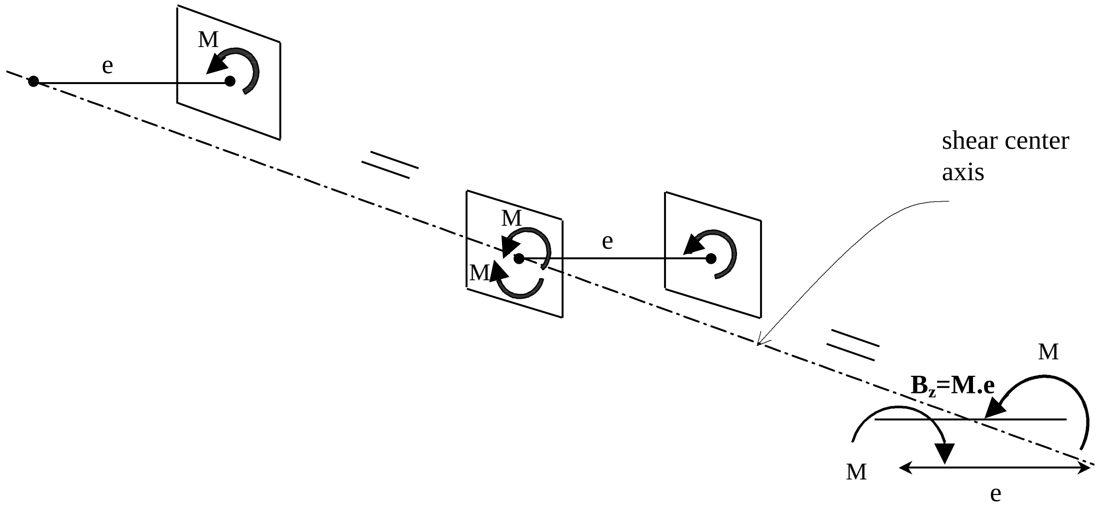

Figure 3.24. Bending moment creating a bimoment

The two theorems formulated by equations (3.56) and (3.59) lead to the important general conclusion that, whenever dealing with a thin-walled beam, the presence of a bimoment and a flexural twist should be expected. That is, in a thin-walled beam torsional stresses, i.e. bimoment, flexural twist and St.Venant twist, can be present even when no external twist moments are present.

3.7. Differential Equation of Open-Section Thin-walled Beams

It was established before that thin-walled beams of rigid cross-section undergo not only bending but also torsion when subjected to a transverse load which does not pass through the shear center.

The relationship between the angle of twist and bimoment has been given as in equations (3.42) and (3.43). Similarly, the relationship between an internal flexural twist and a bimoment was also found in equation (3.54).

Hence, from (3.42) and (3.51)

$$\frac{dM_{\omega}}{dz} = -EI_{\omega}\theta_z^{IV} \tag{3.60}$$

The relationship between the angle of twist θ_z and the external or internal St.Venant torsion found before as in (3.31). Differentiating this equation with respect to z and rearranging,

$$\frac{dM_{sv}}{dz} = GJ\theta_z^{''} \tag{3.61}$$

In Fig. 3.25 a length dz of a beam is shown loaded by internal and external forces. From the conditions of equilibrium,

$$dM_{sv} + dM_{\omega} = dM_{tot} = m\,dz \tag{3.62}$$

or

$$\frac{dM_{sv}}{dz} + \frac{dM_{\omega}}{dz} = \frac{dM_{tot}}{dz} = m \tag{3.63}$$

can be obtained.

where m is an external twisting moment per unit length at the point given by the coordinate z.

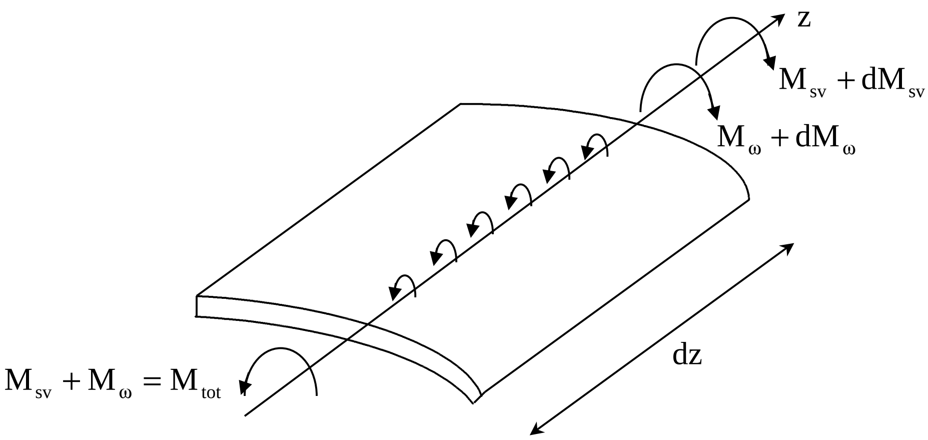

Figure 3.25. Elemental beam loaded by internal and external forces

Substituting equations (3.60) and (3.61) into (3.63)

$$GJ\theta_z'' - EI_{\omega}\theta_z^{IV} = m \tag{3.64}$$

Dividing both sides of equation (3.64) by EI_{ω} and defining a new dimensionless characteristic number k by

$$k^2 = \frac{GJ}{EI_{\omega}} \tag{3.65}$$

and rearranging the equation (3.64) gives

$$\theta_z^{IV} - k^2\theta_z'' = -\frac{m}{EI_{\omega}} \tag{3.66}$$

Equation (3.66) is the governing differential equation of open-section thin-walled beams.

4. METHODS OF ANALYSIS

4.1. Introduction

Based on Vlasov's theory of thin walled beams and the CCM, an approximate method is presented for the analysis of non-planar coupled shear wall structures.

The method presented in this study for the analysis of non-planar coupled shear walls is the CCM. The CCM used in this thesis has also been called ‘‘continuous medium technique’’, the ‘‘continuum method’’ and the ‘‘shear connection method’’ in the literature.

In the analysis of non-planar coupled shear walls, both the flexural and the torsional behaviours have to be taken into account. The deformations of a coupled shear wall subjected to lateral loading are not always confined to its plane. For this reason, the present analysis is a three dimensional analysis of coupled shear walls (see Fig. 4.1). The CCM was developed by assuming that the discrete system of connections, in the form of individual coupling beams or floor slabs, could be replaced by continuous laminae as shown in Fig. 4.2. Tso & Biswas (1973) presented an analysis for a nonlanar coupled shear wall with no change in the properties along the height and an arbitrary lateral load employing the CCM.

In this study, the theory of thin walled beams of open sections is used to describe the behaviour of the piers in non-planar coupled shear walls. The effect of the out-of-plane stiffness of the floor slabs is assumed to be included in the stiffness of the connecting beam in the application of the CCM.

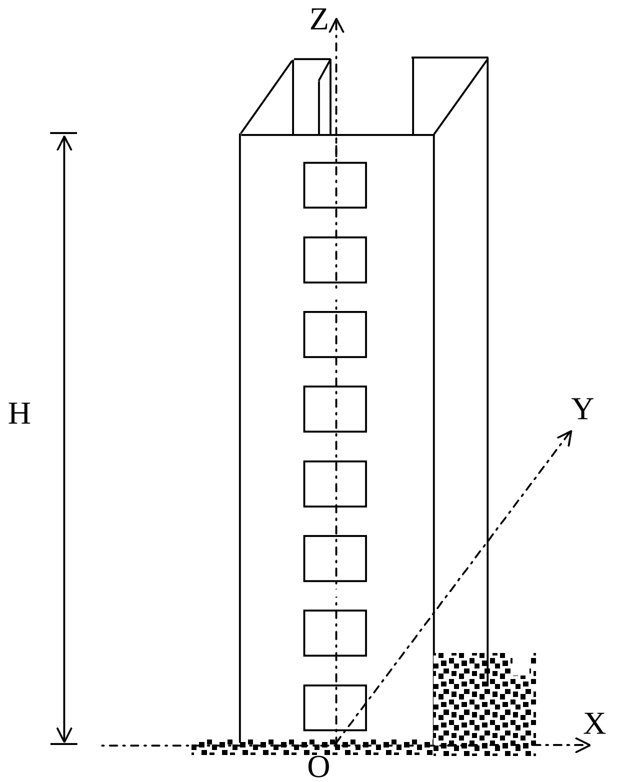

Figure 4.1. Non-planar coupled shear wall

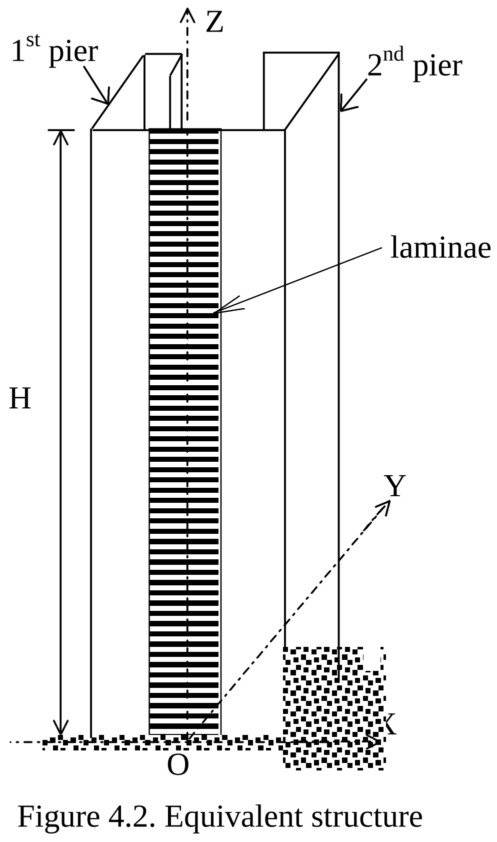

Figure 4.2. Equivalent structure

4.2. Continuous Connection Method (CCM)

This method allows a broad look at the behaviour of planar and non-planar coupled shear wall structures and, simultaneously, gives a good understanding of the relative influences of the piers and the connecting beams in resisting lateral forces.

The CCM was first originated by Chitty in 1940s and subsequently developed by Beck (1962), but probably the most comprehensive treatment has been done by Rosman (1964). The importance of torsional analysis in the design of non-planar coupled shear walls using the CCM was first studied by Glück (1970). Then it has been extended by Tso and Biswas (1973).

In its most basic form the theory assumes that the elastic structural properties of the coupled wall system remain constant over the height and the points of inflection of all the beams are at mid-span. In this method, the individual connecting beams are replaced by continuous laminae. Under the effect of lateral loads, the walls induce shear forces in the laminae as shown in Fig. 4.3.

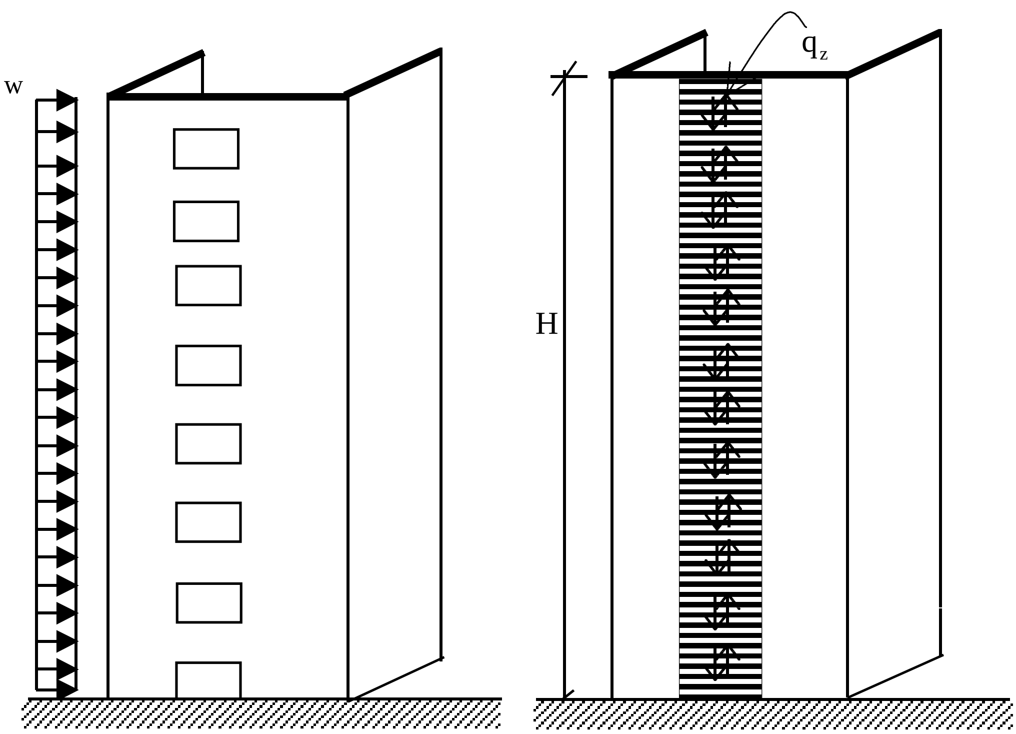

Figure 4.3. (a) Discrete system (b) Substitute system

In this study, the CCM is used for the analysis of non-planar coupled shear walls on rigid foundation subjected to lateral loads. The warping of the piers due to twist has been considered, as well as their bending, in the analysis. The compatibility equation has been written at the mid-points of the connecting beams. The differential equations for the compatibility of the displacements and the equilibrium of the forces are used in the analysis. After the application of the loading and boundary conditions, mathematical solutions are obtained for the determination of the shears and moments in the beams and the walls.

The basic assumptions of the CCM for non-planar coupled shear walls can be summarized as follows:

1. The geometric and mechanical properties are constant throughout each region along the height.
2. The discrete set of connecting beams with bending stiffness EI_{C_i} are replaced by an equivalent continuous connecting medium of flexural rigidity with EI_{C_i}/h per unit length in the vertical direction.
3. Vlasov's theory for thin-walled beams of open section is valid for each pier, separately.
4. The outline of a transverse section of the coupled shear wall at a floor level remains unchanged (due to the rigid diaphragm assumption for floors). Hence, the axis of each connecting beam remains straight and does not change its length. Furthermore, the slope and curvature at the ends of a connecting beam in the vertical plane are equal.
5. The rotational stiffness constants at the ends of a connecting beam are equal.
6. The discrete shear forces in the connecting beams are replaced by an equivalent continuous distribution q_i, per unit length in the vertical direction along the mid-points of the connecting laminae.
7. The torsional stiffness of the connecting beams is neglected.

4.3 Comparison of the Results of the Present Method for Non-planar Coupled Shear Walls with those of the Frame Method

The frame analysis, which is utilized for frame systems composed of beams and columns, cannot be used for the analysis of multistory shear walls. An idealized frame structure can be utilized to simulate the behaviour of the shear walls. The basic difference between the frame analysis for walls and the method for frame systems is that the effect of the finite widths of the members, in particular those of the walls, cannot be neglected in the former. Therefore, the term ‘‘wide-column-frame analogy’’ is generally used to describe the aforementioned method to refer to the application of the latter method to the former case.

The wide-column-frame analogy is popular in design offices for the analysis of shear/core wall buildings. This analogy was developed first by Clough et al. (1964) and Macleod (1967) for the analysis of plane coupled shear wall structures. Basically, the method treats the walls and lintel beams as discrete frame members with the finite width of the walls allowed for by horizontal rigid arms incorporated in the beam elements. It is also commonly known as the frame method (see Fig. 4.4).

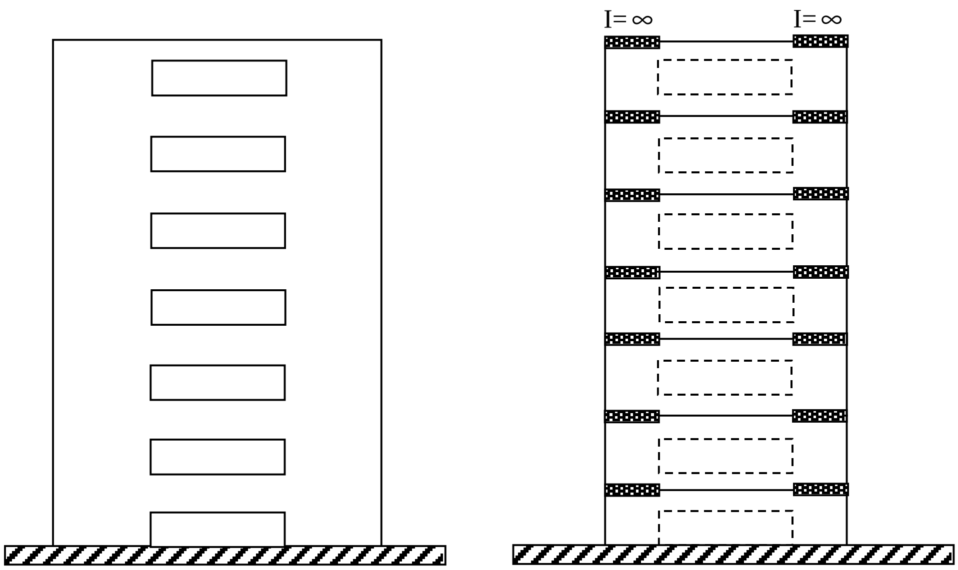

Figure 4.4. Equivalent frame model for planar coupled shear walls

The warping phenomenon of open sections have a significant influence on the behaviour of shear wall structures. Therefore, it is recommended that the warping phenomenon be given serious consideration in the analysis and design of open section shear walls.

As mentioned previously, open section shear walls resist torsion mainly by the out-of-plane bending or warping of the walls. These open sections subject to interaction effects of surrounding beams or slabs resist torsion to a great extent by the continously distributed membrane or St.Venant shear stresses. The analogous frame in this study, is similar to the equivalent frame method.

The frame method was extended to analyze the three dimensional coupled shear/core wall structures by treating the non-planar shear/core walls as assemblies of two dimensional planar wall units individually as discrete column members residing at the centroidal axis of the wall units as shown in Fig. 4.5(a)-(b) respectively. In the extended method, in order to allow connection between adjacent planar wall units to form the non-planar walls, the nodes are placed along the vertical wall joints instead of column members at the centers of the wall units and to the ends of the coupling beams. The connecting beams are rigidly connected to the rigid arms such that the rotations of the beams at the beamwall joints are equal to those of the rigid arms. This method was developed in the 1970s by Macleod.

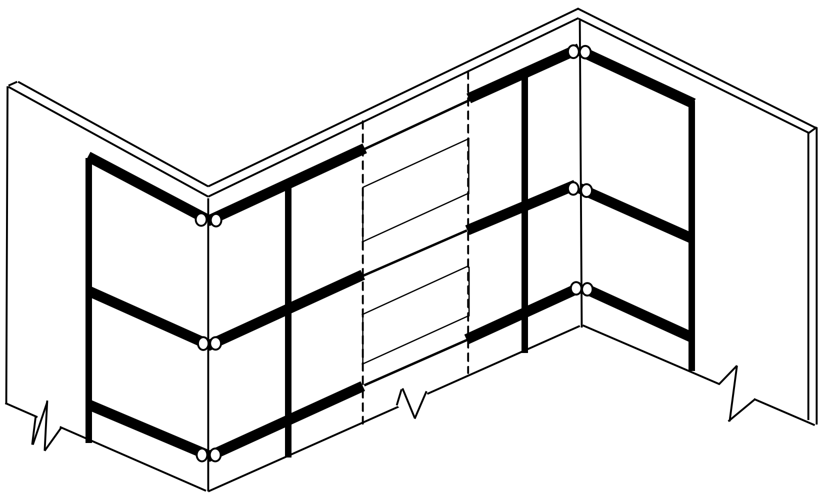

(a)

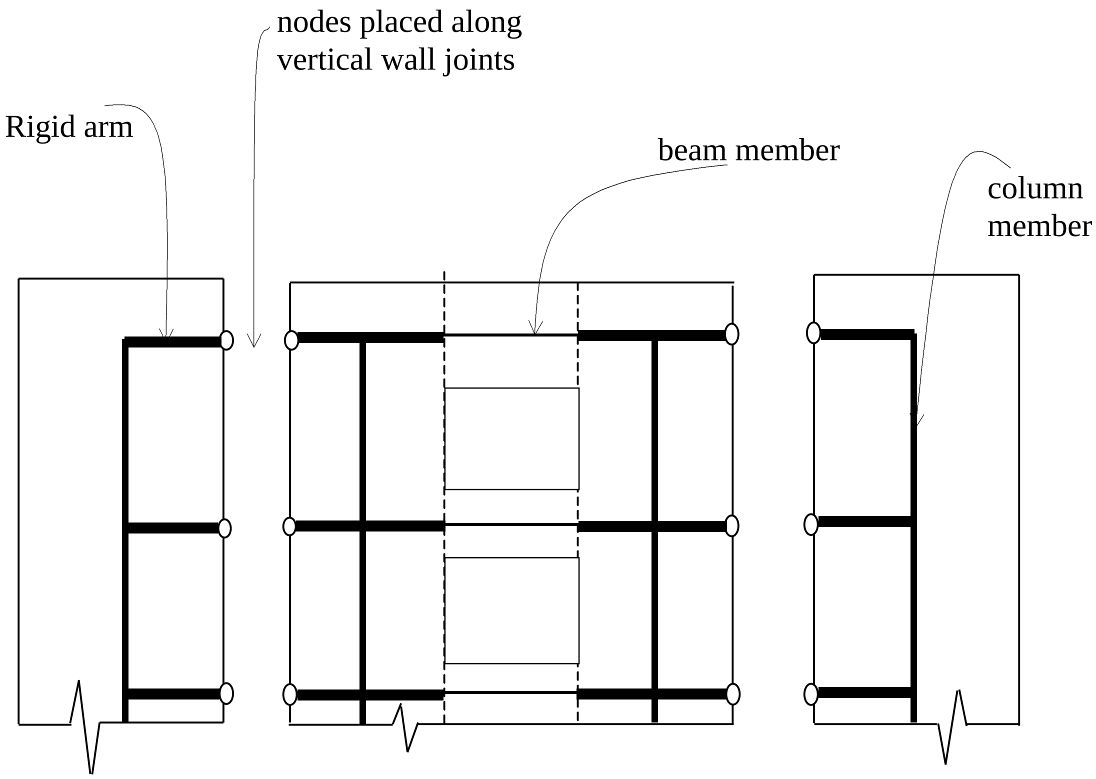

(b)

Figure 4.5. Conventional wide-column-frame analogy for analysis of three dimensional coupled wall structures.

The coupled non-planar wall structure studied by Tso and Biswas (1973) shown in Fig. 4.6 is analyzed using the Macleod's (1977) frame method. The structure consists of three planar walls interconnected to form a U-channel shaped wall assembly. The central wall panel has a row of openings and is thus in effect a pair of coupled shear walls. The coupled non-planar wall structure is therefore actually composed of four planar wall units and a row of coupling beams. The four planar wall units are modeled by solid wall elements. Fig. 4.7 shows the arrangement of the wall and beam elements used in the analysis. Only one layer of elements is shown Fig. 4.7 in which ‘‘h_e’’ is the height of the element. The presented example model tested by Tso and Biswas (1973), neglects the shear deformation of the walls.

Similarly, Vlasov theory, ignores shear deformation in the walls, which yields overstiffed results.

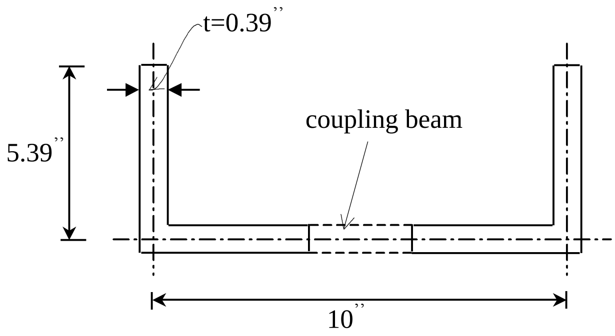

Figure 4.6. Plan of non-planar coupled shear wall tested by Tso and Biswas

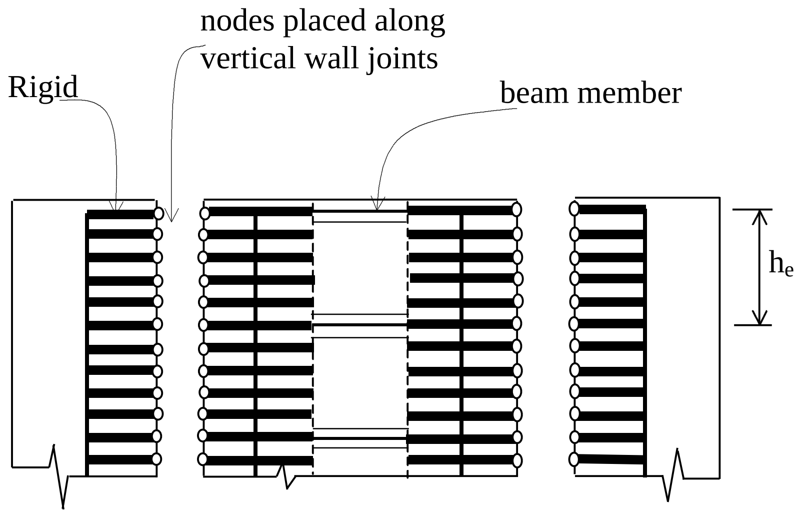

Figure 4.7. Arrangement of wall and beam elements

This method is suitable because all the nodes are placed at the edges of the wall units and, therefore, coupling between adjacent wall units, whether planar or non-planar, can be done simply by connecting them together. Therefore, it is specially designed for modelling wall units connected to other walls at both edges. Such a method of beam wall coupling has the advantage that no rotational degrees of freedom are required, hence, solid wall elements with no rotational degrees of freedom can be coupled with the beam elements directly. The results are plotted in

Fig. 4.8 where the theoretical and experimental results obtained by Tso and Biswas are also plotted for comparison. The figure shows that Tso and Biswas's theory, which neglects the shear deformation of the walls, underestimates the lateral deflection of the structure. The proposed frame method agrees fairly reasonably with the experimental results.

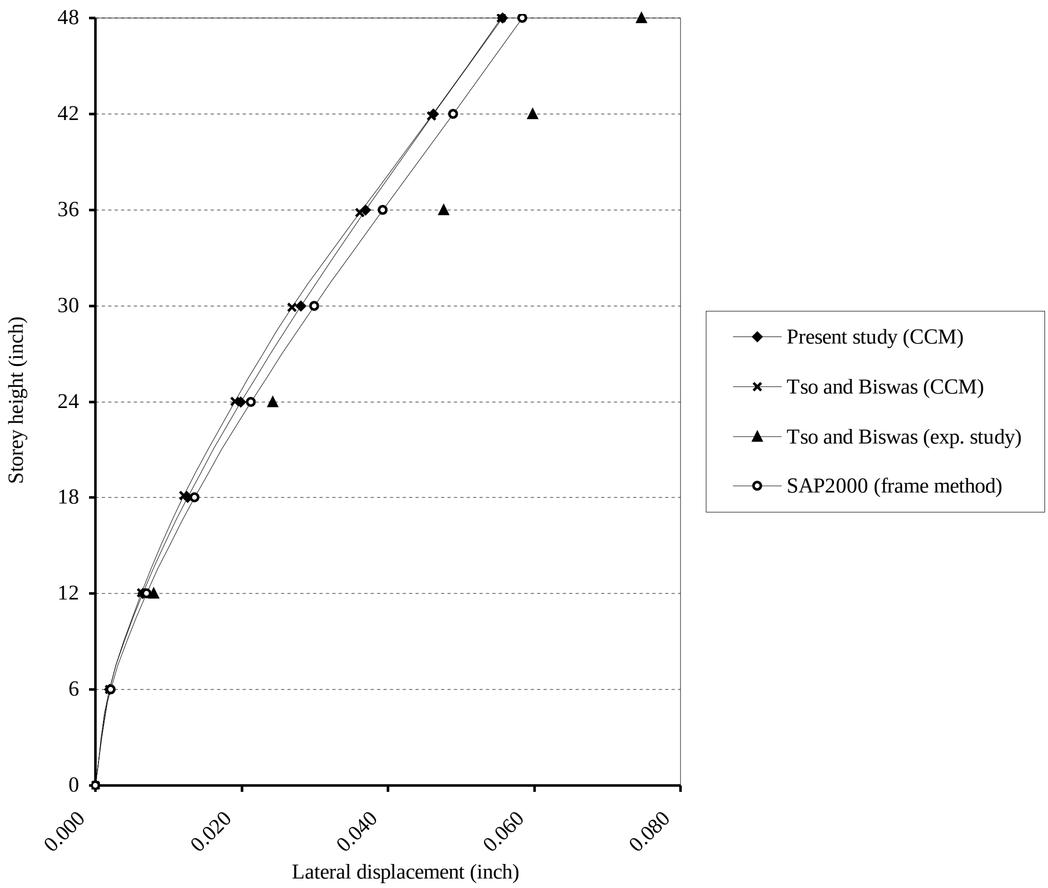

Figure 4.8. The lateral displacements in the X direction of the model studied by Tso& Biswas

5. FORMULATION FOR NON-PLANAR COUPLED SHEAR WALLS UNDER STATIC LOADS

5.1. General Information

Based on Vlasov's theory of thin-walled beams and the continous medium technique, an approximate method is presented for the analysis of non-planar coupled shear walls subjected to lateral loads which produce combined bending and torsional deformations.

The non-planar system of coupled shear walls shown in Fig. 4.1 with global axes OX,OY and OZ, the origin being at the mid-point of the connecting beam. The X-axis is along the longitudinal direction of the connecting beams. The Z-axis is the vertical axis and the Y-axis is in the horizontal plane perpendicular to the X-axis. The plan of the non-planar coupled shear wall is shown in Fig. 5.1 with the mid-point of the clear span at the base denoted as point O.

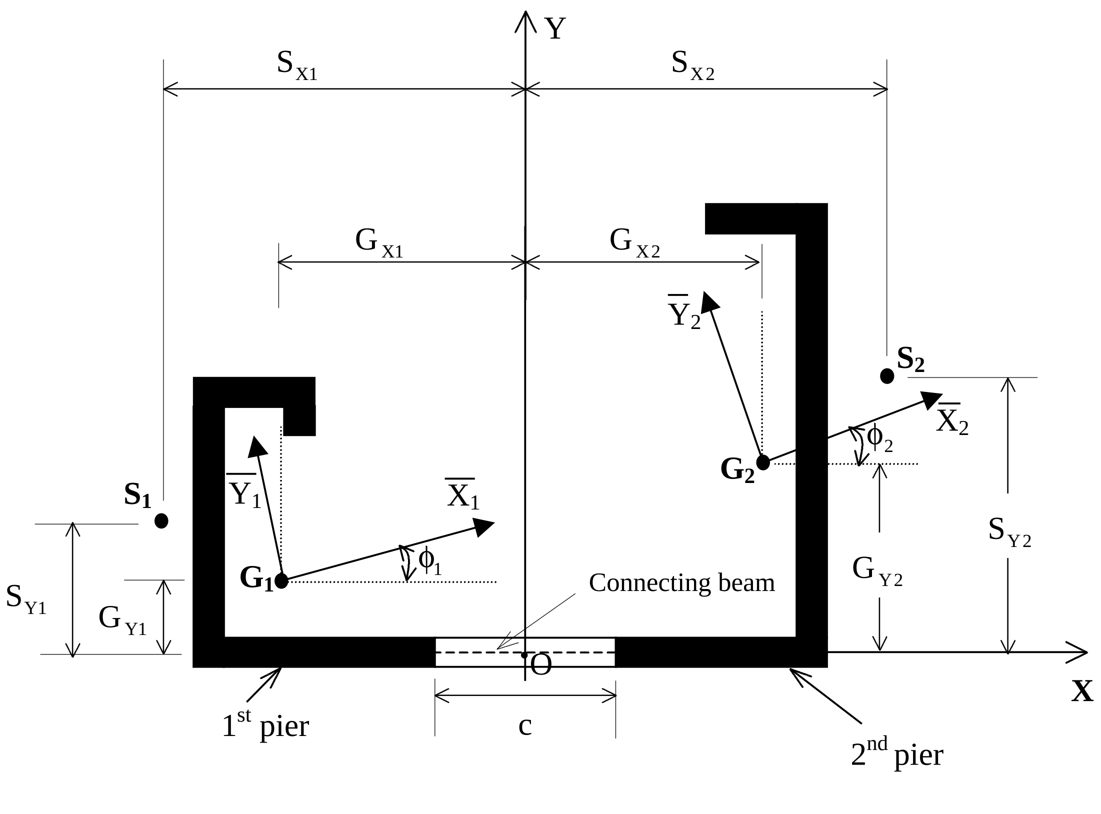

Figure 5.1. Plan of non-planar coupled shear wall

Referring to the axes, OX and OY, the location of the centroids of the piers are taken to be (G_{X1}, G_{Y1}) and (G_{Y1}, G_{Y2}), respectively. The subscripts, 1 and 2, refer to the parameters associated with the left and the right piers, respectively, throughout this study. Similarly, the shear centers of the piers are located at (S_{X1}, S_{Y1}) and (S_{X2}, S_{Y2}), respectively. The coordinates referred to the principal axes of wall j (j=1 and 2) which are represented by $(\overline{X}_j, \overline{Y}_j)$, making an angle ϕ_j with the respective global axes shown in Fig. 5.1. The $\overline{Z}_j$ axis is parallel to the global Z axis. The displacement vector of the shear center of each wall in its local system of axes can be written as

$$D_j = \begin{bmatrix} u_j \\ v_j \\ \theta_j \end{bmatrix} \tag{5.1}$$

where u_j and v_j are the lateral displacements of shear centers with reference to the principal axes of wall j (j=1,2) and θ_j is a function of rotation about $\overline{Z}_j$ axis.

The equilibrium equations of the whole structure, refer to the (X,Y,Z) system of axes. The transformation of the geometric and pyhsical properties of the shear walls into this system is possible by combined rotation and translation. The rotation matrix and the translation matrix can be expressed, respectively, as follows:

$$R_j = \begin{bmatrix} \mathrm{Cos}\phi_j & \mathrm{Sin}\phi_j & 0 \\ -\mathrm{Sin}\phi_j & \mathrm{Cos}\phi_j & 0 \\ 0 & 0 & 1 \end{bmatrix} \tag{5.2}$$

$$T_j = \begin{bmatrix} 1 & 0 & -S_{Yj} \\ 0 & 1 & S_{Xj} \\ 0 & 0 & 1 \end{bmatrix} \tag{5.3}$$

in which S_{Xj} and S_{Yj} are the coordinates of the shear center of wall j relative to the global axes.

The displacement vector of the shear wall in local axes passing through the shear center are related to the corresponding global displacements u, v, and θ, in which

$$D = \begin{bmatrix} u \\ v \\ \theta \end{bmatrix} \tag{5.4}$$

where u and v are the displacements in the X and Y directions of the global axes, and θ is the rotation about the Z axis. Therefore, the transformation of the displacement vector can be expressed as

$$D_j = R_j T_j D \tag{5.5}$$

Substituting the expressions (5.1-4) into (5.5),

$$\begin{bmatrix} u_j \\ v_j \\ \theta_j \end{bmatrix} = \begin{bmatrix} Cos\phi_j & Sin\phi_j & -S_{yj} \\ -Sin\phi_j & Cos\phi_j & S_{xj} \\ 0 & 0 & 1 \end{bmatrix} \begin{bmatrix} u \\ v \\ \theta \end{bmatrix} \tag{5.6}$$

From these geometric relationships, the local displacements u_j, v_j and θ_j (j=1,2) parallel to the global axes at the shear centers of walls 1 and 2 may be expressed in terms of the global displacements u, v, and θ by

$$u_j = u - S_{Yj}\theta \quad (j=1,2) \tag{5.7}$$

$$v_j = v + S_{Xj}\theta \quad (j=1,2) \tag{5.8}$$

and

$$\theta_j = \theta \qquad (j=1,2) \tag{5.9}$$

Consider two sets of axes Oxy and $O\bar{x}\bar{y}$, the latter being inclined at an angle ϕ with the former (see Fig. 5.2).

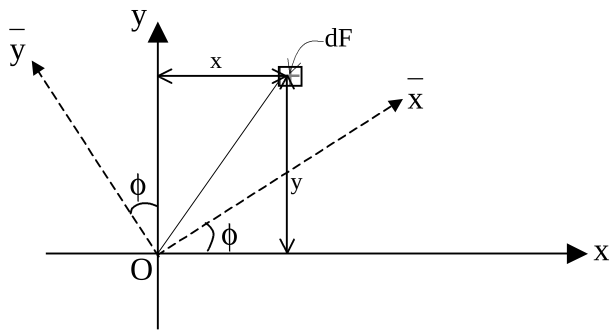

Figure 5.2. Rotation of axes

Any point in the plane can be described by the coordinates (x, y) or by $(\bar{x}, \bar{y})$. These coordinates are related by a rotation matrix with the following transformation.

$$\begin{bmatrix} \bar{x} \\ \bar{y} \end{bmatrix} = \begin{bmatrix} \mathrm{Cos}\phi & \mathrm{Sin}\phi \\ -\mathrm{Sin}\phi & \mathrm{Cos}\phi \end{bmatrix} \begin{bmatrix} x \\ y \end{bmatrix} \tag{5.10}$$

In addition to this, applying the rotation matrix (5.10), to the moments of inertia of a cross-section, the moments of a inertia with respect to the system of axes $O\bar{x}\bar{y}$ can be found in a straightforward manner. It should be noted that, to calculate the moments of inertia with respect to the system of axes $O\bar{x}\bar{y}$ in terms of the moments of inertia with respect to the system of axes Oxy starting from their definitons:

$$\overline{I_x} = \iint_A \bar{y}^2 dA = \iint_A (-x\mathrm{Sin}\phi + y\mathrm{Cos}\phi)^2 dA \tag{5.11}$$

$$\overline{I_y} = \iint_A \overline{x}^2 dA = \iint_A (xCos\phi + ySin\phi)^2 dA \tag{5.12}$$

$$\overline{I_{xy}} = \iint_A \overline{xy}^2 dA = \iint_A (xCos\phi + ySin\phi) \cdot (-xSin\phi + yCos\phi) dA \tag{5.13}$$

From (5.11-13), using the definitons of the moments of inertia with respect to the system of axes Oxy, the relations in (5.11-13) can be rewritten as follows:

$$\overline{I_x} = I_x Cos^2\phi + I_y Sin^2\phi - 2I_{xy} Sin\phi Cos\phi \tag{5.14}$$

$$\overline{I_y} = I_x Sin^2\phi + I_y Cos^2\phi + 2I_{xy} Sin\phi Cos\phi \tag{5.15}$$

$$\overline{I_{xy}} = (I_x - I_y) Sin\phi Cos\phi + I_{xy} (Cos^2\phi - Sin^2\phi) \tag{5.16}$$

The assumptions in the foregoing analysis were given in Chapter 4.

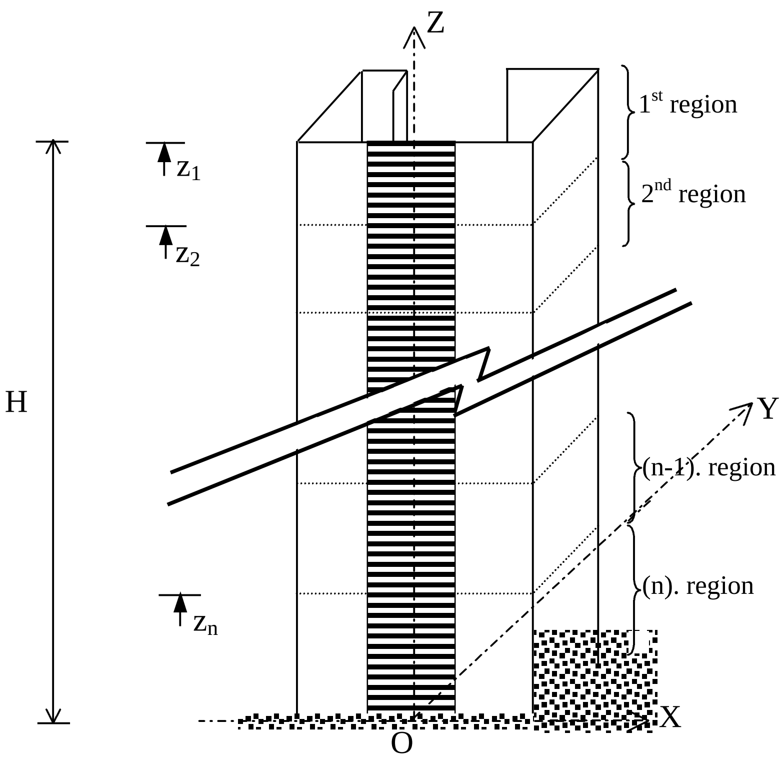

Figure 5.3. Equivalent structure

In view of assumption 4, the overall cross-section of the structure can not be deformed in its own plane. The movements of any point on the contour can then be expressed in terms of the global generalized displacement variables, which consist of two horizontal displacements, u and v, and a rotation, θ, about the point O (see Fig. 5.1).

In order to understand assumption 6 mentioned in Chapter 4, the general displacement of a connecting beam and the moments induced at the ends are shown in Fig. 5.4.

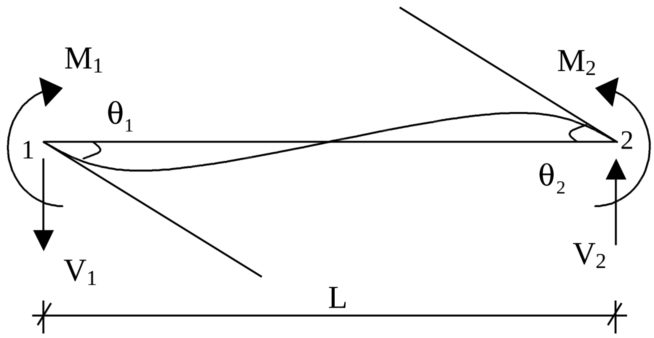

Figure 5.4. General displacement of a connecting beam

The floor slabs surrounding the coupled shear wall system are rigid in their own planes and flexible normal to these planes, so that the cross-sections of the walls remain undistorted in plan. Because of this assumption, actual rotations θ_1 and θ_2 of the connecting beam are equal to each other as shown in Fig. 5.4. The end moments M_1 and M_2 may be considered as being caused by a combination of moments due to the fixed end moments developed by the transverse loading on the member, relative translation of the ends of the member and by the actual rotations of the ends, θ_1 and θ_2 of the member.

Using the slope deflection method, the general form of the left end moment can be written as follows:

$$M_1 = \frac{EI_c}{L}\left(4\theta_1 + 2\theta_2 + 6\psi\right) + M_{12} \tag{5.17}$$

Since $\theta_1 = \theta_2 = \theta$, $\psi = 0$ and assuming there is no transverse loading (This is a logical assumption for this analysis). Hence, M_1 and M_2 can be rewritten, respectively, as follows:

$$M_1 = \frac{6EI_c}{L}\theta \tag{5.18}$$

$$M_2 = \frac{6EI_c}{L}\theta \tag{5.19}$$

Since M_1 and M_2 are equal, they can be called by the same name as M. Considering the free body diagram of the connecting beam in Fig. 5.4, the summation of the moments about the left end being equal to zero, yields

$$V_2 = \frac{2M}{L} \tag{5.20}$$

From the equilibrium of vertical forces

$$V_1 = V_2 = V \tag{5.21}$$

Taking moment about the mid-point of the member yields

$$M_{mp} = \frac{2M}{L} \times \frac{L}{2} - M = 0 \tag{5.22}$$

meaning that the bending moment at the mid-points of the connecting beams vanish.

5.2. Formulation

5.2.1. Compatibility Equations

While obtaining the compatibility equations in non-planar coupled shear wall analysis, it is assumed that all rows of connecting laminae will be cut through the mid-points, which are the points of zero moment. The compatibility of the relative vertical displacements, on the two sides of the mid-points of the connecting laminae, occur as a result of five actions. The prime, denotes differentiation with respect to z, during the formulation.

5.2.1.1. The Relative Vertical Displacements due to the Deflections and Rotations of the Piers

The first contribution to the total relative displacement at the mid-point of a laminae is due to the deflection and rotation of the piers. These are caused by the bending of the piers in the principal directions and the twisting of the piers about the shear centers. The non-planar system of coupled shear walls given in Fig. 5.5, in which $\overline{G_{Xj}}$, $\overline{G_{Yj}}$ (j=1,2) are the distances of the centroids from point O, measured along the principal directions of the piers, will be considered for deriving the compatibility equation.

The vertical displacement due to bending can be obtained as the product of the slope at the section considered and the distance of point O from the neutral axis. In addition, vertical displacement arises due to the twisting of the piers, and is equal to the value of the twist at the section considered, times the sectorial area, ω, at point O.

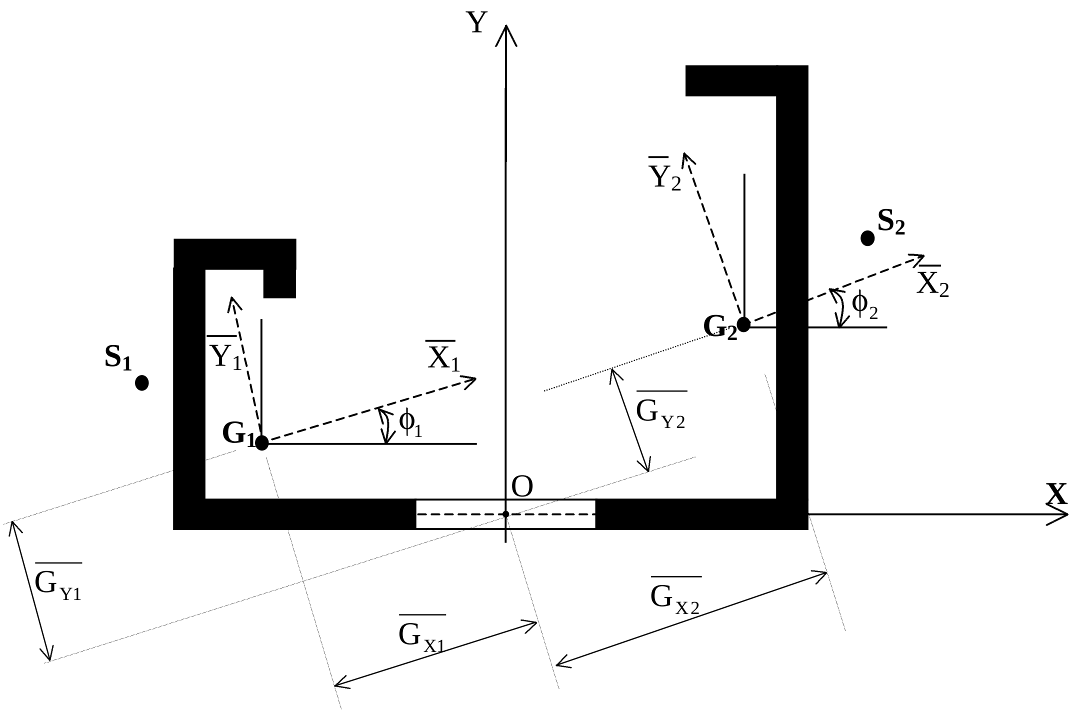

Figure 5.5. Cross-section of a non-planar coupled shear wall

Graphically, the vertical displacements to the left and right of the cut due to bending and twisting can be shown as in Fig. 5.6. Here, the downwards displacements of the end on the left of the cut and the upwards displacements of the end on the right of it will be taken to be positive in expressing the relative vertical displacements.

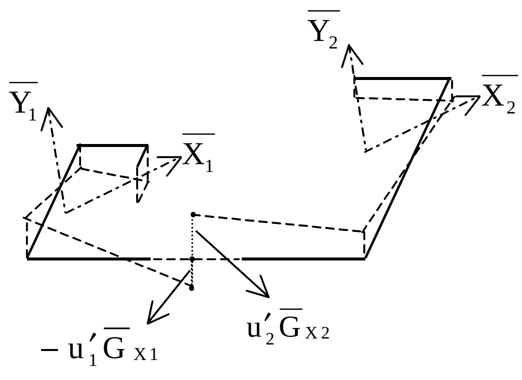

a) Bending in $\overline{X}_1$ and $\overline{X}_2$ directions

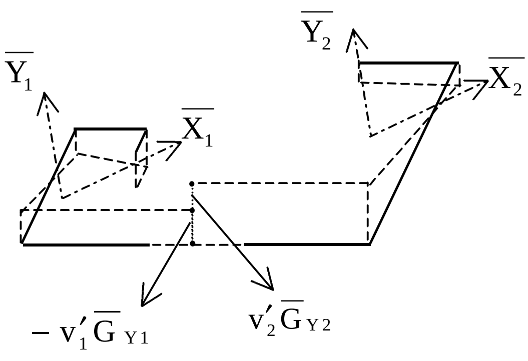

b) Bending in $\overline{Y_1}$ and $\overline{Y_2}$ directions

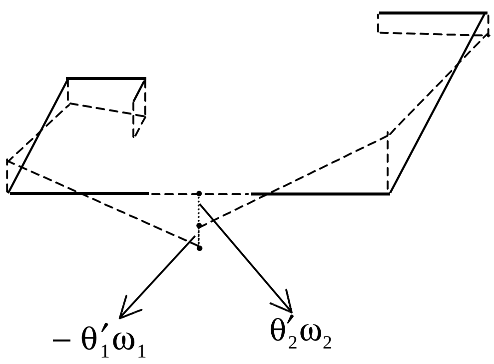

c) Twisting about the shear centers

Figure 5.6. Relative displacements at the mid-point of the lamina due to the deflection and rotation of the wall

Let δ_1 denote the total relative vertical displacement due to the deflections and rotations of the piers, which can be given as

$$\delta_1 = \left(u_2'\overline{G_{X2}} - u_1'\overline{G_{X1}}\right) + \left(v_2'\overline{G_{Y2}} - v_1'\overline{G_{Y1}}\right) - \left(\theta_2'\omega_2 - \theta_1'\omega_1\right) \tag{5.23}$$

The first two terms in equation (5.23), represent the contributions due to the bending of the piers in the principal directions and the last represents the contribution due to the twisting of the piers. ω_1 and ω_2 are the sectorial areas at points on the left and right side of the cut.

A detailed exposition of thin-walled beam theory and the definition of sectorial area with formulas were made in Chapter 3. Substituting equations (5.7-9) into (5.23), yields

$$\begin{aligned}\delta_1 = S_{Y1}G_{X1}\theta' - S_{Y2}G_{X2}\theta' - S_{X1}G_{Y1}\theta' + S_{X2}G_{Y2}\theta' \\ -G_{X1}u' + G_{X2}u'G_{Y1}v' + G_{Y2}v' + \theta'\omega_1 - \theta'\omega_2\end{aligned} \tag{5.24}$$

Rearranging the equation (5.24)

$$\delta_{1i} = u_i'a + v_i'b + \theta_i'(\omega + d) \qquad (i=1,2,...,n) \tag{5.25}$$

$$\omega = \omega_1 - \omega_2 \tag{5.26}$$

where i is the region number and

$$a = G_{X2} - G_{X1} \tag{5.27}$$

$$b = G_{Y2} - G_{Y1} \tag{5.28}$$

$$d = S_{X2}G_{Y2} - S_{Y2}G_{X2} + S_{Y1}G_{X1} - S_{X1}G_{Y1} \tag{5.29}$$

5.2.1.2. The Relative Vertical Displacement due to Axial Deformation of the Piers

The axial force, T, produces axial deformation in the piers and in turn causes additional relative vertical displacement along the cut, which in turn produces compressive force in one pier and tensile in the other as shown in Fig. 5.7.

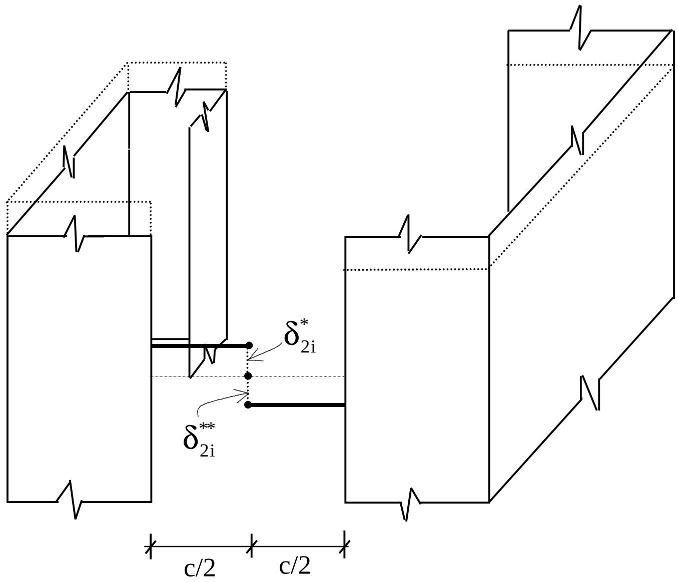

Figure 5.7. Relative displacements due to axial forces in the piers

From the vertical force equilibrium for a dz element of one pier the axial force at any height can be shown to be related to q_i by

$$q_i = -T_i' \qquad (i=1,2,..,n) \qquad (5.30)$$

The normal strain being defined as $\frac{\sigma}{E} = \frac{T}{EA}$, the total axial elongation of pier 1 can be written as

$$\delta^{*}_{2i} = -\frac{1}{E}\sum_{j=i+1}^{n}\frac{1}{A_{1j}}\int_{z_{j+1}}^{z_j} T_j dz - \frac{1}{E}\left(\frac{1}{A_{1i}}\right)\int_{z_{i+1}}^{z_i} T_i dz \qquad (i=1,2,...,n) \qquad (5.31)$$

Similarly, the total axial shortening for pier 2 is

$$\delta_{2i}^{**} = -\frac{1}{E}\sum_{j=i+1}^{n}\frac{1}{A_{2j}}\int_{z_{j+1}}^{z_j} T_j dz - \frac{1}{E}\left(\frac{1}{A_{2i}}\right)\int_{z_{i+1}}^{z_i} T_i dz \qquad (i=1,2,...,n) \qquad (5.32)$$

From (5.31-32), the total relative displacement due to the change of length in the piers can be written as

$$\delta_{2i} = -\frac{1}{E}\sum_{j=i+1}^{n}\left[\left(\frac{1}{A_{1j}}+\frac{1}{A_{2j}}\right)\int_{z_{j+1}}^{z_j} T_j dz\right] - \frac{1}{E}\left(\frac{1}{A_{1i}}+\frac{1}{A_{2i}}\right)\int_{z_{i+1}}^{z} T_i dz \quad (i=1,2,...,n) \quad (5.33)$$

5.2.1.3. The Relative Vertical Displacement due to Bending of the Laminae

A point load P at the end of a cantilever beam of length L, causes an end deflection equal to $\left(\delta = \frac{PL^3}{3EI}\right)$. Hence, the shear force in each lamina of dz height is as follows:

$$P = q_i \, dz \qquad (5.34)$$

in which causes relative displacements (see Fig. 5.8).

$$\delta_{3i}^{*} = -\frac{q_i \, dz \left(c/2\right)^3}{\frac{3EI_{ci}}{h_i} dz} \qquad (i=1,2,...,n) \qquad (5.35)$$

and

$$\delta_{3i}^{**} = -\frac{q_i \, dz \left(c/2\right)^3}{\frac{3EI_{ci}}{h_i} dz} \qquad (i=1,2,...,n) \qquad (5.36)$$

where h_i is the storey height in region i and c is the clear span of the laminae. Therefore, the total relative displacement caused by the from shear forces in the laminae, that is shown in Fig. 5.8, can be obtained by adding expressions (5.35) and (5.36) as

$$\delta_{3i} = \delta_{3i}^{*} + \delta_{3i}^{**} = -\frac{h_i\, c^3}{12EI_{ci}}\, q_i \qquad (i=1,2,...,n) \qquad (5.37)$$

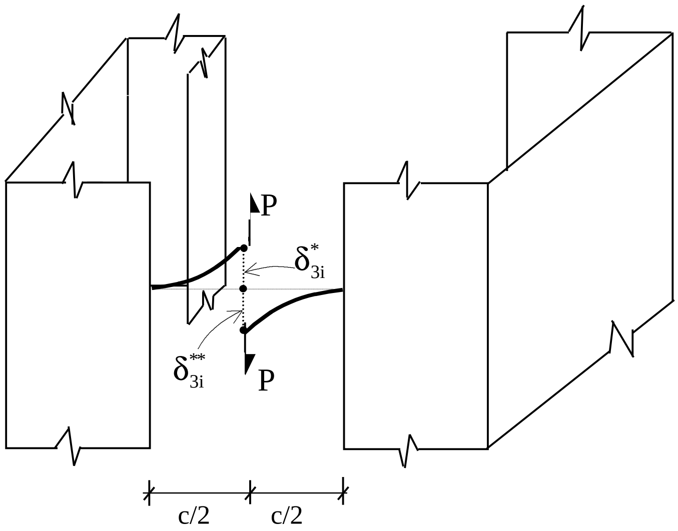

Figure 5.8. Relative displacement of laminae due to bending

5.2.1.4. The relative vertical displacement due to shearing effect in the laminae

The same shear force q_i as it was mentioned before, causes a shear deformation in the beam given by equation

$$\delta_4 = \delta_4^{*} + \delta_4^{**} = -\frac{q_i\,(c/2)\,dz}{G\,\frac{A_c^{*}}{h_i}\,dz} + -\frac{q_i\,(c/2)\,dz}{G\,\frac{A_c^{*}}{h_i}\,dz} = -\frac{q_i\, c\, h_i}{GA_c^{*}} \qquad (i=1,2,...,n) \quad (5.38)$$

However, for rectangular sections, effective cross-sectional shear area $A_{ci}^{\bullet}$ can be considered as in equation (5.39).

$$A_{ci}^{\bullet} = \frac{A_{ci}}{\mu_c} \tag{5.39}$$

where μ_c is a constant, equal to 1.2.

Therefore, the total relative vertical displacement due to shearing effect in the laminae can be written as follow

$$\delta_4 = -\frac{1.2\, q_i\, c\, h_i}{GA_{ci}} \qquad (i=1,2,...,n) \tag{5.40}$$

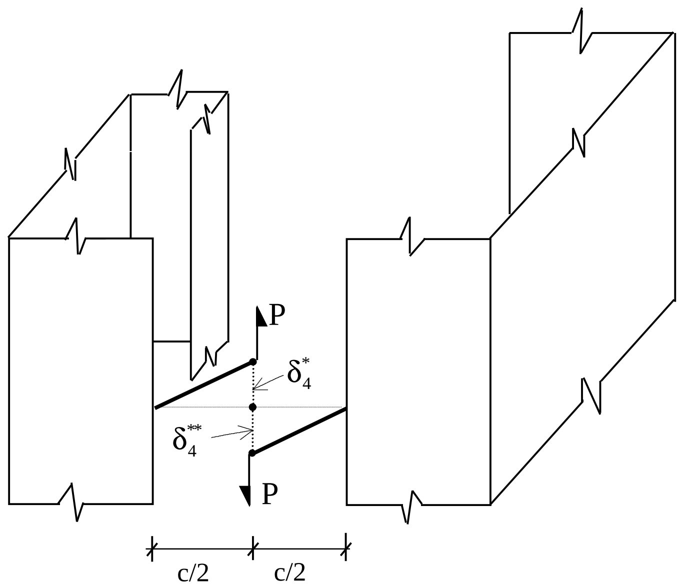

Figure 5.9. Relative displacement of connecting beam due to beam shear deflection

5.2.1.5. The relative vertical displacement due to the flexibility of the connections

In elastic condition cases, beam will take shape as it is shown in Fig. 5.10. In rigid cases, it is formed as shown in case 1. The relative vertical displacement due to rotational spring in the first pier can be written as in

$$\delta_5^* = -\alpha \times \frac{c}{2} \tag{5.41}$$

The moment value in that spring is equal to (M=kα). k is the rotational spring constant. From this relation it is clear that (α=M/k). Therefore, substituting this expression into (5.41)

$$\delta_5^* = -\frac{M}{k} \times \frac{c}{2} \tag{5.42}$$

can be obtained.

M in equation (5.42), is the moment at the end-point of the connecting beam. It is equal to ($M=P\times\frac{c}{2}$) at the mid-point of the connecting beam due to the equilibrium. Also it is known that ($P = q_i h_i$). Therefore, the total relative vertical displacement due to the flexibility connections can be written as shown in

$$\delta_5 = \delta_5^* + \delta_5^{**} = -\frac{q_i h_i c^2}{2C_{cbi}} \qquad (i=1,2,...,n) \tag{5.43}$$

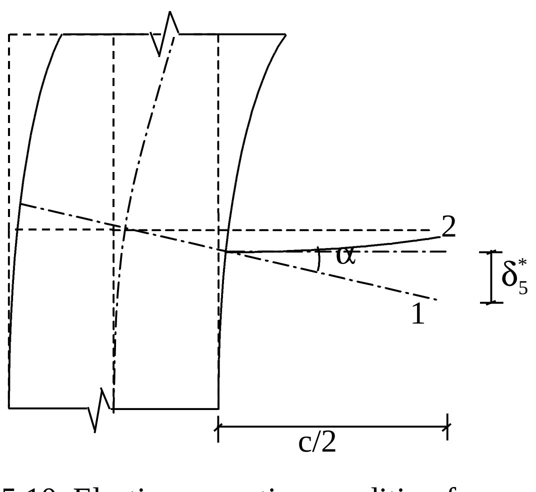

Figure 5.10. Elastic connection condition for connecting beams

Under lateral loads the two ends of the connecting beam experience vertical displacements at the cuts consisting of contributions $\left(\delta_1, \delta_2, \delta_3, \delta_4 \text{ and } \delta_5\right)$ as explained before. Since, the two piers are connected, the compatibility condition stipulates that the relative displacements must vanish, i.e.,

$$\delta_{1i}+\delta_{2i}+\delta_{3i}+\delta_{4i}+\delta_{5i}=0 \tag{5.44}$$

Therefore, the compatibility equation for the vertical displacement in region i can be written as

$$\begin{aligned} & u'a+v_i'b+\theta_i'(\omega+d)- \\ & \qquad \frac{1}{E}\sum_{j=i+1}^{n}\left[\left(\frac{1}{A_{1j}}+\frac{1}{A_{2j}}\right)\int_{z_{j+1}}^{z_j}T_j\,dz\right]-\frac{1}{E}\left(\frac{1}{A_{1i}}+\frac{1}{A_{2i}}\right)\int_{z_{i+1}}^{z}T_i\,dz+ \\ & \qquad\qquad \frac{T_i'}{E}\left[\frac{1.2h_ic}{GA_{ci}}+\frac{h_ic^3}{12EI_{ci}}+\frac{h_ic^2}{2C_{cbi}}\right]=0 \qquad (i=1,2,\ldots,n) \end{aligned} \tag{5.45}$$

Differentiating (5.45) with respect to z

$$u_i''a+v_i''b+\theta_i''(\omega+d)-\frac{1}{E}\left[\left(\frac{1}{A_{1i}}+\frac{1}{A_{2i}}\right)T_i\right]+\frac{T_i''}{E}[\gamma_{ci}]=0 \qquad (i=1,2,...,n) \tag{5.46}$$

in which

$$\gamma_{ci}=\frac{1.2h_ic}{GA_{ci}}+\frac{h_ic^3}{12EI_{ci}}+\frac{h_ic^2}{2C_{cbi}} \tag{5.47}$$

5.3. Force equilibrium equations

The coordinate system and positive directions of bending and twisting moments M_x and M_y are adopted as shown vectorially in Fig. 5.11. The internal moments acting on the different components of the coupled shear wall are shown in in the figure.

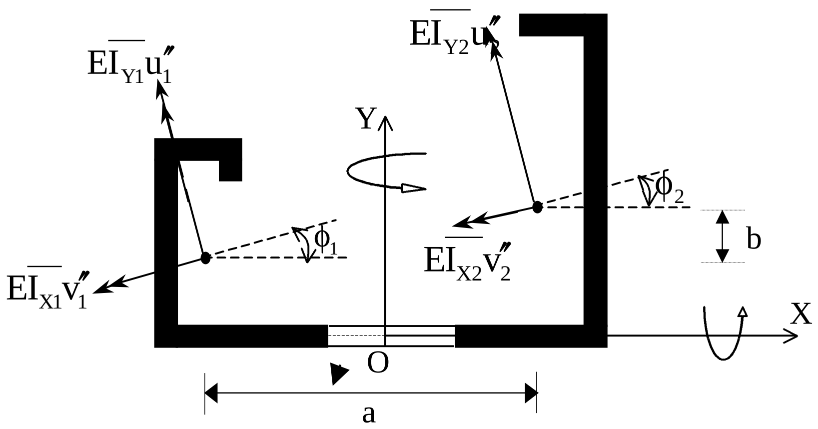

Figure 5.11. Internal moments acting on the components of the coupled shear wall

These internal moments, along with the couple produced by the axial force, T, balance the external moments. For equilibrium of moments about X and Y axes, the following relationships can be derived using Vlasov's theory of thin walled beams.

$$M_{ey} = E\left(\overline{I_{Y1}}u_1''\cos\phi_1 - \overline{I_{X1}}v_1''\sin\phi_1 + \overline{I_{Y2}}u_2''\cos\phi_2 - \overline{I_{X2}}v_2''\sin\phi_2\right) + Ta \tag{5.48}$$

$$M_{ex} = E\left(\overline{I_{Y1}}u_1''\sin\phi_1 + \overline{I_{X1}}v''\cos\phi_1 + \overline{I_{Y2}}u_2''\sin\phi_2 + \overline{I_{X2}}v_2''\cos\phi_2\right) + Tb \quad 5.49)$$

On substituting the local displacement expressions given before in (5.7-9) into expressions (5.48-49), defined above, the moment components are found, in terms of the global displacements at point O, as

$$M_{eyi} = EI_Y u_i'' + EI_{XY} v_i'' - EI_{\theta y} \theta_i'' + T_i a \qquad \text{(i=1,2,...n)} \tag{5.50}$$

$$M_{exi} = EI_{XY} u_i'' + EI_X v_i'' + EI_{\theta x} \theta_i'' + T_i b \qquad \text{(i=1,2,...,n)} \tag{5.51}$$

in which

$$I_y = I_{Y1} + I_{Y2} \tag{5.52}$$

$$I_x = I_{X1} + I_{X2} \tag{5.53}$$

$$I_{xy} = I_{XY1} + I_{XY2} \tag{5.54}$$

$$I_{\theta x} = S_{X1} I_{X1} + S_{X2} I_{X2} - S_{Y1} I_{XY1} - S_{Y2} I_{XY2} \tag{5.55}$$

$$I_{\theta y} = S_{Y1} I_{Y1} + S_{Y2} I_{Y2} - S_{X1} I_{XY1} - S_{X2} I_{XY2} \tag{5.56}$$

Terms I_{Yj} and I_{Xj} are the second moments of area, and I_{XYj} is the product of inertia of pier j (j=1,2) about axes parallel to global axes and passing through the centroid. $\overline{I_{Xj}}$ and $\overline{I_{Yj}}$ are the second moments of area of pier j (j=1,2) about its respective principal axes.

In order to obtain the twisting moment equilibrium equation, the coupled shear wall will be cut through by an horizontal plane such that an upper free body diagram is isolated from the rest of the structure.

The internal twisting moments (torque) in the structure consists of two parts; one contributed by the individual piers as shown in Fig. 5.12 and the other due to the resistance of the connecting laminae, in other words, the differential effect of the shear flow q_i in the connecting medium as shown in Fig. 5.13 (related to warping).

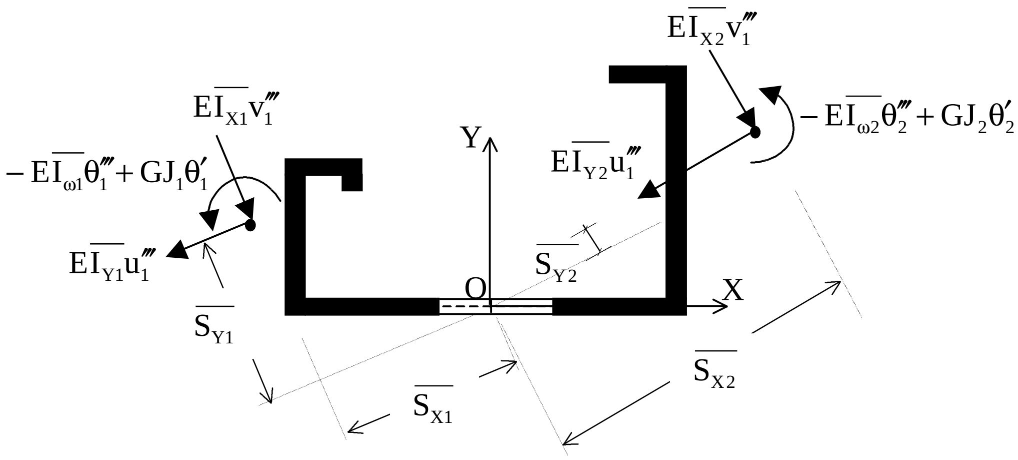

Figure 5.12. Internal torques and shear forces

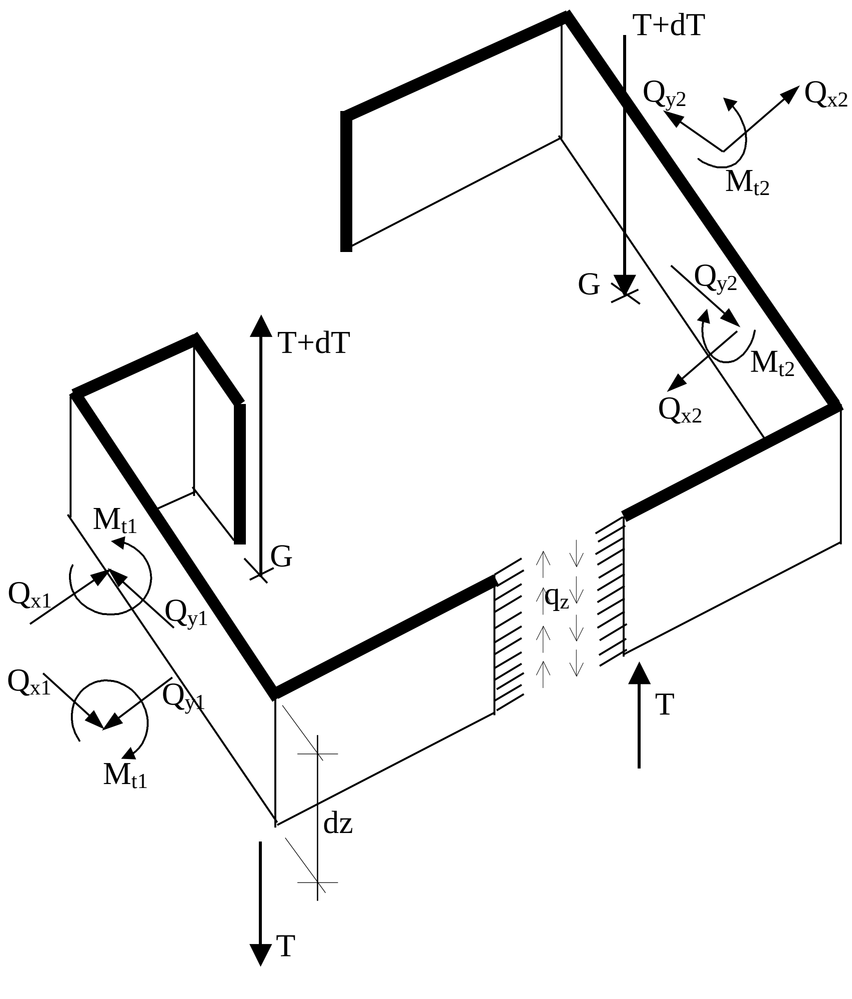

Figure 5.13. Shear forces and torques due to shear flow in connecting medium

In addition, there are shear forces Q_{x1}, Q_{y1}, Q_{x2}, Q_{y2}, and torques M_{t1} and M_{t2}, developed in the section due to the shear force, q, in the laminae, as shown in Fig. 5.14.

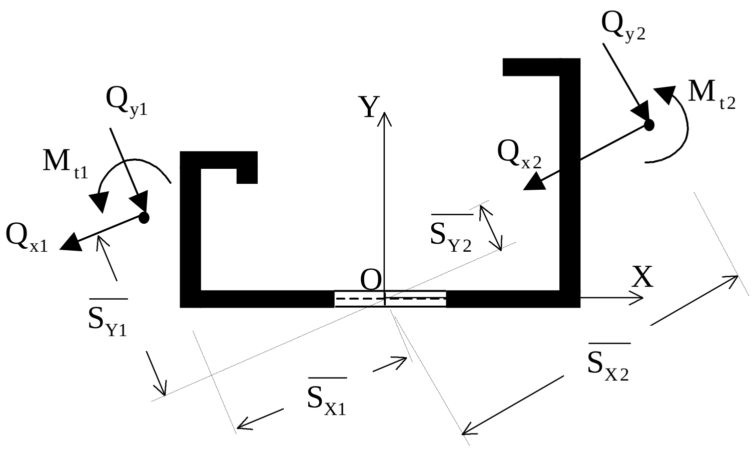

Figure 5.14. Torques and shear forces due to beam shear q_i

All quantities are related to the shear centers of piers 1 and 2. In order to determine the twisting moment due to the shear flow q_i, the relationship between the force components in the piers and q_i may be determined from the free body diagram of Fig. 5.13.

Let $\overline{M_{et}}$ be the resultant torque about point O, which is due to the resistance offered by the piers. It can be written as (see Fig. 5.12)

$$\begin{aligned}\overline{M_{et}} = {} & G\left(J_1\theta_1' + J_2\theta_2'\right) + E\left(I_{Y1}u_1''' + I_{XY1}v_1'''\right)\overline{S_{Y1}} \\ & + E\left(I_{Y2}u_1''' + I_{XY2}v_2'''\right)\overline{S_{Y2}} - E\left(I_{X1}v_1''' + I_{XY2}u_1'''\right)\overline{S_{X1}} \\ & - E\left(I_{X2}v_2''' + I_{XY2}u_2'''\right)\overline{S_{X2}} - E\left(I_{\omega 1}\theta_1''' + I_{\omega 2}\theta_2'''\right)\end{aligned} \tag{5.57}$$

On substituting the expressions (5.7-9) into (5.57), the resultant resisting torque of the piers for all regions in the structure are found as

$$\overline{M_{eti}} = GJ\theta_i' + EI_{\theta y}u_i''' - EI_{\theta x}v_i''' - EI_{\omega}\theta_i''' \qquad \text{(i=1,2,...,n)} \tag{5.58}$$

in which $I_{\theta x}$ and $I_{\theta y}$ are defined in (5.55-56) and

$$J = J_1 + J_2 \tag{5.59}$$

$$\begin{aligned} I_\omega = I_{\omega 1} + I_{\omega 2} + S_{X1}^2 I_{X1} + S_{X2}^2 I_{X2} + S_{Y1}^2 I_{Y1} + S_{Y2}^2 I_{Y2} \\ - 2S_{X1}S_{Y1}I_{XY1} - 2S_{X2}S_{Y2}I_{XY2} \end{aligned} \tag{5.60}$$

Let $\overline{\overline{M_{et}}}$ be the resultant torque due to the additional forces and torques about the point O as shown in Fig. 5.14.

The shear forces, q , in the laminae produce bimoments on the piers. For pier 1, the bimoment dB_{z1} is caused by the external force qdz and is equal to the product of this force and the principal sectorial area ω_1 of the point of its application. Therefore, it can be written in the following form

$$dB_{z1} = q \;\; dz\,\omega_1 \tag{5.61}$$

and analogously for pier 2

$$dB_{z2} = -q \;\; dz\,\omega_2 \tag{5.62}$$

These bimoments produce the flexural twists M_{t1} and M_{t2}, related to pole 1 and 2, respectively. Using the relation obtained in (3.54), yields

$$M_{t1} = \frac{dB_{z1}}{dz} = q \;\; \omega_1 \tag{5.63}$$

$$M_{t2} = \frac{dB_{z2}}{dz} = q \;\; \omega_2 \tag{5.64}$$

The resultant torque, $\overline{\overline{M_{et}}}$, due to these additional forces and torques about the point, O, is, then, found as

$$\overline{\overline{M_{et}}} = M_{t1} + M_{t2} - Q_{x1}\overline{S_{Y1}} + Q_{y1}\overline{S_{X1}} - Q_{x2}\overline{S_{Y2}} + Q_{y2}\overline{S_{X2}} \tag{5.65}$$

These additional forces and torques acting on an element are shown in Fig. 5.13. From the consideration of equilibrium of moment about $\overline{Y_1}$ and $\overline{X_1}$ axes for one pier, the following relations can be obtained as follows, respectively:

$$Q_{x1}\,dz + q\ \ dz\,\overline{G_{X1}} = 0 \tag{5.66}$$

$$Q_{y1}\,dz + q\ \ dz\,\overline{G_{y1}} = 0 \tag{5.67}$$

Thus

$$Q_{x1} = -q\ \ \overline{G_{X1}} \tag{5.68}$$

and

$$Q_{y1} = -q\ \ \overline{G_{Y1}} \tag{5.69}$$

Similar consideration for the other wall gives

$$Q_{x2} = q\ \ \overline{G_{X2}} \tag{5.70}$$

$$Q_{y2} = q\ \ \overline{G_{Y2}} \tag{5.71}$$

Substituting (5.68-71) in (5.65), using (5.29) and simplifying, the resultant twisting moment, about the vertical axis through O, due to the component shears and torques

$$\overline{\overline{M_{et}}} = (\omega + d)q \qquad (5.72)$$

Equating the external twisting moment to the internal resisting moments, the equilibrium of the isolated part of the coupled shear wall above an arbitrary horizontal plane is established. Finally, the foregoing equilibrium for all regions of the structure can be written as follows:

$$M_{eti} = -EI_{\theta x} v_i''' + EI_{\theta y} u_i''' - EI_{\omega} \theta_i''' + GJ\theta_i' - (\omega + d)T_i' \qquad (i=1,2,...,n) \qquad (5.73)$$

Finally, using the compatibility equation (5.45) and the three equilibrium equations (5.50), (5.51), and (5.73), the 4n unknowns of the problem, namely u, v, θ and T can be found under the applied loadings M_{exi}, M_{eyi}, and M_{eti}.

5.4. Method of Solution

For any given lateral loading on the shear wall system, the values of the applied moments and torque, M_{ex}, M_{ey} and M_{et}, at any height of the structure can be found from statics. The deformation of the structure is then found by obtaining the solution of the system of differential equations (5.45), (5.50), (5.51) and (5.73). It is more convenient to reduce the 4n unknowns to n unknowns, T_i, and solve the n equations subjected to appropriate boundary conditions.

Derivatives of equations (5.45), (5.50) and (5.51) with respect to z are as follows:

$$M'_{eyi} = E\,I_y\,u'''_i + E\,I_{xy}\,v'''_i - E\,I_{\theta y}\,\theta'''_i + T'_i a \qquad (i=1,2,\ldots,n) \qquad (5.74)$$

$$M'_{exi} = E\,I_{xy}\,u'''_i + E\,I_x\,v'''_i + E\,I_{\theta x}\,\theta'''_i + T'_i b \qquad (i=1,2,...,n) \qquad (5.75)$$

$$u'''_i a + v'''_i b + \theta'''_i(\omega + d) = \frac{1}{E}\left[\frac{1}{A_1} + \frac{1}{A_2}\right]T'_i - \frac{\gamma T'''_i}{E} \qquad (i=1,2,\ldots,n) \qquad (5.76)$$

Equating the u'''_i expressions obtained from (5.74) and (5.75)

$$u'''_i = \frac{M'_{eyi} - E\,I_{xy}\,v'''_i + E\,I_{\theta y}\,\theta'''_i - T'_i a}{E\,I_y} = \frac{M'_{exi} - E\,I_x\,v'''_i - E\,I_{\theta x}\,\theta'''_i - T'_i b}{E\,I_{xy}} \qquad (5.77)$$

Similar procedure for v'''_i yields

$$v'''_i = \frac{M'_{eyi} - E\,I_y\,u'''_i + E\,I_{\theta y}\,\theta'''_i - T'_i a}{E\,I_{xy}} = \frac{M'_{exi} - E\,I_{xy}\,u'''_i - E\,I_{\theta x}\,\theta'''_i - T'_i b}{E\,I_x} \qquad (5.78)$$

from (5.77) and (5.78), u'''_i and v'''_i are found in a straightforward manner yielding

$$v_i'''E\left(I_x I_y - I_{xy}^2\right) = -E\theta_i'''\left(I_y I_{\theta x} + I_{xy} I_{\theta y}\right) + T_i'\left(a I_{xy} - b I_y\right) - M_{eyi}' I_{xy} + M_{exi}' I_y \tag{5.79}$$

$$-u_i'''E\left(I_x I_y - I_{xy}^2\right) = -E\theta_i'''\left(I_x I_{\theta y} + I_{xy} I_{\theta x}\right) + T_i'\left(a I_x - b I_{xy}\right) + M_{exi}' I_{xy} - M_{eyi}' I_x \tag{5.80}$$

Dividing both equations by $\left(I_x I_y - I_{xy}^2\right)$

$$v_i''' = \frac{1}{E}\left(-E\theta_i'''\frac{\left(I_{xy} I_{\theta y} + I_y I_{\theta x}\right)}{\left(I_x I_y - I_{xy}^2\right)} + T_i'\frac{\left(a I_{xy} - b I_y\right)}{\left(I_x I_y - I_{xy}^2\right)} - \frac{M_{eyi}' I_{xy}}{\left(I_x I_y - I_{xy}^2\right)} + \frac{M_{exi}' I_y}{\left(I_x I_y - I_{xy}^2\right)}\right) \tag{5.81}$$

$$u_i''' = \frac{1}{E}\left(E\theta_i'''\frac{\left(I_{\theta y} I_x + I_{xy} I_{\theta x}\right)}{\left(I_x I_y - I_{xy}^2\right)} - T_i'''\frac{\left(a I_x - b I_{xy}\right)}{\left(I_x I_y - I_{xy}^2\right)} - \frac{M_{exi}' I_{xy}}{\left(I_x I_y - I_{xy}^2\right)} + \frac{M_{eyi}' I_x}{\left(I_x I_y - I_{xy}^2\right)}\right) \tag{5.82}$$

Here and in the sequel the following definitions apply:

$$\frac{1}{A} = \left[\frac{1}{A_1} + \frac{1}{A_2}\right] + aK_3 + bK_4 \tag{5.83}$$

$$\Delta = \left(I_x I_y - I_{xy}^2\right) \tag{5.84}$$

$$K_1 = \frac{\left(I_x I_{\theta y} + I_{xy} I_{\theta x}\right)}{\Delta} \tag{5.85}$$

$$K_2 = \frac{\left(I_{xy} I_{\theta y} + I_y I_{\theta x}\right)}{\Delta} \tag{5.86}$$

$$K_3 = \frac{\left(a\,I_x - b\,I_{xy}\right)}{\Delta} \tag{5.87}$$

$$K_4 = -\frac{\left(a\,I_{xy} - b\,I_y\right)}{\Delta} \tag{5.88}$$

With the definitions (5.84-88), (5.81-82) are put into the following forms:

$$v_i''' = \frac{1}{E}\left(-E\,\theta_i'''K_2 - T_i'K_4 - \frac{M_{eyi}'\,I_{xy}}{\Delta} + \frac{M_{exi}'\,I_y}{\Delta} \right) \tag{5.89}$$

$$u_i''' = \frac{1}{E}\left(E\,\theta_i'''K_1 - T_i'K_3 - \frac{M_{exi}'\,I_{xy}}{\Delta} + \frac{M_{eyi}'\,I_x}{\Delta} \right) \tag{5.90}$$

Substituting (5.89) and (5.90) into (5.73)

$$\begin{aligned} M_{eti} = & -EI_{\theta x}\,\frac{1}{E}\left(-E\,\theta_i'''K_2 - T_i'K_4 - \frac{M_{eyi}'\,I_{xy}}{\Delta} + \frac{M_{exi}'\,I_y}{\Delta} \right) \\ & + EI_{\theta y}\,\frac{1}{E}\left(E\,\theta_i'''K_1 - T_i'K_3 - \frac{M_{exi}'\,I_{xy}}{\Delta} + \frac{M_{eyi}'\,I_x}{\Delta} \right) \\ & - EI_{\omega}\theta_i''' + GJ\theta_i' - (\omega + d)T_i' \qquad (i = 1,2,\ldots,n) \end{aligned} \tag{5.91}$$

Reorganizing (5.91),

$$\begin{aligned} M_{eti} = & -T_i'(w + d) + T_i'I_{\theta x}\,K_4 - T_i'I_{\theta y}K_3 \\ & + EI_{\theta x}\,\theta_i'''K_2 + EI_{\theta y}\theta_i'''K_1 - E\,I_{\omega}\,\theta_i''' \\ & + M_{eyi}'\,\frac{\left(I_x\,I_{\theta y} + I_{xy}I_{\theta x}\right)}{\Delta} - M_{exi}'\,\frac{\left(I_{xy}\,I_{\theta y} + I_yI_{\theta x}\right)}{\Delta} + G\,J\,\theta_i' \end{aligned} \tag{5.92}$$

Simplifying (5.92) further,

$$M_{eti} = -T_i'\left[w + d - I_{\theta x} K_4 + I_{\theta y} K_3\right]$$
$$- E\theta_i'''\left[I_\omega - I_{\theta x} K_2 - I_{\theta y} K_1\right] + M_{eyi}' K_1 - M_{exi}' K_2 + GJ\theta_i' \tag{5.93}$$

Here, making the following definitions

$$r = w + d - I_{\theta x} K_4 + I_{\theta y} K_3 \tag{5.94}$$

$$\bar{I}_\omega = I_\omega - I_{\theta x} K_2 - I_{\theta y} K_1 \tag{5.95}$$

and substituting them in (5.93) yields

$$M_{eti} = -T_i' r - E\theta_i''' \bar{I}_\omega + M_{eyi}' K_1 - M_{exi}' K_2 + GJ\theta_i' \tag{5.96}$$

With the help of expressions (5.85-88), (5.94) can be rearranged as follows:

$$r = w + d - I_{\theta x}\left[-\frac{\left(a I_{xy} - b I_y\right)}{\Delta}\right] + I_{\theta y}\left[\frac{\left(a I_x - b I_{xy}\right)}{\Delta}\right] \tag{5.97}$$

$$r = w + d + \frac{a I_{xy} I_{\theta x} - b I_y I_{\theta x}}{\Delta} + \frac{a I_x I_{\theta y} - b I_{xy} I_{\theta y}}{\Delta} \tag{5.98}$$

$$r = w + d + a\left[\frac{\left(I_x I_{\theta y} + I_{xy} I_{\theta x}\right)}{\Delta}\right] - b\left[\frac{\left(I_{xy} I_{\theta y} + I_y I_{\theta x}\right)}{\Delta}\right] \tag{5.99}$$

and

$$r = w + d + a K_1 - b K_2 \tag{5.100}$$

Reorganizing the compatibility equation (5.76),

$$u_i'' a + v_i'' b + (\omega + d)\theta_i'' - \frac{1}{E}\left[\frac{1}{A_1} + \frac{1}{A_2}\right] T_i + \frac{T_i''\gamma_i}{E} = 0 \tag{5.101}$$

Substituting expressions (5.89-90) into (5.101),

$$\theta_i'' = \frac{1}{Er}\left[-M_{eyi}K_3 - M_{exi}K_4 + \frac{T_i}{A} - T_i''\gamma_i\right] \tag{5.102}$$

$$\theta_i'''E\overline{I_\omega} - GJ\theta_i' = K_1M_{eyi}' - K_2M_{exi}' - T_i'r - M_{eti} \tag{5.103}$$

$$\theta_i''''E\overline{I_\omega} - GJ\theta_i'' = K_1M_{eyi}'' - K_2M_{exi}'' - T_i''r - M_{eti}' \tag{5.104}$$

Eliminating θ from equations (5.102) and (5.104),

$$\begin{aligned}&\frac{\overline{I_\omega}}{r}\left(-M_{eyi}''K_3 - M_{exi}''K_4 + \frac{T_i''}{A} - T_i''''\gamma_i\right) +\\ &\qquad \frac{GJ}{Er}K\left(M_{eyi}K_3 + M_{exi}K_4 - \frac{T_i}{A} + T_i''\gamma_i\right)\\ &\qquad\qquad = M_{eyi}''\,K_1 - M_{exi}''\,K_2 - T_i''r - M_{eti}'\end{aligned} \tag{5.105}$$

Simplifying equation (5.105), the single fourth order governing differential equation for the axial force T_i is obtained as follows:

$$\begin{aligned}&T_i''''\left(\gamma_i\overline{I_\omega}\right) - T_i''\left(\frac{\overline{I_\omega}}{A} + \frac{GJ\gamma_i}{E} + r^2\right) + T_i\left(\frac{GJ}{EA}\right) =\\ &\qquad -M_{eyi}''\left(\overline{I_\omega}K_3 + K_1r\right) - M_{exi}''\left(\overline{I_\omega}K_4 - K_2r\right) +\\ &\qquad\qquad \frac{GJ}{E}\left(M_{eyi}K_3 + M_{exi}K_4\right) + M_{eti}'r\end{aligned} \tag{5.106}$$

Equation (5.106) can be written in another form as

$$\begin{aligned}&T_i''''(\beta_{1i}) - T_i''(\beta_{2i}) + T_i(\beta_{3i}) = -M_{eyi}''\left(\overline{I_\omega}K_3 + K_1r\right)\\ &\qquad - M_{exi}''\left(\overline{I_\omega}K_4 - K_2r\right) + \frac{GJ}{E}\left(M_{eyi}K_3 + M_{exi}K_4\right) + M_{eti}'r\end{aligned} \tag{5.107}$$

in which

$$\beta_{1i} = \gamma_i \overline{I_\omega} \tag{5.108}$$

$$\beta_{2i} = \frac{\overline{I_\omega}}{A} + \frac{GJ\gamma_i}{E} + r^2 \tag{5.109}$$

$$\beta_{3i} = \frac{GJ}{EA} \tag{5.110}$$

The problem of static analysis of non-planar coupled shear walls reduces to the solution of equation (5.107). M_{exi} and M_{eyi} are the external bending moments and M_{eti} is the external twisting moment about the respective global axes and can be written as shown below, for a general horizontal concentrated force at the top and a general uniformly distributed load along the total height:

$$M_{exi} = P_y(H - z) + \frac{w_y(H - z)}{2} \tag{5.111}$$

$$M'_{exi} = -P_y - w_y(H - z) \tag{5.112}$$

$$M''_{exi} = w_y \tag{5.113}$$

$$M'''_{exi} = 0 \tag{5.114}$$

$$M_{eyi} = P_x(H - z) + \frac{w_x(H - z)}{2} \tag{5.115}$$

$$M'_{eyi} = -P_x - w_x(H - z) \tag{5.116}$$

$$M''_{eyi} = w_x \tag{5.117}$$

$$M'''_{eyi} = 0 \tag{5.118}$$

$$M_{eti} = P_x(-d_{py}) + P_y(d_{px}) + w_x(H-z)(-d_{wy}) + w_y(H-z)\,d_{wx} \tag{5.119}$$

$$M'_{eti} = w_x\,d_{wy} - w_y\,d_{wx} \tag{5.120}$$

$$M''_{eti} = 0 \tag{5.121}$$

Using these expressions, T_i function is found as follows:

$$T_i = D1_i * \mathrm{Sinh}[\alpha_{1i} * z_i] + D2_i * \mathrm{Cosh}[\alpha_{1i} * z_i] + D3_i * \mathrm{Sinh}[\alpha_{2i} * z_i]$$

$$+ D4_i * \mathrm{Cosh}[\alpha_{2i} * z_i] + \frac{1}{2\beta_3^2 E}\left(2\beta_2 GJ\left(K_3 w_x + K_4\,w_y\right) + \beta_3\right) +$$

$$\left(-2E\left(\overline{I_\omega}\,K_3\,w_x - d_{wy}\,r\,w_x + K_1\,r\,w_x\,\overline{I_\omega}\,K_4\,w_y + d_{wx}\,r\,w_y - K_2\,r\,w_y\right) + GJ\left(H - z_i\right)\right)$$

$$\left(2K_3P_x + 2K_4P_y + HK_3w_x + HK_4w_y - \left(K_3w_x + K_4w_y\right)z_i\right)$$

$$(i=1,2,\ldots,n) \tag{5.122}$$

Boundary conditions can be used to determine the integration constants in equation (5.122). Then substituting those constants, T_i function can be obtained in a straightforward manner.

5.5. Boundary Conditions

A single fourth order governing differential equation for the axial force T is obtained. To find the axial force expressions in the n regions, one needs 4×n boundary conditions to determine the 4n integration constants.

1- For a structure which is rigidly fixed at the base (z=0)

$$u_i = v_i = \theta_i = 0 \tag{5.123}$$

$$u_i' = v_i' = \theta_i' = 0 \tag{5.124}$$

Applying equation (5.45) at z=0 using (5.124),

$$T_n'\big|_{z=0} = 0 \tag{5.125}$$

2- From equation (5.73), substituting θ_i''', u_i''' and v_i''' from (5.89-90) and (5.102) in terms of T_i' and putting θ_i'=0, the second boundary condition at the base (z=0) yields

$$\begin{aligned} M_{etn} - I_{\theta y}\left[\frac{\left(M_{eyn}' I_x - M_{exn}' I_{xy}\right)}{\Delta} + \frac{K_1}{r}\left(-M_{eyn}' K_3 - M_{exn}' K_4 + \frac{T_n'}{A} - \gamma T_n'''\right) - T_n' K_3\right] + \\ I_{\theta x}\left[\frac{\left(M_{exn}' I_y - M_{eyn}' I_{xy}\right)}{\Delta} - \frac{K_2}{r}\left(-M_{eyn}' K_3 - M_{exn}' K_4 + \frac{T_n'}{A} - \gamma T_n'''\right) - T_n' K_4\right] + \\ \frac{I_\omega}{r}\left[-M_{eyn}' K_3 - M_{exn}' K_4 + \frac{T_n'}{A} - \gamma T_n''''\right] + (\omega + d) T_n' = 0 \end{aligned} \tag{5.126}$$

3- The axial force at the top (z=H) is equal to zero.

$$T_1\big|_{z=H} = 0 \tag{5.127}$$

4- At the top (z=H), the bimoment (B_z) is zero, so that

$$\theta''_{i|_{z=H}} = 0 \tag{5.128}$$

and hence, from equation (3.57)

$$B_z = -EI_\omega \theta''_i = \frac{-I_\omega}{r}\left[-M_{eyi}K_3 - M_{exi}K_4 + \frac{T_i}{A} - T''_i \gamma_i\right] = 0 \tag{5.129}$$

5- From vertical force equilibrium at height z_i on one side of the point of contraflexure

$$T_{i-1|_{z=z_i}} = T_{i|_{z=z_i}} \qquad i=(2,3,\ldots,n) \tag{5.130}$$

6- From continuity condition, applying the compatibility equation for the two neighbouring regions i and i-1 at height $z=z_i$, the following equation is obtained

$$T'_{(i-1)|z=z_i}\left(\frac{c^3h_{(i-1)}}{12EI_{c_{(i-1)}}} + \frac{1.2ch_{(i-1)}}{GA_{c_{(i-1)}}} + \frac{c^2h_{(i-1)}}{2C_{cb_{(i-1)}}}\right) = T'_{i\,|z=z_i}\left(\frac{c^3h_i}{12EI_{ci}} + \frac{1.2ch_i}{GA_{ci}} + \frac{c^2h_i}{2C_{cb_i}}\right) \tag{5.131}$$

7- The total twisting moments of the two neighboring regions i and i-1, at height z_i being equal to each other

$$\begin{aligned} M_{eti} - EI_{\theta y}u'''_i + EI_{\theta x}v'''_i + EI_\omega \theta'''_i - GJ\theta'_i + (\omega + d)T'_i = M_{et(i-1)} - \\ EI_{\theta y}u'''_{(i-1)} + EI_{\theta x}v'''_{(i-1)} + EI_\omega \theta'''_{(i-1)} - GJ\theta'_{(i-1)} + (\omega + d)T'_{(i-1)} \end{aligned} \tag{5.132}$$

Expressing all functions in terms of T and after some necessary arrangements,

$$C_1 T'''_{(i-1)} - C_2 T'''_i + C_3 T'_{(i-1)} - C_4 T'_i = 0 \tag{5.133}$$

in which

$$C_1 = \frac{\gamma_{(i-1)} K_1 I_{\theta y}}{r} + \frac{\gamma_{(i-1)} K_2 I_{\theta x}}{r} - \frac{I_\omega \gamma_{(i-1)}}{r}$$

$$C_2 = \frac{\gamma_i K_1 I_{\theta y}}{r} + \frac{\gamma_i K_2 I_{\theta x}}{r} - \frac{I_\omega \gamma_i}{r}$$

$$C_3 = \frac{-I_{\theta y} K_1}{Ar} + I_{\theta y} K_3 - \frac{I_{\theta x} K_2}{Ar} - I_{\theta x} K_4 + \frac{I_\omega}{Ar} + (\omega + d) \tag{5.134}$$

$$C_4 = \frac{-I_{\theta y} K_1}{Ar} + I_{\theta y} K_3 - \frac{I_{\theta x} K_2}{Ar} - I_{\theta x} K_4 + \frac{I_\omega}{Ar} + (\omega + d)$$

8- Applying the bimoment expression for the two neighbouring regions i and i-1, at height z_i,

$$B_{i|_{z=z_i}} = B_{i-1|_{z=z_i}} \tag{5.135}$$

To determine the integration constants, the boundary conditions at the top, bottom and between each pair of consecutive sections are used. Using the boundary conditions above, the integration constants D_1 to D_4 can be found. Substituting these integration constants, in expression (5.122), the general solution for T_i (i=1,2,…,n) are found.

5.6. Determination of θ (rotation) function in a shear wall

The rotation expressions in n regions can be found by substituting the T_i expressions into equation (5.102) and after integrating two times with respect to z,

$$\theta_i = \frac{1}{Er} \int \left(\int - M_{eyi} K_3 - M_{exi} K_4 + \frac{T_i}{A} - T_i'' \gamma_{ci} \right) dz \;) dz \;) + G_{1i} z_i + G_{2i} z_i$$

$$\text{(i=1,2,…,n)} \tag{5.136}$$

To determine the integration constants, $2\times n$ boundary conditions are needed.
The boundary conditions for the unknowns in θ function are as follows:

1,2- Due to the complete fixity, there is no rotation or warping at the base. Hence,

$$\theta_n\,|_{z=0} = 0 \tag{5.137}$$

$$\theta'_n\,|_{z=0} = 0 \tag{5.138}$$

3,4- From the continuity condition at $z=z_i$, applying the compatibility equation for two neighbouring sections i and i-1 at height $z=z_i$, the following equality is obtained:

$$\theta_i\,\Big|_{z=z_i} = \theta_{i-1}\,\Big|_{z=z_i} \tag{5.139}$$

$$\theta'_i\,\Big|_{z=z_i} = \theta'_{i-1}\,\Big|_{z=z_i} \tag{5.140}$$

can be written.

5.7. Determination of the lateral displacement functions (u and v) in a shear wall

Integrating (5.89) and (5.90) twice with respect to z,

$$u_i = \frac{1}{E}\int\left(\int\left(\frac{M_{eyi}I_x - M_{exi}I_y}{\Delta} + \theta''_i EK_1 - T_i K_3\right)dz\right)dz\ \Big) + R_{1i}z_i + R_{2i} \tag{5.141}$$

$$v_i = \frac{1}{E}\int\left(\int\left(\frac{M_{exi}I_y - M_{eyi}I_x}{\Delta} + \theta''_i EK_2 - T_i K_4\right)dz\right)dz\ \Big) + N_{1i}z_i + N_{2i}$$

$$(i=1,2,\ldots,n) \tag{5.142}$$

Substituting from (5.102) and (5.122) into (5.141) and (5.142) u and v can be expressed in terms of the variable z only. In the resulting expressions of u and v, there are 4n integration constants R_i, N_i to be determined from the boundary conditions of the problem. These boundary conditions are the equivalence of the horizontal displacements and slopes of every pair of neighboring regions at their common boundary and the vanishing of the horizontal displacements and slopes at the bottom are

$$u_n = v_n \Big|_{z=0} = 0 \tag{5.143}$$

$$u'_n = v'_n \Big|_{z=0} = 0 \tag{5.144}$$

For the first group of boundary conditions applying the compatibility equation (5.45) for two neighboring regions i and i-1 at height $z=z_i$ using

$$u_i \Big|_{z=z_i} = u_{i-1} \Big|_{z=z_i} \tag{5.145}$$

$$v_i \Big|_{z=z_i} = v_{i-1} \Big|_{z=z_i} \tag{5.146}$$

$$u'_i \Big|_{z=z_i} = u'_{i-1} \Big|_{z=z_i} \qquad (i=2,3,\ldots,n) \tag{5.147}$$

$$v'_i \Big|_{z=z_i} = v'_{i-1} \Big|_{z=z_i} \qquad (i=2,3,\ldots,n) \tag{5.148}$$

Using these boundary conditions, the lateral displacement functions can be obtained easily.

6. NUMERICAL RESULTS

6.1. Introduction

In this study non-planar shear walls coupled with connecting beams are analyzed under lateral loading. The analysis is performed using Vlasov's thin-walled beam theory in conjunction with the CCM. The analysis carried out in the previous chapters, employing the CCM, has been implemented as a computer program in Fortran language and various examples have been solved by applying it to different structures.

In order to confirm the prepared computer program in Fortran language, a broad literature survey has been made during the research process. At the end of the literature survey, it was seen that in the previous research works the cross-sections of the piers were simple geometric shapes and showed some degree of symmetry. In addition to this, each pier was taken as a star section in which the sectorial area and the warping moment of inertia is equal to zero everywhere in the cross-section. To justify the results of the example structure in the literature (Tso & Biswas, 1973), the model structure is solved both by the present method (CCM) and by the SAP2000 structural analysis program (one dimensional frame members or frame method).

To illustrate the application of the presented theory, various examples have been solved in this study. The proposed approach is useful in studying a shear wall in which there is a complexity in geometry. There is no warping in examples 6.1-5, 6.12 and 6.17 in which the sectorial area values at all points in both piers are identically equal to zero. Despite the fact that no warping is handled in the literature, so far, all other examples in this thesis do involve warping. A computer program has been prepared to analyze the three commonly used loading conditions, i.e., a concentrated load at the top, a uniformly distributed load and a torque. Pairs of shear walls of arbitrary cross-sectional shape with the properties of the connecting beams varying from region to region in the vertical direction and having elastic beam-wall connections have been considered, also.

6.2. Numerical Applications

Example 1:

In the first example, a non-planar coupled shear wall considered by Tso and Biswas (1973) has been solved both by the computer program prepared in the present work and the SAP2000 structural analysis program and the displacements, thus obtained, have been compared with those given in the original work. The dimensions of this example shear wall model are same as those given by the authors in the original model.

The geometry and the plan of the section is given in Fig. 6.1. The non-planar coupled shear wall system rests on a rigid foundation and is loaded by a horizontal load 25 lb, in the plane of the connecting beams acting at the top. The total height is 48 in, the storey height is 6 in, the thickness of the wall is 0.39 in, the height of the connecting beams is 1.5 in and the elasticity and shear moduli of the model are E = $0.40\text{x}10^6$ psi and G = $0.148\text{x}10^6$ psi, respectively.

The cross-section having been formed by two angles, each angle has its shear center at the intersection of its sides. The sectorial areas are equal to zero at all points of the cross-section. Hence, the warping moment of inertia, for this example, is identically equal to zero for each pier.

The comparison of the lateral displacements and rotations along the height and the axial forces at the bottom found by the program prepared in the present work, together with those given in the literature and the SAP2000 structural analysis program, are presented in Tables 6.1-3, expressing the percentage differences. The results found are given in Figs. 6.2-3, also.

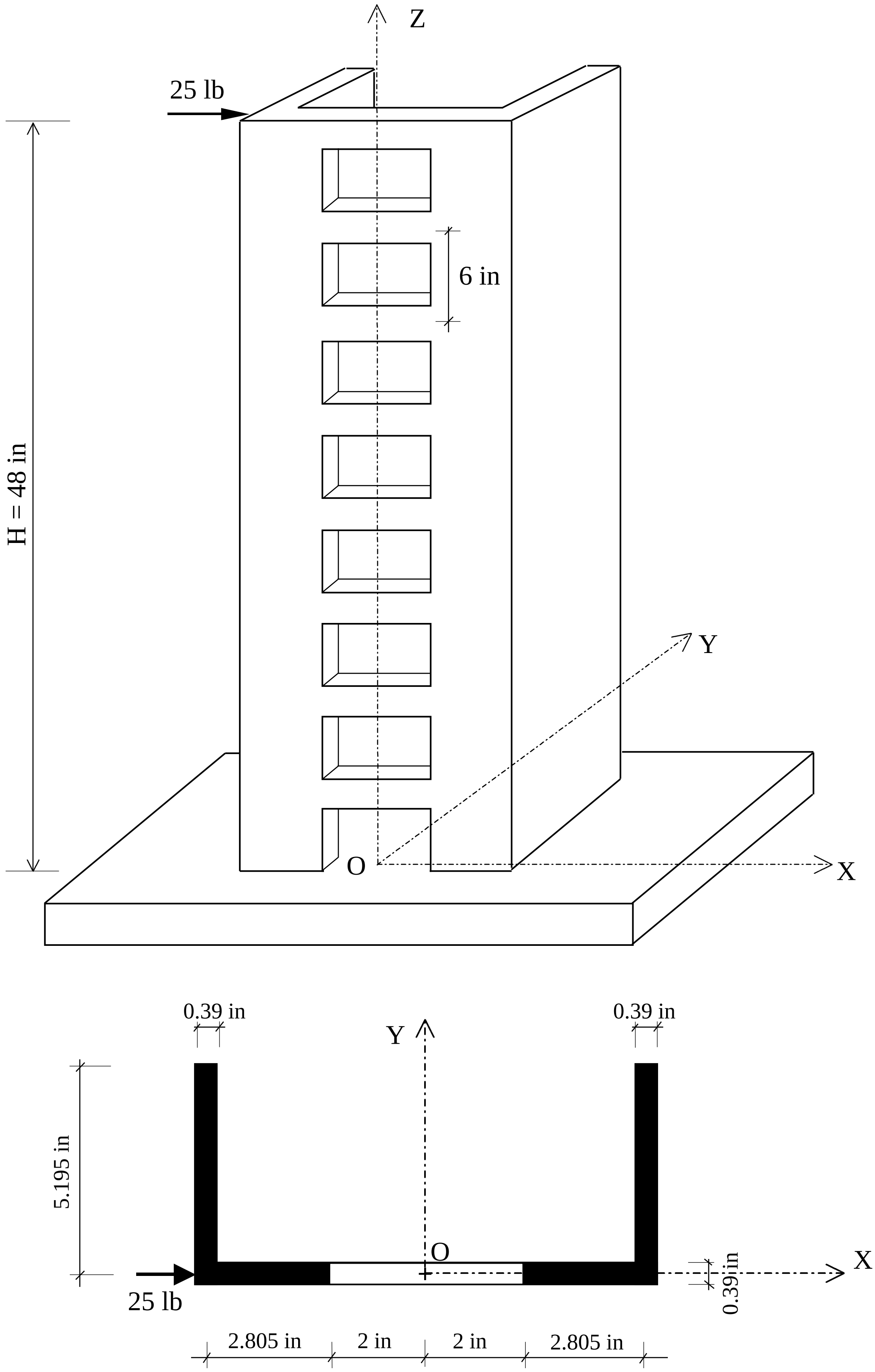

Figure 6.1. Geometrical properties of the model studied by Tso and Biswas

Table 6.1. Comparison of the lateral displacements in the X direction obtained from the present program and SAP2000 in Example 1

Lateral displacements in X direction (inch)								
Storey number	Storey height (inch)	Present study (CCM)	Tso & Biswas (CCM)		Experimental study (Tso&Biswas)		SAP2000 (frame method)	
		Lateral displacement (inch)	Lateral displacement (inch)	% difference of present study compared to Tso & Biswas	Lateral displacement (inch)	% difference of present study compared to Exp. study	Lateral displacement (inch)	% difference of present study compared to SAP2000
8	48	0.055694	0.055494	0.361	0.074678	25.421	0.058410	4.650
7	42	0.046195	0.045966	0.499	0.059742	22.676	0.048923	5.576
6	36	0.036914	0.036180	2.028	0.047639	22.514	0.039268	5.995
5	30	0.028068	0.026910	4.304	–	–	0.029951	6.287
4	24	0.019883	0.019056	4.341	0.024206	17.859	0.021282	6.574
3	18	0.012594	0.012103	4.057	–	–	0.013527	6.897
2	12	0.006480	0.006338	2.244	0.007983	18.826	0.006989	7.283
1	6	0.001960	0.001959	0.059	–	–	0.002132	8.068
0	0	0.000000	0.000000	0.000	0.000000	0.000	0.000000	0.000

Table 6.2. Comparison of the rotations about the Z direction obtained from the present program and SAP2000 in Example 1

Rotations about Z direction (rad)								
Storey number	Storey height (inch)	Present study (CCM)	Tso & Biswas (CCM)		Experimental study (Tso&Biswas)		SAP2000 (Frame method)	
		Rotation (radian)	Rotation (rad)	% difference of present study compared to Tso & Biswas	Rotation (rad)	% difference of present study compared to Exp. study	Rotation (rad)	% difference of present study compared to SAP2000
8	48	-0.010507	-0.010650	1.340	-0.011083	5.195	-0.010912	3.712
7	42	-0.008607	-0.008790	2.080	-0.008994	4.299	-0.008956	3.897
6	36	-0.006759	-0.006930	2.467	-0.007567	10.677	-0.007039	3.978
5	30	-0.005018	-0.005172	2.977	–	–	-0.005229	4.035
4	24	-0.003439	-0.003567	3.585	-0.005019	31.482	-0.003586	4.099
3	18	-0.002079	-0.002191	5.115	–	–	-0.002170	4.194
2	12	-0.001001	-0.001045	4.173	-0.001299	22.962	-0.001046	4.302
1	6	-0.000275	-0.000255	7.937	–	–	-0.000288	4.514
0	0	0.000000	0.000000	0.000	0.000000	0.000	0.000000	0.000

Table 6.3. Comparison of the axial forces at the bottom obtained from the present program and SAP2000 in Example 1

Axial forces at the bottom (lb)		
SAP2000 (frame method)	Present study (CCM)	% difference of present study compared to SAP2000
128.209	131.539	2.597

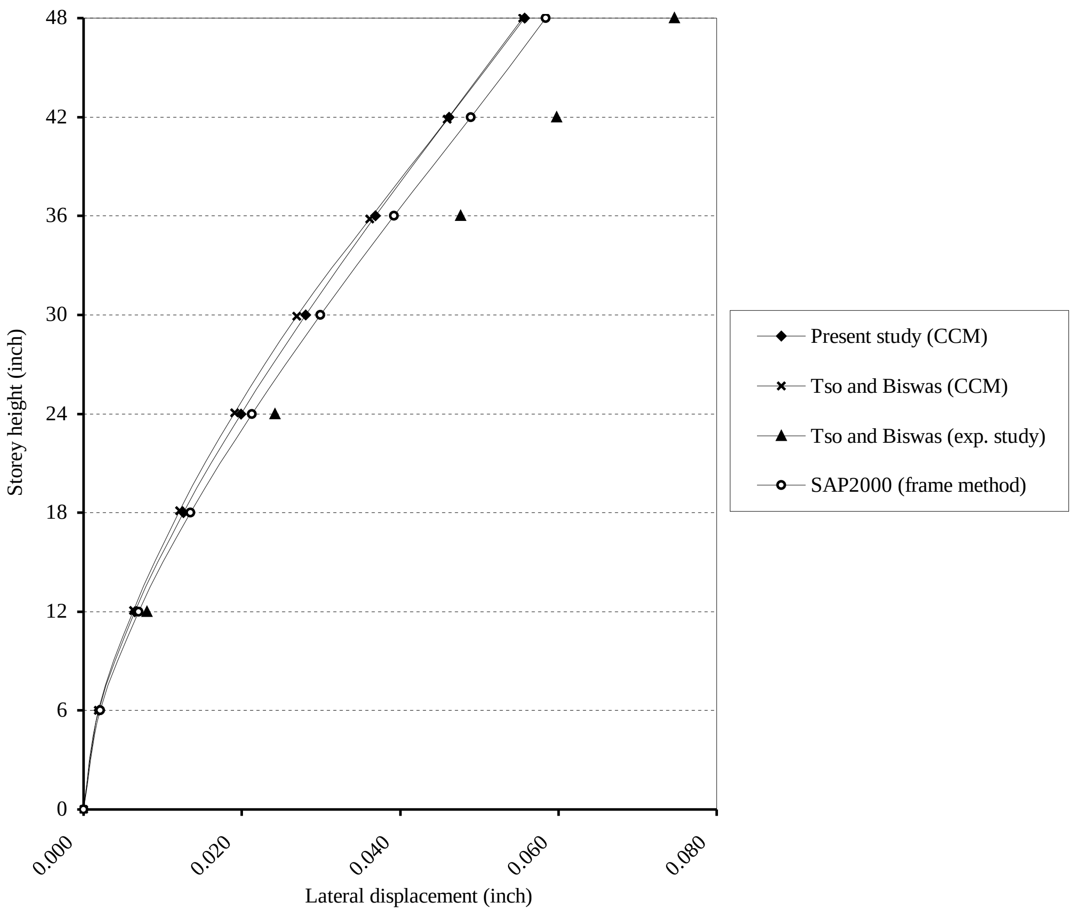

Figure 6.2. The lateral displacements in the X direction in Example 1

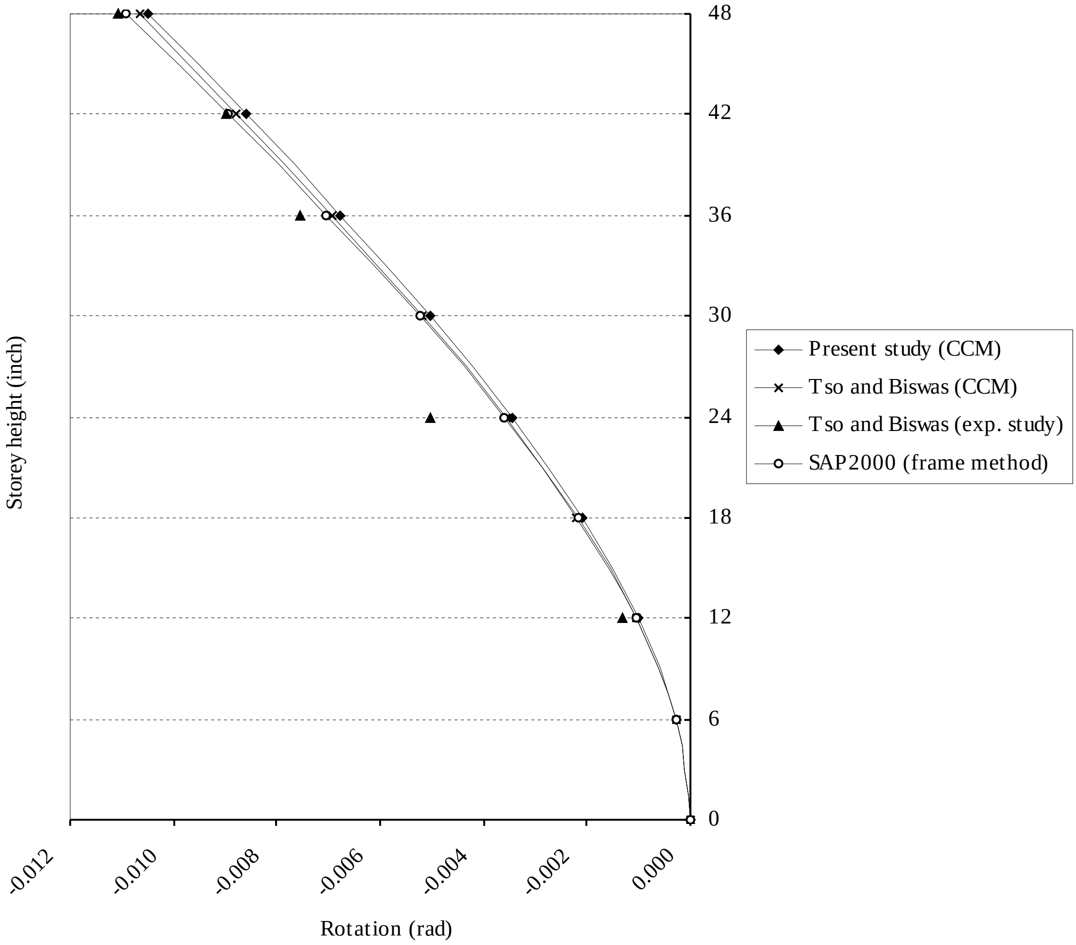

Figure 6.3. The rotations about the Z direction in Example 1

Example 2:

In this example, a non-planar coupled shear wall system has been solved to show the agreement in the results where the system rests on a rigid foundation. The total height of the shear wall is 24 m, the storey height is 3 m, the thickness of the wall is 0.3 m, the height of the connecting beams is 0.5 m and the elasticity and shear moduli of the structure are $E = 2.85\times10^6$ kN/m^2 and $G = 1055556$ kN/m^2, respectively. The concentrated horizontal force 100 kN is applied at the top of the shear wall as seen in Fig. 6.4. Both T-section piers in this system, have their shear centers at the intersection of their branches. Therefore, the sectorial areas are equal to zero at all points of the cross-section. The warping moments of inertia are all equal to zero, also.

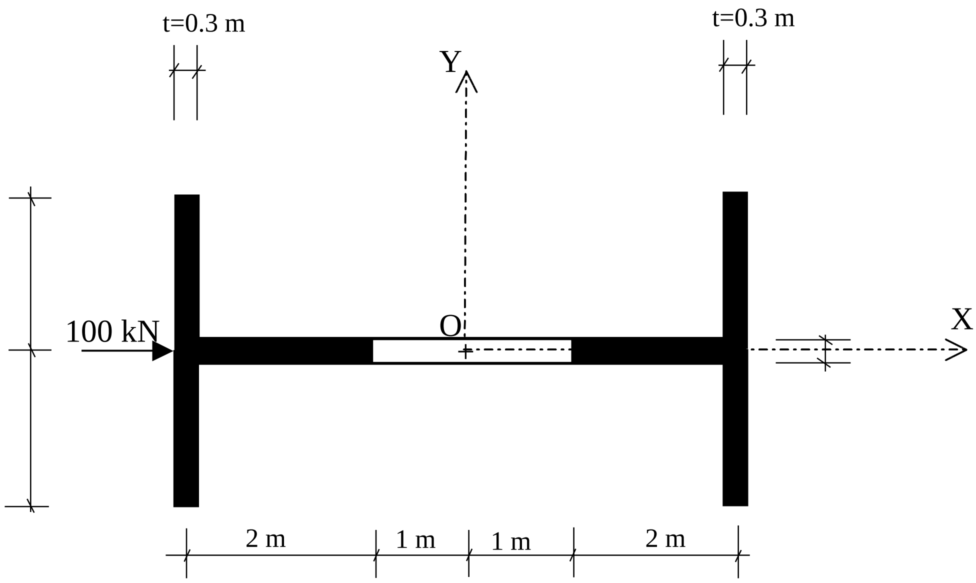

Figure 6.4. Cross-sectional view of the structure in Example 2

The comparison of the axial forces at the base and the lateral displacements in the X direction for the structure found by the program prepared in the present work and the SAP2000 structural analysis program are presented in Tables 6.4-5, expressing the percentage differences. The results are shown in Fig. 6.5, also. Obviously, the other displacements are identically zero due to the symmetry in the structure and the loading.

Table 6.4. Comparison of the axial forces at the bottom obtained from the present program and SAP2000 in Example 2

Axial forces at the bottom (kN)		
SAP2000 (frame method)	Present study (CCM)	% difference of present study compared to SAP2000
329.723	326.287	1.042

Table 6.5. Comparison of the lateral displacements in the X direction obtained from the present program and SAP2000 in Example 2

Storey number	Storey height (m)	SAP2000 (frame method)	Present study (CCM)	
		Lateral displacement (m)	Lateral displacement (m)	% difference of present study compared to SAP2000
8	24.0	0.021324	0.022165	3.943
7	21.0	0.018030	0.018480	2.497
6	18.0	0.014626	0.014854	1.559
5	15.0	0.011246	0.011351	0.938
4	12.0	0.008011	0.008052	0.513
3	9.0	0.005053	0.005064	0.208
2	6.0	0.002543	0.002542	0.050
1	3.0	0.000729	0.000726	0.371
0	0.0	0.000000	0.000000	0.000

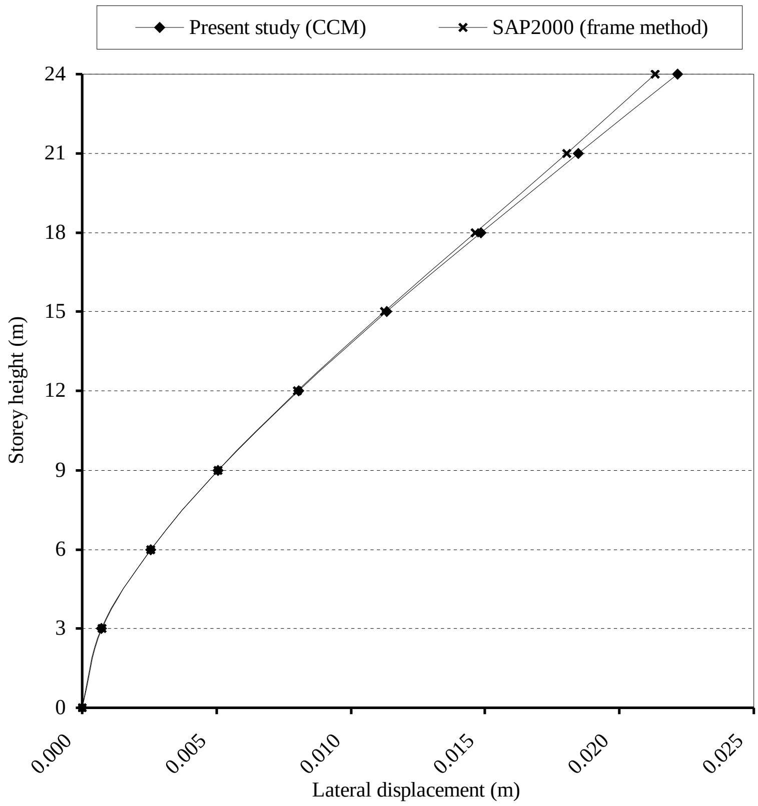

Figure 6.5. The lateral displacements in the X direction in Example 2

Example 3:

In this example, a non-planar non-symmetrical coupled shear wall with a cross-section as shown in Fig. 6.6 is considered. The total height of the shear wall is 40 m, the storey height is 4 m and the height of the connecting beams is 0.7 m. The elasticity and shear moduli are $E=2.85x10^6$ kN/m^2 and $G=1055556$ kN/m^2, respectively. The loading comprises a 50 kN and a 30 kN concentrated horizontal forces as shown in the figure. Under this loading, the model structure is subjected to a twisting moment at the top.

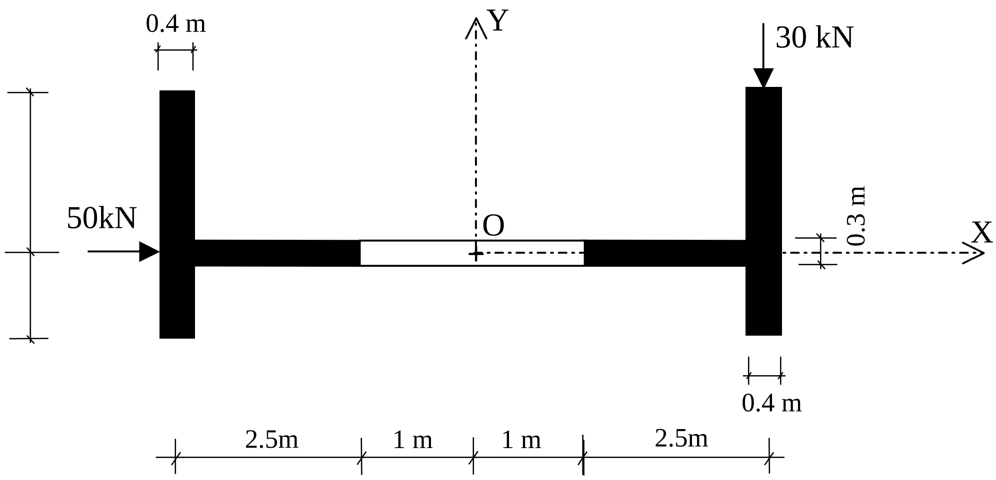

Figure 6.6. Cross-sectional view of the structure in Example 3

The comparison of the lateral displacements and rotations along the height and the axial forces at the bottom, found by the present program and the SAP2000, structural analysis program are presented in Tables 6.6-9, expressing the percentage differences. The results found are shown in Figs. 6.7-9, also.

Table 6.6. Comparison of the lateral displacements in the X direction obtained from the present program and SAP2000 in Example 3

Storey number	Storey height (m)	SAP2000 (frame method)	Present study (CCM)	
		Lateral displacement (m)	Lateral displacement (m)	% difference of present study compared to SAP2000
10	40.0	0.023436	0.023513	0.330
9	36.0	0.020348	0.020298	0.245
8	32.0	0.017221	0.017127	0.544
7	28.0	0.014146	0.014046	0.708
6	24.0	0.011190	0.011100	0.802
5	20.0	0.008412	0.008340	0.850
4	16.0	0.005873	0.005822	0.875
3	12.0	0.003642	0.003610	0.876
2	8.0	0.001811	0.001795	0.900
1	4.0	0.000517	0.000512	1.023
0	0.0	0.000000	0.000000	0.000

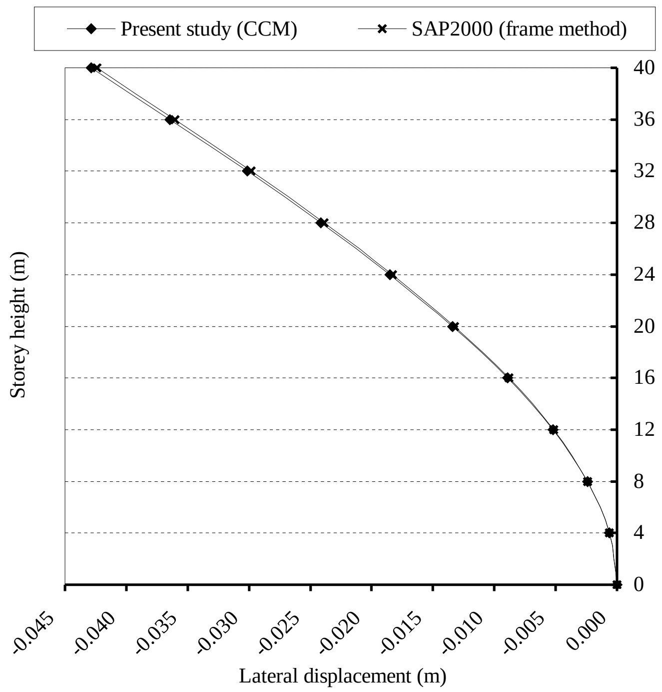

Figure 6.7. The lateral displacements in the X direction in Example 3

Table 6.7. Comparison of the lateral displacements in the Y direction obtained from the present program and SAP2000 in Example 3

Storey number	Storey height (m)	SAP2000 (frame method)	Present study (CCM)	
		Lateral displacement (m)	Lateral displacement (m)	% difference of present study compared to SAP2000
10	40.0	-0.042379	-0.042845	1.101
9	36.0	-0.036044	-0.036440	1.099
8	32.0	-0.029835	-0.030163	1.100
7	28.0	-0.023881	-0.024143	1.099
6	24.0	-0.018309	-0.018509	1.094
5	20.0	-0.013244	-0.013389	1.096
4	16.0	-0.008816	-0.008912	1.087
3	12.0	-0.005150	-0.005206	1.082
2	8.0	-0.002374	-0.002399	1.068
1	4.0	-0.000615	-0.000621	1.018
0	0.0	0.000000	0.000000	0.000

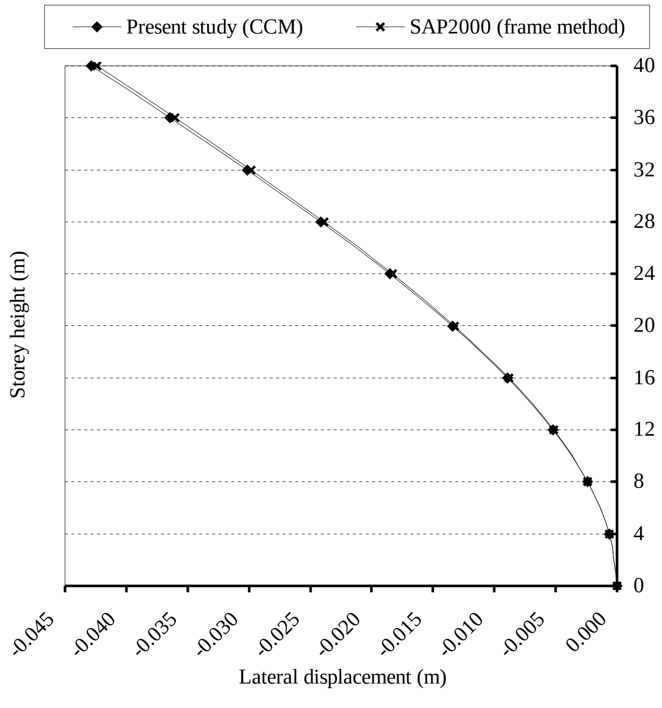

Figure 6.8. The lateral displacements in the Y direction in Example 3

Table 6.8. Comparison of the rotations about the Z direction obtained from the present program and SAP2000 in Example 3

Storey number	Storey height (m)	SAP2000 (frame method)	Present study (CCM)	
		Lateral displacement (m)	Lateral displacement (m)	% difference of present study compared to SAP2000
10	40.0	-0.042379	-0.042845	1.101
9	36.0	-0.036044	-0.036440	1.099
8	32.0	-0.029835	-0.030163	1.100
7	28.0	-0.023881	-0.024143	1.099
6	24.0	-0.018309	-0.018509	1.094
5	20.0	-0.013244	-0.013389	1.096
4	16.0	-0.008816	-0.008912	1.087
3	12.0	-0.005150	-0.005206	1.082
2	8.0	-0.002374	-0.002399	1.068
1	4.0	-0.000615	-0.000621	1.018
0	0.0	0.000000	0.000000	0.000

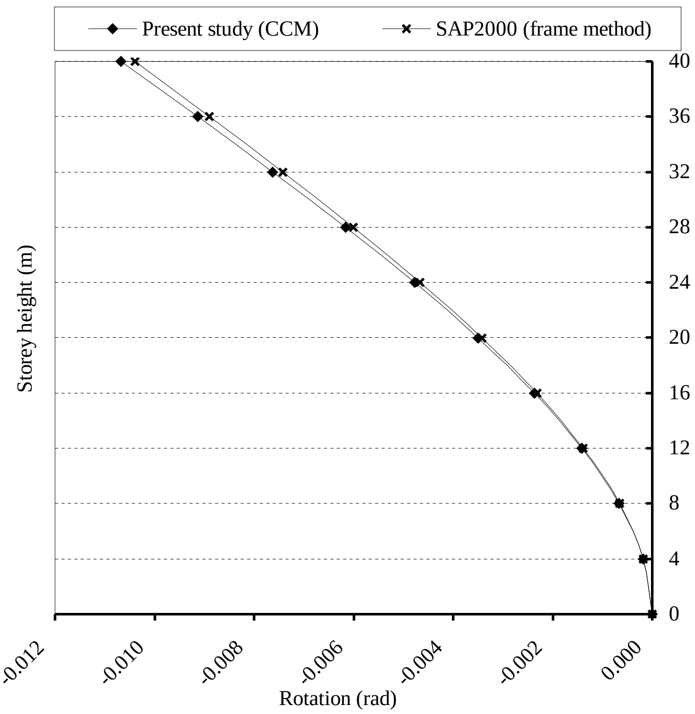

Figure 6.9. The rotations about the Z direction in Example 3

Table 6.9. Comparison of the axial forces at the bottom obtained from the present program and SAP2000 in Example 3

Axial forces at the bottom (kN)		
SAP2000 (frame method)	Present study (CCM)	% difference of present study compared to SAP2000
284.932	289.177	1.468

Example 4:

In this example, the Tso & Biswas model (1973) has been solved for a different loading condition both by the present method and the SAP2000 structural analysis program for comparison. The total height of the shear wall is 48 in, the storey height is 6 in, the thickness of the wall is 0.39 in, the height of the connecting beams is 1.5 in and the elasticity and the shear moduli of the structure are $E = 0.40x10^6$ psi and $G = 0.148x10^6$ psi, respectively. The concentrated horizontal force 25 lb is applied at the top of the structure as shown Fig. 6.10.

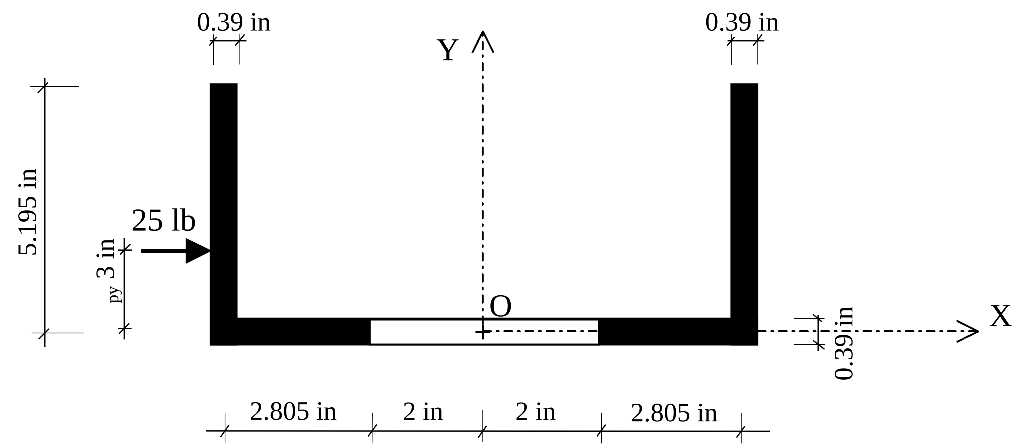

Figure 6.10. Cross-sectional view of the structure in Example 4

The comparison of the axial forces at the base, the lateral displacements in the X direction and the rotations for the shear wall in this model found by the present program and the SAP2000 structural analysis program are presented in Tables 6.10-12, expressing the percentage differences. The results found are shown in Figs. 6.11-12, also.

Table 6.10. Comparison of the displacements in the X direction obtained from the present program and SAP2000 in Example 4

Storey number	Storey height (inch)	SAP2000 (frame method)	Present study (CCM)	
		Lateral displacement (inch)	Lateral displacement (inch)	% difference of present study compared to SAP2000
8	48.0	0.091150	0.087217	4.315
7	42.0	0.075780	0.072017	4.966
6	36.0	0.060374	0.057193	5.270
5	30.0	0.045629	0.043125	5.489
4	24.0	0.032032	0.030202	5.713
3	18.0	0.020033	0.018834	5.985
2	12.0	0.010125	0.009484	6.333
1	6.0	0.002996	0.002786	7.018
0	0.0	0.000000	0.000000	0.000

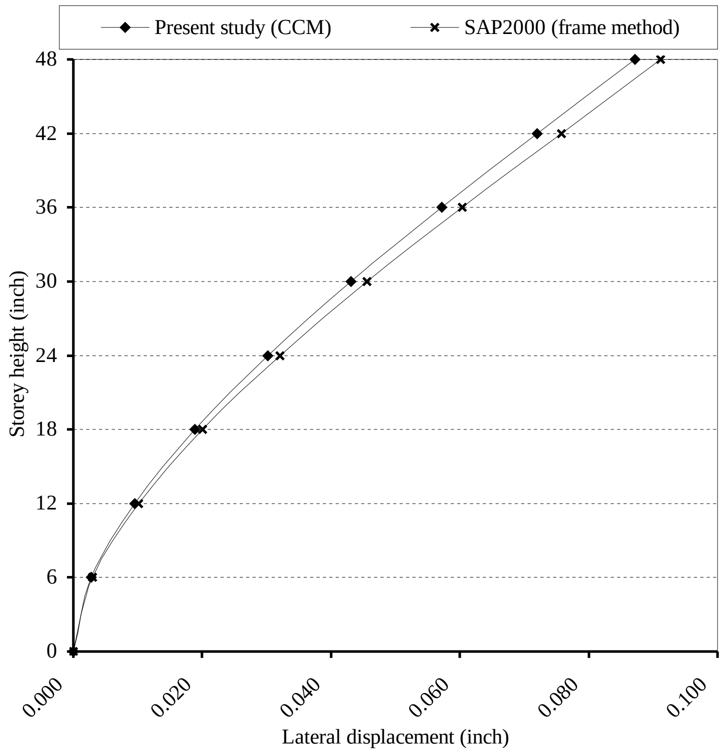

Figure 6.11. The lateral displacements in the X direction in Example 4

Table 6.11. Comparison of the rotations about the Z direction obtained from the present program and SAP2000 in Example 4

Storey no	Storey height (m)	Present study (CCM)	SAP2000 (Frame method)	
		Rotation (radian)	Rotation (radian)	% difference with present study
8	48.0	-0.025382	-0.026233	3.352
7	42.0	-0.020746	-0.021459	3.436
6	36.0	-0.016243	-0.016805	3.457
5	30.0	-0.012009	-0.012424	3.456
4	24.0	-0.008181	-0.008464	3.457
3	18.0	-0.004904	-0.005074	3.467
2	12.0	-0.002330	-0.002411	3.482
1	6.0	-0.000627	-0.000650	3.684
0	0.0	0.000000	0.000000	0.000

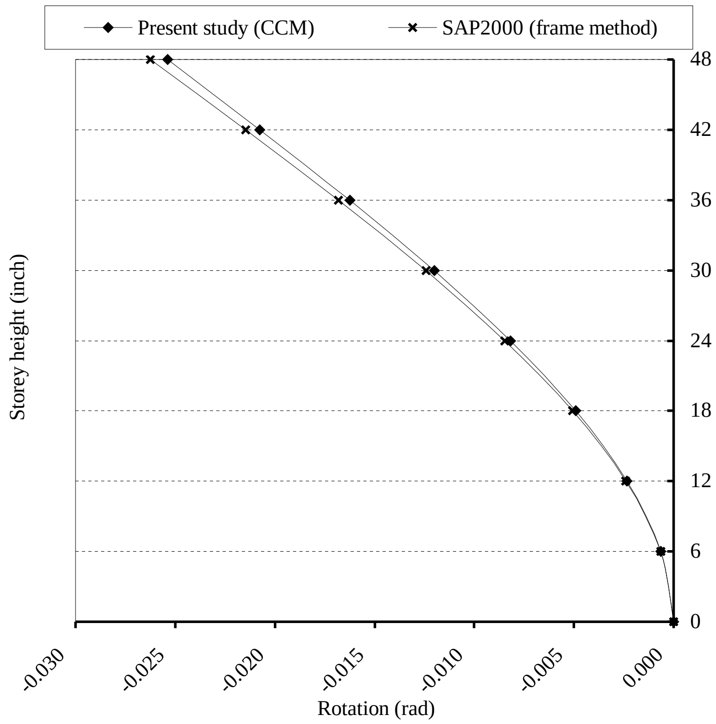

Figure 6.12. The rotations about the Z direction in Example 4

Table 6.12. Comparison of the axial forces at the bottom obtained from the present program and SAP2000 in Example 4

Axial forces at the bottom (lb)		
SAP2000 (frame method)	Present study (CCM)	% difference of present study compared to SAP2000
141.707	143.981	1.604

Example 5:

In this example, a non-planar non-symmetrical coupled shear wall with a cross-section as shown in Fig. 6.13 is considered. The total height of the shear wall is 24 m, the storey height is 3 m, the thickness of the wall is 0.3 m, the height of the connecting beams is 0.5 m and the elasticity and shear moduli are E=2.85x10^6 kN/m^2 and G=1055556 kN/m^2, respectively. The concentrated horizontal force 300 kN is applied at the top of the shear wall as shown in the figure.

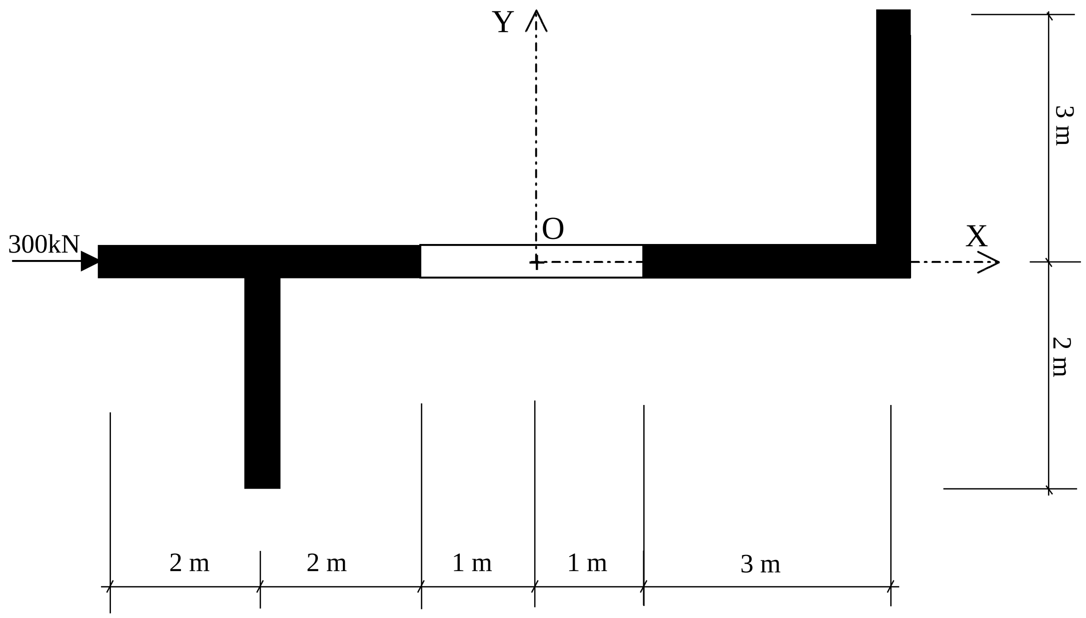

Figure 6.13. Cross-sectional view of the structure in Example 5

The comparison of the lateral displacements and rotations along the height and the axial forces at the bottom, found by the present program and the SAP2000, structural analysis program are presented in Tables 6.13-16, expressing the percentage differences. The results found are given in Figs. 6.14-16, also.

Table 6.13. Comparison of the lateral displacements in the X direction obtained from the present program and SAP2000 in Example 5

Storey number	Storey height (m)	SAP2000 (frame method)	Present study (CCM)	
		Lateral displacement (m)	Lateral displacement (m)	% difference of present study compared to SAP2000
8	24.0	0.050336	0.051931	3.168
7	21.0	0.041939	0.042884	2.254
6	18.0	0.033501	0.034035	1.594
5	15.0	0.025311	0.025591	1.108
4	12.0	0.017658	0.017790	0.746
3	9.0	0.010863	0.010912	0.453
2	6.0	0.005303	0.005315	0.217
1	3.0	0.001466	0.001464	0.111
0	0.0	0.000000	0.000000	0.000

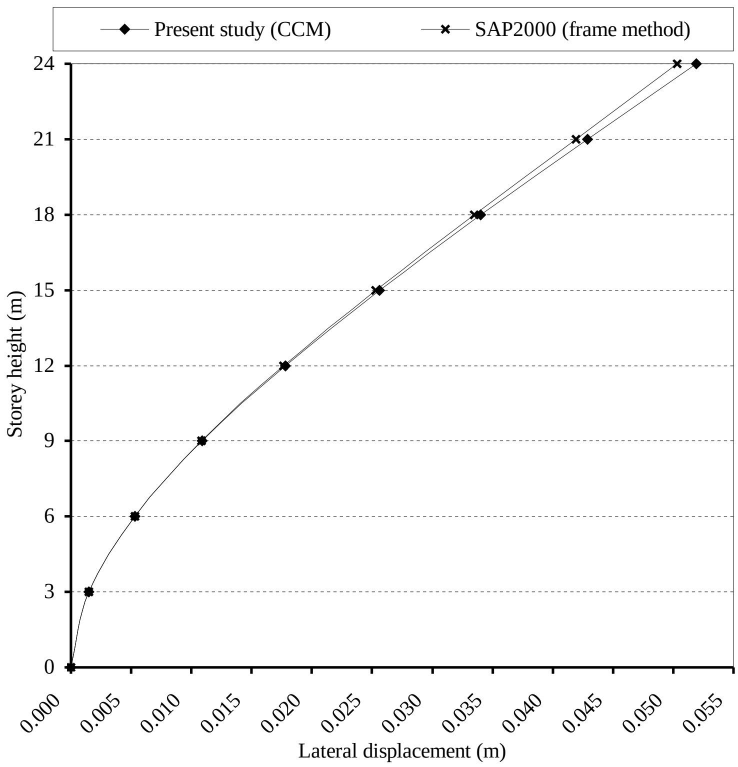

Figure 6.14. The lateral displacements in the X direction in Example 5

Table 6.14. Comparison of the displacements in the Y direction obtained from the present program and SAP2000 in Example 5

Storey number	Storey height (m)	SAP2000 (frame method)	Present study (CCM)	
		Lateral displacement (m)	Lateral displacement (m)	% difference of present study compared to SAP2000
8	24.0	-0.044967	-0.045340	0.829
7	21.0	-0.036597	-0.036885	0.788
6	18.0	-0.028483	-0.028696	0.748
5	15.0	-0.020890	-0.021037	0.704
4	12.0	-0.014081	-0.014174	0.661
3	9.0	-0.008322	-0.008373	0.610
2	6.0	-0.003878	-0.003899	0.542
1	3.0	-0.001014	-0.001019	0.514
0	0.0	0.000000	0.000000	0.000

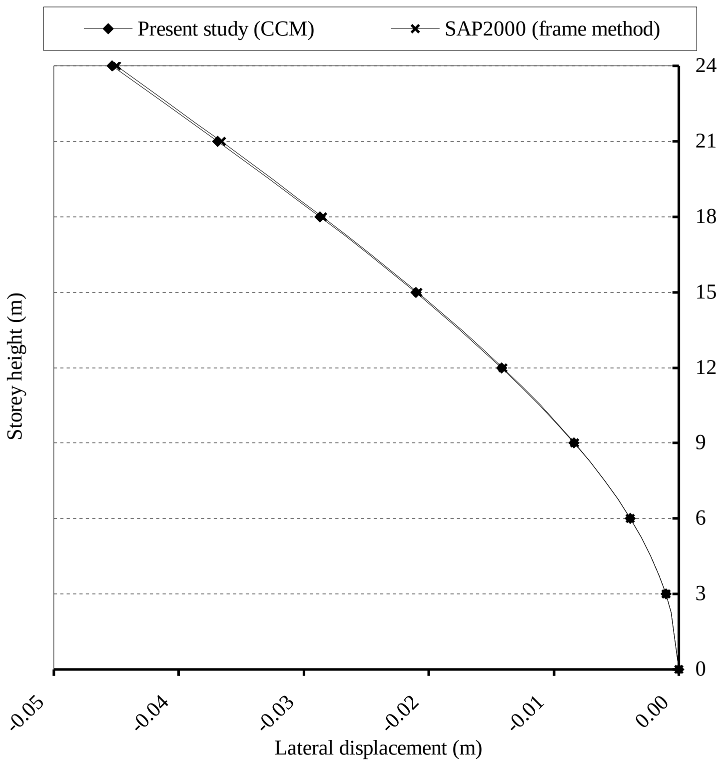

Figure 6.15. The lateral displacements in the Y direction in Example 5

Table 6.15. Comparison of the rotations about the Z direction obtained from the present program and SAP2000

Storey no	Storey height (m)	Present study (CCM)	SAP2000 (Frame method)	
		Rotation (radian)	Rotation (radian)	% Difference with present study
8	24.0	-0.002411	-0.002493	3.417
7	21.0	-0.002025	-0.002122	4.816
6	18.0	-0.001642	-0.001735	5.673
5	15.0	-0.001267	-0.001344	6.045
4	12.0	-0.000908	-0.000964	6.115
3	9.0	-0.000577	-0.000612	6.078
2	6.0	-0.000292	-0.000309	5.837
1	3.0	-0.000084	-0.000088	5.432
0	0.0	0.000000	0.000000	0.000

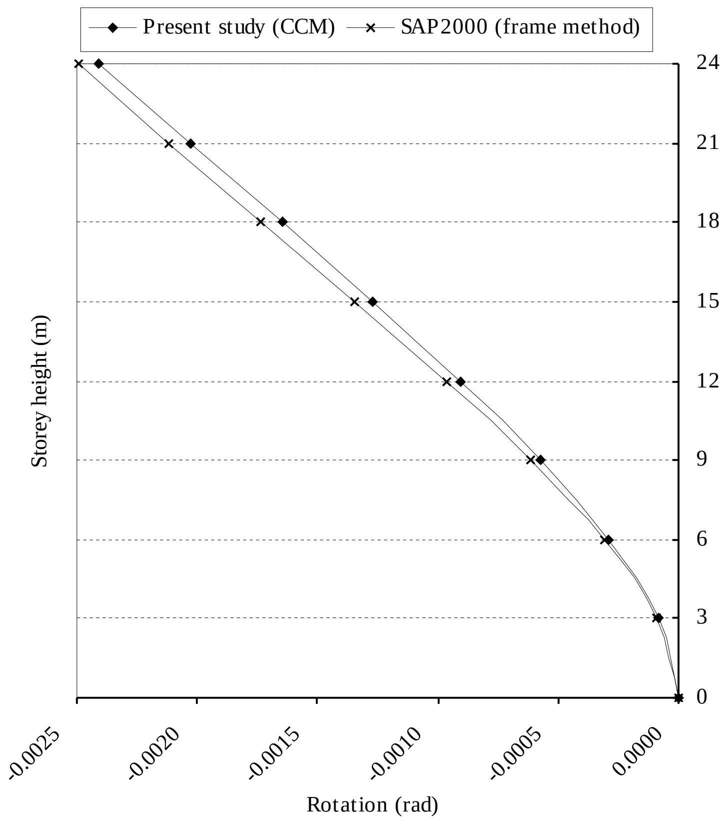

Figure 6.16. The rotations about the Z direction in Example 5

Table 6.16. Comparison of the axial forces at the bottom obtained from the present program and SAP2000 in Example 5

Axial forces at the bottom (kN)		
SAP2000 (frame method)	Present study (CCM)	% difference of present study compared to SAP2000
755.830	756.104	0.036

Example 6:

In this example, a non-planar non-symmetrical coupled shear wall with a cross-section as shown in Fig. 6.17 is considered. The total height of the shear wall is 24 m, the storey height is 3 m, the thickness of the wall is 0.4 m, the height of the connecting beams is 0.7 m and the elasticity and shear moduli are E = 2.85×10^6 kN/m^2 and G = 1055556 kN/m^2, respectively. The loading comprises a 250 kN and a 100 kN concentrated horizontal forces as shown in the figure. Since there are non zero sectorial area values in the left pier, as shown in Fig. 6.18, there is warping in this example, whereas, there was no warping in the previous examples and the open section shear walls in the literature.

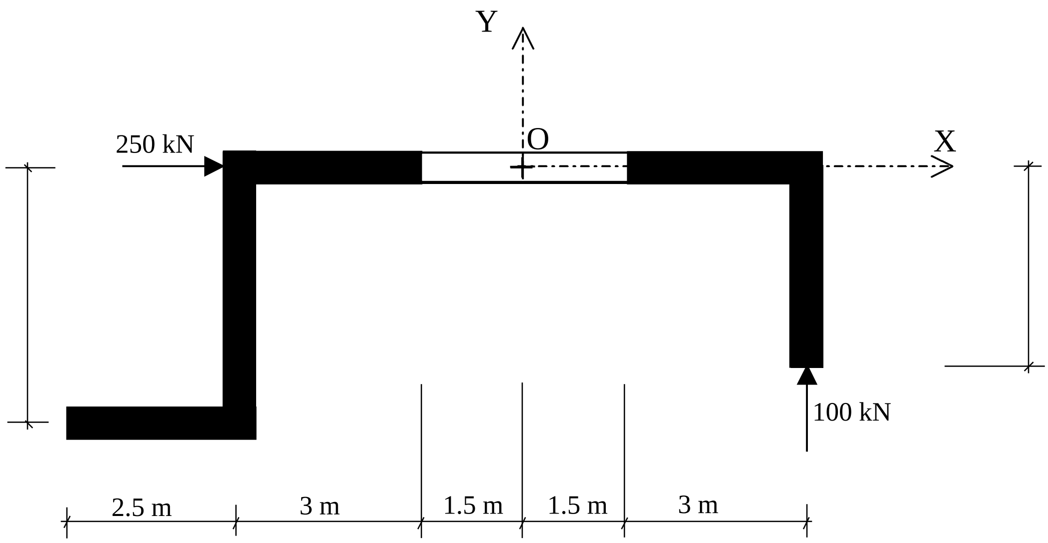

Figure 6.17. Cross-sectional view of the structure in Example 6

The comparison of the axial forces found by the present program together with SAP2000 are presented in Table 6.17. The comparison of the lateral displacements and rotations, found by the present program and the SAP2000, structural analysis program are presented in Tables 6.18-20, expressing the percentage differences. The results found are given in Figs. 6.19-21, also.

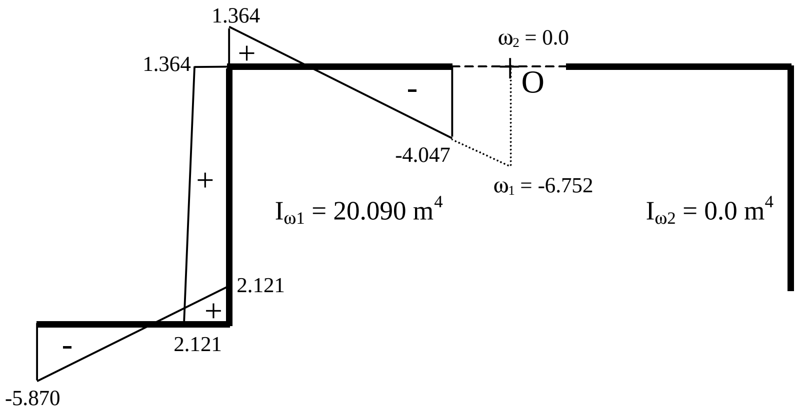

Figure 6.18. The principal sectorial area diagram of the structure in Example 6

Table 6.17. Comparison of the axial forces at the bottom obtained from the present program and SAP2000 in Example 6

Axial forces at the bottom (kN)		
SAP2000 (frame method)	Present study (CCM)	% difference of present study compared to SAP2000
606.157	609.201	0.502

Table 6.18. Comparison of the lateral displacements in the X direction obtained from the present program and SAP2000 in Example 6

Storey number	Storey height (m)	SAP2000 (frame method)	Present study (CCM)	
		Lateral displacement (m)	Lateral displacement (m)	% difference of present study compared to SAP2000
8	24.0	0.020180	0.020010	0.840
7	21.0	0.016787	0.016526	1.556
6	18.0	0.013388	0.013120	2.004
5	15.0	0.010106	0.009874	2.293
4	12.0	0.007053	0.006879	2.473
3	9.0	0.004349	0.004237	2.584
2	6.0	0.002135	0.002078	2.669
1	3.0	0.000596	0.000579	2.824
0	0.0	0.000000	0.000000	0.000

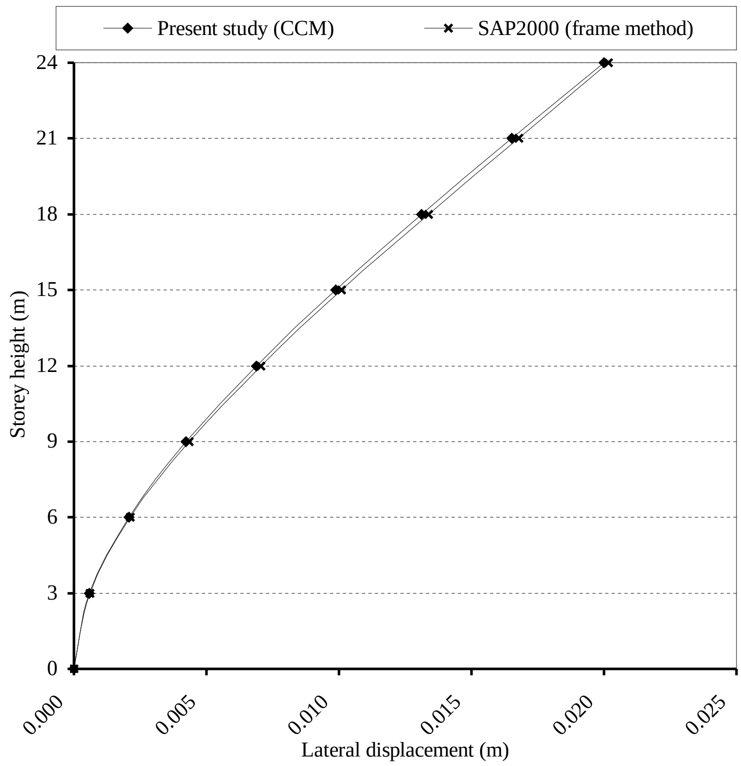

Figure 6.19. The lateral displacements in the X direction in Example 6

Table 6.19. Comparison of the lateral displacements in the Y direction obtained from the present program and SAP2000 in Example 6

Storey number	Storey height (m)	SAP2000 (frame method) Lateral displacement (m)	Present study (CCM) Lateral displacement (m)	Present study (CCM) % difference of present study compared to SAP2000
8	24.0	0.011867	0.011745	1.030
7	21.0	0.009620	0.009536	0.876
6	18.0	0.007456	0.007398	0.777
5	15.0	0.005441	0.005403	0.696
4	12.0	0.003645	0.003622	0.633
3	9.0	0.002138	0.002125	0.619
2	6.0	0.000986	0.000980	0.588
1	3.0	0.000254	0.000253	0.415
0	0.0	0.000000	0.000000	0.000

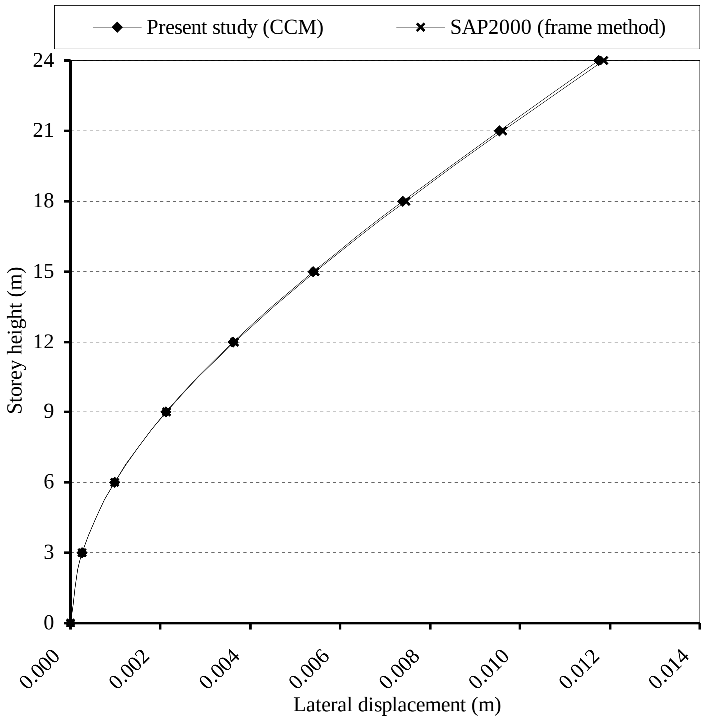

Figure 6.20. The lateral displacements in the Y direction in Example 6

Table 6.20. Comparison of the rotations about the Z direction obtained from the present program and SAP2000 in Example 6

Storey number	Storey height (m)	SAP2000 (frame method) Rotation (rad)	Present study (CCM) Rotation (rad)	Present study (CCM) % difference of present study compared to SAP2000
8	24.0	0.006591	0.006458	2.022
7	21.0	0.005384	0.005270	2.109
6	18.0	0.004210	0.004118	2.182
5	15.0	0.003105	0.003036	2.219
4	12.0	0.002107	0.002060	2.214
3	9.0	0.001256	0.001228	2.222
2	6.0	0.000592	0.000578	2.301
1	3.0	0.000157	0.000153	2.333
0	0.0	0.000000	0.000000	0.000

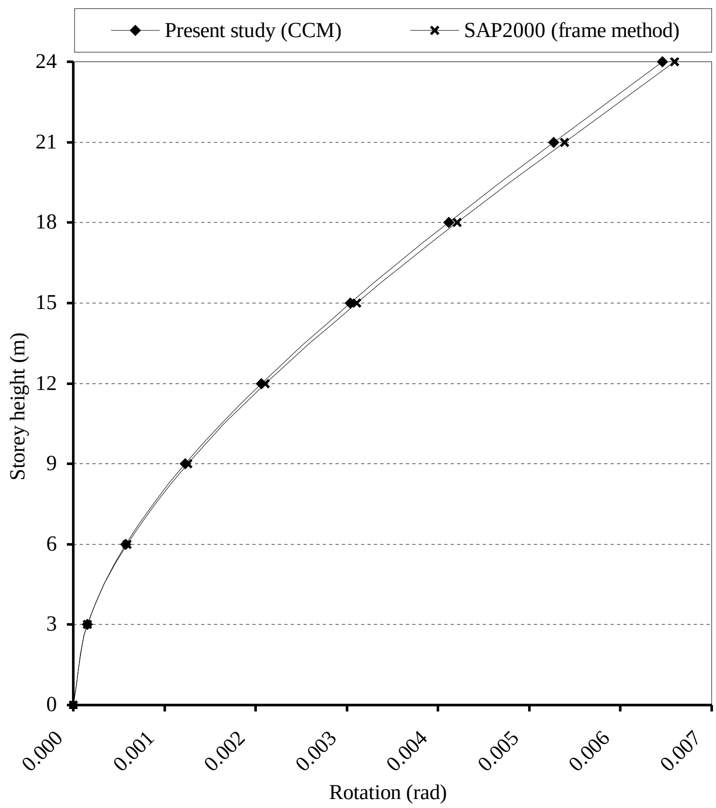

Figure 6.21. The rotations about the Z direction in Example 6

Example 7:

In this example, a non-planar non-symmetrical coupled shear wall with a cross-section as in Fig. 6.22 is considered. The total height of the shear wall is 48 m, the storey height is 3 m, the thickness of the wall is 0.4 m, the height of the connecting beams is 0.5 m and the elasticity and shear moduli are $E = 2.85\text{x}10^6$ kN/m^2 and $G = 1055556$ kN/m^2, respectively. The concentrated horizontal force 250 kN acts at the top. The sectorial area diagram for this system is given in Fig. 6.23.

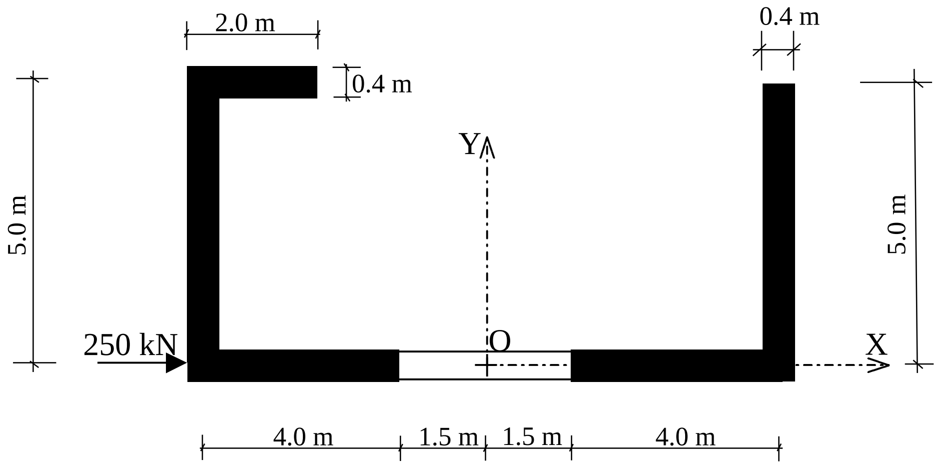

Figure 6.22. Cross-sectional view of the structure in Example 7

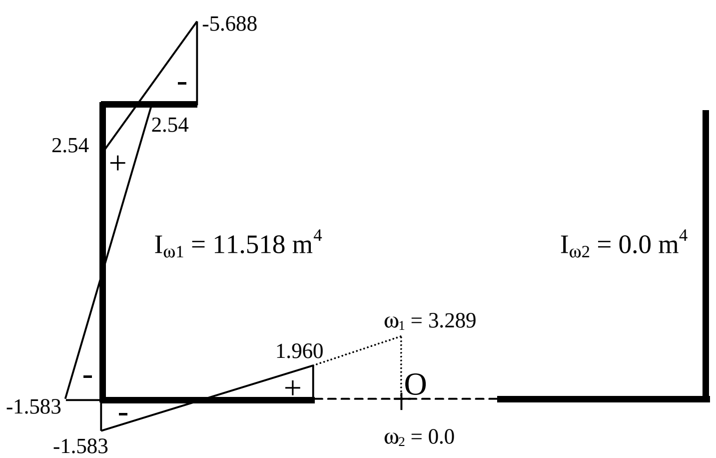

Figure 6.23. The principal sectorial area diagram of the structure in Example 7

The comparison of the lateral displacements and rotations along the height and the axial forces at the bottom, found by the present program and the SAP2000, structural analysis program are presented in Tables 6.21-24, expressing the percentage differences. The results found are given in Fig. 6.24, also.

Table 6.21. Comparison of the lateral displacements in the X direction obtained from the present program and SAP2000 in Example 7

Storey number	Storey height (m)	SAP2000 (frame method)	Present study (CCM)	
		Lateral displacement (m)	Lateral displacement (m)	% difference of present study compared to SAP2000
16	48.0	0.092629	0.093988	1.467
15	45.0	0.084831	0.085838	1.188
14	42.0	0.076998	0.077731	0.952
13	39.0	0.069186	0.069707	0.752
12	36.0	0.061452	0.061810	0.582
11	33.0	0.053852	0.054087	0.436
10	30.0	0.046442	0.046587	0.312
9	27.0	0.039283	0.039363	0.205
8	24.0	0.032441	0.032477	0.109
7	21.0	0.025985	0.025992	0.028
6	18.0	0.019996	0.019987	0.047
5	15.0	0.014562	0.014546	0.111
4	12.0	0.009788	0.009770	0.183
3	9.0	0.005791	0.005777	0.248
2	6.0	0.002712	0.002703	0.328
1	3.0	0.000717	0.000713	0.591
0	0.0	0.000000	0.000000	0.000

Table 6.22. Comparison of the lateral displacements in the Y direction obtained from the present program and SAP2000 in Example 7

Storey number	Storey height (m)	SAP2000 (frame method)	Present study (CCM)	
		Lateral displacement (m)	Lateral displacement (m	% difference of present study compared to SAP2000
16	48.0	-0.013858	-0.013630	1.648
15	45.0	-0.012656	-0.012427	1.808
14	42.0	-0.011454	-0.011231	1.943
13	39.0	-0.010260	-0.010050	2.051
12	36.0	-0.009082	-0.008889	2.130
11	33.0	-0.007930	-0.007756	2.196
10	30.0	-0.006813	-0.006659	2.256
9	27.0	-0.005739	-0.005607	2.299
8	24.0	-0.004718	-0.004608	2.325
7	21.0	-0.003761	-0.003673	2.347
6	18.0	-0.002879	-0.002811	2.355
5	15.0	-0.002085	-0.002036	2.361
4	12.0	-0.001392	-0.001360	2.295
3	9.0	-0.000818	-0.000800	2.261
2	6.0	-0.000380	-0.000372	2.156
1	3.0	-0.000099	-0.000097	2.020
0	0.0	0.000000	0.000000	0.000

Table 6.23. Comparison of the rotations about the Z direction obtained from the present program and SAP2000 in Example 7

Storey no	Storey height (m)	Present study (CCM)	SAP2000 (Frame method)	
		Rotation (radian)	Rotation (radian)	% Difference with present study
16	48.0	-0.009240	-0.009319	0.856
15	45.0	-0.008400	-0.008478	0.934
14	42.0	-0.007565	-0.007640	0.994
13	39.0	-0.006742	-0.006811	1.030
12	36.0	-0.005936	-0.005999	1.069
11	33.0	-0.005153	-0.005210	1.112
10	30.0	-0.004399	-0.004449	1.137
9	27.0	-0.003681	-0.003723	1.149
8	24.0	-0.003004	-0.003039	1.156
7	21.0	-0.002376	-0.002404	1.162
6	18.0	-0.001804	-0.001825	1.157
5	15.0	-0.001295	-0.001310	1.160
4	12.0	-0.000857	-0.000867	1.173
3	9.0	-0.000499	-0.000504	1.077
2	6.0	-0.000229	-0.000232	1.151
1	3.0	-0.000059	-0.000060	1.042
0	0.0	0.000000	0.000000	0.000

Table 6.24. Comparison of the axial forces at the bottom obtained from the present program and SAP2000 in Example 7

Axial forces at the bottom (kN)		
SAP2000 (frame method)	Present study (CCM)	% difference of present study compared to SAP2000
892.048	889.274	0.311

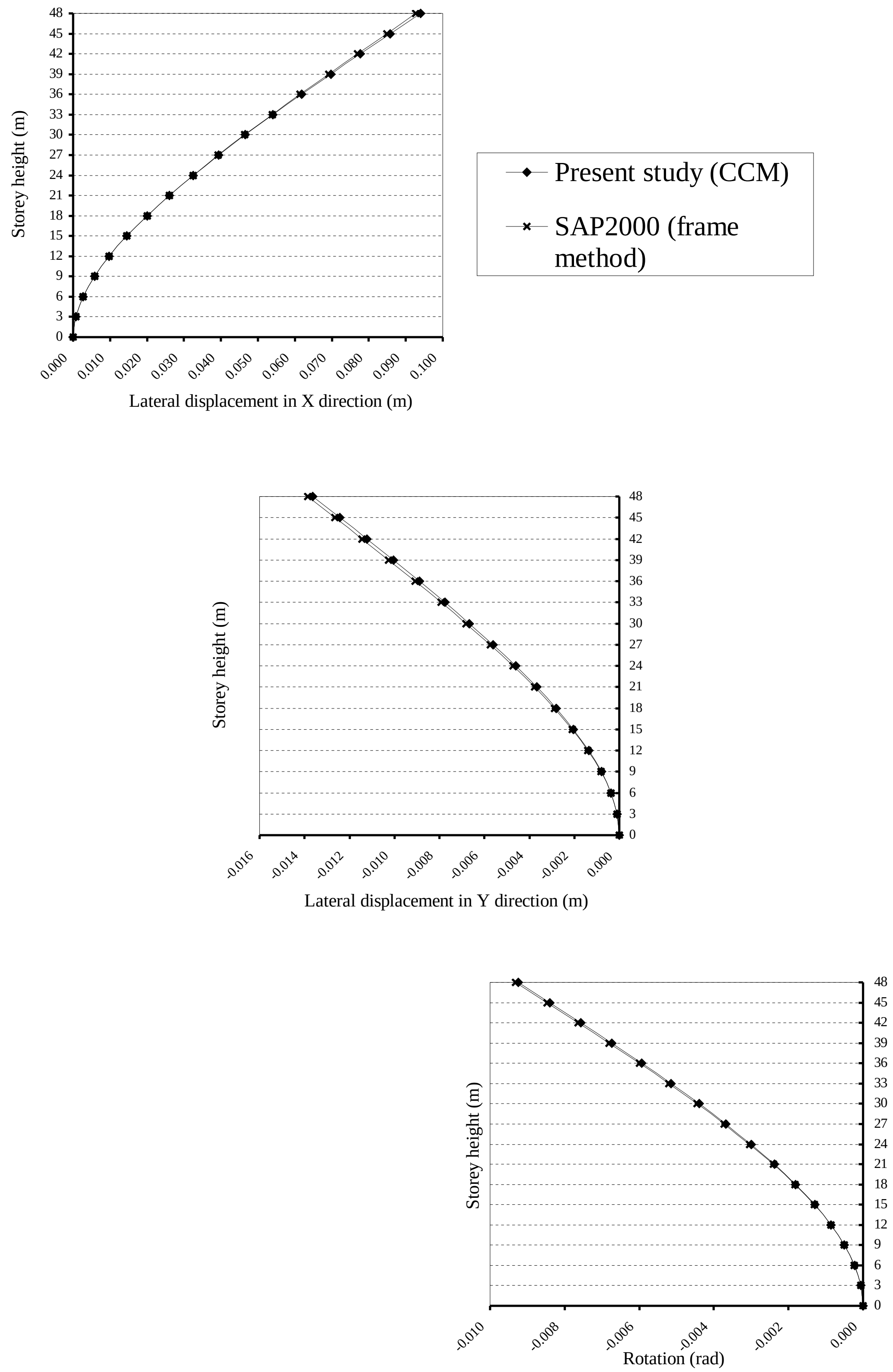

Figure 6.24. The lateral displacements and the rotations along the height in Example 7

Example 8:

In this example, a non-planar non-symmetrical coupled shear wall with a cross-section in Fig. 6.25 is considered. The total height of the shear wall is 48 m, the storey height is 3 m, the thickness of the wall is 0.4 m, the height of the connecting beams is 0.5 m and the elasticity and shear moduli are $E = 2.85x10^6$ kN/m^2 and $G = 1055556$ kN/m^2, respectively. The concentrated horizontal force 250 kN is applied at the top of the shear wall. The sectorial area diagram for this system is given in Fig. 6.26.

The comparison of the axial forces at the bottom, the lateral displacements and rotations along the height found by the present program and SAP2000 are presented in Tables 6.25-28, expressing the percentage differences. The results found are given in Fig. 6.27, also.

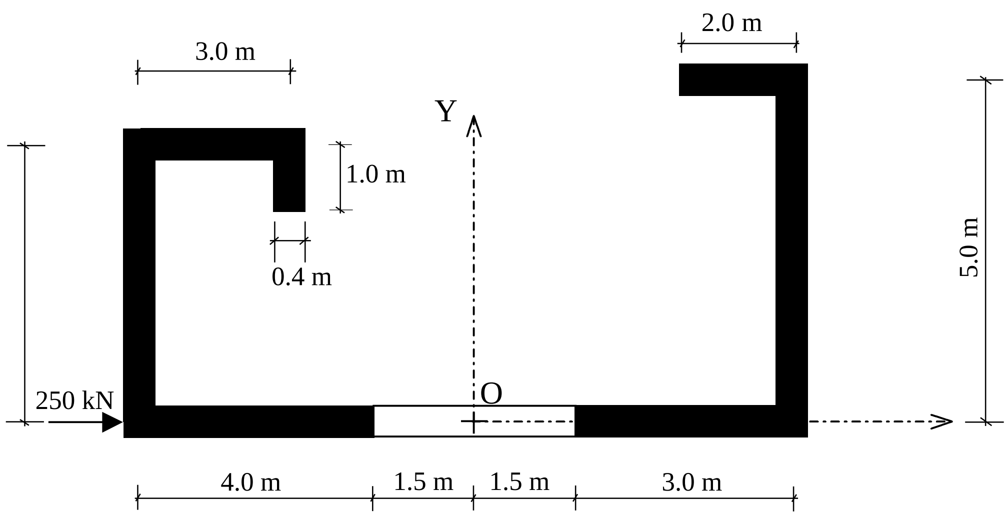

Figure 6.25. Cross-sectional view of the structure in Example 8

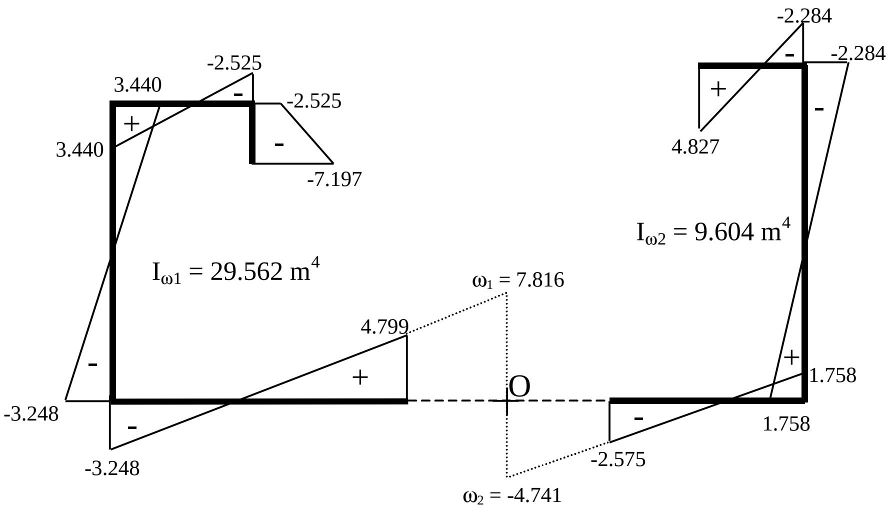

Figure 6.26. The principal sectorial area diagram of the structure in Example 8

Table 6.25. Comparison of the axial forces obtained from the present program and SAP2000 in Example 8

Axial forces at the bottom (kN)		
SAP2000 (frame method)	Present study (CCM)	% difference of present study compared to SAP2000
867.012	863.808	0.370

Table 6.26. Comparison of the lateral displacements in the X direction obtained from the present program and SAP2000 in Example 8

Storey number	Storey height (m)	SAP2000 (frame method)	Present study (CCM)	
		Lateral displacement (m)	Lateral displacement (m)	% difference of present study compared to SAP2000
16	48.0	0.094538	0.095731	1.262
15	45.0	0.086435	0.087317	1.021
14	42.0	0.078313	0.078951	0.815
13	39.0	0.070231	0.070678	0.637
12	36.0	0.062248	0.062549	0.483
11	33.0	0.054423	0.054613	0.349
10	30.0	0.046816	0.046924	0.232
9	27.0	0.039490	0.039541	0.129
8	24.0	0.032513	0.032525	0.038
7	21.0	0.025958	0.025946	0.045
6	18.0	0.019904	0.019880	0.122
5	15.0	0.014440	0.014412	0.196
4	12.0	0.009666	0.009639	0.277
3	9.0	0.005694	0.005673	0.365
2	6.0	0.002655	0.002642	0.503
1	3.0	0.000698	0.000693	0.734
0	0.0	0.000000	0.000000	0.000

Table 6.27. Comparison of the lateral displacements in the Y direction obtained from the present program and SAP2000 in Example 8

Storey number	Storey height (m)	SAP2000 (frame method)	Present study (CCM)	
		Lateral displacement (m)	Lateral displacement (m)	% difference of present study compared to SAP2000
16	48.0	-0.008478	-0.008511	0.386
15	45.0	-0.007691	-0.007720	0.373
14	42.0	-0.006909	-0.006935	0.370
13	39.0	-0.006139	-0.006161	0.366
12	36.0	-0.005386	-0.005406	0.377
11	33.0	-0.004658	-0.004675	0.369
10	30.0	-0.003959	-0.003974	0.382
9	27.0	-0.003296	-0.003309	0.402
8	24.0	-0.002676	-0.002687	0.399
7	21.0	-0.002104	-0.002113	0.414
6	18.0	-0.001586	-0.001594	0.480
5	15.0	-0.001130	-0.001136	0.514
4	12.0	-0.000742	-0.000746	0.515
3	9.0	-0.000427	-0.000430	0.778
2	6.0	-0.000194	-0.000196	1.099
1	3.0	-0.000049	-0.000050	1.215
0	0.0	0.000000	0.000000	0.000

Table 6.28. Comparison of the rotations about the Z direction obtained from the present program and SAP2000 in Example 8

Storey number	Storey height (m)	SAP2000 (frame method)	Present study (CCM)	
		Rotation (rad)	Rotation (rad)	% difference of present study compared to SAP2000
16	48.0	-0.004614	-0.004497	2.537
15	45.0	-0.004162	-0.004062	2.409
14	42.0	-0.003716	-0.003630	2.303
13	39.0	-0.003280	-0.003207	2.231
12	36.0	-0.002856	-0.002795	2.141
11	33.0	-0.002449	-0.002398	2.073
10	30.0	-0.002063	-0.002021	2.049
9	27.0	-0.001700	-0.001666	2.004
8	24.0	-0.001364	-0.001337	1.952
7	21.0	-0.001059	-0.001038	1.945
6	18.0	-0.000787	-0.000772	1.885
5	15.0	-0.000552	-0.000542	1.887
4	12.0	-0.000356	-0.000349	1.889
3	9.0	-0.000201	-0.000197	1.752
2	6.0	-0.000090	-0.000088	1.924
1	3.0	-0.000022	-0.000022	1.888
0	0.0	0.000000	0.000000	0.000

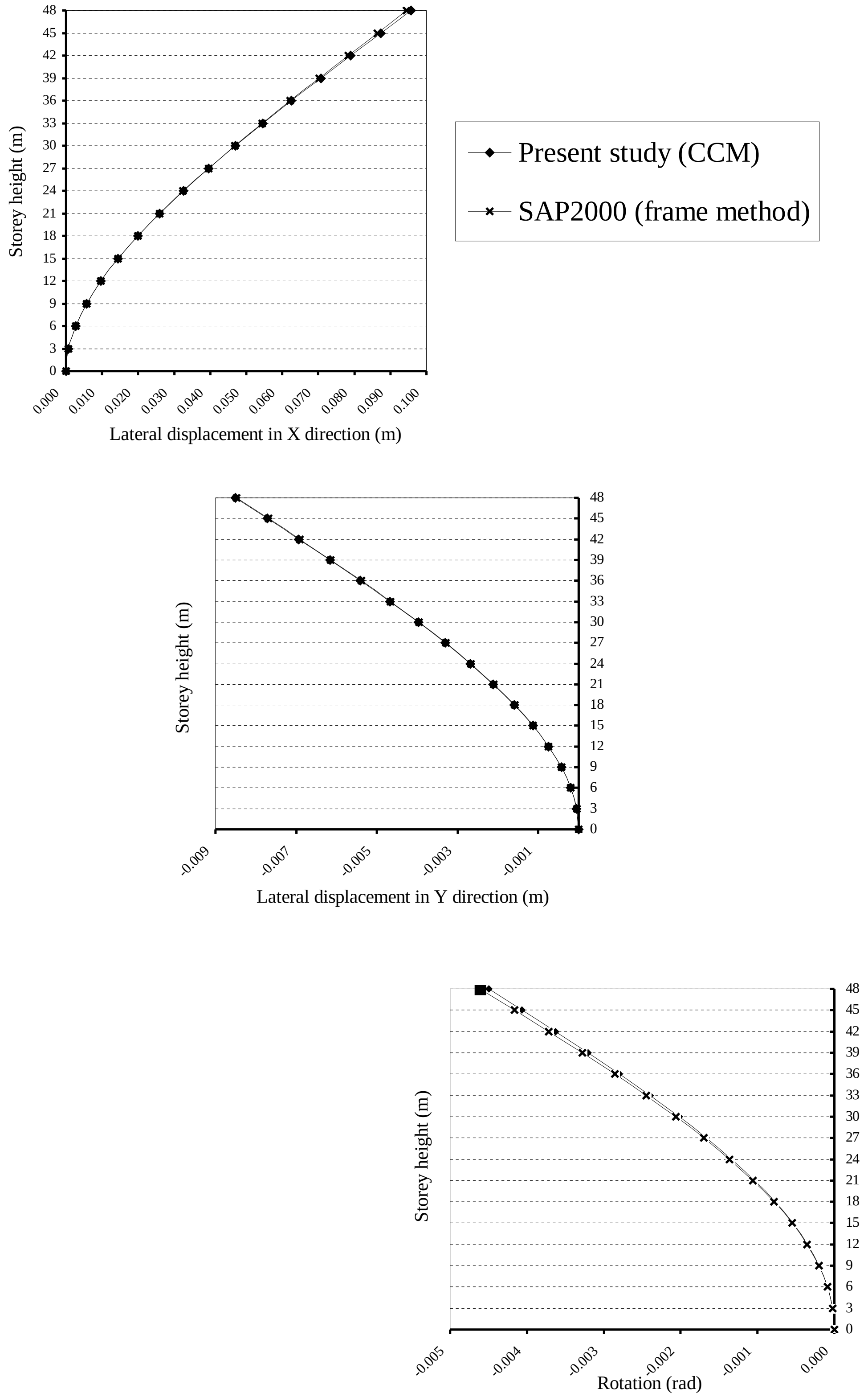

Figure 6.27. The lateral displacements and the rotations along the height in Example 8

Example 9:

In this example, a non-planar non-symmetrical coupled shear wall with a cross-section as shown in Fig. 6.28 is considered. The total height of the shear wall is 48 m, the storey height is 3 m, the thickness of the wall is 0.4 m, the height of the connecting beams is 0.5 m and the elasticity and shear moduli are $E = 2.85x10^6$ kN/m^2 and $G = 1055556$ kN/m^2, respectively. The loading comprises a 300 kN and a 250 kN concentrated horizontal forces as shown in the figure. The sectorial area diagram for this system is given in Fig. 6.29.

The comparison of the axial forces at the bottom, the lateral displacements and rotations along the height, found by the present program and SAP2000, are presented in Tables 6.29-32, expressing the percentage differences. The results found are given in Figs. 6.30-32, also.

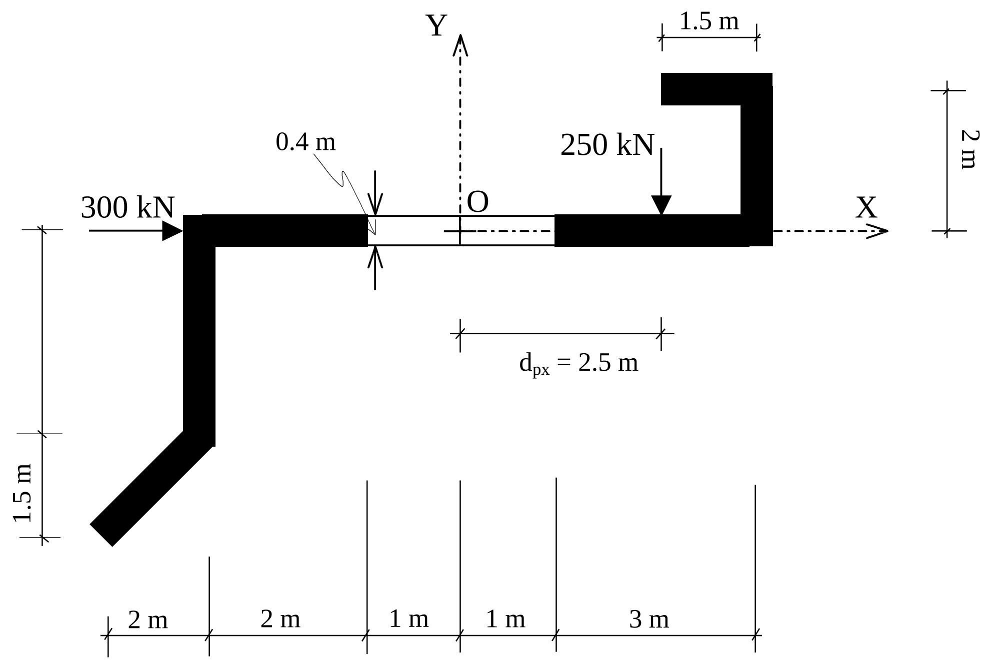

Figure 6.28. Cross-sectional view of the structure in Example 9

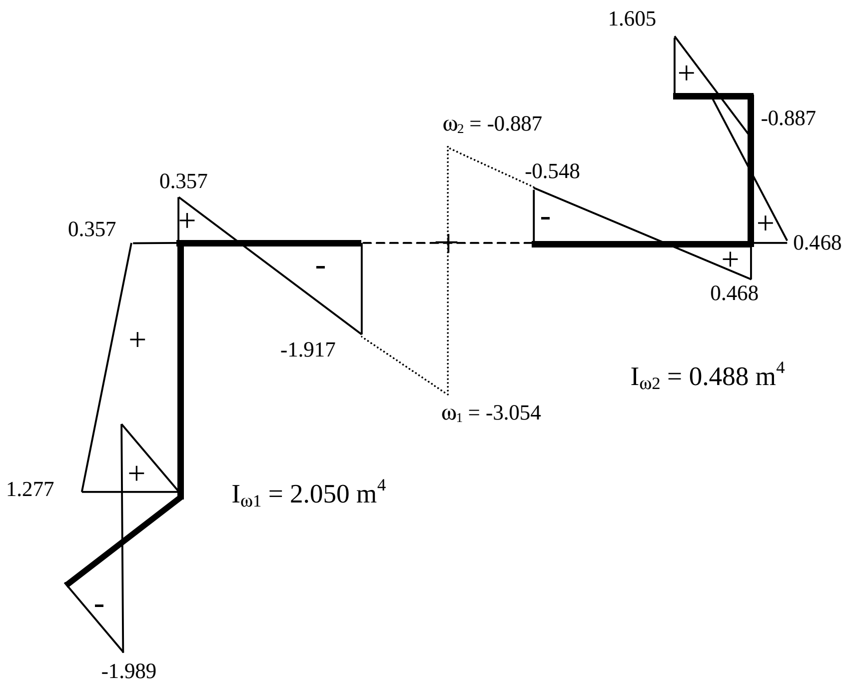

Figure 6.29. The principal sectorial area diagram of the structure in Example 9

Table 6.29. Comparison of the axial forces at the bottom obtained from the present and SAP2000 in Example 9

Axial forces at the bottom (kN)		
SAP2000 (frame method)	Present study (CCM)	% difference of present study compared to SAP2000
1682.472	1690.807	0.495

Table 6.30. Comparison of the lateral displacements in the X direction obtained from the present program and SAP2000 in Example 9

Storey number	Storey height (m)	SAP2000 (frame method)	Present study (CCM)	
		Lateral displacement (m)	Lateral displacement (m)	% difference of present study compared to SAP2000
10	30.0	0.177371	0.175575	1.013
9	27.0	0.152472	0.150406	1.355
8	24.0	0.127673	0.125668	1.571
7	21.0	0.103568	0.101792	1.714
6	18.0	0.080686	0.079219	1.818
5	15.0	0.059530	0.058398	1.901
4	12.0	0.040606	0.039805	1.972
3	9.0	0.024459	0.023960	2.039
2	6.0	0.011720	0.011472	2.113
1	3.0	0.003190	0.003118	2.244
0	0.0	0.000000	0.000000	0.000

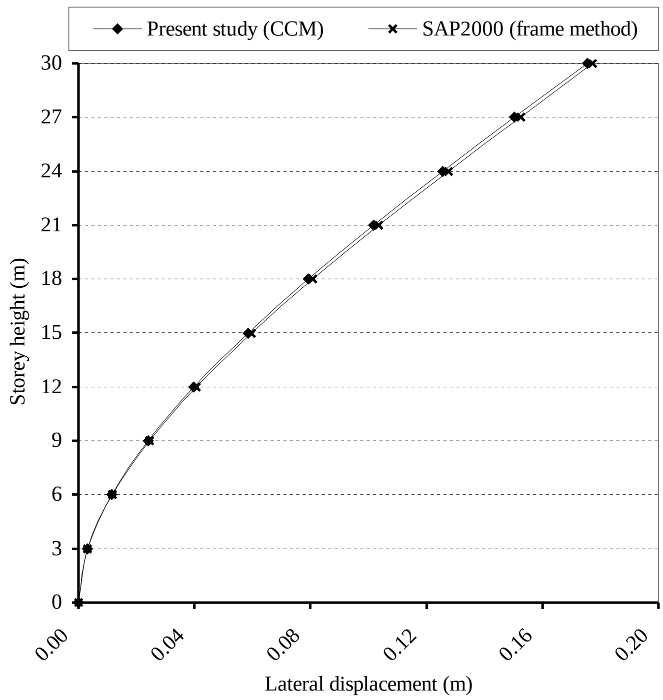

Figure 6.30. The lateral displacements in the X direction in Example 9

Table 6.31. Comparison of the lateral displacements in the Y direction obtained from the present program and SAP2000 in Example 9

Storey number	Storey height (m)	SAP2000 (frame method)	Present study (CCM)	
		Lateral displacement (m)	Lateral displacement (m)	% difference of present study compared to SAP2000
10	30.0	-0.280582	-0.277793	0.994
9	27.0	-0.239188	-0.236636	1.067
8	24.0	-0.198491	-0.196278	1.115
7	21.0	-0.159351	-0.157519	1.149
6	18.0	-0.122609	-0.121164	1.179
5	15.0	-0.089093	-0.088019	1.205
4	12.0	-0.059637	-0.058902	1.233
3	9.0	-0.035090	-0.034645	1.270
2	6.0	-0.016326	-0.016111	1.317
1	3.0	-0.004282	-0.004221	1.433
0	0.0	0.000000	0.000000	0.000

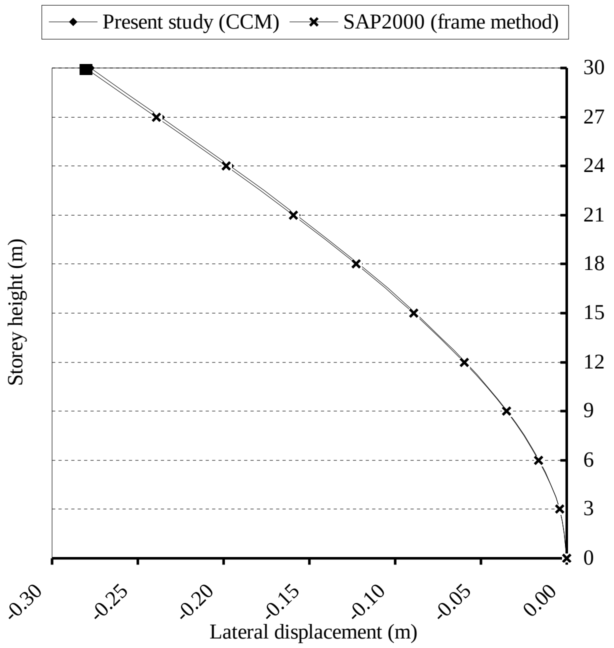

Figure 6.31. The lateral displacements in the Y direction in Example 9

Table 6.32. Comparison of the rotations about the Z direction obtained from the present program and SAP2000 in Example 9

Storey number	Storey height (m)	SAP2000 (frame method)	Present study (CCM)	
		Rotation (rad)	Rotation (rad)	% difference of present study compared to SAP2000
10	30.0	-0.018421	-0.018060	1.958
9	27.0	-0.015681	-0.015382	1.910
8	24.0	-0.012997	-0.012754	1.869
7	21.0	-0.010421	-0.010230	1.837
6	18.0	-0.008005	-0.007861	1.805
5	15.0	-0.005803	-0.005700	1.769
4	12.0	-0.003871	-0.003804	1.734
3	9.0	-0.002266	-0.002227	1.703
2	6.0	-0.001047	-0.001029	1.745
1	3.0	-0.000272	-0.000267	1.948
0	0.0	0.000000	0.000000	0.000

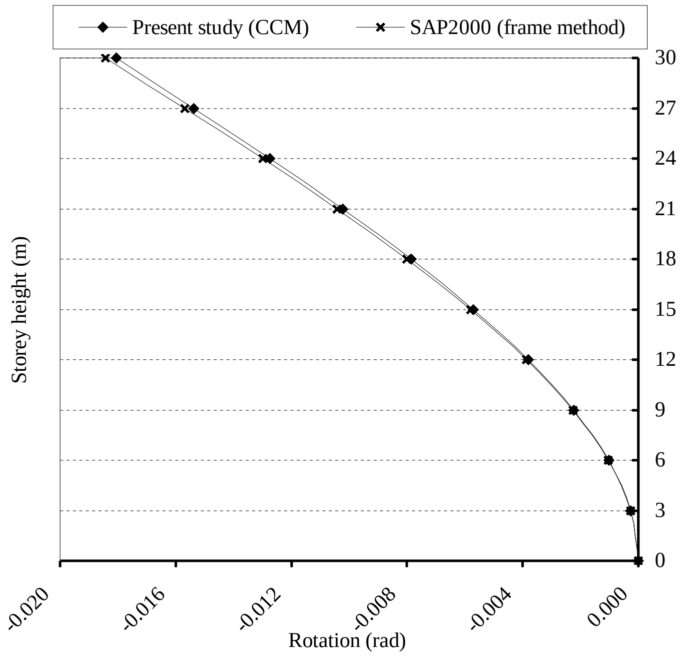

Figure 6.32. The rotations about the Z direction in Example 9

Example 10:

In this example, a non-planar non-symmetrical coupled shear wall with a cross-section as shown in Fig. 6.33 is considered. The total height of the shear wall is 30 m, the storey height is 3 m and the thicknesses of the piers and the connecting beams are shown in the figure. The height of the connecting beams is 0.7 m and the elasticity and shear moduli are $E = 2.85\text{x}10^6$ kN/m^2 and $G = 1055556$ kN/m^2, respectively. The external torque, 2500 kN-m, acts at the top of the structure. The sectorial area diagram for this system is given in Fig. 6.34.

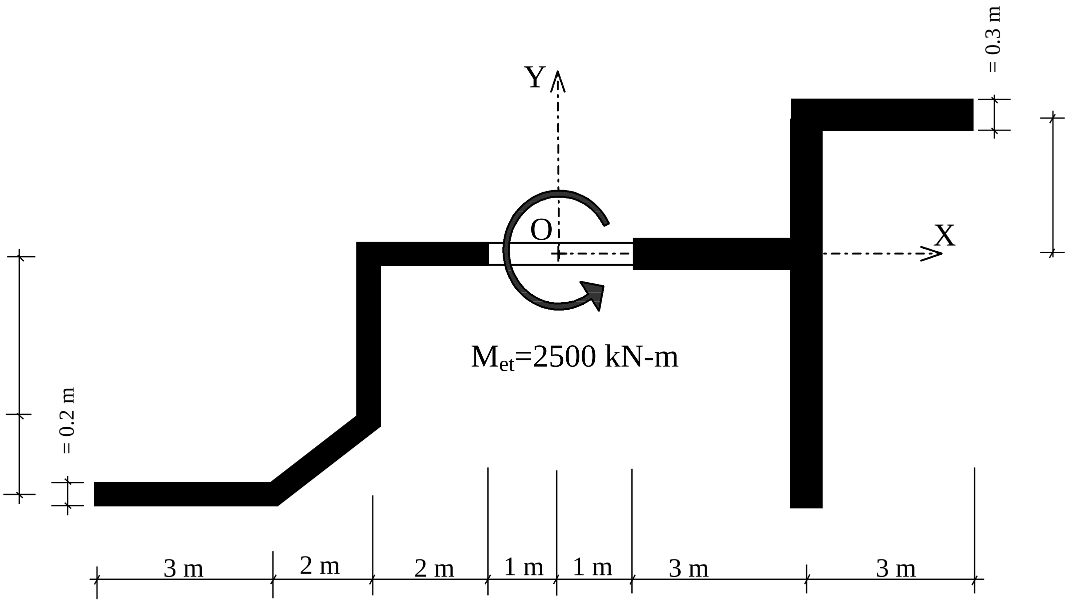

Figure 6.33. Cross-sectional view of the structure in Example 10

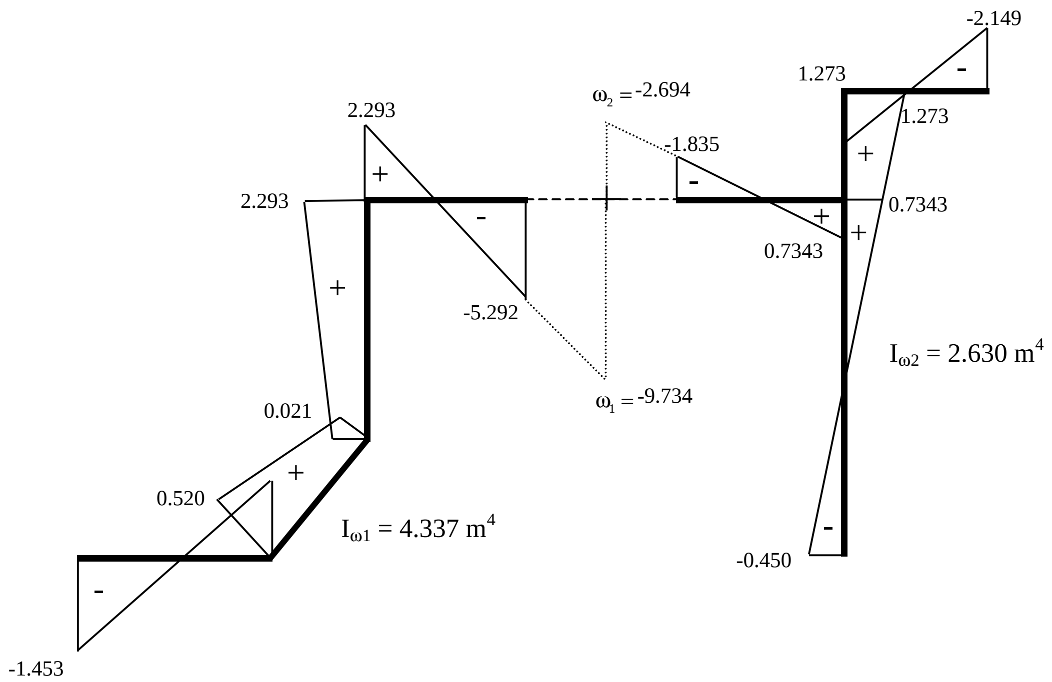

Figure 6.34. The principal sectorial area diagram of the structure in Example 10

The comparison of the axial forces at the bottom, the lateral displacements and the rotations found by the present program and SAP2000 are presented in Tables 6.33-36, expressing the percentage differences. The results found are given in Figs. 6.35-37, also.

Table 6.33. Comparison of the axial forces at the bottom obtained from the present program and SAP2000 in Example 10

Axial forces at the bottom (kN)		
SAP2000 (frame method)	Present study (CCM)	% difference of present study compared to SAP2000
172.892	170.920	1.141

Table 6.34. Comparison of the lateral displacements in the X direction obtained from the present program and SAP2000 in Example 10

Storey number	Storey height (m)	SAP2000 (frame method)	Present study (CCM)	
		Lateral displacement (m)	Lateral displacement (m)	% difference of present study compared to SAP2000
10	30.0	0.081546	0.079807	2.133
9	27.0	0.069317	0.067881	2.072
8	24.0	0.057350	0.056193	2.017
7	21.0	0.045884	0.044982	1.967
6	18.0	0.035159	0.034486	1.916
5	15.0	0.025419	0.024945	1.866
4	12.0	0.016906	0.016600	1.811
3	9.0	0.009866	0.009693	1.756
2	6.0	0.004540	0.004464	1.665
1	3.0	0.001173	0.001155	1.557
0	0.0	0.000000	0.000000	0.000

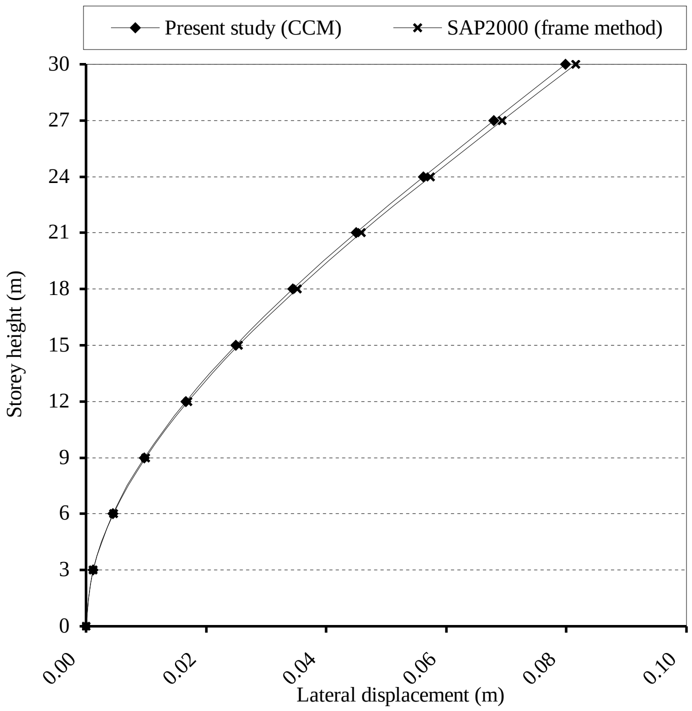

Figure 6.35. The lateral displacements in the X direction in Example 10

Table 6.35. Comparison of the lateral displacements in the Y direction obtained from the present program and SAP2000 in Example 10

Storey number	Storey height (m)	SAP2000 (frame method)	Present study (CCM)	
		Lateral displacement (m)	Lateral displacement (m)	% difference of present study compared to SAP2000
10	30.0	-0.168018	-0.164819	1.904
9	27.0	-0.143046	-0.140344	1.889
8	24.0	-0.118563	-0.116344	1.871
7	21.0	-0.095057	-0.093295	1.853
6	18.0	-0.073017	-0.071679	1.833
5	15.0	-0.052940	-0.051981	1.811
4	12.0	-0.035330	-0.034697	1.791
3	9.0	-0.020700	-0.020333	1.775
2	6.0	-0.009575	-0.009405	1.780
1	3.0	-0.002491	-0.002445	1.865
0	0.0	0.000000	0.000000	0.000

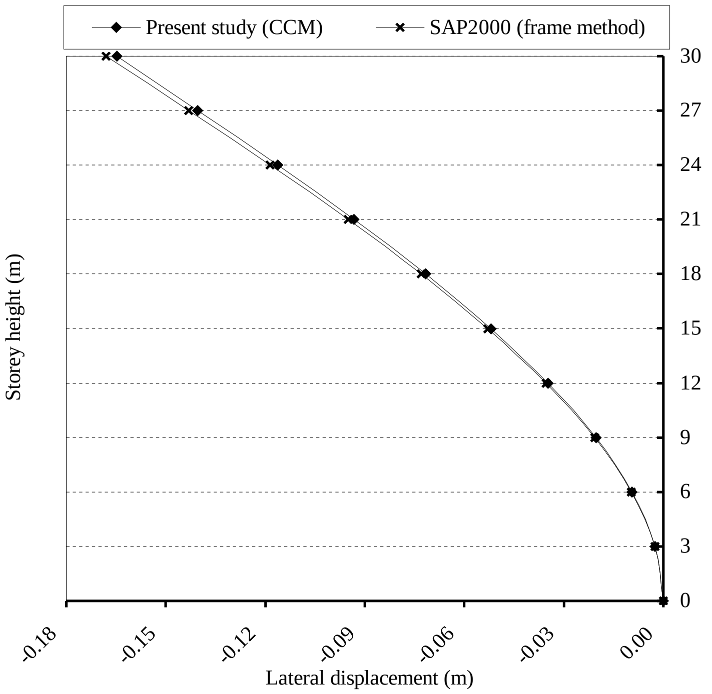

Figure 6.36. The lateral displacements in the Y direction in Example 10

Table 6.36. Comparison of the rotations about the Z direction obtained from the present program and SAP2000 in Example 10

Storey number	Storey height (m)	SAP2000 (frame method)	Present study (CCM)	
		Rotation (rad)	Rotation (rad)	% difference of present study compared to SAP2000
10	30.0	0.062865	0.061776	1.732
9	27.0	0.053534	0.052611	1.723
8	24.0	0.044383	0.043624	1.711
7	21.0	0.035594	0.034991	1.695
6	18.0	0.027350	0.026892	1.676
5	15.0	0.019838	0.019509	1.658
4	12.0	0.013245	0.013028	1.638
3	9.0	0.007764	0.007638	1.617
2	6.0	0.003594	0.003535	1.635
1	3.0	0.000936	0.000920	1.754
0	0.0	0.000000	0.000000	0.000

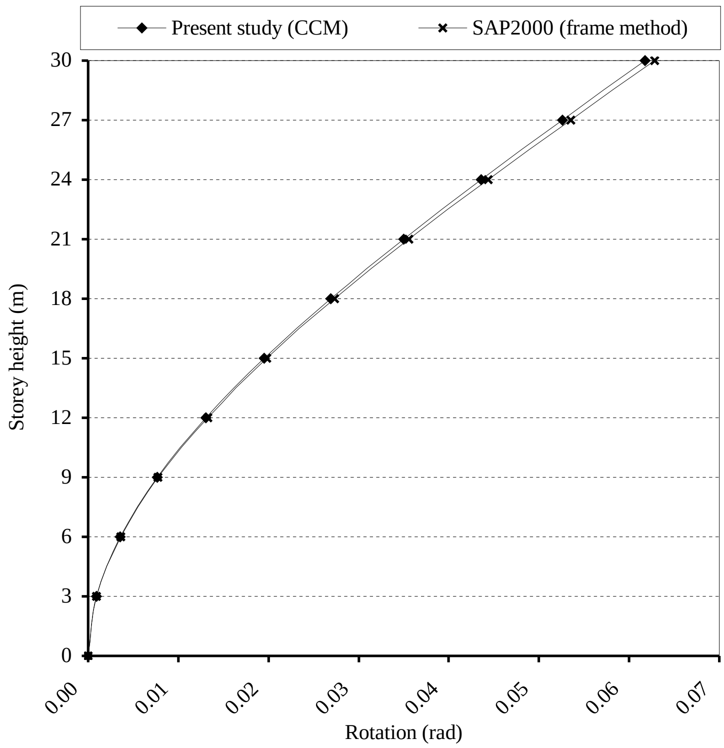

Figure 6.37. The rotations about the Z direction in Example 10

Example 11:

In this example, a non-planar non-symmetrical coupled shear wall (Fig. 6.38) with a cross-section as shown in Fig. 6.39 is considered. The total height of the shear wall is 36 m, the storey height is 3 m, the thickness of the wall is 0.4 m, the height of the connecting beams is 0.5 m and the elasticity and shear moduli are $E = 2.85x10^6$ kN/m^2 and $G = 1055556$ kN/m^2, respectively. The uniform horizontal force 3 kN/m^2 acts along the height as shown in Figs. 6.38-39.

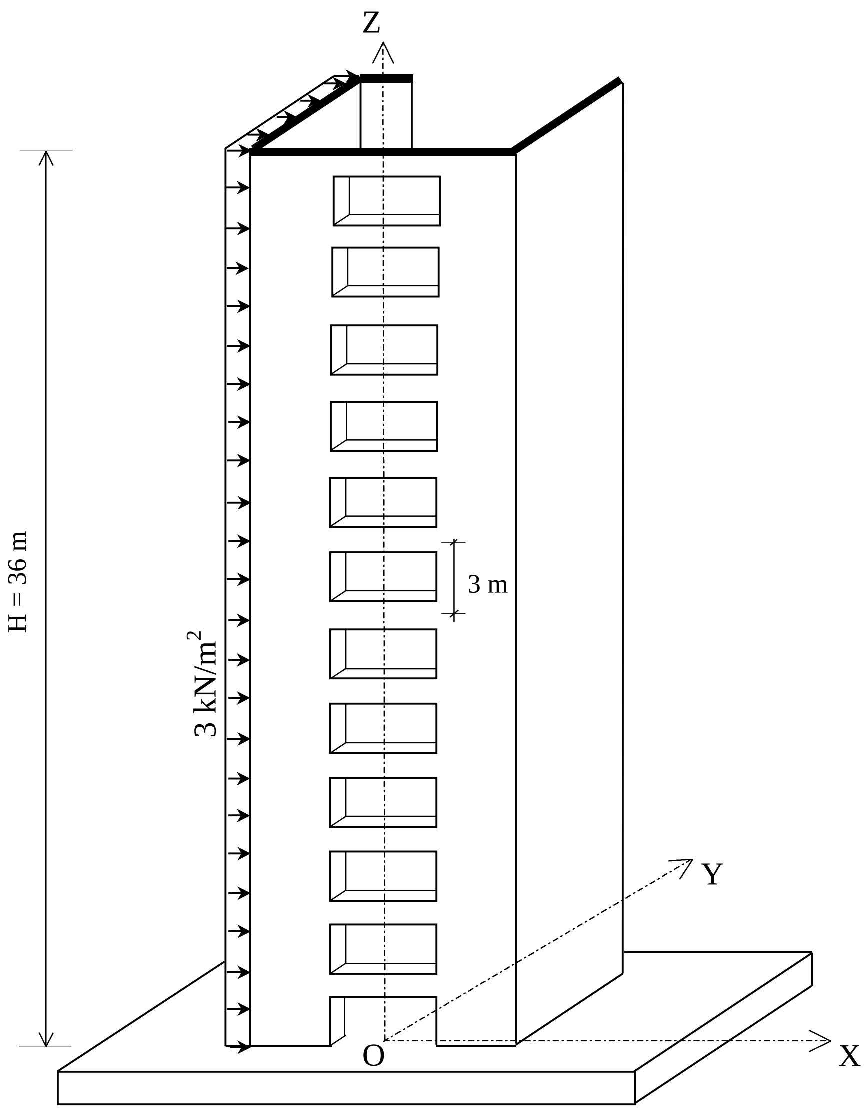

Figure 6.38. Geometrical properties and loading of the structure in Example 11

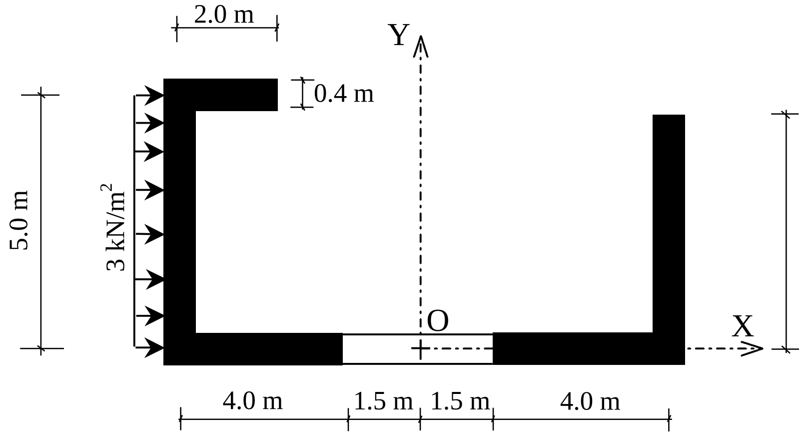

Figure 6.39. Cross-sectional view of the structure in Example 11

The comparison of the axial forces at the bottom, the lateral displacements and the rotations along the height found by the present program and SAP2000 are presented in Tables 6.37-40, expressing the percentage differences. The results found are given in Figs. 6.40-42, also.

Table 6.37. Comparison of the axial forces at the bottom obtained from the present program and SAP2000 in Example 11

Axial forces at the bottom (kN)		
SAP2000 (frame method)	Present study (CCM)	% difference of present study compared to SAP2000
526.359	523.667	0.511

Table 6.38. Comparison of the lateral displacements in the X direction obtained from the present program and SAP2000 in Example 11

Storey number	Storey height (m)	SAP2000 (frame method) Lateral displacement (m)	Present study (CCM) Lateral displacement (m)	Present study (CCM) % difference of present study compared to SAP2000
12	36.0	0.053832	0.054478	1.201
11	33.0	0.049039	0.049489	0.918
10	30.0	0.044106	0.044404	0.676
9	27.0	0.038989	0.039172	0.470
8	24.0	0.033686	0.033787	0.299
7	21.0	0.028242	0.028285	0.152
6	18.0	0.022744	0.022749	0.024
5	15.0	0.017325	0.017310	0.089
4	12.0	0.012169	0.012145	0.194
3	9.0	0.007516	0.007494	0.298
2	6.0	0.003671	0.003655	0.447
1	3.0	0.001010	0.001003	0.700
0	0.0	0.000000	0.000000	0.000

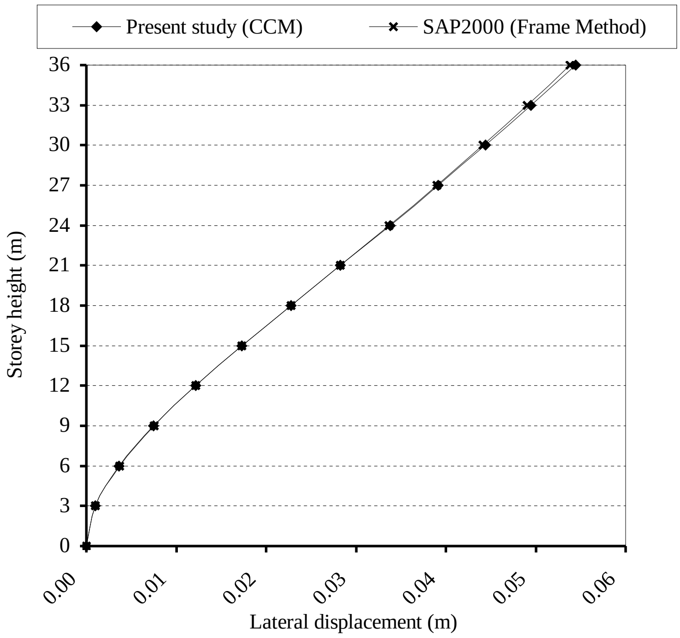

Figure 6.40. The lateral displacements in the X direction in Example 11

Table 6.39. Comparison of the lateral displacements in the Y direction obtained from the present program and SAP2000 in Example 11

Storey number	Storey height (m)	SAP2000 (frame method)	Present study (CCM)	
		Lateral displacement (m)	Lateral displacement (m)	% difference of present study compared to SAP2000
12	36.0	-0.013588	-0.013442	1.077
11	33.0	-0.012214	-0.012072	1.159
10	30.0	-0.010826	-0.010694	1.222
9	27.0	-0.009423	-0.009303	1.270
8	24.0	-0.008013	-0.007907	1.318
7	21.0	-0.006608	-0.006520	1.334
6	18.0	-0.005234	-0.005163	1.363
5	15.0	-0.003919	-0.003866	1.351
4	12.0	-0.002706	-0.002669	1.364
3	9.0	-0.001642	-0.001620	1.345
2	6.0	-0.000787	-0.000777	1.280
1	3.0	-0.000212	-0.000210	1.123
0	0.0	0.000000	0.000000	0.000

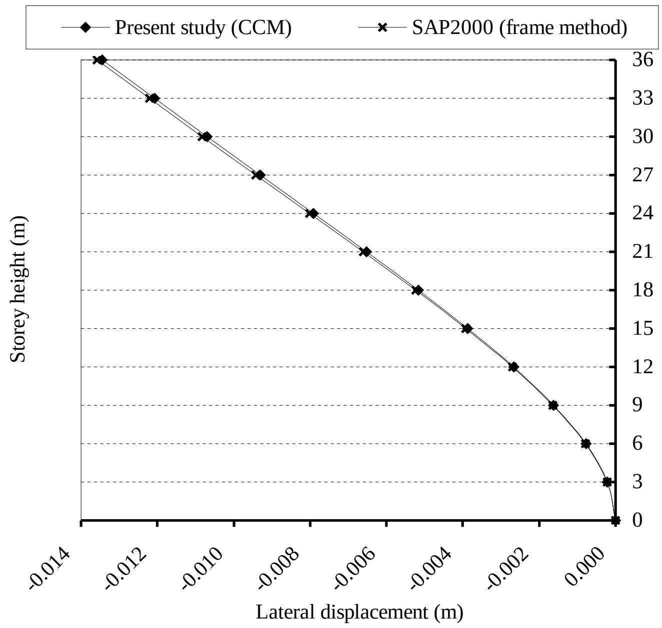

Figure 6.41. The lateral displacements in the Y direction in Example 11

Table 6.40. Comparison of the rotations about the Z direction obtained from the present program and SAP2000 in Example 11

Storey number	Storey height (m)	SAP2000 (frame method) Rotation (rad)	Present study (CCM) Rotation (rad)	Present study (CCM) % difference of present study compared to SAP2000
12	36.0	-0.007220	-0.007180	0.552
11	33.0	-0.006464	-0.006425	0.607
10	30.0	-0.005703	-0.005667	0.636
9	27.0	-0.004940	-0.004907	0.672
8	24.0	-0.004178	-0.004150	0.681
7	21.0	-0.003428	-0.003403	0.723
6	18.0	-0.002699	-0.002680	0.709
5	15.0	-0.002010	-0.001995	0.733
4	12.0	-0.001380	-0.001369	0.775
3	9.0	-0.000832	-0.000826	0.727
2	6.0	-0.000397	-0.000394	0.852
1	3.0	-0.000106	-0.000106	0.468
0	0.0	0.000000	0.000000	0.000

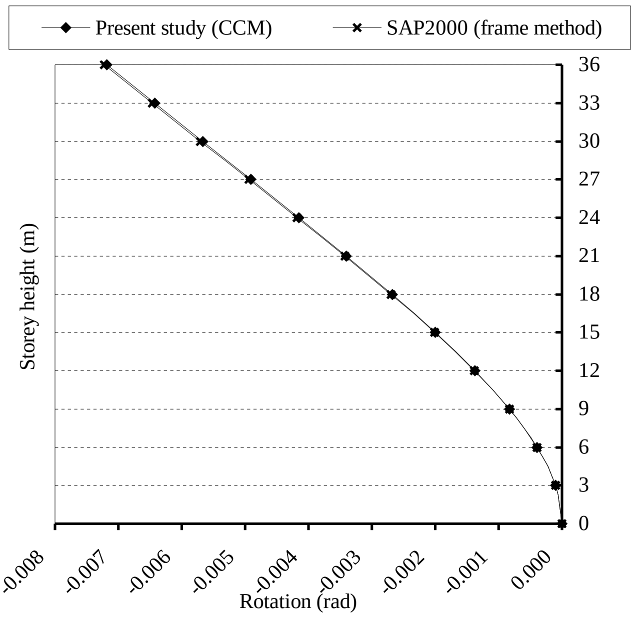

Figure 6.42. The rotations about the Z direction in Example 11

Example 12:

In this example, a non-planar coupled shear wall which rests on a rigid foundation is loaded by a horizontal force 300 kN (see Fig. 6.43). The present work considers the variations of connecting beams and storey heights from one region to another. The total height is 26 m and the storey heights for the upper and lower regions are 3 m and 3.5 m,respectively. The thickness of the wall is 0.39 m and the height of the connecting beams is 0.5 m.

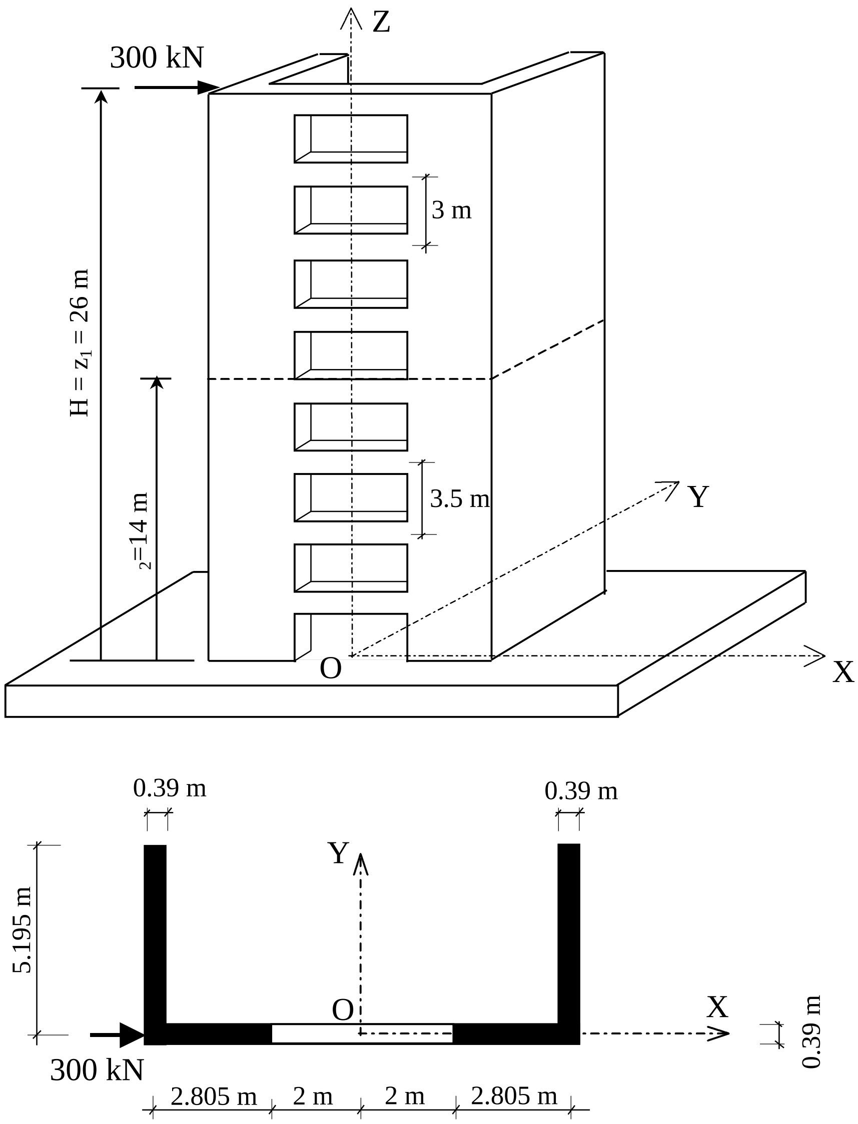

Figure 6.43. Geometrical properties of the structure in Example 12

The elasticity modulus for the complete wall is $E = 2.85x10^6$ kN/m^2 and the shear modulus is $G = 1055556$ kN/m^2. The comparison of the axial forces at the bottom, the lateral displacements and the rotations along the height found by the program prepared in the present work and the SAP2000 structural analysis program are presented in Tables 6.41-43, expressing the percentage differences. The results found are given in Figs. 6.44-45, also.

Table 6.41. Comparison of the axial forces at the bottom obtained from the present program and SAP2000 in Example 12

Axial forces at the bottom (kN)		
SAP2000 (frame method)	Present study (CCM)	% difference of present study compared to SAP2000
459.714	449.635	2.193

Table 6.42. Comparison of the lateral displacements in the X direction obtained from the present program and SAP2000 in Example 12

Storey number	Storey height (m)	SAP2000 (frame method)	Present study (CCM)	
		Lateral displacement (m)	Lateral displacement (m)	% difference of present study compared to SAP2000
8	26.0	0.091914	0.095333	3.720
7	23.0	0.077331	0.079753	3.132
6	20.0	0.062819	0.064483	2.649
5	17.0	0.048752	0.049846	2.245
4	14.0	0.035517	0.036192	1.901
3	10.5	0.021705	0.022049	1.584
2	7.0	0.010480	0.010618	1.318
1	3.5	0.002849	0.002879	1.052
0	0.0	0.000000	0.000000	0.000

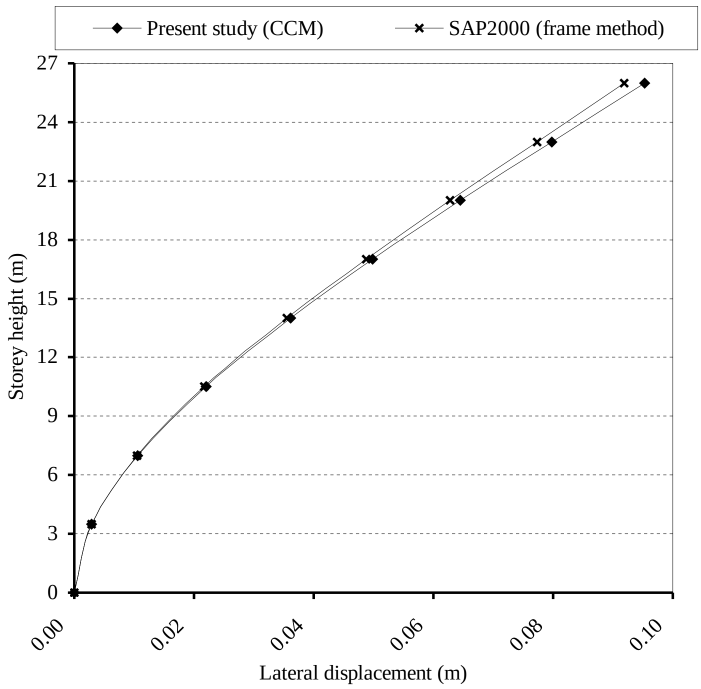

Figure 6.44. The lateral displacements in the X direction in Example 12

Table 6.43. Comparison of the rotations about the Z direction obtained from the present program and SAP2000 in Example 12

Storey number	Storey height (m)	SAP2000 (frame method)	Present study (CCM)	
		Rotation (rad)	Rotation (rad)	% difference of present study compared to SAP2000
8	26.0	-0.006483	-0.006533	0.778
7	23.0	-0.005423	-0.005448	0.454
6	20.0	-0.004378	-0.004386	0.178
5	17.0	-0.003373	-0.003373	0.012
4	14.0	-0.002439	-0.002434	0.207
3	10.5	-0.001476	-0.001471	0.315
2	7.0	-0.000706	-0.000703	0.479
1	3.5	-0.000190	-0.000189	0.643
0	0.0	0.000000	0.000000	0.000

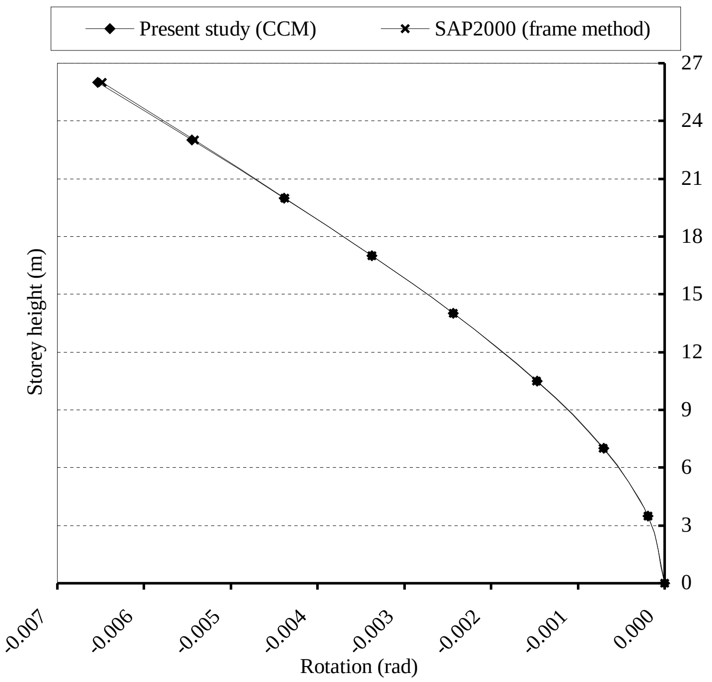

Figure 6.45. The rotations about the Z direction in Example 12

Example 13:

In this example, a non-planar non-symmetrical coupled shear wall (Fig. 6.46) with a cross-section as shown in Fig. 6.47 is considered. The story heights for the two regions are given in Fig. 6.46. The system is loaded by a horizontal force 250 kN as seen in Figs. 6.46-47.

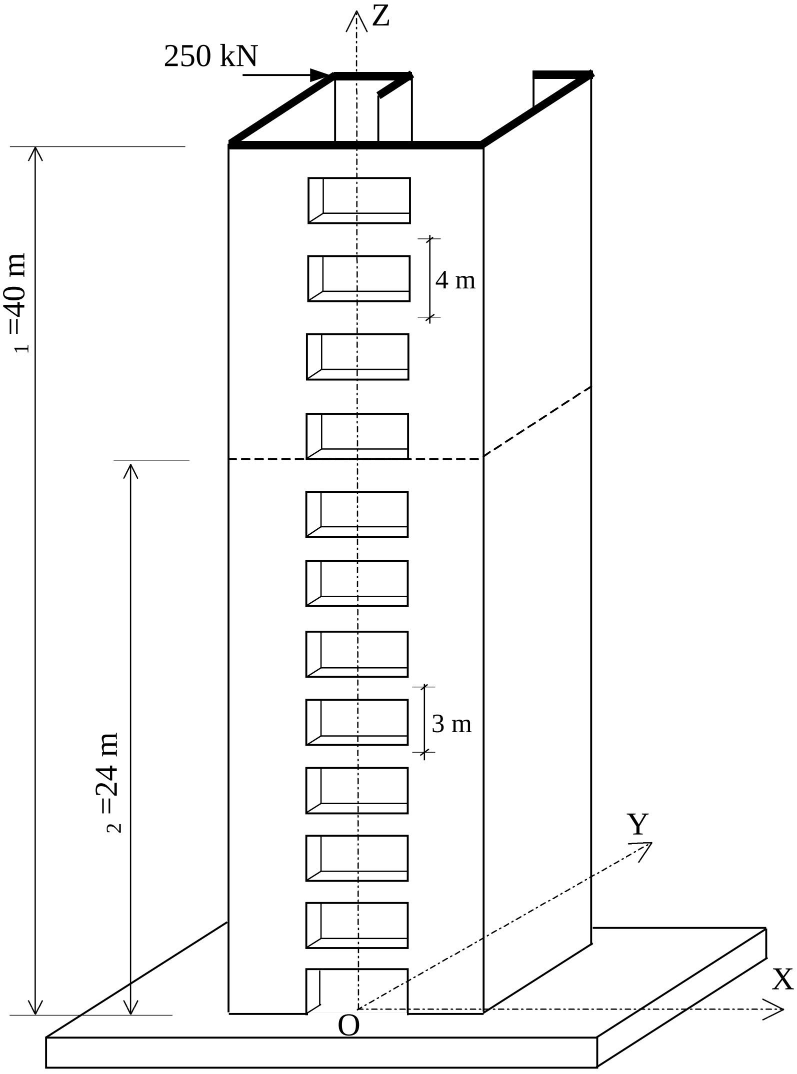

Figure 6.46. Geometrical properties and loading of the structure in Example 13

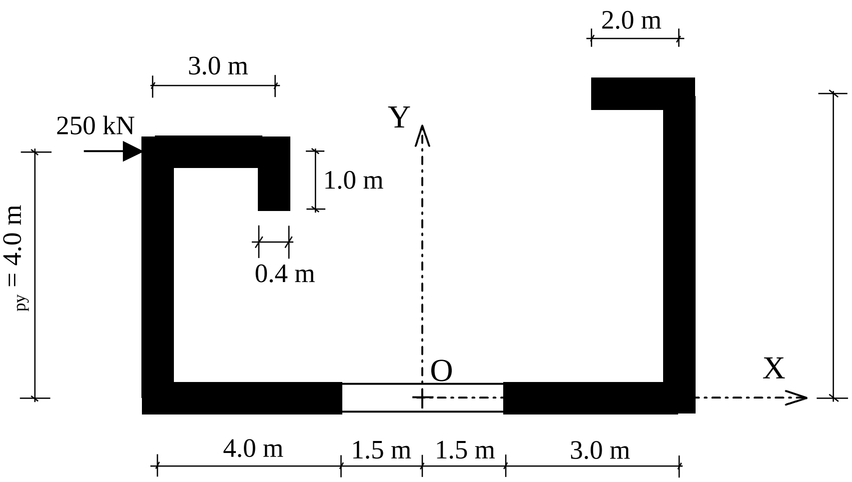

Figure 6.47. Cross-sectional view of the structure in Example 13

The total height of the shear wall is 40 m and the height of the connecting beams for the upper and lower regions are 0.4 m and 0.6 m, respectively. The material properties of the structure are $E = 2.85x10^6$ kN/m^2 and $G = 1055556$ kN/m^2.

The comparison of the axial forces at the bottom, the lateral displacements and the rotations along the height found by the present program and SAP2000 are presented in Tables 6.44-47, expressing the percentage differences. The results found are given in Figs. 6.48-50, also.

Table 6.44. Comparison of the axial forces at the bottom obtained from the present program and SAP2000 in Example 13

Axial forces at the bottom (kN)		
SAP2000 (frame method)	Present study (CCM)	% difference of present study compared to SAP2000
619.368	609.071	1.663

Table 6.45. Comparison of the lateral displacements in the X direction obtained from the present program and SAP2000 in Example 13

Storey number	Storey height (m)	SAP2000 (frame method)	Present study (CCM)	
		Lateral displacement (m)	Lateral displacement (m)	% difference of present study compared to SAP2000
12	40.0	0.078948	0.081646	3.417
11	36.0	0.066723	0.068867	3.213
10	32.0	0.054765	0.056418	3.018
9	28.0	0.043426	0.044635	2.785
8	24.0	0.033072	0.033867	2.404
7	21.0	0.026103	0.026645	2.075
6	18.0	0.019828	0.020184	1.795
5	15.0	0.014277	0.014498	1.550
4	12.0	0.009499	0.009627	1.349
3	9.0	0.005570	0.005635	1.170
2	6.0	0.002588	0.002614	0.999
1	3.0	0.000679	0.000684	0.737
0	0.0	0.000000	0.000000	0.000

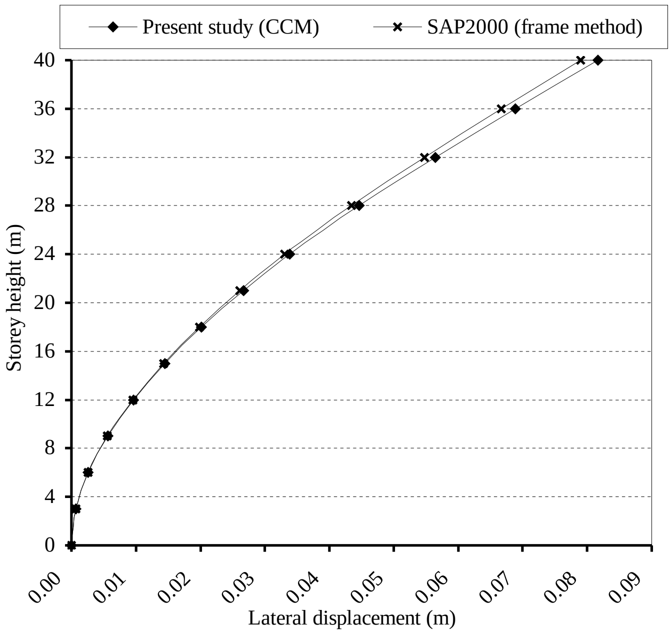

Figure 6.48. The lateral displacements in the X direction in Example 13

Table 6.46. Comparison of the lateral displacements in the Y direction obtained from the present program and SAP2000 in Example 13

Storey number	Storey height (m)	SAP2000 (frame method) Lateral displacement (m)	Present study (CCM) Lateral displacement (m)	Present study (CCM) % difference of present study compared to SAP2000
12	40.0	-0.008136	-0.008199	0.769
11	36.0	-0.006918	-0.006970	0.757
10	32.0	-0.005725	-0.005767	0.738
9	28.0	-0.004581	-0.004614	0.725
8	24.0	-0.003512	-0.003537	0.701
7	21.0	-0.002774	-0.002793	0.683
6	18.0	-0.002101	-0.002115	0.686
5	15.0	-0.001504	-0.001514	0.646
4	12.0	-0.000991	-0.000998	0.685
3	9.0	-0.000574	-0.000578	0.666
2	6.0	-0.000262	-0.000264	0.875
1	3.0	-0.000067	-0.000068	1.155
0	0.0	0.000000	0.000000	0.000

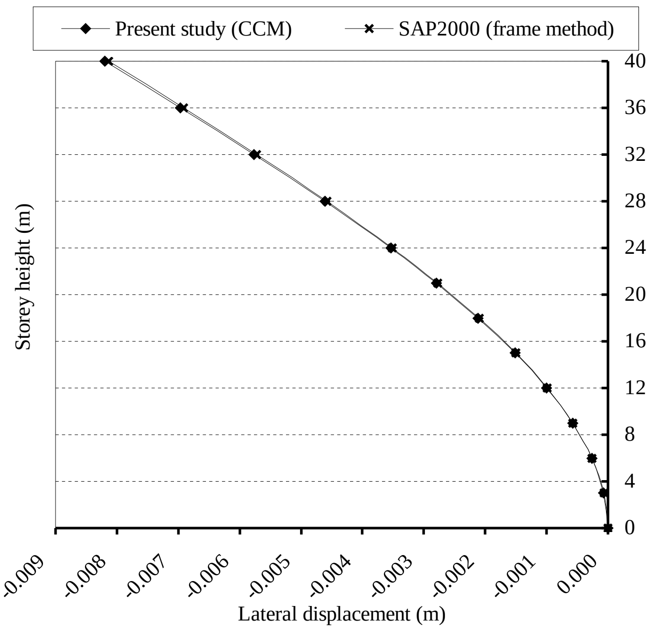

Figure 6.49. The lateral displacements in the Y direction in Example 13

Table 6.47. Comparison of the rotations about the Z direction obtained from the present program and SAP2000 in Example 13

Storey number	Storey height (m)	SAP2000 (frame method)	Present study (CCM)	
		Rotation (rad)	Rotation (rad)	% difference of present study compared to SAP2000
12	40.0	-0.007674	-0.007511	2.120
11	36.0	-0.006543	-0.006410	2.037
10	32.0	-0.005434	-0.005328	1.957
9	28.0	-0.004365	-0.004284	1.848
8	24.0	-0.003357	-0.003299	1.728
7	21.0	-0.002653	-0.002610	1.615
6	18.0	-0.002008	-0.001977	1.520
5	15.0	-0.001434	-0.001413	1.448
4	12.0	-0.000942	-0.000929	1.378
3	9.0	-0.000543	-0.000536	1.334
2	6.0	-0.000247	-0.000244	1.349
1	3.0	-0.000063	-0.000062	1.550
0	0.0	0.000000	0.000000	0.000

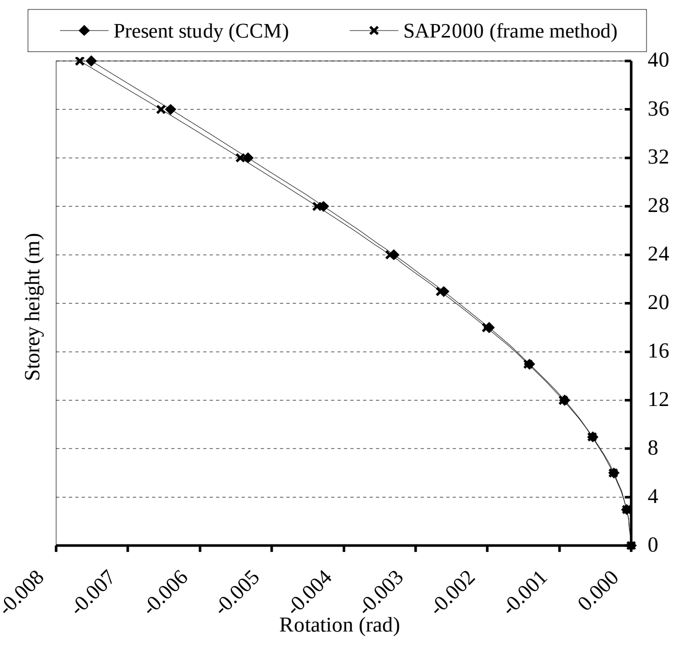

Figure 6.50. The rotations about the Z direction in Example 13

Example 14:

In this example, a non-planar non-symmetrical coupled shear wall (Fig. 6.51) with a cross-section as shown in Fig. 6.52 is considered. The concentrated horizontal force 500 kN acts on the system. This loading causes a twisting moment on the structure.

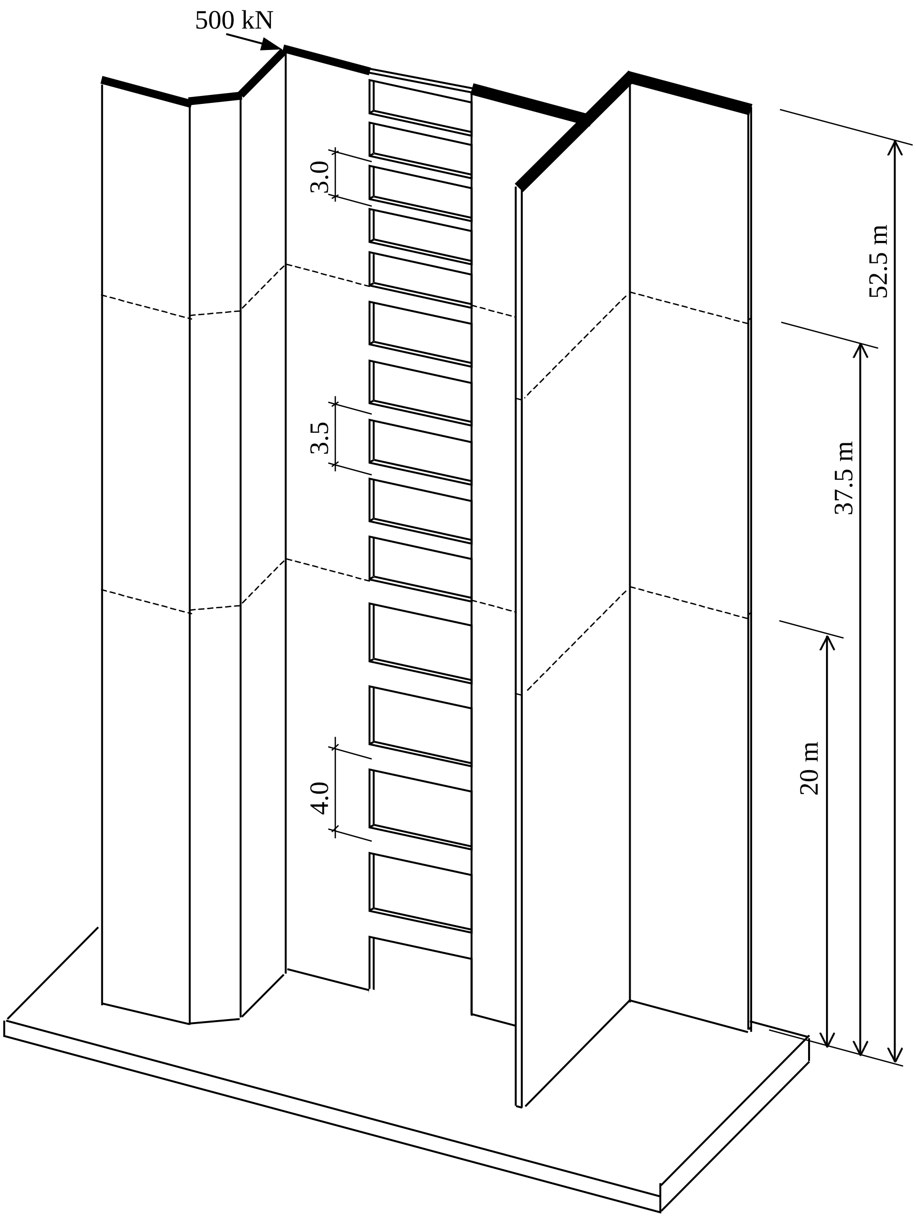

Figure 6.51. Geometric properties and loading of the structure in Example 14

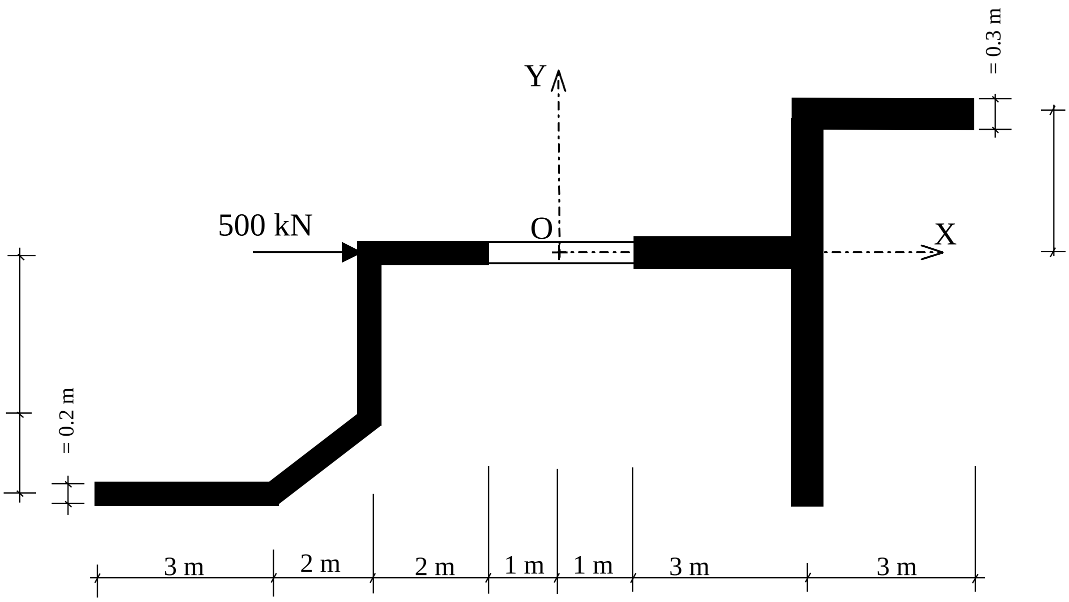

Figure 6.52. Cross-sectional view of the structure in Example 14

The total height of the shear wall is 52.5 m and for each section, starting from the top, the storey heights are 3 m, 3.5 m and 4 m, respectively. The thickness of the wall is 0.3 m, the height of the connecting beams are 0.4 m, 0.5 m, 0.6 m and the material properties of the system are as $E = 2.85x10^6$ kN/m^2 and $G = 1055556$ kN/m^2.

The comparison of the lateral displacements and the rotations along the height and the axial forces at the bottom, found by the present program and SAP2000, are presented in Tables 6.48-51, expressing the percentage differences. The results found are given in Fig. 6.52, also.

Table 6.48. Comparison of the lateral displacements in the X direction obtained from the present program and SAP2000 in Example 14

Storey number	Storey height (m)	SAP2000 (frame method)	Present study (CCM)	
		Lateral displacement (m)	Lateral displacement (m)	% difference of present study compared to SAP2000
15	52.5	0.380120	0.382336	0.583
14	49.5	0.348050	0.349671	0.466
13	46.5	0.316100	0.317237	0.360
12	43.5	0.284510	0.285266	0.266
11	40.5	0.253580	0.253998	0.165
10	37.5	0.223560	0.223681	0.054
9	34.0	0.189930	0.189819	0.058
8	30.5	0.158020	0.157786	0.148
7	27.0	0.128080	0.127804	0.216
6	23.5	0.100450	0.100142	0.307
5	20.0	0.075460	0.075119	0.451
4	16.0	0.050500	0.050190	0.614
3	12.0	0.029800	0.029580	0.739
2	8.0	0.013940	0.013825	0.822
1	4.0	0.003680	0.003649	0.838
0	0.0	0.000000	0.000000	0.000

Table 6.49. Comparison of the lateral displacements in the Y direction obtained from the present program and SAP2000 in Example 14

Storey number	Storey height (m)	SAP2000 (frame method)	Present study (CCM)	
		Lateral displacement (m)	Lateral displacement (m)	% difference of present study compared to SAP2000
15	52.5	-0.407390	-0.400179	1.770
14	49.5	-0.372880	-0.366226	1.784
13	46.5	-0.338570	-0.332489	1.796
12	43.5	-0.304680	-0.299184	1.804
11	40.5	-0.271440	-0.266530	1.809
10	37.5	-0.239090	-0.234747	1.816
9	34.0	-0.202760	-0.199061	1.824
8	30.5	-0.168250	-0.165184	1.822
7	27.0	-0.135910	-0.133445	1.814
6	23.5	-0.106100	-0.104185	1.805
5	20.0	-0.079200	-0.077764	1.814
4	16.0	-0.052460	-0.051515	1.801
3	12.0	-0.030550	-0.030004	1.788
2	8.0	-0.014060	-0.013813	1.759
1	4.0	-0.003640	-0.003579	1.685
0	0.0	0.000000	0.000000	0.000

Table 6.50. Comparison of the rotations about the Z direction obtained from the present program and SAP2000 in Example 14

Storey number	Storey height (m)	SAP2000 (frame method)	Present study (CCM)	
		Rotation (rad)	Rotation (rad)	% difference of present study compared to SAP2000
15	52.5	0.069000	0.065931	4.448
14	49.5	0.063200	0.060411	4.412
13	46.5	0.057430	0.054923	4.365
12	43.5	0.051740	0.049499	4.332
11	40.5	0.046140	0.044168	4.274
10	37.5	0.040680	0.038964	4.219
9	34.0	0.034530	0.033095	4.155
8	30.5	0.028680	0.027502	4.106
7	27.0	0.023180	0.022245	4.033
6	23.5	0.018100	0.017385	3.951
5	20.0	0.013510	0.012983	3.898
4	16.0	0.008930	0.008597	3.725
3	12.0	0.005190	0.004999	3.689
2	8.0	0.002380	0.002294	3.618
1	4.0	0.000612	0.000592	3.347
0	0.0	0.000000	0.000000	0.000

Table 6.51. Comparison of the axial forces obtained from the present program and SAP2000 in Example 14

Axial forces at the bottom (kN)		
SAP2000 (frame method)	Present study (CCM)	% difference of present study compared to SAP2000
2305.960	2312.305	0.275

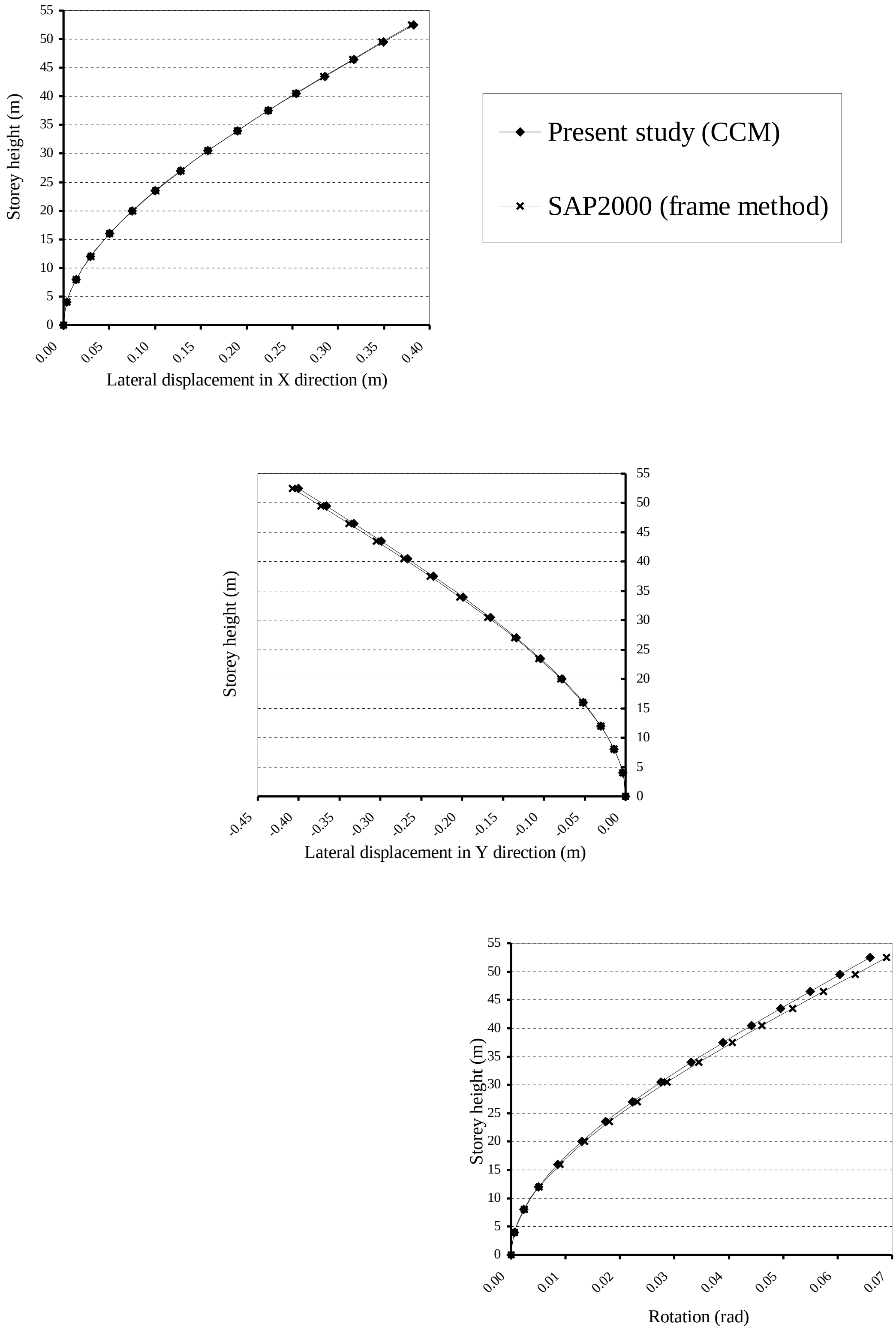

Figure 6.52. The lateral displacements and the rotations along the height in Example14

Example 15:

In this study, the method of analysis and the program prepared, is achieved when there is an elastic beam-wall connections in non-planar coupled shear wall. The comparison of the top displacements found by the program prepared in the present work and the SAP2000 structural analysis program, which are influenced by the variation of the connection stiffness, are presented in Table 6.52, expressing the percentage differences. The results found are given in Figs. 6.54-56. The total height of the shear wall is 36 m, the storey height is 3 m, the height of the connecting beams is 0.5 m and the elasticity and shear moduli are E = 2.85x10^6 kN/m^2 and G = 1055556 kN/m^2, respectively. The concentrated horizontal force 250 kN acts at the top as shown in Fig. 6.53.

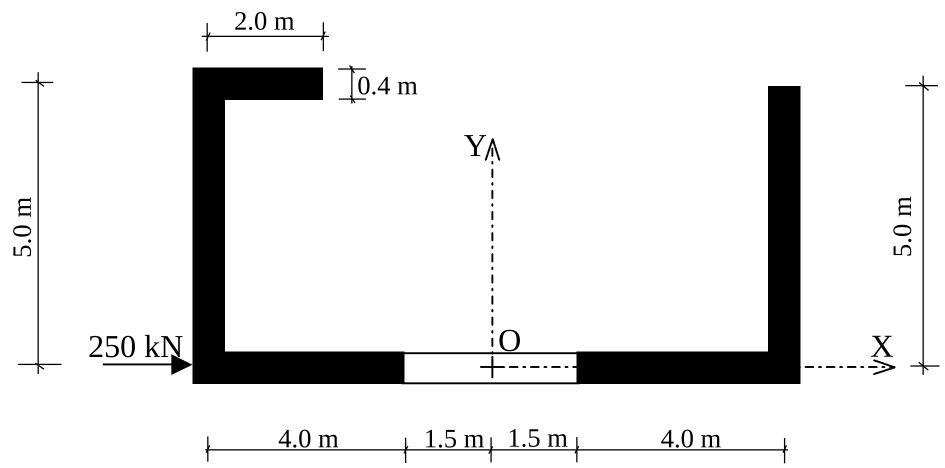

Figure 6.53. Cross-sectional view of the structure in Example 15

Table 6.52. Comparison of the results for the lateral displacements and the rotation at the top for various elastic beam-wall connection stiffnesses (C_{cb}) in Example 15

C_{cb} kN-m/rad	**Lateral displacements in X direction (m)**			**Lateral displacements in Y direction (m)**			**Rotations about Z direction (rad)**		
	SAP2000	Present study	% difference	SAP2000	Present study	% difference	SAP2000	Present study	% difference
10^0	0.144095	0.143019	0.747	-0.015975	-0.015554	2.634	-0.006972	-0.006865	1.531
10^1	0.143992	0.142893	0.763	-0.015966	-0.015543	2.650	-0.006969	-0.006862	1.535
10^2	0.142967	0.141655	0.918	-0.015872	-0.015432	2.771	-0.006942	-0.006830	1.615
10^3	0.133856	0.130931	2.185	-0.015040	-0.014473	3.768	-0.006702	-0.006552	2.244
10^4	0.092924	0.088512	4.748	-0.011300	-0.010680	5.484	-0.005622	-0.005451	3.045
10^5	0.058771	0.059031	0.443	-0.008179	-0.008044	1.653	-0.004720	-0.004686	0.729
10^6	0.052625	0.054218	3.027	-0.007617	-0.007613	0.049	-0.004558	-0.004561	0.057
10^7	0.051954	0.053706	3.372	-0.007556	-0.007567	0.152	-0.004540	-0.004547	0.161
10^8	0.051912	0.053654	3.356	-0.007552	-0.007563	0.144	-0.004539	-0.004546	0.154
10^9	0.051874	0.053649	3.422	-0.007549	-0.007562	0.177	-0.004538	-0.004546	0.173
10^{10}	0.051873	0.053649	3.423	-0.007548	-0.007562	0.190	-0.004538	-0.004546	0.172
Rigid case	0.051873	0.053649	3.423	-0.007548	-0.007562	0.190	-0.004538	-0.004546	0.172

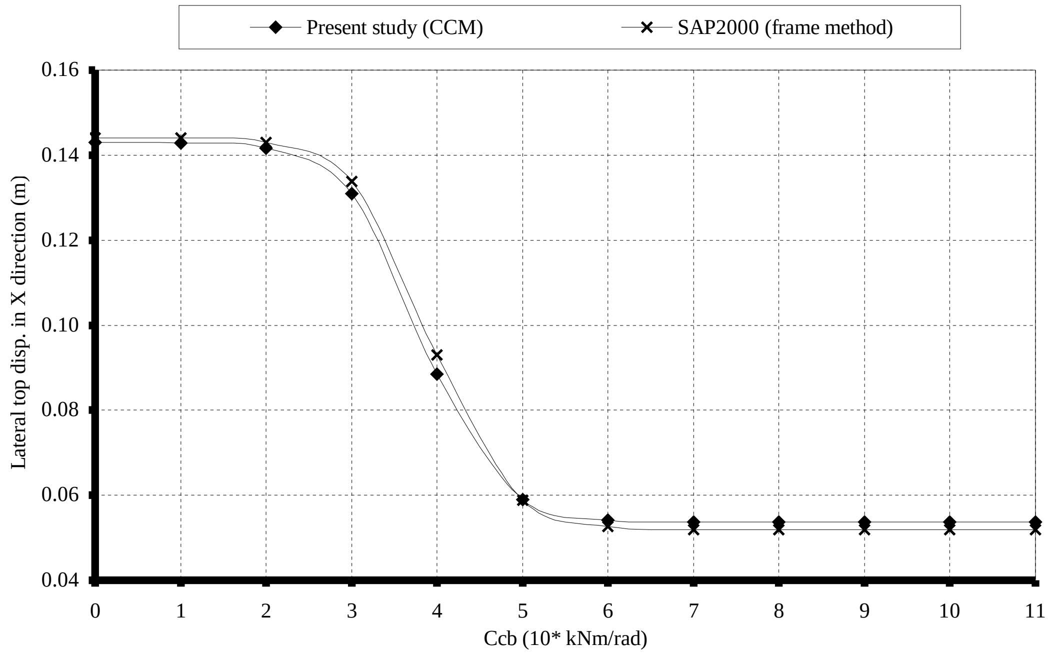

Figure 6.54. The effect of the variation of the connection stiffness on the maximum top displacement in the X direction in Example 15

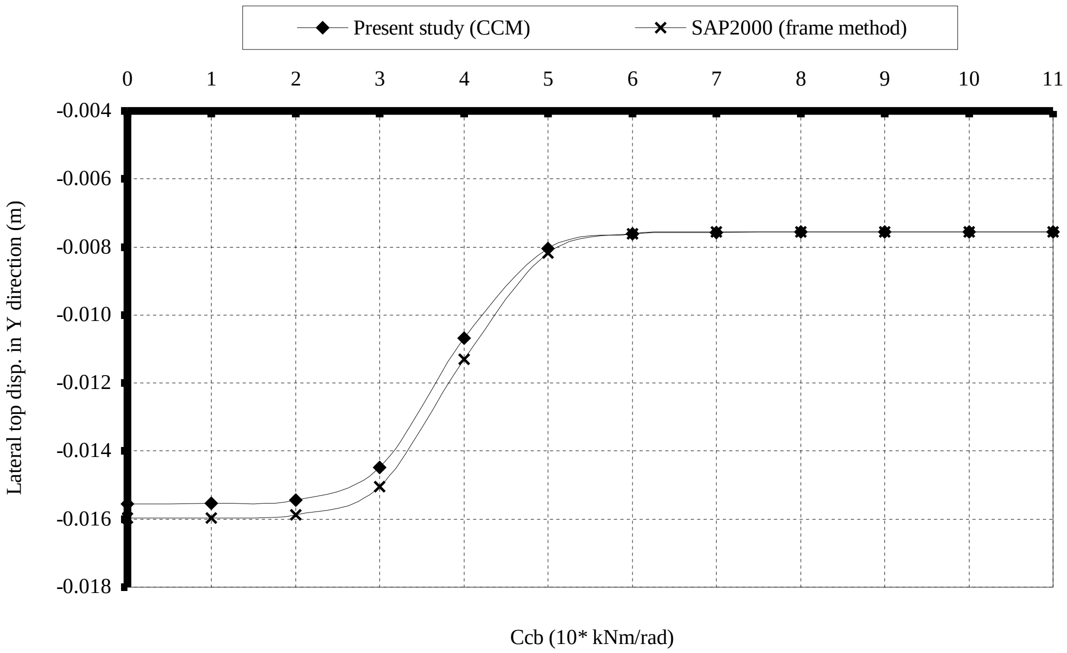

Figure 6.55. The effect of the variation of the connection stiffness on the maximum top displacement in the Y direction in Example 15

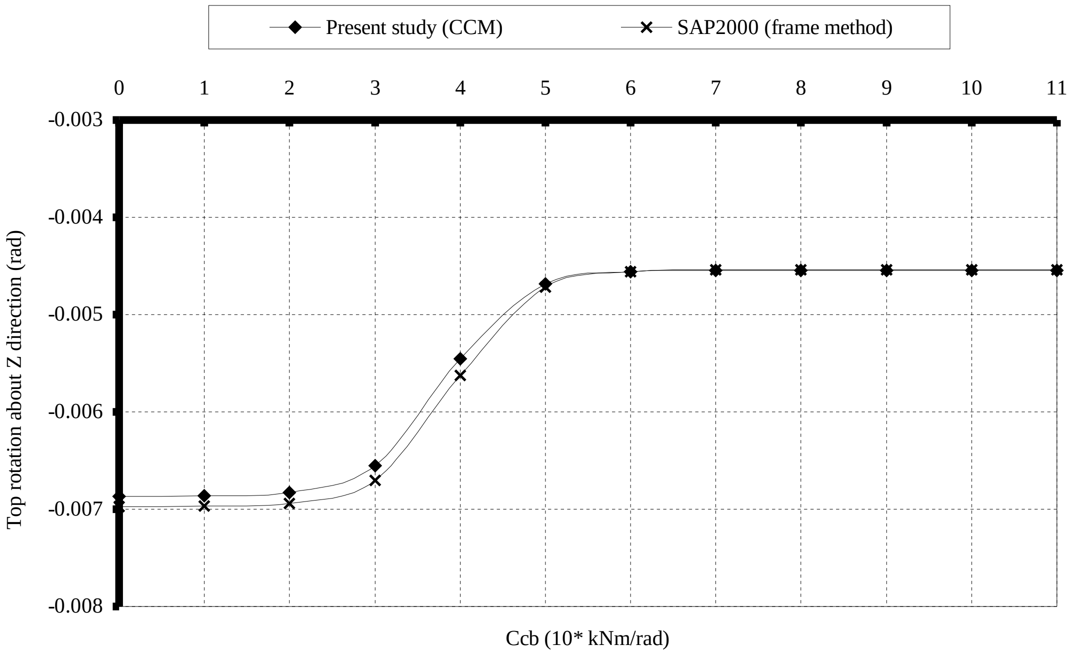

Figure 6.56. The effect of the variation of the connection stiffness on the maximum top rotation about the Z direction in example 15

Example 16:

In this example, a non-planar non-symmetrical coupled shear wall with a cross-section as shown in Fig. 6.58 is considered. The structure is composed of three regions having different connection stiffnesses which are starting from the top $1x10^3$ kNm/rad, $2x10^3$ kNm/rad and $3x10^3$ kNm/rad, respectively (see Fig. 6.58). The total height of the shear wall is 48 m, the storey height is 3 m, the thickness of the wall is 0.4 m, the height of the connecting beams is 0.5 m and the elasticity and shear moduli are $E = 2.85x10^6$ kN/m^2 and $G = 1055556$ kN/m^2, respectively. The concentrated horizontal force 250 kN acts at the top of the shear wall as seen in Figs. 6.57-58.

The comparison of the lateral displacements and the rotations, found by the present program and SAP2000, are presented in Tables 6.53-55, expressing the percentage differences. The results found are given in Figs. 6.59-61, also.

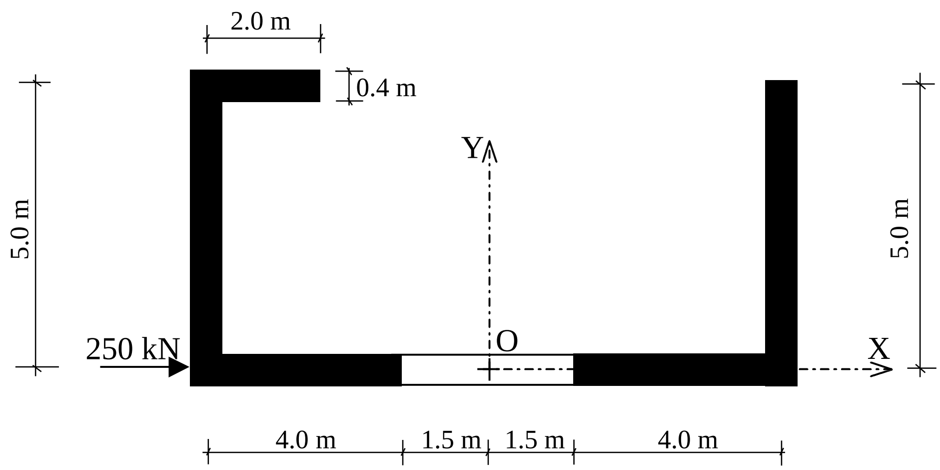

Figure 6.57. Cross-sectional view of the structure in Example 16

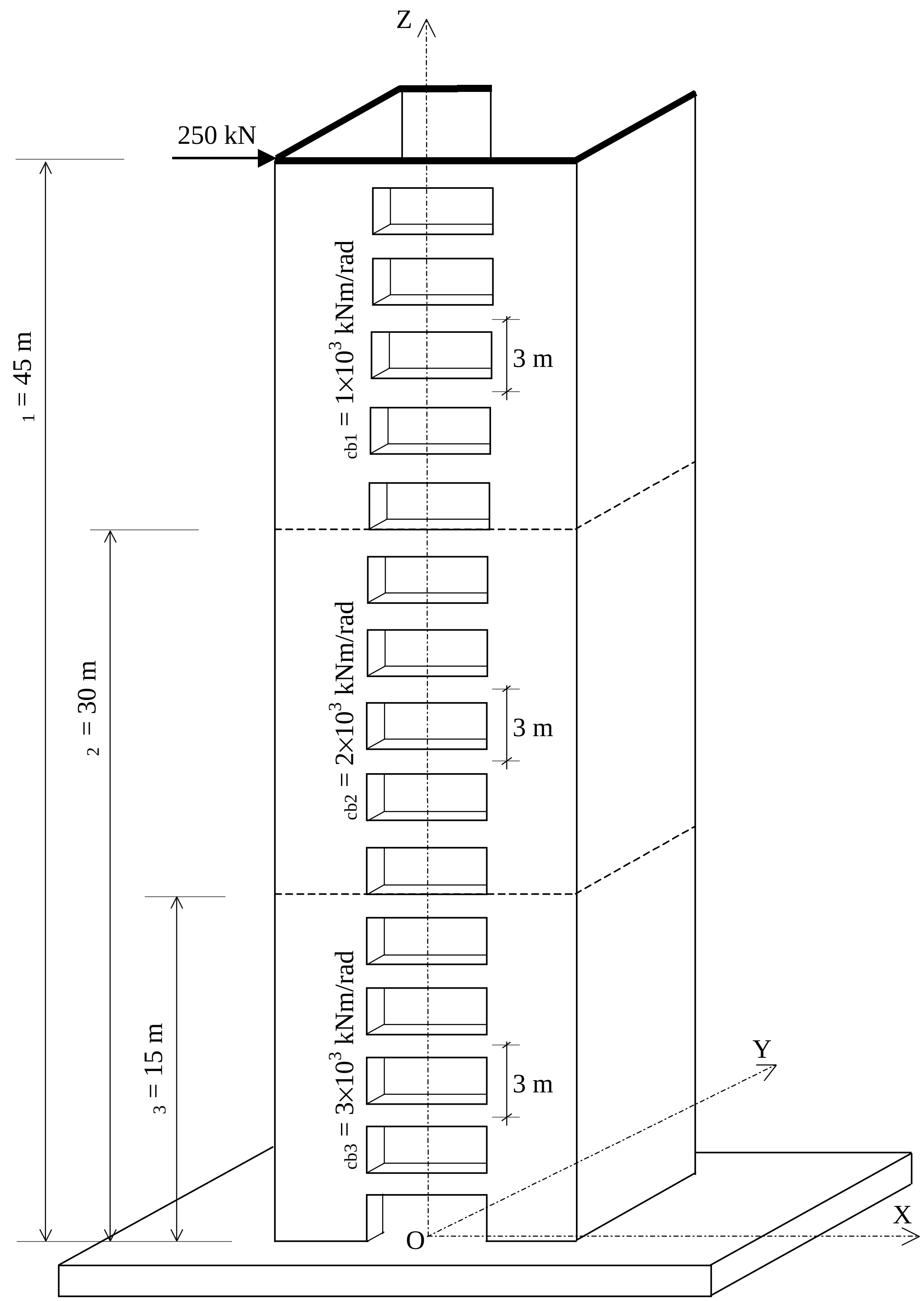

Figure 6.58. Geometrical properties and loading of the structure in Example 16

Table 6.53. Comparison of the lateral displacements in the X direction obtained from the present program and SAP2000 in Example 16

Storey number	Storey height (m)	SAP2000 (frame method)	Present study (CCM)	
		Lateral displacement (m)	Lateral displacement (m)	% difference of present study compared to SAP2000
15	45.0	0.237582	0.229247	3.508
14	42.0	0.213883	0.206332	3.530
13	39.0	0.190385	0.183625	3.551
12	36.0	0.167308	0.161334	3.571
11	33.0	0.144870	0.139667	3.591
10	30.0	0.123289	0.118836	3.612
9	27.0	0.102775	0.099046	3.628
8	24.0	0.083525	0.080488	3.635
7	21.0	0.065743	0.063352	3.637
6	18.0	0.049634	0.047830	3.634
5	15.0	0.035409	0.034123	3.631
4	12.0	0.023278	0.022434	3.625
3	9.0	0.013449	0.012963	3.610
2	6.0	0.006140	0.005919	3.601
1	3.0	0.001577	0.001520	3.602
0	0.0	0.000000	0.000000	0.000

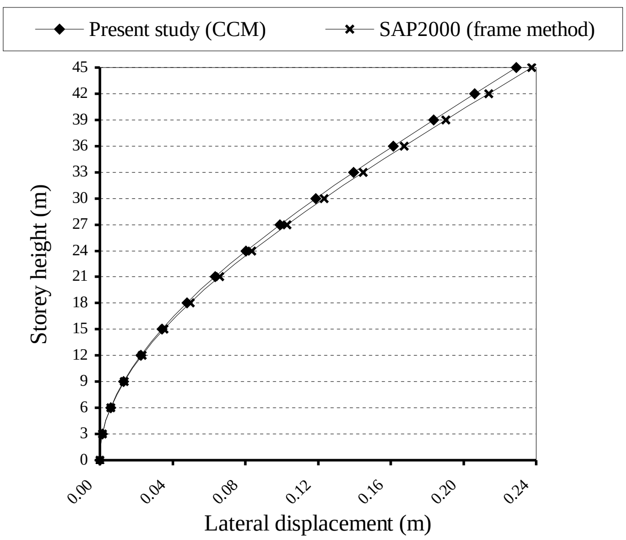

Figure 6.59. The lateral displacements in the X direction in Example16

Table 6.54. Comparison of the lateral displacements in the Y direction obtained from the present program and SAP2000 in Example 16

Storey number	Storey height (m)	SAP2000 (frame method)	Present study (CCM)	
		Lateral displacement (m)	Lateral displacement (m)	% difference of present study compared to SAP2000
15	45.0	-0.026023	-0.024696	5.101
14	42.0	-0.023441	-0.022242	5.114
13	39.0	-0.020880	-0.019811	5.121
12	36.0	-0.018364	-0.017422	5.129
11	33.0	-0.015916	-0.015098	5.137
10	30.0	-0.013559	-0.012862	5.143
9	27.0	-0.011316	-0.010734	5.147
8	24.0	-0.009208	-0.008735	5.142
7	21.0	-0.007257	-0.006885	5.125
6	18.0	-0.005486	-0.005206	5.097
5	15.0	-0.003919	-0.003721	5.063
4	12.0	-0.002580	-0.002450	5.026
3	9.0	-0.001493	-0.001418	4.993
2	6.0	-0.000682	-0.000649	4.862
1	3.0	-0.000175	-0.000167	4.592
0	0.0	0.000000	0.000000	0.000

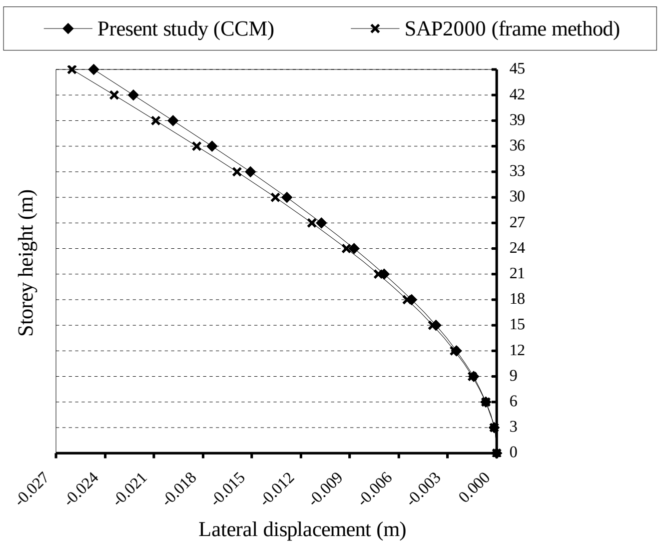

Figure 6.60. The lateral displacements in the Y direction in Example 16

Table 6.55. Comparison of the rotations about the Z direction obtained from the present program and SAP2000 in Example 16

Storey number	Storey height (m)	SAP2000 (frame method)	Present study (CCM)	
		Rotation (rad)	Rotation (rad)	% difference of present study compared to SAP2000
15	45.0	-0.011868	-0.011498	3.122
14	42.0	-0.010690	-0.010356	3.121
13	39.0	-0.009523	-0.009225	3.127
12	36.0	-0.008376	-0.008114	3.130
11	33.0	-0.007260	-0.007032	3.135
10	30.0	-0.006185	-0.005991	3.136
9	27.0	-0.005162	-0.005000	3.143
8	24.0	-0.004200	-0.004068	3.137
7	21.0	-0.003310	-0.003206	3.132
6	18.0	-0.002502	-0.002424	3.117
5	15.0	-0.001787	-0.001732	3.096
4	12.0	-0.001176	-0.001140	3.069
3	9.0	-0.000680	-0.000659	3.024
2	6.0	-0.000311	-0.000301	3.088
1	3.0	-0.000080	-0.000077	2.904
0	0.0	0.000000	0.000000	0.000

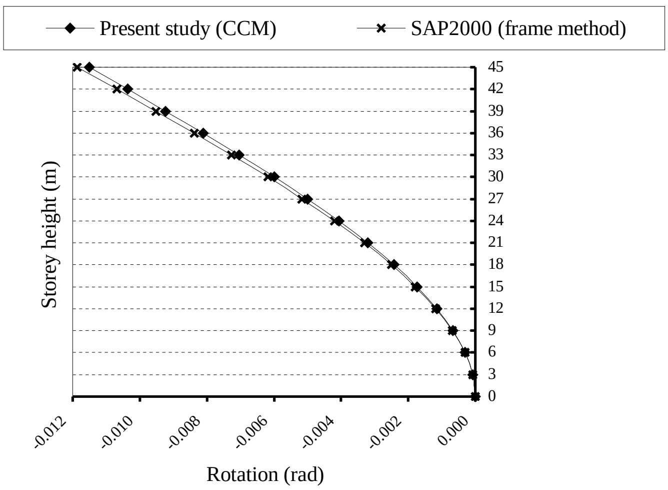

Figure 6.61. The rotations about the Z direction in Example 16

Example 17:

In this example, a non-planar coupled shear wall model considered by Tso and Biswas (1973) has been solved when St. Venant's torsional effect is neglected to find its effect on the deformations. The total height of the shear wall is 48 in, the storey height is 6 in, the thickness of the wall is 0.39 in, the height of the connecting beams is 1.5 in and the elasticity and shear moduli of the structure are $E = 0.40x10^6$ psi and $G = 0.148x10^6$ psi, respectively. The model rests on a rigid base and is loaded by a horizontal force 25 lb, in the plane of the connecting beams acting at the top as shown in Fig. 6.62.

The comparison of the lateral displacements and rotations along the height and the axial forces at the bottom found by the present program and SAP2000 are presented in Tables 6.56-58, expressing the percentage differences. The results found are given in Figs. 6.63-64, also.

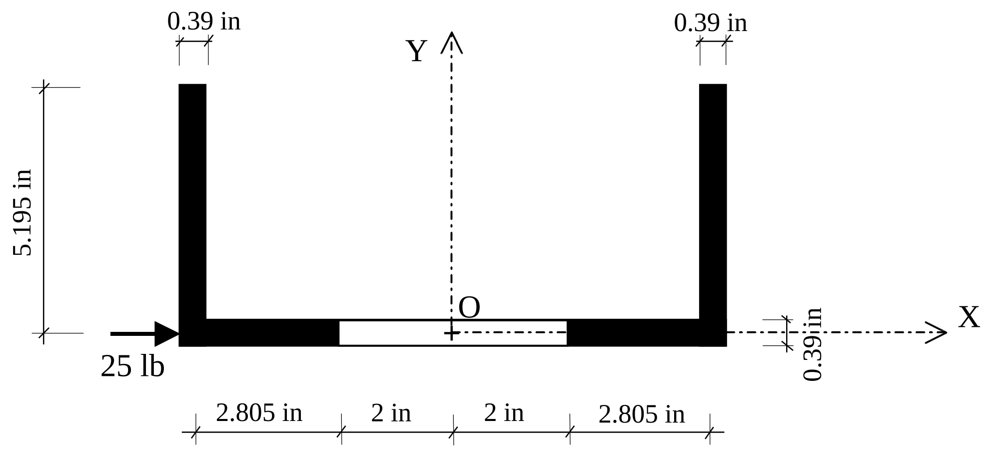

Figure 6.62. Cross-sectional view of the model structure in Example 17

Table 6.56. Comparison of the lateral displacements in the X direction obtained from the present program and SAP2000 in Example 17

Lateral displacements in X direction (inch)								
Storey number	Storey height (inch)	Present study (CCM)			SAP2000 (frame method)			Exp. study (Tso&Biswas)
		Torsional stiffness included	Torsional stiffness ignored	% difference	Torsional stiffness included	Torsional stiffness ignored	% difference	
8	48	0.055694	0.062739	12.650	0.058410	0.065032	11.337	0.074678
7	42	0.046195	0.051882	12.310	0.048923	0.054275	10.940	0.059742
6	36	0.036914	0.041291	11.857	0.039268	0.043392	10.502	0.047639
5	30	0.028068	0.031234	11.280	0.029951	0.032936	9.966	–
4	24	0.019883	0.021980	10.548	0.021282	0.023260	9.294	0.024206
3	18	0.012594	0.013808	9.641	0.013527	0.014672	8.465	–
2	12	0.006480	0.007031	8.509	0.006989	0.007509	7.440	0.007983
1	6	0.001960	0.002100	7.160	0.002132	0.002264	6.191	–
0	0	0.000000	0.000000	0.000	0.000000	0.000000	0.000	0.000000

Table 6.57. Comparison of the rotations about the Z direction obtained from the present program and SAP2000 in Example 17

Rotation about Z direction (rad)								
Storey number	Storey height (inch)	Present study (CCM)			SAP2000 (frame method)			Exp. study (Tso&Biswas)
		Torsional stiffness included	Torsional stiffness ignored	% difference	Torsional stiffness included	Torsional stiffness ignored	% difference	
8	48	-0.010507	-0.013853	31.846	-0.010912	-0.014029	28.565	-0.011083
7	42	-0.008607	-0.011305	31.352	-0.008956	-0.011472	28.093	-0.008994
6	36	-0.006759	-0.008835	30.711	-0.007039	-0.008975	27.504	-0.007567
5	30	-0.005018	-0.006518	29.887	-0.005229	-0.006627	26.736	–
4	24	-0.003439	-0.004431	28.854	-0.003586	-0.004511	25.795	-0.005019
3	18	-0.002079	-0.002653	27.599	-0.002170	-0.002704	24.608	–
2	12	-0.001001	-0.001261	25.982	-0.001046	-0.001288	23.136	-0.001299
1	6	-0.000275	-0.000341	23.965	-0.000288	-0.000350	21.528	–
0	0	0.000000	0.000000	0.000	0.000000	0.000000	0.000	0.000000

Table 6.58. Comparison of the axial forces at the bottom obtained from the present program and SAP2000 in Example 17

Axial forces at the bottom (lb)					
Present study (CCM)			SAP2000 (frame method)		
Torsional stiffness included	Torsional stiffness ignored	% difference	Torsional stiffness included	Torsional stiffness ignored	% difference
130.539	133.187	2.029	128.209	130.664	1.915

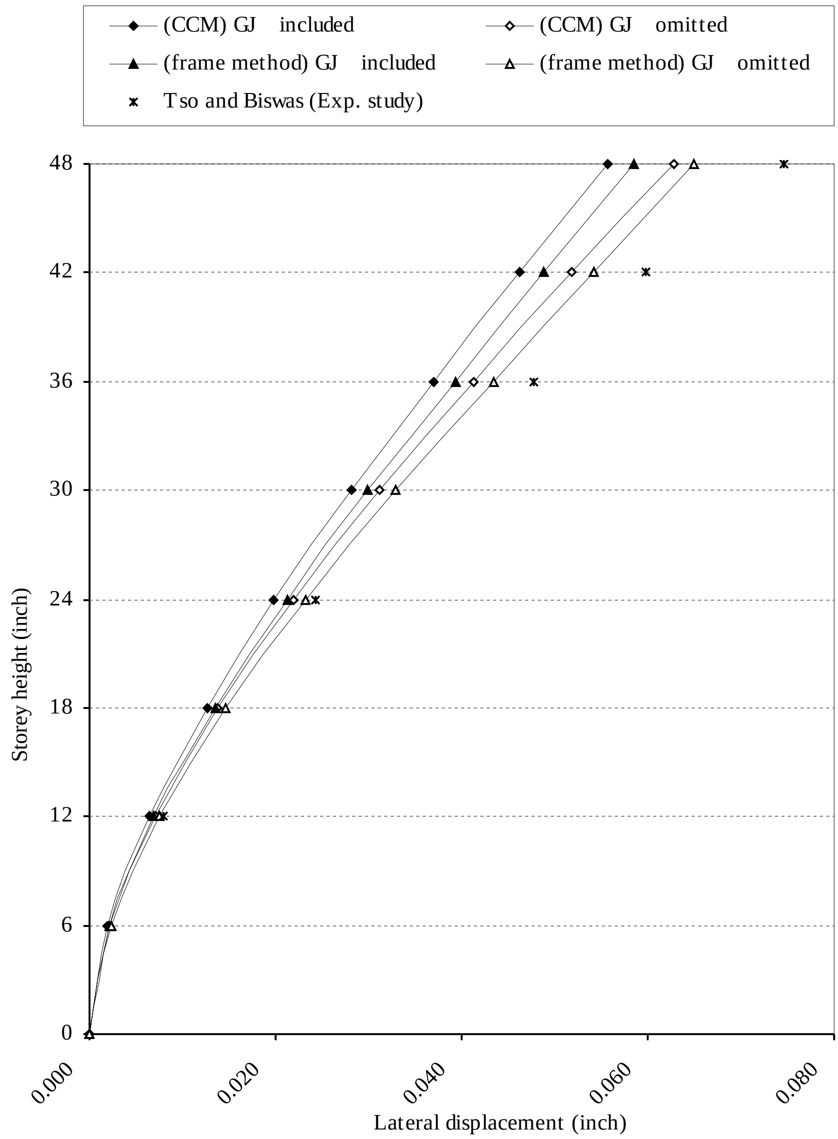

Figure 6.63. The lateral displacements in the X direction in Example 17

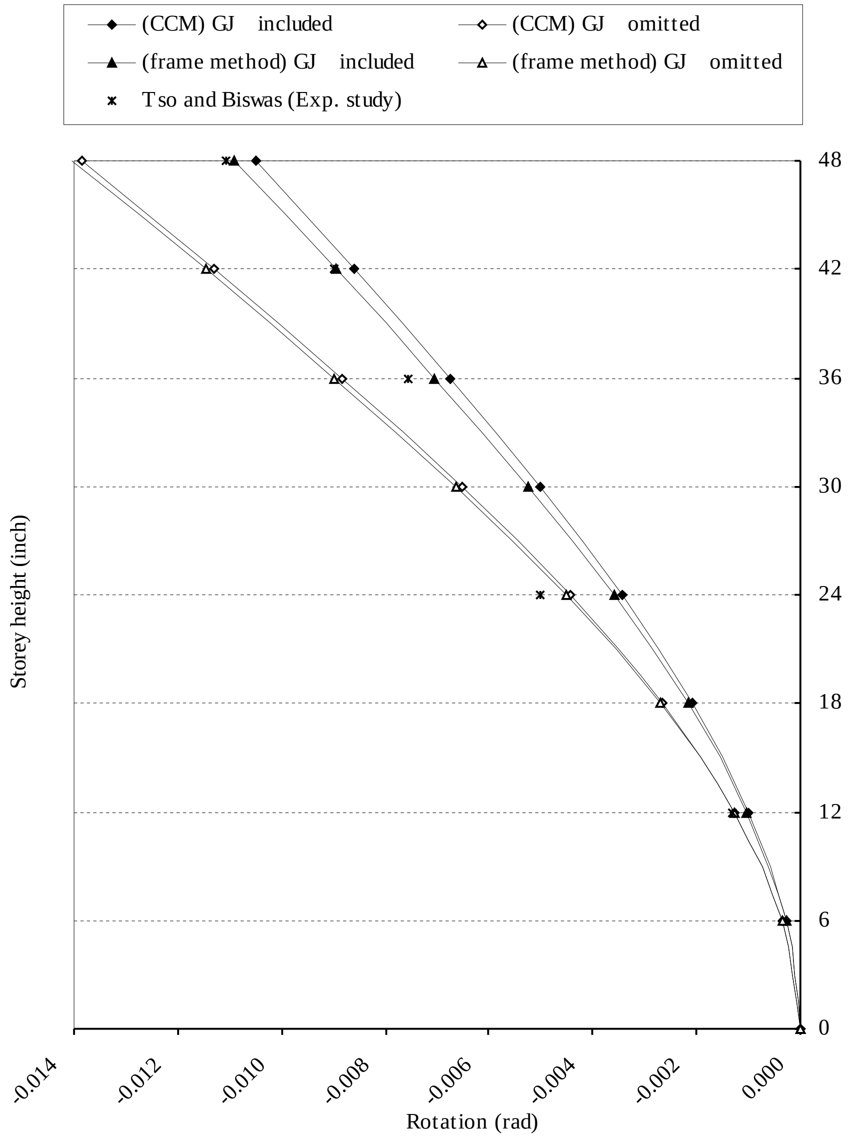

Figure 6.64. The rotations about the Z direction in Example 17

Example 18:

In this example, a non-planar coupled non-symmetrical coupled shear wall with a cross-section as shown in Fig. 6.65 is considered. The system has been solved when St. Venant's torsional effect is neglected to find its influence on the deformations. The total height of the shear wall is 48 m, the storey height is 3 m, the thickness of the wall is 0.4 m, the height of the connecting beams is 0.5 m and the elasticity and shear moduli are $E = 2.85x10^6$ kN/m^2 and $G = 1055556$ kN/m^2, respectively. The concentrated horizontal force 250 kN acts at the top of the shear wall.

The comparison of the lateral displacements and the rotations along the height and the axial forces at the bottom, found by the present program and SAP2000, are presented in Tables 6.59-62, expressing the percentage differences. The results found are given in Figs. 6.66-68, also.

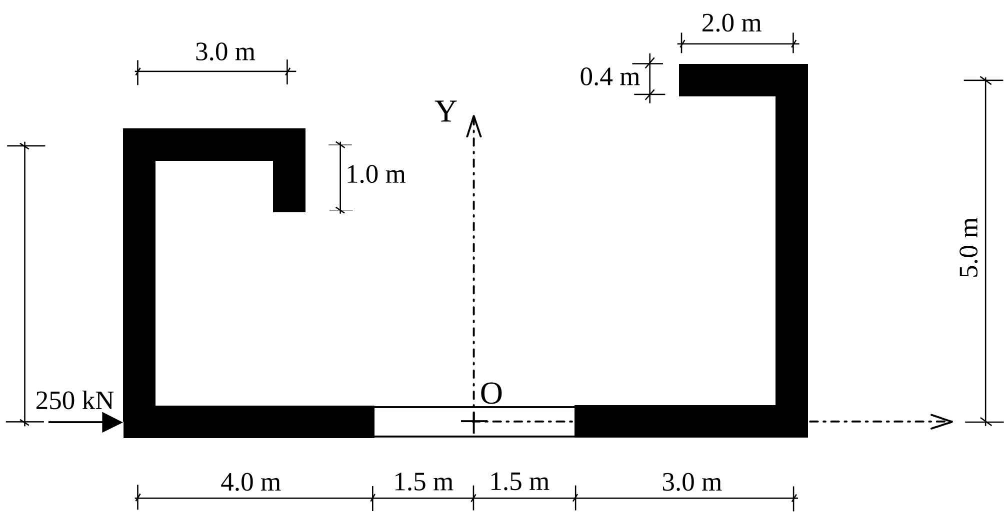

Figure 6.65. Cross-sectional view of the structure in Example 18

Table 6.59. Comparison of the lateral displacements in the X direction obtained from the present program and SAP2000 in Example 18

Lateral displacements in X direction (m)							
Storey number	Storey height (m)	Present study (CCM)			SAP2000 (frame method)		
		Torsional stiffness included	Torsional stiffness ignored	% difference	Torsional stiffness included	Torsional stiffness ignored	% difference
16	48.0	0.095731	0.096895	1.217	0.094538	0.095645	1.171
15	45.0	0.087317	0.088368	1.203	0.086435	0.087432	1.153
14	42.0	0.078951	0.079888	1.188	0.078313	0.079201	1.134
13	39.0	0.070678	0.071505	1.170	0.070231	0.071014	1.115
12	36.0	0.062549	0.063268	1.150	0.062248	0.062928	1.092
11	33.0	0.054613	0.055229	1.128	0.054423	0.055005	1.069
10	30.0	0.046924	0.047442	1.103	0.046816	0.047305	1.045
9	27.0	0.039541	0.039967	1.077	0.039490	0.039892	1.018
8	24.0	0.032525	0.032867	1.049	0.032513	0.032835	0.990
7	21.0	0.025946	0.026211	1.019	0.025958	0.026208	0.963
6	18.0	0.019880	0.020076	0.988	0.019904	0.020089	0.929
5	15.0	0.014412	0.014549	0.955	0.014440	0.014570	0.900
4	12.0	0.009639	0.009728	0.920	0.009666	0.009749	0.859
3	9.0	0.005673	0.005723	0.885	0.005694	0.005741	0.825
2	6.0	0.002642	0.002664	0.848	0.002655	0.002676	0.791
1	3.0	0.000693	0.000698	0.810	0.000698	0.000704	0.860
0	0.0	0.000000	0.000000	0.000	0.000000	0.000000	0.000

Table 6.60. Comparison of the lateral displacements in the Y direction obtained from the present program and SAP2000 in Example 18

Lateral displacements in Y direction (m)							
Storey number	Storey height (m)	Present study (CCM)			SAP2000 (frame method)		
		Torsional stiffness included	Torsional stiffness ignored	% difference	Torsional stiffness included	Torsional stiffness ignored	% difference
16	48.0	-0.008511	-0.008839	3.858	-0.008478	-0.008781	3.574
15	45.0	-0.007720	-0.008016	3.837	-0.007691	-0.007964	3.550
14	42.0	-0.006935	-0.007199	3.813	-0.006909	-0.007153	3.532
13	39.0	-0.006161	-0.006395	3.784	-0.006139	-0.006354	3.502
12	36.0	-0.005406	-0.005609	3.752	-0.005386	-0.005574	3.491
11	33.0	-0.004675	-0.004849	3.716	-0.004658	-0.004818	3.435
10	30.0	-0.003974	-0.004120	3.677	-0.003959	-0.004094	3.410
9	27.0	-0.003309	-0.003429	3.633	-0.003296	-0.003407	3.368
8	24.0	-0.002687	-0.002783	3.586	-0.002676	-0.002764	3.288
7	21.0	-0.002113	-0.002187	3.535	-0.002104	-0.002172	3.232
6	18.0	-0.001594	-0.001649	3.480	-0.001586	-0.001637	3.216
5	15.0	-0.001136	-0.001175	3.422	-0.001130	-0.001166	3.186
4	12.0	-0.000746	-0.000771	3.360	-0.000742	-0.000765	3.100
3	9.0	-0.000430	-0.000444	3.294	-0.000427	-0.000441	3.279
2	6.0	-0.000196	-0.000202	3.225	-0.000194	-0.000200	3.093
1	3.0	-0.000050	-0.000052	3.154	-0.000049	-0.000051	3.441
0	0.0	0.000000	0.000000	0.000	0.000000	0.000000	0.000

Table 6.61. Comparison of the rotations about the Z direction obtained from the present program and SAP2000 in Example 18

Rotations about Z direction (rad)							
Storey number	Storey height (m)	Present study (CCM)			SAP2000 (frame method)		
		Torsional stiffness included	Torsional stiffness ignored	% difference	Torsional stiffness included	Torsional stiffness ignored	% difference
16	48.0	-0.004497	-0.005056	12.432	-0.004614	-0.005136	11.313
15	45.0	-0.004062	-0.004566	12.417	-0.004162	-0.004633	11.317
14	42.0	-0.003630	-0.004081	12.399	-0.003716	-0.004136	11.302
13	39.0	-0.003207	-0.003604	12.380	-0.003280	-0.003650	11.280
12	36.0	-0.002795	-0.003140	12.358	-0.002856	-0.003179	11.310
11	33.0	-0.002398	-0.002694	12.335	-0.002449	-0.002725	11.270
10	30.0	-0.002021	-0.002270	12.312	-0.002063	-0.002295	11.246
9	27.0	-0.001666	-0.001871	12.288	-0.001700	-0.001891	11.235
8	24.0	-0.001337	-0.001501	12.266	-0.001364	-0.001517	11.217
7	21.0	-0.001038	-0.001166	12.246	-0.001059	-0.001178	11.237
6	18.0	-0.000772	-0.000867	12.229	-0.000787	-0.000875	11.182
5	15.0	-0.000542	-0.000608	12.219	-0.000552	-0.000614	11.232
4	12.0	-0.000349	-0.000392	12.216	-0.000356	-0.000396	11.236
3	9.0	-0.000197	-0.000222	12.223	-0.000201	-0.000224	11.443
2	6.0	-0.000088	-0.000099	12.245	-0.000090	-0.000100	11.483
1	3.0	-0.000022	-0.000025	12.284	-0.000022	-0.000025	11.161
0	0.0	0.000000	0.000000	0.000	0.000000	0.000000	0.000

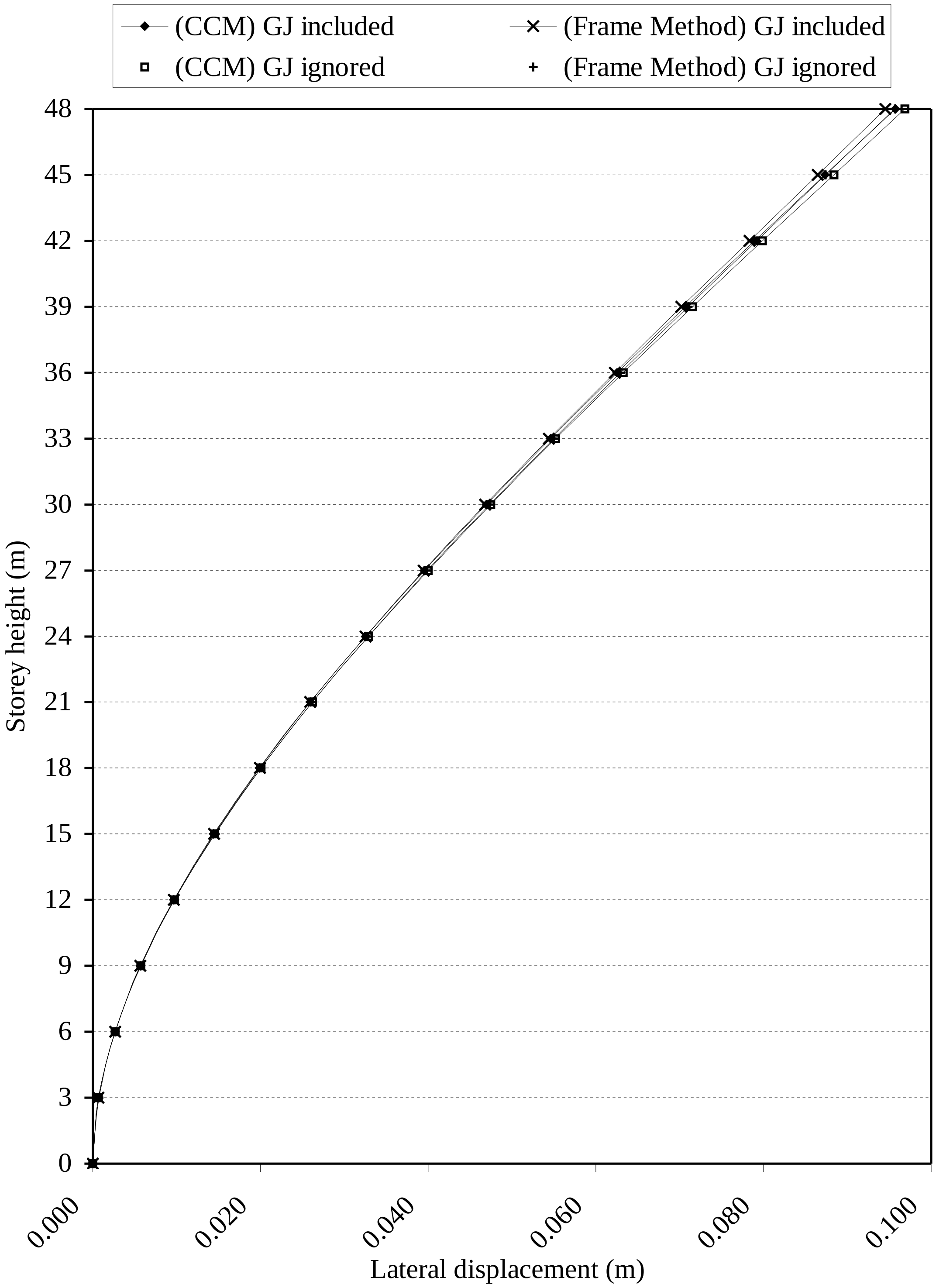

Figure 6.66. The lateral displacements in the X direction in Example 18

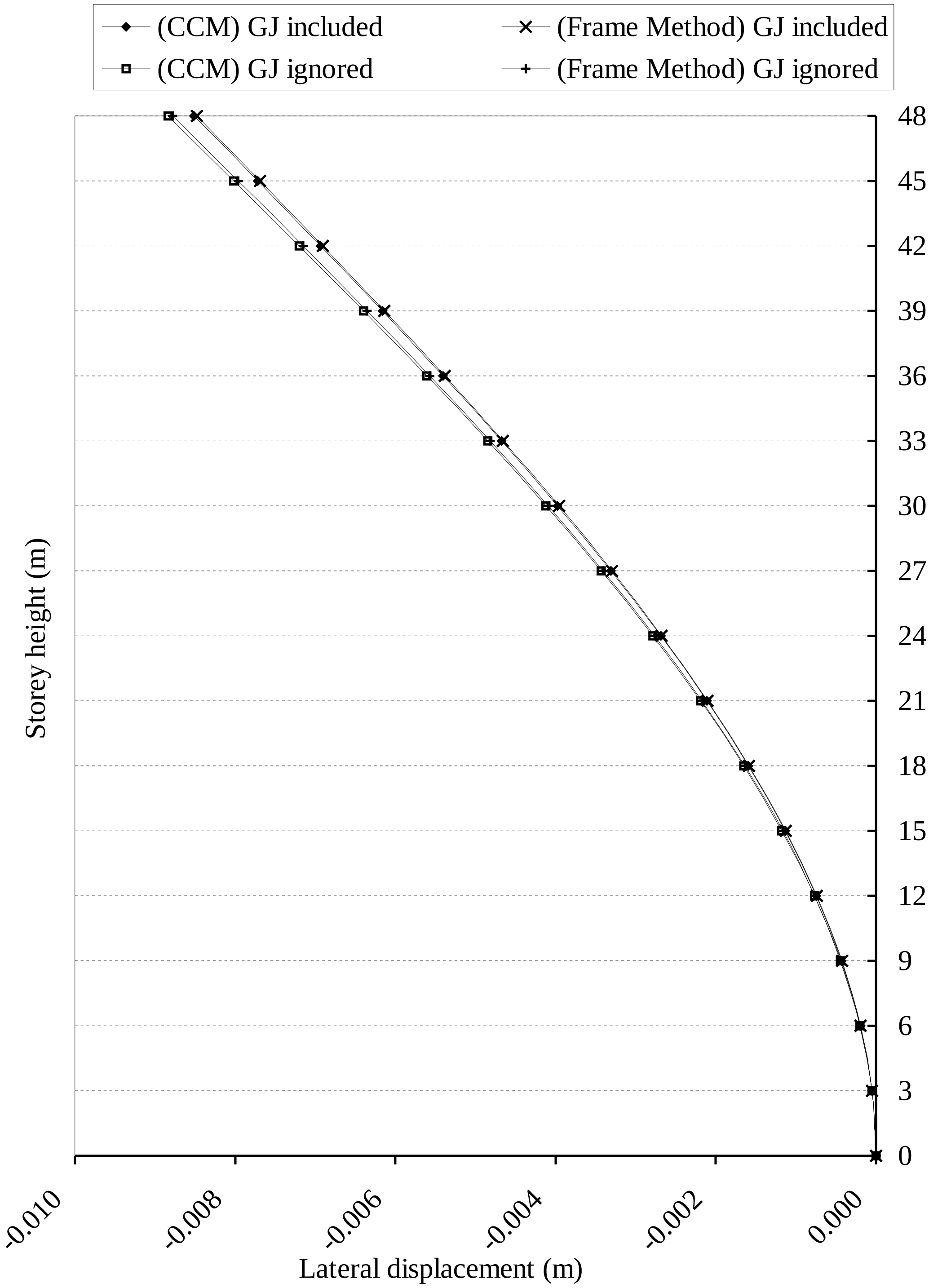

Figure 6.67. The lateral displacements in the Y direction in Example 18

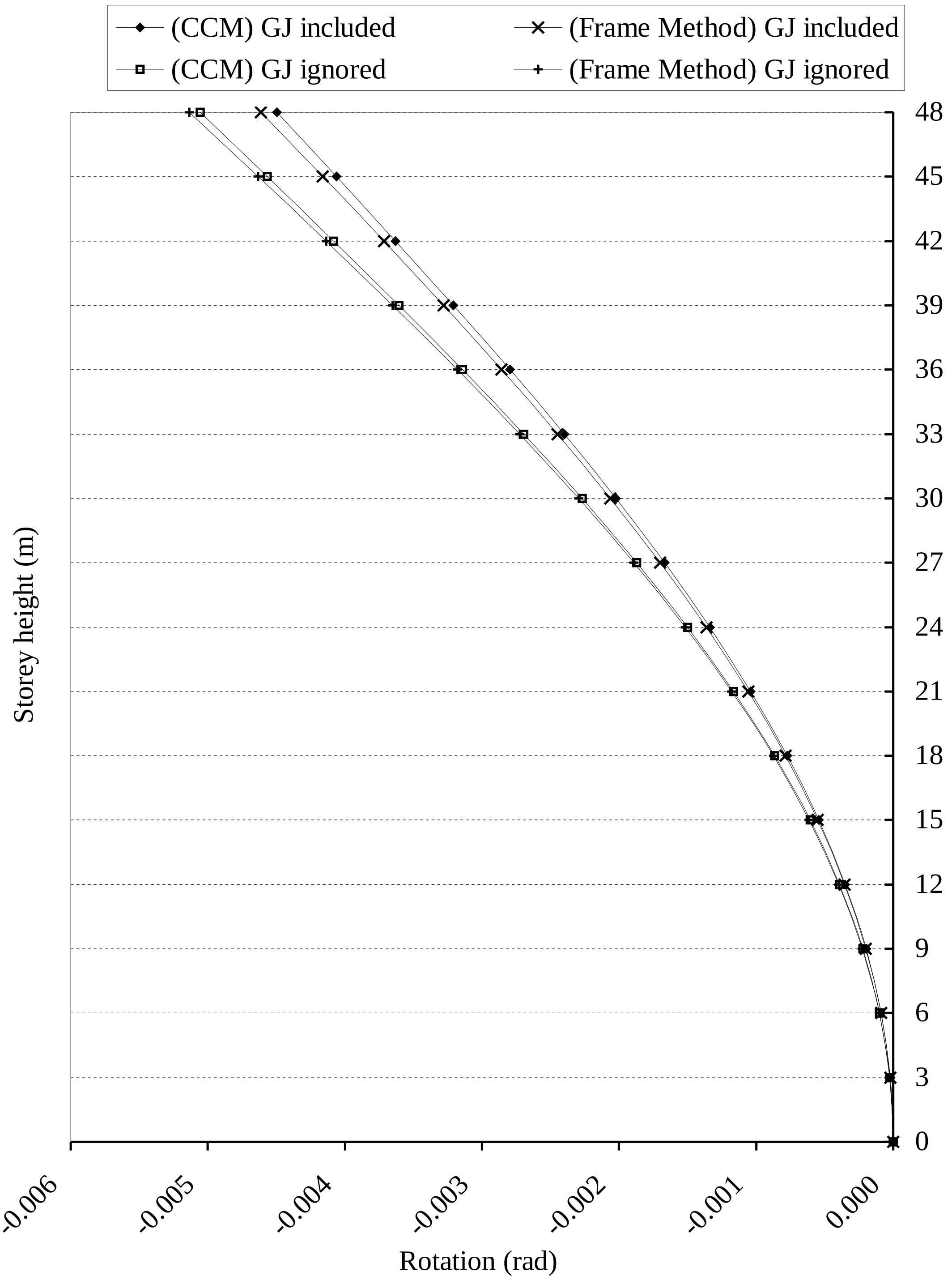

Figure 6.68. The rotations about the Z direction in Example 18

Table 6.62. Comparison of the axial forces at the bottom obtained from the present program and SAP2000 in Example 18

Axial forces at the bottom (kN)					
Present study (CCM)			SAP2000 (frame method)		
Torsional stiffness included	Torsional stiffness ignored	% difference	Torsional stiffness included	Torsional stiffness ignored	% difference
863.808	858.074	0.664	867.012	861.723	0.610

Example 19:

In this example, a non-planar non-symmetrical coupled shear wall with a cross-section as shown in Fig. 6.69 is considered. The system has been solved when St. Venant's torsional effect is neglected to find its effect on the deformations. The total height of the shear wall is 48 m, the storey height is 3 m, the thickness of the wall is 0.4 m, the height of the connecting beams is 0.5 m and the elasticity and shear moduli are $E = 2.85x10^6$ kN/m^2 and $G = 1055556$ kN/m^2, respectively. The loading comprises a 250 kN and a 350 kN concentrated horizontal forces as shown in the figure.

The comparison of the axial forces at the bottom, the lateral displacements and the rotations along the height, found by the present program and SAP2000, are presented in Tables 6.63-66, expressing the percentage differences. The results found are given in Fig. 6.70-72, also.

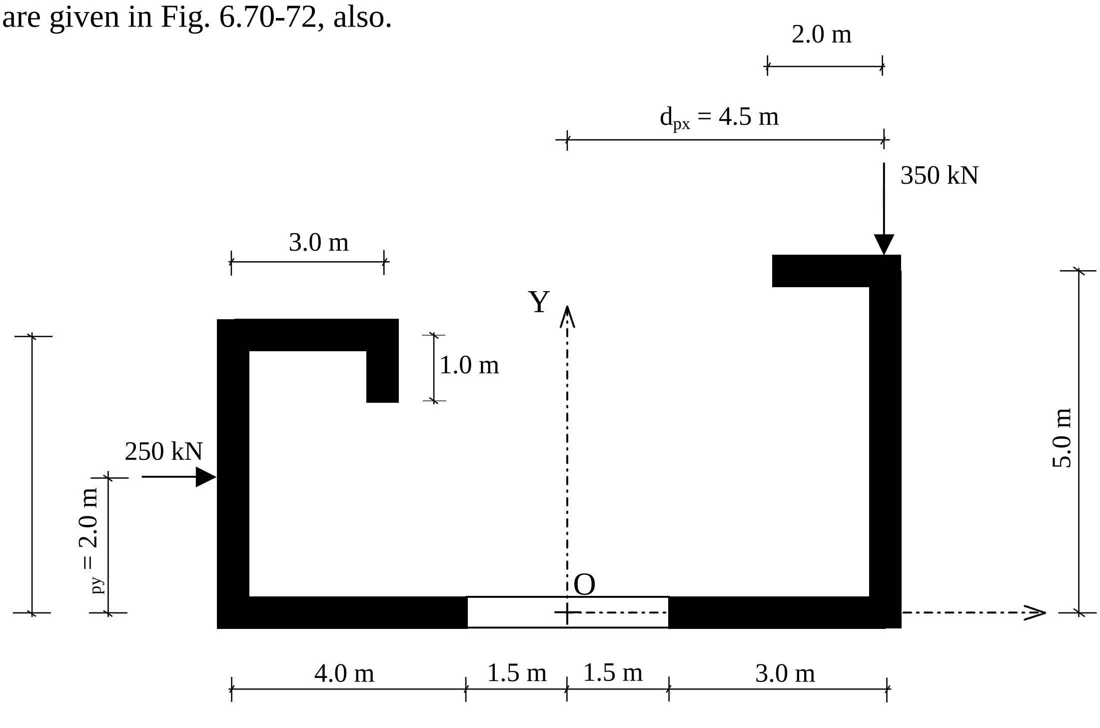

Figure 6.69. Cross-sectional view of the structure in Example 19

Table 6.63. Comparison of the axial forces at the bottom obtained from the present program and SAP2000 in Example 19

Axial forces at the bottom (kN)					
Present study (CCM)			SAP2000 (frame method)		
Torsional stiffness included	Torsional stiffness ignored	% difference	Torsional stiffness included	Torsional stiffness ignored	% difference
682.322	651.376	4.536	685.502	657.371	4.104

Table 6.64. Comparison of the lateral displacements in the X direction obtained from the present program and SAP2000 in Example 19

Lateral displacements in the X direction (m)							
Storey no	Storey height (m)	Present study (CCM)			SAP2000 (frame method)		
		Torsional stiffness included	Torsional stiffness ignored	% diff.	Torsional stiffness included	Torsional stiffness ignored	% diff.
16	48.0	0.144970	0.151235	4.321	0.144705	0.150567	4.051
15	45.0	0.131837	0.137489	4.287	0.131754	0.137036	4.009
14	42.0	0.118792	0.123836	4.246	0.118839	0.123548	3.963
13	39.0	0.105921	0.110369	4.200	0.106057	0.110206	3.912
12	36.0	0.093315	0.097185	4.147	0.093506	0.097113	3.858
11	33.0	0.081063	0.084378	4.089	0.081284	0.084370	3.797
10	30.0	0.069260	0.072047	4.024	0.069489	0.072083	3.733
9	27.0	0.058001	0.060295	3.954	0.058222	0.060356	3.665
8	24.0	0.047387	0.049225	3.878	0.047589	0.049298	3.591
7	21.0	0.037523	0.038947	3.796	0.037698	0.039023	3.515
6	18.0	0.028520	0.029578	3.709	0.028664	0.029647	3.429
5	15.0	0.020497	0.021238	3.616	0.020608	0.021297	3.343
4	12.0	0.013582	0.014060	3.519	0.013661	0.014105	3.250
3	9.0	0.007915	0.008185	3.416	0.007964	0.008216	3.164
2	6.0	0.003646	0.003767	3.309	0.003672	0.003784	3.050
1	3.0	0.000946	0.000976	3.198	0.000954	0.000982	2.935
0	0.0	0.000000	0.000000	0.000	0.000000	0.000000	0.000

Table 6.65. Comparison of the lateral displacements in the Y direction obtained from the present program and SAP2000 in Example 19

Lateral displacements in the Y direction (m)							
Storey no	Storey height (m)	Present study (CCM)			SAP2000 (frame method)		
		Torsional stiffness included	Torsional stiffness ignored	% diff.	Torsional stiffness included	Torsional stiffness ignored	% diff.
16	48.0	-0.167053	-0.168821	1.058	-0.167922	-0.169530	0.958
15	45.0	-0.151423	-0.153018	1.053	-0.152213	-0.153663	0.953
14	42.0	-0.135914	-0.137338	1.048	-0.136626	-0.137921	0.948
13	39.0	-0.120649	-0.121906	1.042	-0.121283	-0.122426	0.942
12	36.0	-0.105750	-0.106844	1.035	-0.106308	-0.107303	0.936
11	33.0	-0.091338	-0.092276	1.027	-0.091823	-0.092675	0.928
10	30.0	-0.077537	-0.078326	1.018	-0.077950	-0.078668	0.921
9	27.0	-0.064467	-0.065117	1.008	-0.064813	-0.065404	0.912
8	24.0	-0.052251	-0.052772	0.997	-0.052535	-0.053008	0.900
7	21.0	-0.041012	-0.041416	0.986	-0.041237	-0.041605	0.892
6	18.0	-0.030872	-0.031173	0.973	-0.031045	-0.031318	0.879
5	15.0	-0.021954	-0.022165	0.960	-0.022080	-0.022271	0.865
4	12.0	-0.014381	-0.014517	0.946	-0.014466	-0.014590	0.857
3	9.0	-0.008275	-0.008352	0.930	-0.008327	-0.008397	0.841
2	6.0	-0.003760	-0.003795	0.914	-0.003787	-0.003818	0.819
1	3.0	-0.000961	-0.000969	0.897	-0.000970	-0.000978	0.825
0	0.0	0.000000	0.000000	0.000	0.000000	0.000000	0.000

Table 6.66. Comparison of the rotations about the Z direction obtained from the present program and SAP2000 in Example 19

Rotation about Z direction (rad)							
Storey no	Storey height (m)	Present study (CCM)			SAP2000 (frame method)		
		Torsional stiffness included	Torsional stiffness ignored	% diff.	Torsional stiffness included	Torsional stiffness ignored	% diff.
16	48.0	-0.024455	-0.027464	12.307	-0.024747	-0.027516	11.189
15	45.0	-0.022164	-0.024880	12.255	-0.022425	-0.024923	11.139
14	42.0	-0.019891	-0.022317	12.194	-0.020121	-0.022353	11.093
13	39.0	-0.017655	-0.019795	12.124	-0.017856	-0.019825	11.027
12	36.0	-0.015471	-0.017335	12.044	-0.015645	-0.017360	10.962
11	33.0	-0.013360	-0.014957	11.955	-0.013508	-0.014978	10.882
10	30.0	-0.011338	-0.012682	11.856	-0.011463	-0.012699	10.783
9	27.0	-0.009424	-0.010531	11.747	-0.009527	-0.010545	10.685
8	24.0	-0.007635	-0.008523	11.628	-0.007718	-0.008535	10.586
7	21.0	-0.005990	-0.006679	11.499	-0.006055	-0.006688	10.454
6	18.0	-0.004507	-0.005019	11.361	-0.004555	-0.005026	10.340
5	15.0	-0.003203	-0.003562	11.213	-0.003237	-0.003568	10.226
4	12.0	-0.002096	-0.002328	11.054	-0.002119	-0.002333	10.099
3	9.0	-0.001205	-0.001336	10.886	-0.001219	-0.001340	9.926
2	6.0	-0.000547	-0.000606	10.709	-0.000554	-0.000608	9.747
1	3.0	-0.000140	-0.000154	10.521	-0.000142	-0.000155	9.155
0	0.0	0.000000	0.000000	0.000	0.000000	0.000000	0.000

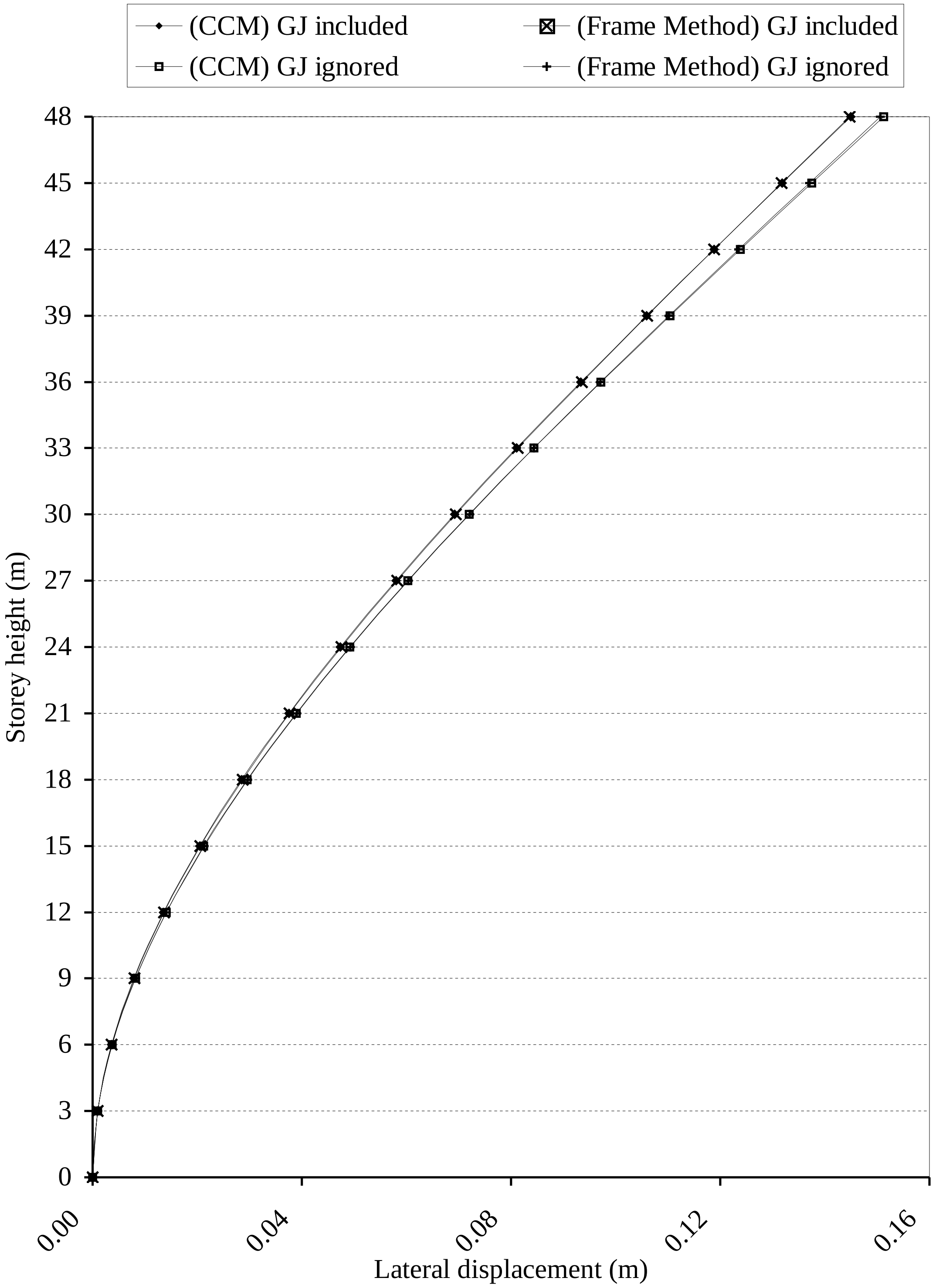

Figure 6.70. The lateral displacements in the X direction in Example 19

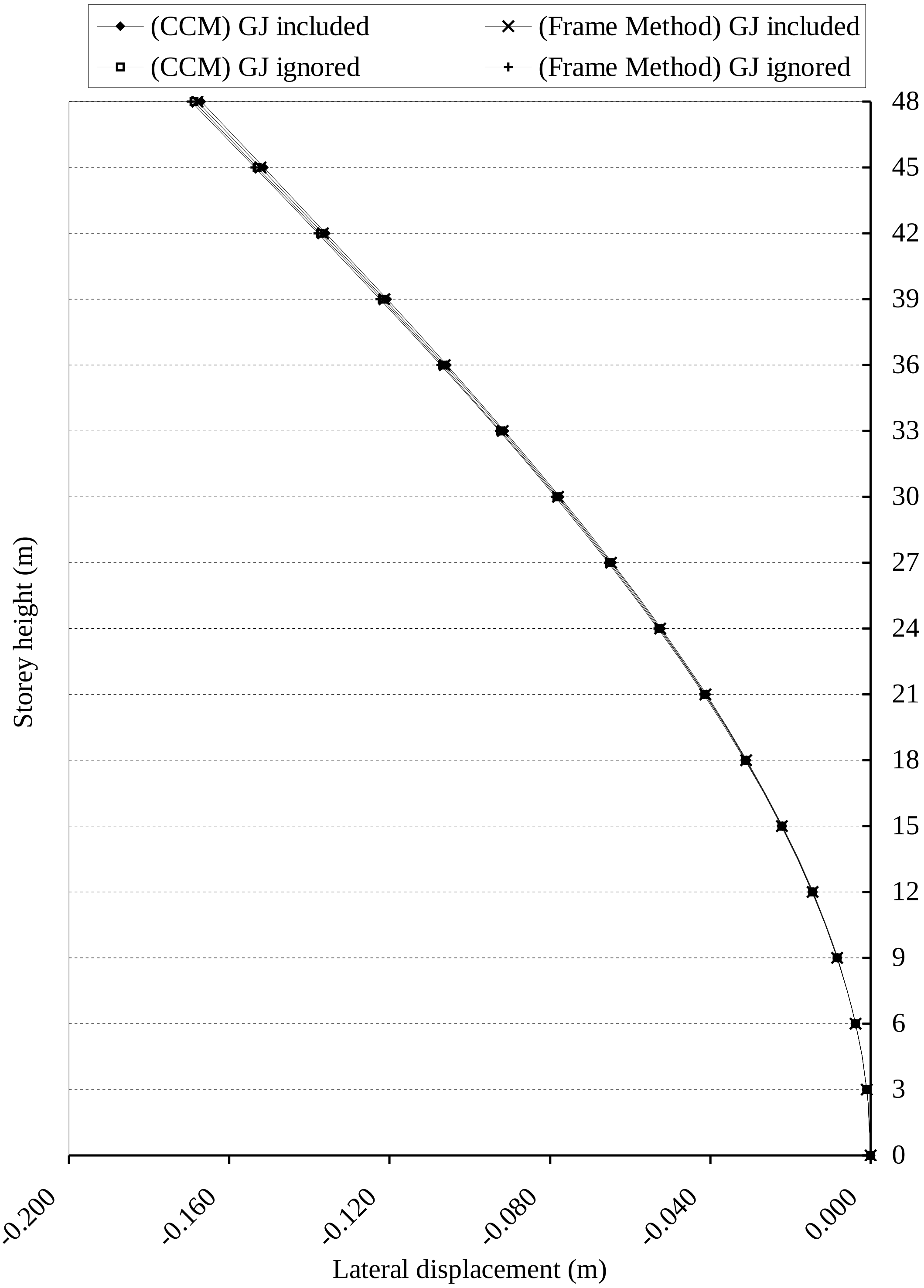

Figure 6.71. The lateral displacements in the Y direction in Example 19

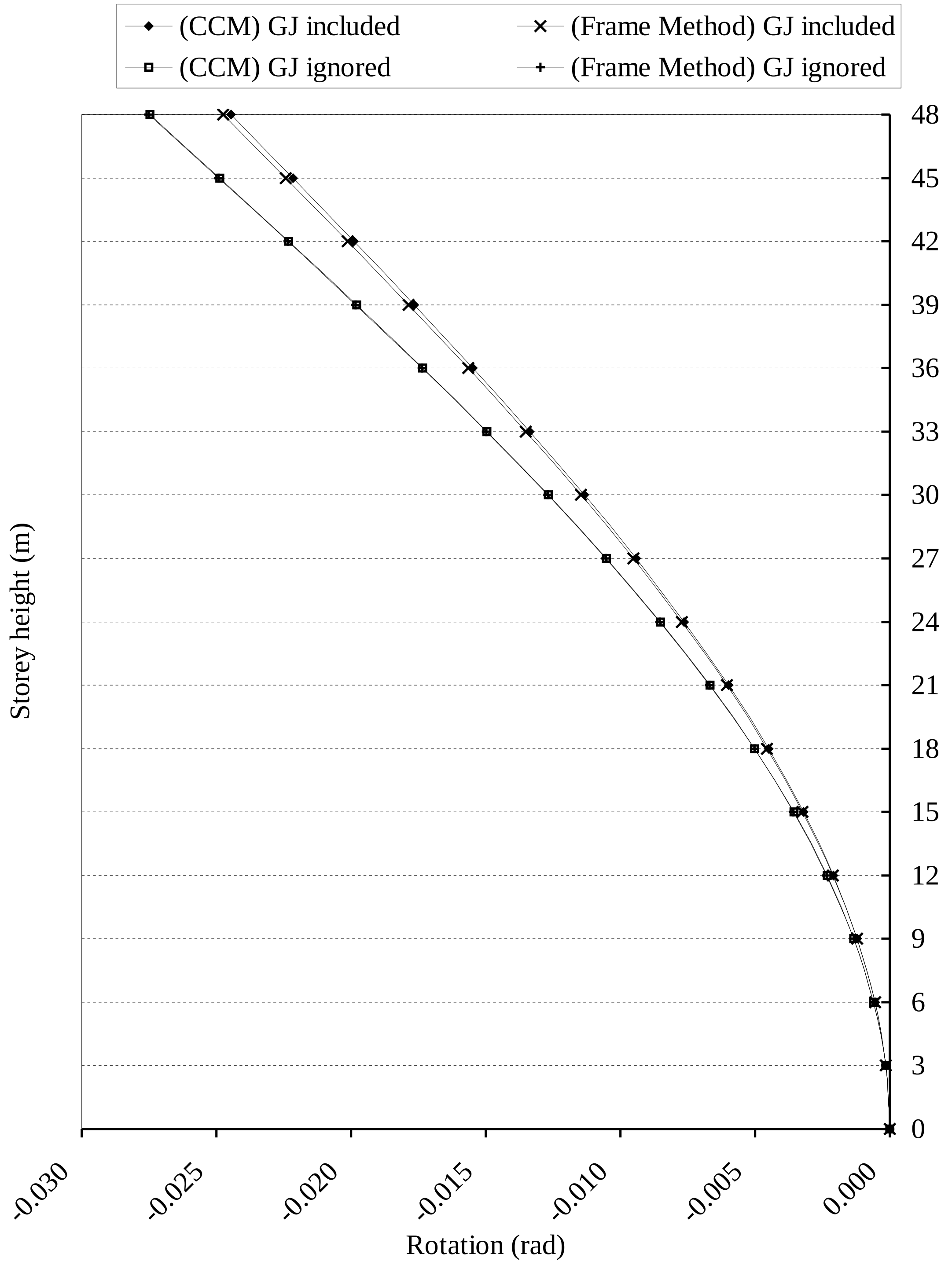

Figure 6.72. The rotations about the Z direction in Example 19

7. CONCLUSIONS

In this study non-planar shear walls coupled with connecting beams are analyzed under lateral loading. The analysis is performed using Vlasov's thin-walled beam theory in conjunction with the CCM. The analysis carried out in the previous chapters, employing the CCM, has been implemented as a computer program in Fortran language and various examples have been solved by applying it to different structures.

In the first example, a non-planar coupled shear wall considered by Tso and Biswas (1973) has been solved both by the computer program prepared in the present work and the SAP2000 structural analysis program and the displacements, thus obtained, have been compared with those given in the literature. The deflections and the rotation along the height of the structure were presented where the theoretical and experimental results of Tso and Biswas were also plotted for comparison (see Figs. 6.2-3). As can be seen, the results of the present study compares perfectly with those of Tso and Biswas and SAP2000, whereas, the experimental results are appreciably different. This was expected, because all three former works ignore shear deformations in the piers and the experimental work, naturally, comprises them.

In the examples, from second to fifth, both piers are assigned as star sections, in which the sectorial areas are equal to zero at all points of the cross-section. Hence, the warping moments of inertia are zero for each pier. The results obtained have been compared with those of SAP2000 and a perfect match has been observed. In the third example, the thicknesses of the flange and the web are assigned to be unequal. In the fourth example, the Tso and Biswas model structure (1973) has been solved for a different loading condition. In the fifth example, a non-symmetrical coupled shear wall is considered.

In the sixth example, a non-symmetrical non-planar coupled shear wall structure in which the left pier has non-zero sectorial area values is considered. There is warping in this example, whereas, warping has never been considered in the examples in the previous studies. The results obtained have been compared with those of SAP2000 and a perfect match has been observed.

In the eighth example, a non-symmetrical structure in which both sections have non-zero sectorial values is considered. The investigations showed that when straight parts in the cross-section are bent into polygonal shapes, the stiffness was greatly increased. The lateral displacements and the rotations along the height have been plotted in Fig. 6.27 for comparison with those of SAP2000 and a perfect match has been observed.

In the tenth example, an arbitrary non-symmetrical structure in which the thicknesses of the piers are assigned to be unequal. In this example, an external torque acts at the top of the structure. The results obtained have been compared with those of SAP2000 and a good agreement has been observed.

In the eleventh example, the uniform horizontal force acts along the height of a non-symmetrical coupled shear wall system. The lateral displacements and the rotations along the height is plotted for comparison with those of SAP2000 and a perfect match has been observed.

The twelflth and thirteenth examples, consider non-planar coupled shear walls in which the storey heights for the two regions are considered to be unequal. The results obtained have been compared with those of SAP2000 and a perfect match has been observed.

In the fourteenth example, a non-planar non-symmetrical complex structure in which the thicknesses of the two piers and the storey heights of the three regions are considered to be unequal. The results obtained have been compared with those of SAP2000 and a perfect match has been observed again.

In the fifteenth example, a non-planar coupled shear wall with elastic beam-wall connections is considered. In Figs. 6.55-57, separate curves have been presented for different connection stiffnesses. Connection stiffness has been varied from 1 to 10^{10}. The results of SAP2000 and the present study have been compared and a perfect match has been observed. With an increase in the connection stiffness, the displacements decreased, as expected.

In the sixteenth example, a non-symmetrical non-planar coupled shear wall with three regions and different connection stiffnesses in them is considered (see Fig.

6.59). The results obtained have been compared with those of SAP2000 and a good agreement has been observed.

In the seventeenth example, a non-planar coupled shear wall model structure considered by Tso and Biswas (1973) has been solved neglecting St. Venant's torsional effects. In order to simplify the analysis, Arviddson (1997) did not take into account the St. Venant's torsional stiffness of the piers. It is true that the solution is greatly simplified and the order of the governing differential equation in (5.107) is reduced from four to three. However, this example indicated that its effect on the displacements, especially on the rotations is far from being irrelevant.

In the eighteenth and nineteenth examples, non-symmetrical structures have been solved with different loading conditions when St. Venant's torsional effect is neglected. The results obtained have been compared with those of SAP2000 and it is observed that neglecting the foregoing effect has little influence on the displacements. In this example, only the rotations have appreciable loss of accuracy, as mentioned by Arviddson (1997).

The method proposed in this study, has two main advantages, which are that the data preparation is much easier compared to equivalent frame method for non-planar coupled shear walls and the computation time needed is much shorter compared to other methods. Hence, the method presented in this study is very useful for predesign purposes while determining the dimensions of non-planar coupled shear wall structures.

REFERENCES

ACI Committee 442, 1987, Response of Buildings to Lateral Forces, (ACI442r-71), American Concrete Institute, Detroit, 26 p.

AKSOGAN, O., ARSLAN, H. M. and AKAVCI, S. S., 2003, Stiffened Coupled Shear Walls on Elastic Foundation with Flexible Connections and Stepwise Changes in Width, Iranian Journal of Science and Technology, Transaction B, 27(B1), pp. 37-46.

ARSLAN, H. M., 1999, Kesit Değişikliği Olan Güçlendirilmiş Boşluklu Deprem Perdelerinin Dinamik Analizi, Doktora Tezi, Ç.Ü. Fen Bilimleri Enstitüsü, Adana, 172 s.

ARSLAN, H. M., AKSOGAN, O. and CHOO, B. S., 2004, Free Vibrations of Flexibly Connected Elastically Supported Stiffened Coupled Shear Walls with Stepwise Changes in Width, Iranian Journal of Science and Technology, Transaction B, 28(B5), pp. 605-614.

ARVIDSSON, K., 1997, Non-planar Coupled Shear Walls in Multistory Buildings, Proceedings of the Institution of Civil Engineers, Structures and Buildings, 122, pp. 326-333.

BECK, H., 1962, Contribution to the Analysis of Coupled Shear Walls, Journal of the American Concrete Institute, 59(8), pp.1055-1070.

BİKÇE, M., 2002, Çok Sıra Boşluklu Deprem Perdelerinin Statik ve Dinamik Analizi, Doktora Tezi, Ç. Ü. Fen Bilimleri Enstitüsü, Adana, 206 s.

CLOUGH, I. P. K. and WILSON E. L., 1964, Structural Analysis of Multistory Buildings, Journal of Structural Division, ASCE, 90(19).

COULL, A. and PURI, R. D., 1968, Analysis of Coupled Shear Walls of Variable Cross-section, Building Science, 2, pp.181-188.

COULL, A. and SMITH, B. S., 1966, Analysis of Shear Wall Structures, Symposium of Tall Buildings, Southampton, England, pp.138-158.

COULL, A. and SMITH, B. S., 1991, Tall Building Structures: Analysis and Design, John Wiley & Sons, New York, 537 p.

COULL, A. and SUBEDI, N. K., 1972, Coupled Shear Walls with Two and Three Bands of Openings, Building Science, Pergamon Press, 7, Great Britain, pp.81-86.

DOĞAN, E., 1995, Coupled Shear Walls with Slitted Connecting Beams, MSc. Thesis, Middle East Technical University, Ankara, 99 p.

GJELSVIK, A., 1981, The Theory of Thin-walled Bars, John Wiley and Sons, USA, 248 p.

GLUCK, J., 1970, Lateral Load Analysis of Asymmetric Multistory Structures, Journal of the Structural Division, ASCE, 96(ST2), Proc. paper 7089, pp.317-333.

HEIDEBRECHT, A. C., ASCE, A. M. and SWIFT, R. D., 1971, Analysis of Asymmetrical Coupled Shear Walls, Journal of Structural Division, ASCE, 97(ST5), pp.1407-1421.

KHAN, M. A. and SMITH, B. S., 1975, Restraining Action of Bracing in Thin-walled Open Section Beams, 59, Part 2, pp.67-68.

KWAN, A. K., 1993, Improved Wide-column Frame Analogy for Shear/Core Wall Analysis, Journal of Structural Engineering, 119, pp. 420-437.

MACLEOD, I. A., and HOSNY, H. M., 1977, Frame Analysis of Shear Wall Cores, Journal of Structural Division , ASCE, 103(10), 2037 p.

ZBIROHOWSKI-KOSCIA, K., 1967, Thin-walled Beams, from Theory to Practice, Crosby Lockwood and Son Ltd.

MENDIS, P., 2001, Warping Analysis of Concrete Cores, Structural Design of Tall Buildings, John Wiley and Sons, 10, pp. 43-52.

ROSMAN, R., 1964, Approximate Analysis of Shear Walls Subjected to Lateral Loads, ACI Journal, Proceedings, 61(6), pp. 717-732.

SOANE, A. J. M., 1967, The Analysis of Interconnected Shear Walls by Analogue Computation, In Tall Buildings, Permagon Press, London, pp.207-221.

SÜMER, Ö. and AŞKAR, G., 1992, Analysis of a Mono-symmetric Core Wall Structure Coupled with Connecting Beams, 59, Part 2, pp.67-78.

TARANATH, B. S., 1988, Structural Analysis and Design of Tall Buildings, McGraw-Hill, Inc., USA, 739 p.

TIMESHENKO, S. and YOUNG, D. H., 1945, Theory of Structures, McGraw-Hill book company, first edition, New York.

TIMESHENKO, S. and GOODIER, J. N., 1951, Theory of Elasticity, McGraw-Hill book company, second edition, Tokyo, 506 p.

TSO, W. K., ASCE, A. M. and BISWAS, J. K., 1973, General Analysis of Non-planar Coupled Shear Walls, Journal of Structural Division, ASCE, 100(ST5), pp.365-380.

VLASOV, V. Z., 1961, Thin-walled Elastic Beams, published for the National Science Foundation, Washington, D.C., the Israel program for scientific translations, Jerusalem, Israel.

WILSON E. L., 1997, SAP2000 Integrated Finite Element Analysis and Design of Structures. 1-2, Computers and Structures, Inc, California, 211 p.

CURRICULUM VITAE

I was born in North Cyprus on 31st December, 1975. After attending the Şehit Tuncer Primary School in Lefkoşa, I attended the secondary and high schools at Bayraktar Türk Maarif College. After this, I started to my BSc. study at the Eastern Mediterranean University in 1993 and graduated from the Department of Civil Engineering in 1997. After working as a Research Assistant for two years at EMU, I finished MSc. programme in Structural Mechanics in 1999. I began to work as a part-time Lecturer at Cyprus International University in 2000. Then I started my PhD. programme at Çukurova University in 2001.

APPENDICES

APPENDIX 1. List of Abbreviations

$$I_y = I_{y1} + I_{y2} \tag{A1.1}$$

$$I_x = I_{x1} + I_{x2} \tag{A1.2}$$

$$I_{xy} = I_{xy1} + I_{xy2} \tag{A1.3}$$

$$I_{\theta y} = S_{Y1} I_{y1} + S_{Y2} I_{y2} - S_{X1} I_{xy1} - S_{X2} I_{xy2} \tag{A1.4}$$

$$I_{\theta x} = S_{X1} I_{x1} + S_{X2} I_{x2} - S_{Y1} I_{xy1} - S_{Y2} I_{xy2} \tag{A1.5}$$

$$I_{\omega} = I_{\omega 1} + I_{\omega 2} + S_{X1}^2 I_{x1} + S_{X2}^2 I_{x2} + S_{Y1}^2 I_{y1} + S_{Y2}^2 I_{y2} - 2S_{X1} S_{Y1} I_{xy1} - 2S_{X2} S_{Y2} I_{xy2} \tag{A1.6}$$

$$\Delta = \left(I_x I_y - I_{xy}^2 \right) \tag{A1.7}$$

$$K_1 = \frac{\left(I_x I_{\theta y} + I_{xy} I_{\theta x} \right)}{\Delta} \tag{A1.8}$$

$$K_2 = \frac{\left(I_{xy} I_{\theta y} + I_y I_{\theta x} \right)}{\Delta} \tag{A1.9}$$

$$K_3 = \frac{\left(a I_x - b I_{xy} \right)}{\Delta} \tag{A1.10}$$

$$K_4 = -\frac{\left(a I_{xy} - b I_y \right)}{\Delta} \tag{A1.11}$$

$$r = \omega + d - I_{\theta x} K_4 + I_{\theta y} K_3 \tag{A1.12}$$

$$\bar{I}_{\omega} = I_{\omega} - I_{\theta x} K_2 - I_{\theta y} K_1 \tag{A1.13}$$

$$\frac{1}{A} = \left[\frac{1}{A_1} + \frac{1}{A_2} \right] + aK_3 + bK_4 \tag{A1.14}$$

$$\beta_{1i} = \gamma_i \bar{I}_{\omega} \tag{A1.15}$$

$$\beta_{2i} = \left(\frac{\bar{I}_{\omega}}{A} + \frac{\gamma_i G J}{E} + r^2 \right) \tag{A1.16}$$

$$\beta_{3i} = \frac{G J}{EA} \tag{A1.17}$$

APPENDIX 2. List of Input Data File of a Computer Program prepared in Fortran Language for the Analysis of Non-planar Coupled Shear Walls using CCM

TITLE

H, a, b, c, h

J, G, Elas

P_x, w_x, d_{py} , d_{wy}

P_y, w_y, d_{px} , d_{wx}

I_x, I_{xy}, I_y

$I_{\theta x}$, $I_{\theta y}$, I_{ω}

I_c, A_c

KSAY, HKAT

H	: Total Height of Shear Wall
h	: Storey Height (HKAT)
Elas	: Modulus of Elasticity,
P_x	: a Concentrated Force in X direction
w_x	: a Uniform Load in X direction
P_y	: a Concentrated Force in Y direction
w_y	: a Uniform Load in Y direction
d_{px}, d_{py}, d_{wx}, d_{wy}	: moment arms of the components of the concentrated force and moment arms of the distributed force components
KSAY	: Storey Number

APPENDIX 3. List of the Computer Program Prepared in Fortran Language for the Analysis of Non-planar Coupled Shear Walls Using CCM

```
*******************************************************************
c
c Three Dimensional Analysis of Non-Planar Coupled Shear Walls (region to region)
c *******************************************************************
PARAMETER (N=50)
IMPLICIT REAL*8 (A-H,K-Z)
c  I and J variables
   REAL*8 Teta(N),U(N),V(N),T(N),ST(N),KYUK(N),KAT(N)
   REAL*8 HKAT(N),HKIR(N),CCB(N),CSB(N),HGKIR(N),Z(N)
    @      ,Ac(N),As(N),EIc(N),EIs(N),GAMA(N),GAMAstf(N)
    @      ,BETA1(N),BETA2(N),BETA3(N),ALFA1(N),ALFA2(N)
    @      ,S(N),Tozel(N),Tozelz(N),Tozelzz(N),Tozelzzz(N)
    @      ,STozel(N),STozelz(N),STozelzz(N),STozelzzz(N)
    @      ,Mx(N),Mxz(N),Mxzz(N),Mxzzz(N)
    @      ,My(N),Myz(N),Myzz(N),Myzzz(N)
    @      ,Mt(N),Mtz(N),Mtzz(N),Mtzzz(N)
    @      ,ZK(N,N),ZB(N),D1(N),D2(N),D3(N),D4(N)
    @      ,REK1(N),REK2(N),REK3(N),REK4(N),C1(N),C2(N)
    @      ,YK(N,N),YB(N),SONUC1(N),SONUC2(N),SONUC3(N),SONUC4(N)
    @      ,G1(N),G2(N),F1(N),F2(N),P1(N),P2(N),eSIW(N),ePRSA(N,N)
    @      ,eDX(N),eDY(N),eEDI(N),eEDJ(N),eTHICK(N),ePRSECAREA(N)
    @      ,CX(N),CY(N),EX(N),EY(N),eCSAREA(N)
    @      ,SIx(N),SIxy(N),SIy(N),EJp(N),PNN(N),ENN(N)
          INTEGER ibsay,BSAY,GSAY,KSAY,PSAY,PN,EN
          CHARACTER*8   CIKTI,GIRDI
          WRITE(*,*)   'GIRDI DOSYASININ ADI'
          READ(*,10)    GIRDI
          WRITE(*,*)   'CIKTI DOSYASININ ADI'
          READ(*,10)    CIKTI
          OPEN(5,FILE=GIRDI,FORM='FORMATTED')
          OPEN(6,FILE=CIKTI,FORM='FORMATTED')
  10 FORMAT(A8)
  20 FORMAT(A50)
  22 FORMAT(1X,30F10.3)
  23 FORMAT(1X,30F13.3)
  25 FORMAT(1X,30F13.4)
    READ(5,20)  BASLIK
          WRITE(6,20) BASLIK
    READ(5,*)   BSAY,GSAY,KSAY,PSAY
          WRITE(6,*) '   BSAY       GSAY       KSAY         PSAY       '
          WRITE(6,*) '----------------------------------------------  '
          WRITE(6,22) BSAY,GSAY,KSAY,PSAY
    ibsay=BSAY+1
  910 FORMAT(A8)
 920 FORMAT(A50)
 922 FORMAT(1X,30F10.3)
 923 FORMAT(1X,30F10.2)
 925 FORMAT(1X,30F13.4)
          WRITE(6,*) '                                          '
          WRITE(6,*) '************************************************    '
          WRITE(6,*) '                                          '
```

```
C     GEOMETRIC PROPERTIES FROM DATA FILE AND CALCULATION OF
C           W(sectorial area) DIAGRAM AND IW(Warping moment of inertia) VALUES
      DO II=1,PSAY
      READ(5,20)  BILGI
      READ(5,*)       eCSAREA(II)
            WRITE(6,*) '  CROSS SECTION AREA   '
            WRITE(6,*) '-----------------------'
            WRITE(6,922)     eCSAREA(II)
      READ(5,*)   CX(II),CY(II)
            WRITE(6,*) '                                          '
            WRITE(6,*) '      CX        CY (Shear center coord. for Glob.Ax.)'
            WRITE(6,*) '---------------------------                         '
            WRITE(6,922) CX(II),CY(II)
      READ(5,*)   EX(II),EY(II)
            WRITE(6,*) '                                          '
            WRITE(6,*) '      EX         EY  (Center of gravity coordinates)'
            WRITE(6,*) '--------------------------                         '
            WRITE(6,922) EX(II),EY(II)
            READ(5,*)   SIx(II),SIxy(II),SIy(II)
            WRITE(6,*) '                                          '
            WRITE(6,*) '     Ix        Ixy       Iy                    '
            WRITE(6,*) '-------------------------------------                 '
            WRITE(6,22) SIx(II),SIxy(II),SIy(II)
      READ(5,*)   EJp(II)
            WRITE(6,*) '                                          '
            WRITE(6,*) '      J              '
            WRITE(6,*) '--------------        '
            WRITE(6,23) EJp(II)
      READ(5,*)   ePN,eEN
            WRITE(6,*) '                                        '
            WRITE(6,*) '      PN         EN    (Number of point on section)'
            WRITE(6,*) '---------------------------                       '
            WRITE(6,922) PN,EN
      READ(5,*)   eSCN,eSx,eSy
            WRITE(6,*) '                                        '
            WRITE(6,*) '      Sx         Sy      (Shear center coordinates)'
            WRITE(6,*) '------------------------                          '
            WRITE(6,922) eSx,eSy
            WRITE(6,*) '                                        '
            WRITE(6,*) '    POINT        X         Y    (point coordinates)'
            WRITE(6,*) '-------------------------------------           '
      DO I=1,ePN
            READ(5,*)   P,eDX(P),eDY(P)
            WRITE(6,922) P,eDX(P),eDY(P)
      ENDDO
            WRITE(6,*) '                                          '
            WRITE(6,*) '     ELEMENT      I        J      THICKNESS         '
            WRITE(6,*) '----------------------------------------------------'-
      DO I=1,eEN
            READ(5,*)   E,eEDI(E),eEDJ(E),eTHICK(E)
            WRITE(6,923) E,eEDI(E),eEDJ(E),eTHICK(E)
      ENDDO
      PNN(II)=ePN
      ENN(II)=eEN
CALL CAIw(II,eCSAREA,ePN,eEN,eSCN,eSx,eSy,P,eDX,eDY,
```

```
     eEDI,eEDJ,eTHICK,ePRSECAREA,ePRSA,eSIW)
       WRITE(6,*) '                                        '
       WRITE(6,*) '************************************************    '
       WRITE(6,*) '                                        '
  ENDDO
  READ(5,20)  BILGI
  READ(5,*)   c,BKTHICK
       WRITE(6,*) '       c        BAG.KİR. KALINLIĞI                '
       WRITE(6,*) '-------------------------------------------        '
       WRITE(6,22) c,BKTHICK
  READ(5,*)   G,Elas
       WRITE(6,*) '                              '
       WRITE(6,*) '      G            Elas               '
       WRITE(6,*) '-------------------------------         '
       WRITE(6,23) G,Elas
       READ(5,*)   Px,Wx,dy
       WRITE(6,*) '                                        '
       WRITE(6,*) '    Px        Wx         dy                      '
       WRITE(6,*) '-------------------------------                  '
       WRITE(6,22) Px,Wx,dy
       READ(5,*)   Py,Wy,dx
       WRITE(6,*) '                                        '
       WRITE(6,*) '    Py        Wy         dx                      '
       WRITE(6,*) '-------------------------------                  '
       WRITE(6,22) Py,Wy,dx
  READ(5,20)  BILGI
       WRITE(6,*) '                                        '
       WRITE(6,*) '-----Kat Yüksekliği------                        '
       WRITE(6,*) '-------------------------                        '
  DO 1 I=1,bsay
       READ(5,*)   HKAT(I)
       WRITE(6,22) HKAT(I)
1 CONTINUE
       HKAT(ibsay)=HKAT(bsay)
       WRITE(6,*) '                                        '
       WRITE(6,*) '-----connection stiffness factor-Ccb-----                '
       WRITE(6,*) '------------------------------------             '
  DO 2 I=1,bsay
       READ(5,*) CCB(I)
       WRITE(6,22) CCB(I)
2 CONTINUE
       CCB(ibsay)=CCB(bsay)
       WRITE(6,*) '                                        '
       WRITE(6,*) '-----connection stiffness constant-Csb-----                '
       WRITE(6,*) '------------------------------------             '
  DO 3 I=1,bsay
       READ(5,*) CSB(I)
       WRITE(6,22) CSB(I)
3 CONTINUE
       CSB(ibsay)=CSB(bsay)
       WRITE(6,*) '                                        '
       WRITE(6,*) '-----beam height------                           '
       WRITE(6,*) '---------------------------                      '
  DO 4 I=1,bsay
       READ(5,*)   HKIR(I)
```

```
      WRITE(6,22) HKIR(I)
4 CONTINUE
      HKIR(ibsay)=HKIR(bsay)
  READ(5,20)  BILGI
      WRITE(6,*) '                                    '
      WRITE(6,*) '-height of stiffening beam---Yerden Mesafe----      '
      WRITE(6,*) '----------------------------------------      '
  DO 5 I=1,ibsay
      READ(5,*)   HGKIR(I),Z(I)
      WRITE(6,22) HGKIR(I),Z(I)
5 CONTINUE
      H     = Z(1)
      WRITE(6,*) '      '
      WRITE(6,*) 'H=    '
      WRITE(6,*)  H
      a     = EX(2)-EX(1)
      WRITE(6,*) '      '
      WRITE(6,*) 'a=    '
      WRITE(6,*)  a
      b     = EY(2)-EY(1)
      WRITE(6,*) '      '
      WRITE(6,*) 'b=    '
      WRITE(6,*)  b
      EJ    = EJp(1)+EJp(2)
      WRITE(6,*) '      '
      WRITE(6,*) 'J=    '
      WRITE(6,*)  EJ
  EIx   = SIx(1)+SIx(2)
      WRITE(6,*) '      '
      WRITE(6,*) 'Ix=    '
      WRITE(6,*)  EIx
      EIxy  = SIxy(1)+SIxy(2)
      WRITE(6,*) '      '
      WRITE(6,*) 'Ixy=    '
      WRITE(6,*)  EIxy
      EIy   = SIy(1)+SIy(2)
      WRITE(6,*) '      '
      WRITE(6,*) 'Iy=    '
      WRITE(6,*)  EIy
  Delta = (EIx*EIy - EIxy**2)
      WRITE(6,*) '      '
      WRITE(6,*) 'Delta=    '
      WRITE(6,*)  Delta
  EIxc  = CX(1)*SIx(1)+CX(2)*SIx(2)-CY(1)*SIxy(1)-CY(2)*SIxy(2)
      WRITE(6,*) '      '
      WRITE(6,*) 'Ixc=    '
      WRITE(6,*)  EIxc
  EIyc  = CY(1)*SIy(1)+CY(2)*SIy(2)-CX(1)*SIxy(1)-CX(2)*SIxy(2)
      WRITE(6,*) '      '
      WRITE(6,*) 'Iyc=    '
      WRITE(6,*)  EIyc
  K1    = (EIxc*EIxy + EIx*EIyc)/Delta
      WRITE(6,*) '      '
      WRITE(6,*) 'K1=    '
      WRITE(6,*)  K1
```

```
 K2    = (EIxc*EIy + EIxy*EIyc)/Delta
        WRITE(6,*) '      '
        WRITE(6,*) 'K2=    '
        WRITE(6,*)  K2
 K3    =       (a*EIx - b*EIxy)/Delta
        WRITE(6,*) '      '
        WRITE(6,*) 'K3=    '
        WRITE(6,*)  K3
 K4    =       (b*EIy - a*EIxy)/Delta
        WRITE(6,*) '      '
        WRITE(6,*) 'K4=    '
        WRITE(6,*)  K4
 ALAN  =  1/((1/eCSAREA(1))+(1/eCSAREA(2))+a*K3+b*K4)
        WRITE(6,*) '      '
        WRITE(6,*) 'Alan=    '
        WRITE(6,*)  ALAN
 d     = CX(2)*EY(2)-CY(2)*EX(2)+CY(1)*EX(1)-CX(1)*EY(1)
        WRITE(6,*) '      '
        WRITE(6,*) 'd=    '
        WRITE(6,*)  d
        w     = ePRSA(1,PNN(1))-ePRSA(2,PNN(2))
        WRITE(6,*) '      '
        WRITE(6,*) 'w=    '
        WRITE(6,*)  w
        r     = w + d + a*K1 - b*K2
        WRITE(6,*) '      '
        WRITE(6,*) 'r=    '
        WRITE(6,*)  r
 EIw   = eSIw(1)+eSIw(2)+CX(1)**2*SIx(1)+CX(2)**2*SIx(2)
@                    +CY(1)**2*SIy(1)+CY(2)**2*SIy(2)
@                    -2*CX(1)*CY(1)*SIxy(1)
@                    -2*CX(2)*CY(2)*SIxy(2)
        WRITE(6,*) '      '
        WRITE(6,*) 'Iw=    '
        WRITE(6,*)  EIw
 EIOw  = EIw - EIyc*K1 - EIxc*K2
        WRITE(6,*) '      '
        WRITE(6,*) 'IOw=    '
        WRITE(6,*)  EIOw
        DO 6 I=1,ibsay
 Ac(I)=BKTHICK*HKIR(I)
 As(I)=BKTHICK*HGKIR(I)
        EIc(I)=(BKTHICK*HKIR(I)**3.)/12.
        EIs(I)=(BKTHICK*HGKIR(I)**3.)/12.
 GAMA(I)=Elas*((c**2*hkat(I))/(2.*Ccb(I))+
-             (c*hkat(I)*1.2)/(Ac(I)*G)+
-             (c**3*hkat(I))/(12.*Elas*EIc(I)))
 GAMAstf(I)=Elas*((c**2)/(2.*Csb(I))+
-               (c*1.2)/(As(I)*G)+
-               (c**3)/(12.*Elas*EIs(I)))
 BETA1(I) = EIOw*GAMA(I)
 BETA2(I) = EIOw/ALAN + (EJ*G*GAMA(I))/Elas + r**2
 BETA3(I) = (EJ*G)/(Elas*ALAN)
 ALFA1(I)=Sqrt((BETA2(I)-Sqrt(BETA2(I)**2
*            -4*BETA1(I)*BETA3(I)))/BETA1(I))/Sqrt(2.)
```

```
      ALFA2(I)=Sqrt((BETA2(I)+Sqrt(BETA2(I)**2
     *           -4*BETA1(I)*BETA3(I)))/BETA1(I))/Sqrt(2.)
      S(I)=GAMA(I)/GAMAstf(I)
c     External force moments (at the region ends)
        Mx(I)    =Py*(H - Z(I)) + (Wy*(H - Z(I))**2)/2.
        Mxz(I)   =-Py - Wy*(H - Z(I))
        Mxzz(I)  =Wy
        Mxzzz(I) =0
        My(I)    =Px*(H - Z(I)) + (Wx*(H - Z(I))**2)/2.
        Myz(I)   =-Px - Wx*(H - Z(I))
        Myzz(I)  =Wx
        Myzzz(I) =0
      Mt(I)    =-(dy*Px) + dx*Py - dy*Wx*(H - Z(I)) + dx*Wy*(H - Z(I))
      Mtz(I)   =dy*Wx - dx*Wy
      Mtzz(I)  =0
      C1(I)=  d+EIyc*K3-EIxc*K4+EIw/(Alan*r)-(EIyc*K1)/(Alan*r)-
     -      (EIxc*K2)/(Alan*r)+w
      C2(I)= -(EIw/r)*GAMA(I)+(GAMA(I)*EIyc*K1)/r+(GAMA(I)*EIxc*K2)/r
    6   CONTINUE
c     WRITE(6,*)'                                   '
c     WRITE(6,*)'  Tozel(I)   Tozelz(I)   Tozelzz(I)   Tozelzzz(I)'
        DO 55 I=1,ibsay
      Tozel(I)= (2*BETA2(I)*G*EJ*(K3*Wx + K4*Wy) +
     -         BETA3(I)*(-2*Elas*(EIOw*K3*Wx - dy*r*Wx + K1*r*Wx +
     -         EIOw*K4*Wy + dx*r*Wy - K2*r*Wy) +
     -         G*EJ*(H - Z(I))*(2*K3*Px + 2*K4*Py + H*K3*Wx +
     -         H*K4*Wy - (K3*Wx + K4*Wy)*Z(I))))/
     -         (2.*BETA3(I)**2*Elas)
      Tozelz(I)= (G*EJ*(-(K3*Wx) - K4*Wy)*(H - Z(I)) -
     -          G*EJ*(2*K3*Px + 2*K4*Py + H*K3*Wx + H*K4*Wy -
     -          (K3*Wx + K4*Wy)*Z(I)))/(2.*BETA3(I)*Elas)
       Tozelzz(I)= (G*EJ*(K3*Wx + K4*Wy))/(BETA3(I)*Elas)
      Tozelzzz(I)=0.
c     WRITE(6,*) Tozel(I),Tozelz(I),Tozelzz(I),Tozelzzz(I)
   55   CONTINUE
c     WRITE(6,*)'                                   '
c     WRITE(6,*)'  STozel(I)   STozelz(I)   STozelzz(I)   STozelzzz(I)'
        DO 56 I=1,ibsay
      STozel(I)= (2*BETA2(I)*G*EJ*(K3*Wx + K4*Wy) +
     -          BETA3(I)*(-2*Elas*(EIOw*K3*Wx - dy*r*Wx + K1*r*Wx +
     -          EIOw*K4*Wy + dx*r*Wy - K2*r*Wy) +
     -          G*EJ*(H - Z(I+1))*(2*K3*Px + 2*K4*Py + H*K3*Wx +
     -          H*K4*Wy - (K3*Wx + K4*Wy)*Z(I+1))))/
     -          (2.*BETA3(I)**2*Elas)
      STozelz(I)= (G*EJ*(-(K3*Wx) - K4*Wy)*(H - Z(I+1)) -
     -           G*EJ*(2*K3*Px + 2*K4*Py + H*K3*Wx + H*K4*Wy -
     -           (K3*Wx + K4*Wy)*Z(I+1)))/(2.*BETA3(I)*Elas)
      STozelzz(I)= (G*EJ*(K3*Wx + K4*Wy))/(BETA3(I)*Elas)
      STozelzzz(I)= 0.
c     WRITE(6,*) STozel(I),STozelz(I),STozelzz(I),STozelzzz(I)
   56   CONTINUE
      TOL=0.00001
c     INTEGRATION CONSTANTS
        IL=1
      IK=0
```

```
        DO I=1,ibsay
          IF(I.EQ.1) THEN
   CALL COEF1A(Tozel(I),Tozelz(I),ALFA1(I),ALFA2(I)
@                                         ,Z(I),S(I),REK1,REKB1)
          CALL COEF1B(Tozel(I),Tozelz(I),Tozelzz(I),ALFA1(I),ALFA2(I)
@                    ,GAMA(I),Z(I),S(I),EIw,ALAN,r,w,REK2,REKB2)
  ENDIF
         IF((I.GT.1).AND.(I.LT.ibsay)) THEN
          CALL COEF2A(ibsay,ALFA1,ALFA2,Z(I),
@             Tozelz,STozelz,GAMA,I,REK1,REKB1)
          CALL COEF2B(ibsay,ALFA1,ALFA2,Z(I),S(I),
@             Tozel,Tozelz,STozel,I,REK2,REKB2)
          CALL COEF2C(ibsay,Tozelz,Tozelzzz,STozelz,STozelzzz,
@              ALFA1,ALFA2,Z(I),C1,C2,I,REK3,REKB3)
          CALL COEF2D(ibsay,Tozel,Tozelz,Tozelzz,STozel,STozelzz,
@            ALFA1,ALFA2,Z(I),S(I),GAMA,EIw,ALAN,r,w,I,REK4,REKB4)
         ENDIF
         IF(I.EQ.ibsay) THEN
        CALL COEF3A(Tozelz(I),ALFA1(I),ALFA2(I),Z(I),REK1,REKB1)
      CALL COEF3B(Tozelz(I),Tozelzzz(I),ALFA1(I),ALFA2(I),
@              Z(I),GAMA(I),Mxz(I),Myz( I),Mt(I),
@              EIw,ALAN,r,w,EIyc,EIxc,EIx,EIy,EIxy,
@              K1,K2,K3,K4,d,Delta,REK2,REKB2)
         ENDIF
         IF(I.EQ.1) THEN
           DO J=1,4
                    ZK(I,J)=ZK(I,J)+REK1(J)
                    ZB(I)=REKB1
                    ZK(I+1,J)=ZK(I+1,J)+REK2(J)
                    ZB(I+1)=REKB2
                   ENDDO
         ENDIF
   IF((I.GT.1).AND.(I.LT.ibsay)) THEN
           DO J=1,8
      ZK(I+IL-3,J+IK-4)=ZK(I+IL-3,J+IK-4)+REK1(J)
                    ZB(I+IL-3)=REKB1
                    ZK(I+IL-2,J+IK-4)=ZK(I+IL-2,J+IK-4)+REK2(J)
                    ZB(I+IL-2)=REKB2
      ZK(I+IL-1,J+IK-4)=ZK(I+IL-1,J+IK-4)+REK3(J)
                    ZB(I+IL-1)=REKB3
                    ZK(I+IL,J+IK-4)=ZK(I+IL,J+IK-4)+REK4(J)
                    ZB(I+IL)=REKB4
    ENDDO
         ENDIF
         IK=IK+4
         IF(I.EQ.ibsay) THEN
           DO J=1,4
                    ZK(I+IL-3,J+IK-8)=ZK(I+IL-3,J+IK-8)+REK1(J)
                    ZB(I+IL-3)=REKB1
                    ZK(I+IL-2,J+IK-8)=ZK(I+IL-2,J+IK-8)+REK2(J)
                    ZB(I+IL-2)=REKB2
    ENDDO
         ENDIF
        IL=IL+3
         do j=1,8
```

```
              REK1(j)=0.d0
              REK2(j)=0.d0
              REK3(j)=0.d0
              REK4(j)=0.d0
            enddo
          ENDDO
      in=4*(ibsay-1)
      WRITE(6,*) '                  '
c     write(6,*) 'Coefficient Matrix'
c     DO I =1,n
c     WRITE(6,22) (zk(I,J),J=1,N)
c           enddo
   77 FORMAT(1X,40F22.10)
c     WRITE(6,*) '                      '
c     write(6,*) 'Right Hand Side Vector'
c     WRITE(6,77) (zb(J),J=1, N)
      CALL GAUSS(ZK,in,ZB,SONUC1)
c     WRITE(6,*) '             '
c     write(6,*) 'Result Vector'
c     WRITE(6,77) (SONUC1(J),J=1,N)
      im=0
          DO I=1,ibsay
      if(I.EQ.ibsay)THEN
          im=im-4
          endif
        D1(I)=D1(I)+SONUC1(I+im)
        D2(I)=D2(I)+SONUC1(I+1+im)
        D3(I)=D3(I)+SONUC1(I+2+im)
        D4(I)=D4(I)+SONUC1(I+3+im)
            im=im+3
      ENDDO
      WRITE(6,*)'                                    '
      WRITE(6,*)'       --T--                          '
          DO I=1,ibsay
      WRITE(6,*)'                                    '
          T(I)= D1(I)*SINH(ALFA1(I)*Z(I))+D2(I)*COSH(ALFA1(I)*Z(I))
     @     +D3(I)*SINH(ALFA2(I)*Z(I))+D4(I)*COSH(ALFA2(I)*Z(I))
     @     +Tozel(I)
      IF((I.GT.1).AND.(I.LT.ibsay)) THEN
          ST(I)= D1(I-1)*SINH(ALFA1(I-1)*Z(I))+D2(I-1)*COSH(ALFA1(I-1)*Z(I))
     @     +D3(I-1)*SINH(ALFA2(I-1)*Z(I))+D4(I-1)*COSH(ALFA2(I-1)*Z(I))
     @     +STozel(I-1)
      WRITE(6,*)  ST(I)
      ENDIF
      WRITE(6,*) 'Z(I)=',Z(I)
      WRITE(6,*)  T(I)
      ENDDO
      WRITE(6,*)'                                    '
c     LATERAL DISPLACEMENTS
      iksay=KSAY+1
      DO I=1,ibsay
       IF(Z(I).EQ.H) THEN
        KAT(iksay)=H
            GOTO 60
              ENDIF
```

```
            DO 70 in=1,iksay
              KAT(iksay-in)=KAT(iksay-in+1)-HKAT(I-1)
                        IF(KAT(iksay-in).LT.TOL) THEN
         KAT(iksay-in)=0.d0
                 GOTO 60
                   ENDIF
               IF(ABS(Z(I)-KAT(iksay-in)).LT.TOL) THEN
         iksay=iksay-in
                 GOTO 60
                   ENDIF
   70  CONTINUE
   60 ENDDO
      iksay=KSAY+1
      write(6,*) '    '
      write(6,*) '--KAT SEViYELERi--'
      write(6,*) '    '
      do in=1,iksay
      im=iksay-in+1
            write(6,*) KAT(im)
            enddo
c     Teta(Z) DISPLACEMENT FUNCTION
            iL=0
      iK=0
            DO I=2,ibsay
            IF(I.LT.ibsay) THEN
         CALL COEF1Y(ibsay,ALFA1,ALFA2,BETA1,BETA2,BETA3
     @               ,Z(I),GAMA,G,EJ,K1,K2,K3,K4,H
     @              ,Px,Py,Wx,Wy,dx,dy,r,EIOw,Alan
     @                                 ,Elas,D1,D2,D3,D4,REK1,REKB1,I)
      CALL COEF2Y(ibsay,ALFA1,ALFA2,BETA1,BETA2,BETA3
     @               ,Z(I),GAMA,G,EJ,K1,K2,K3,K4,H
     @              ,Px,Py,Wx,Wy,dx,dy,r,EIOw,Alan
     @                                 ,Elas,D1,D2,D3,D4,REK2,REKB2,I)
        ENDIF
             IF(I.EQ.ibsay) THEN
            CALL COEF3Y(ibsay,ALFA1,ALFA2,BETA1,BETA2,BETA3
     @               ,Z(I),GAMA,G,EJ,K1,K2,K3,K4,H
     @              ,Px,Py,Wx,Wy,dx,dy,r,EIOw,Alan
     @                 ,Elas,D1,D2,D3,D4,REK1,REKB1,I)
           CALL COEF4Y(ibsay,ALFA1,ALFA2,BETA1,BETA2,BETA3
     @      Z(I),GAMA,G,EJ,K1,K2,K3,K4,H
     @   ,Px,Py,Wx,Wy,dx,dy,r,EIOw,Alan
     @     ,Elas,D1,D2,D3,D4,REK2,REKB2,I)
             ENDIF
             IF(I.LT.ibsay) THEN
            DO J=1,4
                       YK(I+iL-1,J+iK)=YK(I+iL-1,J+iK)+REK1(J)
                       YB(I+iL-1)=REKB1
                       YK(I+iL,J+iK)=YK(I+iL,J+iK)+REK2(J)
                       YB(I+iL)=REKB2
                       ENDDO
             ENDIF
            iK=iK+2
             IF(I.EQ.ibsay) THEN
               DO J=1,2
```

```
                    YK(I+iL-1,J+iK-2)=YK(I+iL-1,J+iK-2)+REK1(J)
                    YB(I+iL-1)=REKB1
                    YK(I+iL,J+iK-2)=YK(I+iL,J+iK-2)+REK2(J)
                    YB(I+iL)=REKB2
       ENDDO
          ENDIF
         iL=iL+1
           do j=1,4
           rek1(j)=0.d0
           rek2(j)=0.d0
           rek3(j)=0.d0
           rek4(j)=0.d0
          enddo
         ENDDO
     in=2*(ibsay-1)
c    write(6,*) 'Coefficient Matrix'
c    DO I =1,in
c     WRITE(6,233) (yk(I,J),J=1,in)
c    enddo
 233 FORMAT(1X,40F22.10)
c    write(6,*) 'Right Hand Side Vector'
c    WRITE(6,233) (yb(J),J=1,in)
     CALL GAUSS(YK,in,YB,SONUC2)
c    write(6,*) 'Result Vector'
c    WRITE(6,22) (SONUC2(J),J=1,in)
     im=0
         DO I=1,ibsay
      G1(I)=G1(I)+SONUC2(I+im)
      G2(I)=G2(I)+SONUC2(I+1+im)
          im=im+1
     ENDDO
         G1(ibsay)=G1(ibsay-1)
     G2(ibsay)=G2(ibsay-1)
C     TETA(Z) FUNCTION
      iksay=KSAY+1
     DO I=1,ibsay
          DO 90 in=1,iksay
          im=iksay-in+1
         CALL TETAFONK(ibsay,iksay,ALFA1,ALFA2,BETA1,BETA2,BETA3
    @          ,GAMA,K1,K2,K3,K4,Elas,G,EJ
    @         ,Px,Py,Wx,Wy,dx,dy,r,EIOw,Alan,H
    @          ,D1,D2,D3,D4,TETA,KAT,I,im,G1,G2)
           IF(ABS(Z(I+1)-KAT(im)).LT.TOL) THEN
        iksay=im
             GOTO 80
             ENDIF
                IF(KAT(im).LT.TOL) THEN
                GOTO 80
             ENDIF
   90  CONTINUE
   80 ENDDO
     iksay=KSAY+1
   24 FORMAT(1X,30F20.12)
     iksay=ksay+1
     WRITE(6,*) '   '
```

```
      WRITE(6,*) 'TETA='
      do I=1,iksay
      J=iksay-I+1
              write(6,24) TETA(J)
              enddo
      in=2*(ibsay-1)
                do j=1,in
                YB(j)=0.d0
                enddo
        do I =1,in
         do J =1,in
               yk(I,J)=0.d0
         enddo
        enddo
                do j=1,4
                rek1(j)=0.d0
                rek2(j)=0.d0
                rek3(j)=0.d0
                rek4(j)=0.d0
                enddo
c      U(Z) DISPLACEMENT FUNCTION
iL=0
iK=0
              DO I=2,ibsay
              IF(I.LT.ibsay) THEN
          CALL COEF1U(ibsay,ALFA1,ALFA2,BETA1,BETA2,BETA3
     @                 ,Z(I),GAMA,G,EJ,K1,K2,K3,K4,H,DELTA
     @               ,Px,Py,Wx,Wy,dx,dy,r,EIOw,Alan,EIx,EIxy
     @                   ,Elas,D1,D2,D3,D4,REK1,REKB1,I)
          CALL COEF2U(ibsay,ALFA1,ALFA2,BETA1,BETA2,BETA3
     @                  ,Z(I),GAMA,G,EJ,K1,K2,K3,K4,H,DELTA
     @               ,Px,Py,Wx,Wy,dx,dy,r,EIOw,Alan,EIx,EIxy
     @                   ,Elas,D1,D2,D3,D4,REK2,REKB2,I)
        ENDIF
  IF(I.EQ.ibsay) THEN
              CALL COEF3U(ibsay,ALFA1,ALFA2,BETA1,BETA2,BETA3
     @                 ,Z(I),GAMA,G,EJ,K1,K2,K3,K4,H,DELTA
     @               ,Px,Py,Wx,Wy,dx,dy,r,EIOw,Alan,EIx,EIxy
     @                   ,Elas,D1,D2,D3,D4,REK1,REKB1,I)
                CALL COEF4U(ibsay,ALFA1,ALFA2,BETA1,BETA2,BETA3
     @                 ,Z(I),GAMA,G,EJ,K1,K2,K3,K4,H,DELTA
     @               ,Px,Py,Wx,Wy,dx,dy,r,EIOw,Alan,EIx,EIxy
     @                   ,Elas,D1,D2,D3,D4,REK2,REKB2,I)
               ENDIF
               IF(I.LT.ibsay) THEN
               DO J=1,4
                         YK(I+iL-1,J+iK)=YK(I+iL-1,J+iK)+REK1(J)
                         YB(I+iL-1)=REKB1
                         YK(I+iL,J+iK)=YK(I+iL,J+iK)+REK2(J)
                         YB(I+iL)=REKB2
                        ENDDO
               ENDIF
              iK=iK+2
               IF(I.EQ.ibsay) THEN
                DO J=1,2
```

```
                  YK(I+iL-1,J+iK-2)=YK(I+iL-1,J+iK-2)+REK1(J)
                  YB(I+iL-1)=REKB1
                  YK(I+iL,J+iK-2)=YK(I+iL,J+iK-2)+REK2(J)
                  YB(I+iL)=REKB2
        ENDDO
          ENDIF
          iL=iL+1
           do j=1,4
            rek1(j)=0.d0
            rek2(j)=0.d0
            rek3(j)=0.d0
            rek4(j)=0.d0
           enddo
          ENDDO
      in=2*(ibsay-1)
c     write(6,*) 'Coefficient Matrix'
c     DO I =1,in
c      WRITE(6,233) (yk(I,J),J=1,in)
c     enddo
 234 FORMAT(1X,40F22.10)
c     write(6,*) 'Right Hand Side Vector'
c     WRITE(6,234) (yb(J),J=1,in)
      CALL GAUSS(YK,in,YB,SONUC3)
c     write(6,*) 'Result Vector'
c     WRITE(6,22) (SONUC3(J),J=1,in)
      im=0
          DO I=1,ibsay
        F1(I)=F1(I)+SONUC3(I+im)
        F2(I)=F2(I)+SONUC3(I+1+im)
           im=im+1
      ENDDO
           F1(ibsay)=F1(ibsay-1)
           F2(ibsay)=F2(ibsay-1)
C      U(Z) FONKSIYONU
      iksay=KSAY+1
      DO I=1,ibsay
           DO 91 in=1,iksay
           im=iksay-in+1
          CALL UFONK(ibsay,iksay,ALFA1,ALFA2,BETA1,BETA2,BETA3
     @                   ,GAMA,K1,K2,K3,K4,Elas,G,EJ,DELTA
     @                  ,Px,Py,Wx,Wy,dx,dy,r,EIOw,Alan,H
     @                     ,EIx,EIxy,D1,D2,D3,D4,U,KAT,I,im
     @                  ,F1,F2)
          IF(ABS(Z(I+1)-KAT(im)).LT.TOL) THEN
         iksay=im
              GOTO 81
              ENDIF
                  IF(KAT(im).LT.TOL) THEN
                  GOTO 81
              ENDIF
   91  CONTINUE
   81  ENDDO
      iksay=KSAY+1
      WRITE(6,*) '   '
      WRITE(6,*) 'U= '
```

```
      do I=1,iksay
      J=iksay-I+1
            write(6,24) U(J)
            enddo
      in=2*(ibsay-1)
               do j=1,in
               YB(j)=0.d0
               enddo
       do I =1,in
       do J =1,in
       yk(I,J)=0.d0
       enddo
       enddo
                do j=1,4
                rek1(j)=0.d0
               rek2(j)=0.d0
               rek3(j)=0.d0
               rek4(j)=0.d0
               enddo
c     V(Z) DISPLACEMENT FUNCTION
iL=0
iK=0
DO I=2,ibsay
             IF(I.LT.ibsay) THEN
         CALL COEF1V(ibsay,ALFA1,ALFA2,BETA1,BETA2,BETA3
     @                 ,Z(I),GAMA,G,EJ,K1,K2,K3,K4,H,DELTA
     @               ,Px,Py,Wx,Wy,dx,dy,r,EIOw,Alan,EIy,EIxy
     @                  ,Elas,D1,D2,D3,D4,REK1,REKB1,I)
         CALL COEF2V(ibsay,ALFA1,ALFA2,BETA1,BETA2,BETA3
     @                 ,Z(I),GAMA,G,EJ,K1,K2,K3,K4,H,DELTA
     @               ,Px,Py,Wx,Wy,dx,dy,r,EIOw,Alan,EIy,EIxy
     @                  ,Elas,D1,D2,D3,D4,REK2,REKB2,I)
        ENDIF
            IF(I.EQ.ibsay) THEN
               CALL COEF3V(ibsay,ALFA1,ALFA2,BETA1,BETA2,BETA3
     @                 ,Z(I),GAMA,G,EJ,K1,K2,K3,K4,H,DELTA
     @               ,Px,Py,Wx,Wy,dx,dy,r,EIOw,Alan,EIy,EIxy
     @                  ,Elas,D1,D2,D3,D4,REK1,REKB1,I)
               CALL COEF4V(ibsay,ALFA1,ALFA2,BETA1,BETA2,BETA3
     @                 ,Z(I),GAMA,G,EJ,K1,K2,K3,K4,H,DELTA
     @               ,Px,Py,Wx,Wy,dx,dy,r,EIOw,Alan,EIy,EIxy
     @                  ,Elas,D1,D2,D3,D4,REK2,REKB2,I)
             ENDIF
             IF(I.LT.ibsay) THEN
               DO J=1,4
                      YK(I+iL-1,J+iK)=YK(I+iL-1,J+iK)+REK1(J)
                      YB(I+iL-1)=REKB1
                      YK(I+iL,J+iK)=YK(I+iL,J+iK)+REK2(J)
                      YB(I+iL)=REKB2
                      ENDDO
             ENDIF
             iK=iK+2
             IF(I.EQ.ibsay) THEN
             DO J=1,2
                      YK(I+iL-1,J+iK-2)=YK(I+iL-1,J+iK-2)+REK1(J)
```

```
                  YB(I+iL-1)=REKB1
                  YK(I+iL,J+iK-2)=YK(I+iL,J+iK-2)+REK2(J)
                  YB(I+iL)=REKB2
          ENDDO
           ENDIF
           iL=iL+1
           do j=1,4
            rek1(j)=0.d0
            rek2(j)=0.d0
            rek3(j)=0.d0
            rek4(j)=0.d0
            enddo
           ENDDO
      in=2*(ibsay-1)
 c     write(6,*) 'Coefficient Matrix'
c     DO I =1,in
c      WRITE(6,233) (yk(I,J),J=1,in)
c     enddo
  235 FORMAT(1X,40F22.10)
c     write(6,*) 'Right Hand Side Vector'
c     WRITE(6,235) (yb(J),J=1,in)
     CALL GAUSS(YK,in,YB,SONUC4)
c     write(6,*) 'Result Vector'
c     WRITE(6,22) (SONUC4(J),J=1,in)
     im=0
DO I=1,ibsay
       P1(I)=P1(I)+SONUC4(I+im)
       P2(I)=P2(I)+SONUC4(I+1+im)
            im=im+1
     ENDDO
          P1(ibsay)=P1(ibsay-1)
     P2(ibsay)=P2(ibsay-1)
C      V(Z) FUNCTION
      iksay=KSAY+1
     DO I=1,ibsay
          DO 92 in=1,iksay
          im=iksay-in+1
          CALL VFONK(ibsay,iksay,ALFA1,ALFA2,BETA1,BETA2,BETA3
    @               ,GAMA,K1,K2,K3,K4,Elas,G,EJ,DELTA
    @              ,Px,Py,Wx,Wy,dx,dy,r,EIOw,Alan,H
    @                 ,EIy,EIxy,D1,D2,D3,D4,V,KAT,I,im
    @             ,P1,P2)
            IF(ABS(Z(I+1)-KAT(im)).LT.TOL) THEN
        iksay=im
             GOTO 82
              ENDIF
                  IF(KAT(im).LT.TOL) THEN
                   GOTO 82
              ENDIF
   92  CONTINUE
   82 ENDDO
     iksay=KSAY+1
     WRITE(6,*) '   '
     WRITE(6,*) 'V= '
     do I=1,iksay
```

```
     J=iksay-I+1
           write(6,24) V(J)
           enddo
    WRITE(6,*) '   '
     WRITE(6,*) 'T= '
     do I=1,iksay
     J=iksay-I+1
           write(6,24) T(J)
           enddo

     STOP
     END
*************************************************************************
c    *********      SUBROUTINES       ***************
c    ***********************************************************************
     SUBROUTINE COEF1A(ETozel,ETozelz,EALFA1,EALFA2
    @                                   ,EZ,ES,REK1,REKB1)
           implicit real*8 (A-H,K-Z)
           dimension REK1(8)
c          real*8 EALFA1,EALFA2,EZ,ES
           REK1(1)=EALFA1*ES*Cosh(EALFA1*EZ) + Sinh(EALFA1*EZ)
           REK1(2)=Cosh(EALFA1*EZ) + EALFA1*ES*Sinh(EALFA1*EZ)
           REK1(3)=EALFA2*ES*Cosh(EALFA2*EZ) + Sinh(EALFA2*EZ)
           REK1(4)=Cosh(EALFA2*EZ) + EALFA2*ES*Sinh(EALFA2*EZ)
           REKB1=-ETozel -ES*ETozelz
c          WRITE(6,*) REK1(1),REK1(2)
           RETURN
           END
           SUBROUTINE COEF1B(ETozel,ETozelz,ETozelzz,EALFA1,EALFA2
    @                ,EGAMA,EZ,ES,EEIw,EALAN,Er,Ew,REK2,REKB2)
           implicit real*8 (A-H,K-Z)
           dimension REK2(8)
           REK2(1)= -EALFA1*ES*Ew*Cosh(EALFA1*EZ)+
 ((1-EALAN*EALFA1**2*EGAMA)*EEIw*Sinh(EALFA1*EZ))/(EALAN*Er)
           REK2(2)= -EALFA1*ES*Ew*Sinh(EALFA1*EZ)+
  ((1-EALAN*EALFA1**2*EGAMA)*EEIw*Cosh(EALFA1*EZ))/(EALAN*Er)
           REK2(3)= -EALFA2*ES*Ew*Cosh(EALFA2*EZ)+
  ((1-EALAN*EALFA2**2*EGAMA)*EEIw*Sinh(EALFA2*EZ))/(EALAN*Er)
           REK2(4)= -EALFA2*ES*Ew*Sinh(EALFA2*EZ)+
-  ((1-EALAN*EALFA2**2*EGAMA)*EEIw*Cosh(EALFA2*EZ))/(EALAN*Er)
           REKB2=-((EEIw*ETozel)/(EALAN*Er)
    @     -(EGAMA*EEIw*ETozelzz)/Er-ES*ETozelz*Ew)
           RETURN
           END
           SUBROUTINE COEF2A(ibsay,EALFA1,EALFA2,EZ,
    @            ETozelz,ESTozelz,EGAMA,J,REK1,REKB1)
           implicit real*8 (A-H,K-Z)
           dimension REK1(8),EALFA1(ibsay),EALFA2(ibsay),
    @        ETozelz(ibsay),ESTozelz(ibsay),EGAMA(ibsay)
           REK1(1)=EALFA1(J-1)*EGAMA(J-1)*Cosh(EALFA1(J-1)*EZ)
     REK1(2)=EALFA1(J-1)*EGAMA(J-1)*Sinh(EALFA1(J-1)*EZ)
     REK1(3)=EALFA2(J-1)*EGAMA(J-1)*Cosh(EALFA2(J-1)*EZ)
     REK1(4)=EALFA2(J-1)*EGAMA(J-1)*Sinh(EALFA2(J-1)*EZ)
     REK1(5)=-(EALFA1(J)*EGAMA(J)*Cosh(EALFA1(J)*EZ))
     REK1(6)=-(EALFA1(J)*EGAMA(J)*Sinh(EALFA1(J)*EZ))
```

```
 REK1(7)=-(EALFA2(J)*EGAMA(J)*Cosh(EALFA2(J)*EZ))
 REK1(8)=-(EALFA2(J)*EGAMA(J)*Sinh(EALFA2(J)*EZ))
        REKB1=-(-(EGAMA(J)*ETozelz(J))+EGAMA(J-1)*ESTozelz(J-1))
        RETURN
        END
        SUBROUTINE COEF2B(ibsay,EALFA1,EALFA2,EZ,ES,
@                  ETozel,ETozelz,ESTozel,J,REK2,REKB2)
        implicit real*8 (A-H,K-Z)
        dimension REK2(8),EALFA1(ibsay),EALFA2(ibsay),
@                ETozel(ibsay),ETozelz(ibsay),ESTozel(ibsay)
        REK2(1)=Sinh(EALFA1(J-1)*EZ)
 REK2(2)=Cosh(EALFA1(J-1)*EZ)
 REK2(3)=Sinh(EALFA2(J-1)*EZ)
 REK2(4)=Cosh(EALFA2(J-1)*EZ)
 REK2(5)=-(EALFA1(J)*ES*Cosh(EALFA1(J)*EZ))-Sinh(EALFA1(J)*EZ)
 REK2(6)=-(EALFA1(J)*ES*Sinh(EALFA1(J)*EZ))-Cosh(EALFA1(J)*EZ)
 REK2(7)=-(EALFA2(J)*ES*Cosh(EALFA2(J)*EZ))-Sinh(EALFA2(J)*EZ)
 REK2(8)=-(EALFA2(J)*ES*Sinh(EALFA2(J)*EZ))-Cosh(EALFA2(J)*EZ)
        REKB2=-(-ETozel(J)+ESTozel(J-1)-ES*ETozelz(J))
      RETURN
        END
        SUBROUTINE COEF2C(ibsay,ETozelz,ETozelzzz,ESTozelz,ESTozelzzz,
@              EALFA1,EALFA2,EZ,EC1,EC2,J,REK3,REKB3)
        implicit real*8 (A-H,K-Z)
        dimension REK3(8),EALFA1(ibsay),EALFA2(ibsay),
@          EC1(ibsay),EC2(ibsay),ETozelz(ibsay),ESTozelz(ibsay),
@                        ETozelzzz(ibsay),ESTozelzzz(ibsay)

        REK3(1)= EALFA1(J-1)*(EC1(J-1)+EALFA1(J-1)**2*EC2(J-1))*
@                              Cosh(EALFA1(J-1)*EZ)
 REK3(2)= EALFA1(J-1)*(EC1(J-1)+EALFA1(J-1)**2*EC2(J-1))*
@                              Sinh(EALFA1(J-1)*EZ)
 REK3(3)= EALFA2(J-1)*(EC1(J-1)+EALFA2(J-1)**2*EC2(J-1))*
@                              Cosh(EALFA2(J-1)*EZ)
 REK3(4)= EALFA2(J-1)*(EC1(J-1)+EALFA2(J-1)**2*EC2(J-1))*
@                              Sinh(EALFA2(J-1)*EZ)
 REK3(5)= -(EALFA1(J)*(EC1(J)+EALFA1(J)**2*EC2(J))*
@                          Cosh(EALFA1(J)*EZ))
 REK3(6)= -(EALFA1(J)*(EC1(J)+EALFA1(J)**2*EC2(J))*
@                          Sinh(EALFA1(J)*EZ))
 REK3(7)= -(EALFA2(J)*(EC1(J)+EALFA2(J)**2*EC2(J))*
@                          Cosh(EALFA2(J)*EZ))
REK3(8)= -(EALFA2(J)*(EC1(J)+EALFA2(J)**2*EC2(J))*
@                          Sinh(EALFA2(J)*EZ))
        REKB3=-(-(EC1(J)*ETozelz(J))+EC1(J-1)*ESTozelz(J-1)
@          -EC2(J)*ETozelzzz(J)+EC2(J-1)*ESTozelzzz(J-1))
        RETURN
        END
        SUBROUTINE COEF2D(ibsay,ETozel,ETozelz,ETozelzz,ESTozel,ESTozelzz,
@          EALFA1,EALFA2,EZ,ES,EGAMA,EEIw,EALAN,Er,Ew,J,REK4,REKB4)
        implicit real*8 (A-H,K-Z)
        dimension REK4(8),EALFA1(ibsay),EALFA2(ibsay),EGAMA(ibsay),
@                ETozel(ibsay),ETozelz(ibsay),ESTozel(ibsay),
@                ETozelzz(ibsay),ESTozelzz(ibsay)
        REK4(1)= ((-1+EAlan*EALFA1(J-1)**2*EGAMA(J-1))*EEIw*
```

```
     -      Sinh(EALFA1(J-1)*EZ))/(EAlan*Er)
      REK4(2)= ((-1+EAlan*EALFA1(J-1)**2*EGAMA(J-1))*EEIw*
     -      Cosh(EALFA1(J-1)*EZ))/(EAlan*Er)
      REK4(3)= ((-1+EAlan*EALFA2(J-1)**2*EGAMA(J-1))*EEIw*
     -      Sinh(EALFA2(J-1)*EZ))/(EAlan*Er)
      REK4(4)= ((-1+EAlan*EALFA2(J-1)**2*EGAMA(J-1))*EEIw*
     -      Cosh(EALFA2(J-1)*EZ))/(EAlan*Er)
      REK4(5)= EALFA1(J)*ES*Ew*Cosh(EALFA1(J)*EZ)+
     -      ((1-EAlan*EALFA1(J)**2*EGAMA(J))*EEIw*
     -      Sinh(EALFA1(J)*EZ))/(EAlan*Er)
      REK4(6)= EALFA1(J)*ES*Ew*Sinh(EALFA1(J)*EZ)+
     -      ((1-EAlan*EALFA1(J)**2*EGAMA(J))*EEIw*
     -      Cosh(EALFA1(J)*EZ))/(EAlan*Er)
      REK4(7)= EALFA2(J)*ES*Ew*Cosh(EALFA2(J)*EZ)+
     -      ((1-EAlan*EALFA2(J)**2*EGAMA(J))*EEIw*
     -      Sinh(EALFA2(J)*EZ))/(EAlan*Er)
      REK4(8)= EALFA2(J)*ES*Ew*Sinh(EALFA2(J)*EZ)+
     -      ((1-EAlan*EALFA2(J)**2*EGAMA(J))*EEIw*
     -      Cosh(EALFA2(J)*EZ))/(EAlan*Er)
            REKB4=-((EEIw*(ETozel(J)-ESTozel(J-1)-EAlan*EGAMA(J)*ETozelzz(J)+
     -   EAlan*EGAMA(J-1)*ESTozelzz(J-1)))/(EAlan*Er)+ES*ETozelz(J)*Ew)
      RETURN
            END
      SUBROUTINE COEF3A(ETozelz,EALFA1,EALFA2,EZ,REK1,REKB1)
            implicit real*8 (A-H,K-Z)
            dimension REK1(8)
      REK1(1)=EALFA1*Cosh(EALFA1*EZ)
      REK1(2)=EALFA1*Sinh(EALFA1*EZ)
      REK1(3)=EALFA2*Cosh(EALFA2*EZ)
      REK1(4)=EALFA2*Sinh(EALFA2*EZ)
      REKB1=-ETozelz
      RETURN
            END
      SUBROUTINE COEF3B(ETozelz,ETozelzzz,EALFA1,EALFA2,
     @           EZ,EGAMA,EMxz,EMyz,EMt,
     @           EEIw,EALAN,Er,Ew,EEIyc,EEIxc,EEIx,EEIy,EEIxy,
     @           EK1,EK2,EK3,EK4,Ed,EDelta,REK2,REKB2)
            implicit real*8 (A-H,K-Z)
            dimension REK2(8)
      REK2(1)=-((EALFA1*((-ALAN*EALFA1**2*EGAMA)*EEIw+EEIyc*EK1+
      EEIxc*EK2-EALAN*(EALFA1**2*EGAMA*(EEIyc*EK1+EEIxc*EK2)+
      Er*(Ed+EEIyc*EK3-EEIxc*EK4+Ew))))/(EALAN*Er))
      REK2(2)=0.
        REK2(3)=((EALFA2*((1+EALAN*EALFA2**2*EGAMA)*EEIw+EEIyc*EK1+
EEIxc*EK2-EALAN*(EALFA2**2*EGAMA*(EEIyc*EK1+EEIxc*EK2)+
Er*(Ed+EEIyc*EK3-EEIxc*EK4+Ew))))/(EALAN*Er))
      REK2(4)=0.
      REKB2=((EDelta*(EEIw-EEIyc*EK1-EEIxc*EK2)*ETozelz+
     -     EALAN*((EEIxc*EEIy*EMxz+EEIxy*EEIyc*EMxz-EEIxc*EEIxy*EMyz-
     -      EEIx*EEIyc*EMyz)*Er+EDelta*(Er*(EMt+Ed*ETozelz)-
     -      EEIw*(EK4*EMxz+EK3*EMyz+EGAMA*ETozelzzz)+
     -      EEIyc*(EK1*EK4*EMxz+EK1*EK3*EMyz+EK3*Er*ETozelz+
     -      EGAMA*EK1*ETozelzzz)+
     -      EEIxc*(EK2*EK4*EMxz+EK2*EK3*EMyz-EK4*Er*ETozelz+
     -      EGAMA*EK2*ETozelzzz)+Er*ETozelz*Ew)))/
```

```
-       (EALAN*EDelta*Er))
        RETURN
        END
        SUBROUTINE COEF1Y(ibsay,EALFA1,EALFA2,EBETA1,EBETA2,EBETA3
@                  ,EZ,EGAMA,EG,EEJ,EK1,EK2,EK3,EK4,EH
@                  ,EPx,EPy,EWx,EWy,Edx,Edy,Er,EEIOw,EAlan
@                     ,EElas,ED1,ED2,ED3,ED4,REK1,REKB1,J)

        implicit real*8 (A-H,K-Z)
        dimension REK1(4),EBETA1(ibsay),EBETA2(ibsay),EBETA3(ibsay)
@                 ,EALFA1(ibsay),EALFA2(ibsay),EGAMA(ibsay)
@                 ,ED1(ibsay),ED2(ibsay),ED3(ibsay),ED4(ibsay)
      REK1(1)=1
        REK1(2)=0
        REK1(3)=-1
        REK1(4)=0
        REKB1= -((EALFA1(J)**2*EALFA2(J)**2*EZ**2*
-       (-4*EBETA3(J)*(EAlan*EBETA3(J)*EElas-EEJ*EG)*
-       (EK3*(EPx+EH*EWx)+EK4*(EPy+EH*EWy))+
-        2*EBETA3(J)*(EAlan*EBETA3(J)*EElas-EEJ*EG)*
-       (EK3*EWx+EK4*EWy)*EZ)+
-        2*EALFA1(J)**2*EALFA2(J)**2*EZ*
-       (6*EAlan*EBETA3(J)*
-       (2*EEJ*EG*EGAMA(J)*(EK3*EWx+EK4*EWy)+
-        EBETA3(J)*EElas*EH*
-       (2*EK3*EPx+2*EK4*EPy+EH*EK3*EWx+
-        EH*EK4*EWy))-
-        6*(2*EBETA2(J)*EEJ*EG*(EK3*EWx+EK4*EWy)+
-        EBETA3(J)*(EEJ*EG*EH*
-       (2*EK3*EPx+2*EK4*EPy+EH*EK3*EWx+
-        EH*EK4*EWy)-2*EElas*
-       (EEIOw*EK3*EWx-Edy*Er*EWx+EK1*Er*EWx+
-        EEIOw*EK4*EWy+Edx*Er*EWy-EK2*Er*EWy)))
-        -4*EBETA3(J)*(EAlan*EBETA3(J)*EElas-EEJ*EG)*
-       (EK3*(EPx+EH*EWx)+EK4*(EPy+EH*EWy))*EZ+
-        EBETA3(J)*(EAlan*EBETA3(J)*EElas-EEJ*EG)*
-       (EK3*EWx+EK4*EWy)*EZ**2)+
-        24*EALFA1(J)*EALFA2(J)**2*EBETA3(J)**2*ED2(J)*EElas*
-       (-1+EAlan*EALFA1(J)**2*EGAMA(J))*Sinh(EALFA1(J)*EZ)+
-        24*EBETA3(J)**2*EElas*
-       (EALFA1(J)*EALFA2(J)**2*ED1(J)*
-       (-1+EAlan*EALFA1(J)**2*EGAMA(J))*Cosh(EALFA1(J)*EZ)+
-        EALFA1(J)**2*EALFA2(J)*ED3(J)*
-       (-1+EAlan*EALFA2(J)**2*EGAMA(J))*Cosh(EALFA2(J)*EZ)+
-        EALFA1(J)**2*EALFA2(J)*ED4(J)*
-       (-1+EAlan*EALFA2(J)**2*EGAMA(J))*Sinh(EALFA2(J)*EZ)))/
-       (24.*EAlan*EALFA1(J)**2*EALFA2(J)**2*
-        EBETA3(J)**2*EElas**2*Er)
-        -(EALFA1(J-1)**2*EALFA2(J-1)**2*EZ**2*
-       (-4*EBETA3(J-1)*(EAlan*EBETA3(J-1)*EElas-EEJ*EG)*
-       (EK3*(EPx+EH*EWx)+EK4*(EPy+EH*EWy))+
-        2*EBETA3(J-1)*(EAlan*EBETA3(J-1)*EElas-EEJ*EG)*
-       (EK3*EWx+EK4*EWy)*EZ)+
-        2*EALFA1(J-1)**2*EALFA2(J-1)**2*EZ*
-       (6*EAlan*EBETA3(J-1)*
```

```
-       (2*EEJ*EG*EGAMA(J-1)*(EK3*EWx+EK4*EWy)+
-        EBETA3(J-1)*EElas*EH*
-       (2*EK3*EPx+2*EK4*EPy+EH*EK3*EWx+
-        EH*EK4*EWy))-
-        6*(2*EBETA2(J-1)*EEJ*EG*(EK3*EWx+EK4*EWy)+
-        EBETA3(J-1)*(EEJ*EG*EH*
-       (2*EK3*EPx+2*EK4*EPy+EH*EK3*EWx+
-        EH*EK4*EWy)-2*EElas*
-       (EEIOw*EK3*EWx-Edy*Er*EWx+EK1*Er*EWx+
-        EEIOw*EK4*EWy+Edx*Er*EWy-EK2*Er*EWy)))
-        -4*EBETA3(J-1)*(EAlan*EBETA3(J-1)*EElas-EEJ*EG)*
-       (EK3*(EPx+EH*EWx)+EK4*(EPy+EH*EWy))*EZ+
-        EBETA3(J-1)*(EAlan*EBETA3(J-1)*EElas-EEJ*EG)*
-       (EK3*EWx+EK4*EWy)*EZ**2)+
-        24*EALFA1(J-1)*EALFA2(J-1)**2*
-        EBETA3(J-1)**2*ED2(J-1)*EElas*
-       (-1+EAlan*EALFA1(J-1)**2*EGAMA(J-1))*Sinh(EALFA1(J-1)*EZ)+
-        24*EBETA3(J-1)**2*EElas*
-       (EALFA1(J-1)*EALFA2(J-1)**2*ED1(J-1)*
-       (-1+EAlan*EALFA1(J-1)**2*EGAMA(J-1))*Cosh(EALFA1(J-1)*EZ)
-        +EALFA1(J-1)**2*EALFA2(J-1)*ED3(J-1)*
-       (-1+EAlan*EALFA2(J-1)**2*EGAMA(J-1))*Cosh(EALFA2(J-1)*EZ)
-        +EALFA1(J-1)**2*EALFA2(J-1)*ED4(J-1)*
-       (-1+EAlan*EALFA2(J-1)**2*EGAMA(J-1))*Sinh(EALFA2(J-1)*EZ)
-       ))/(24.*EAlan*EALFA1(J-1)**2*EALFA2(J-1)**2*
-        EBETA3(J-1)**2*EElas**2*Er))
 return
        end
        SUBROUTINE COEF2Y(ibsay,EALFA1,EALFA2,EBETA1,EBETA2,EBETA3
@                ,EZ,EGAMA,EG,EEJ,EK1,EK2,EK3,EK4,EH
@               ,EPx,EPy,EWx,EWy,Edx,Edy,Er,EEIOw,EAlan
@                                   ,EElas,ED1,ED2,ED3,ED4,REK2,REKB2,J)
        implicit real*8 (A-H,K-Z)
        dimension REK2(4),EBETA1(ibsay),EBETA2(ibsay),EBETA3(ibsay)
@               ,EALFA1(ibsay),EALFA2(ibsay),EGAMA(ibsay)
@               ,ED1(ibsay),ED2(ibsay),ED3(ibsay),ED4(ibsay)
 REK2(1)=EZ
        REK2(2)=1
        REK2(3)=-EZ
        REK2(4)=-1
        REKB2= -((EALFA1(J)**2*EALFA2(J)**2*EZ**2*
-       (6*EAlan*EBETA3(J)*
-       (2*EEJ*EG*EGAMA(J)*(EK3*EWx+EK4*EWy)+
-        EBETA3(J)*EElas*EH*
-       (2*EK3*EPx+2*EK4*EPy+EH*EK3*EWx+
-        EH*EK4*EWy))-
-        6*(2*EBETA2(J)*EEJ*EG*(EK3*EWx+EK4*EWy)+
-        EBETA3(J)*(EEJ*EG*EH*
-       (2*EK3*EPx+2*EK4*EPy+EH*EK3*EWx+
-        EH*EK4*EWy)-2*EElas*
-       (EEIOw*EK3*EWx-Edy*Er*EWx+EK1*Er*EWx+
-        EEIOw*EK4*EWy+Edx*Er*EWy-EK2*Er*EWy)))
-        -4*EBETA3(J)*(EAlan*EBETA3(J)*EElas-EEJ*EG)*
-       (EK3*(EPx+EH*EWx)+EK4*(EPy+EH*EWy))*EZ+
-        EBETA3(J)*(EAlan*EBETA3(J)*EElas-EEJ*EG)*
```

```
-       (EK3*EWx+EK4*EWy)*EZ**2)+
-        24*EALFA2(J)**2*EBETA3(J)**2*ED2(J)*EElas*
-       (-1+EAlan*EALFA1(J)**2*EGAMA(J))*Cosh(EALFA1(J)*EZ)+
-        24*EBETA3(J)**2*EElas*
-       (EALFA1(J)**2*ED4(J)*(-1+EAlan*EALFA2(J)**2*EGAMA(J))*
-        Cosh(EALFA2(J)*EZ)+
-        EALFA2(J)**2*ED1(J)*(-1+EAlan*EALFA1(J)**2*EGAMA(J))*
-        Sinh(EALFA1(J)*EZ)+
-        EALFA1(J)**2*ED3(J)*(-1+EAlan*EALFA2(J)**2*EGAMA(J))*
-        Sinh(EALFA2(J)*EZ)))/
-       (24.*EAlan*EALFA1(J)**2*EALFA2(J)**2*
-        EBETA3(J)**2*EElas**2*Er)
-        -(EALFA1(J-1)**2*EALFA2(J-1)**2*EZ**2*
-       (6*EAlan*EBETA3(J-1)*
-       (2*EEJ*EG*EGAMA(J-1)*(EK3*EWx+EK4*EWy)+
-        EBETA3(J-1)*EElas*EH*
-       (2*EK3*EPx+2*EK4*EPy+EH*EK3*EWx+
-        EH*EK4*EWy))-
-        6*(2*EBETA2(J-1)*EEJ*EG*(EK3*EWx+EK4*EWy)+
-        EBETA3(J-1)*(EEJ*EG*EH*
-       (2*EK3*EPx+2*EK4*EPy+EH*EK3*EWx+
-        EH*EK4*EWy)-2*EElas*
-       (EEIOw*EK3*EWx-Edy*Er*EWx+EK1*Er*EWx+
-        EEIOw*EK4*EWy+Edx*Er*EWy-EK2*Er*EWy)))
-        -4*EBETA3(J-1)*(EAlan*EBETA3(J-1)*EElas-EEJ*EG)*
-       (EK3*(EPx+EH*EWx)+EK4*(EPy+EH*EWy))*EZ+
-        EBETA3(J-1)*(EAlan*EBETA3(J-1)*EElas-EEJ*EG)*
-       (EK3*EWx+EK4*EWy)*EZ**2)+
-        24*EALFA2(J-1)**2*EBETA3(J-1)**2*ED2(J-1)*EElas*
-       (-1+EAlan*EALFA1(J-1)**2*EGAMA(J-1))*Cosh(EALFA1(J-1)*EZ)+
-        24*EBETA3(J-1)**2*EElas*
-       (EALFA1(J-1)**2*ED4(J-1)*(-1+EAlan*EALFA2(J-1)**2*
-        EGAMA(J-1))*Cosh(EALFA2(J-1)*EZ)+
-        EALFA2(J-1)**2*ED1(J-1)*(-1+EAlan*EALFA1(J-1)**2*
-        EGAMA(J-1))*Sinh(EALFA1(J-1)*EZ)+
-        EALFA1(J-1)**2*ED3(J-1)*(-1+EAlan*EALFA2(J-1)**2*
-        EGAMA(J-1))*Sinh(EALFA2(J-1)*EZ)))/
-       (24.*EAlan*EALFA1(J-1)**2*EALFA2(J-1)**2*
-        EBETA3(J-1)**2*EElas**2*Er))
        return
        end
        SUBROUTINE COEF3Y(ibsay,EALFA1,EALFA2,EBETA1,EBETA2,EBETA3
@            ,EZ,EGAMA,EG,EEJ,EK1,EK2,EK3,EK4,EH
@           ,EPx,EPy,EWx,EWy,Edx,Edy,Er,EEIOw,EAlan
@              ,EElas,ED1,ED2,ED3,ED4,REK1,REKB1,J)
        implicit real*8 (A-H,K-Z)
        dimension REK1(4),EBETA1(ibsay),EBETA2(ibsay),EBETA3( ibsay)
@           ,EALFA1(ibsay),EALFA2(ibsay),EGAMA(ibsay)
@           ,ED1(ibsay),ED2(ibsay),ED3(ibsay),ED4(ibsay)
 REK1(1)=1
        REK1(2)=0
        REKB1= -(-((EALFA1(J)*EALFA2(J)**2*ED1(J)*
-       (-1+EAlan*EALFA1(J)**2*EGAMA(J))+
-        EALFA1(J)**2*EALFA2(J)*ED3(J)*
-       (-1+EAlan*EALFA2(J)**2*EGAMA(J)))/
```

```
-       (EAlan*EALFA1(J)**2*EALFA2(J)**2*EElas*Er)))
        return
        end
        SUBROUTINE COEF4Y(ibsay,EALFA1,EALFA2,EBETA1,EBETA2,EBETA3
@               ,EZ,EGAMA,EG,EEJ,EK1,EK2,EK3,EK4,EH
@               ,EPx,EPy,EWx,EWy,Edx,Edy,Er,EEIOw,EAlan
@                                   ,EElas,ED1,ED2,ED3,ED4,REK2,REKB2,J)
        implicit real*8 (A-H,K-Z)
        dimension REK2(4),EBETA1(ibsay),EBETA2(ibsay),EBETA3(ibsay)
@               ,EALFA1(ibsay),EALFA2(ibsay),EGAMA(ibsay)
@               ,ED1(ibsay),ED2(ibsay),ED3(ibsay),ED4(ibsay)
 REK2(1)=0
        REK2(2)=1
        REKB2=  -((-24*EALFA2(J)**2*EBETA3(J)**2*ED2(J)*EElas*
-        (-1+EAlan*EALFA1(J)**2*EGAMA(J))-
-         24*EALFA1(J)**2*EBETA3(J)**2*ED4(J)*EElas*
-        (-1+EAlan*EALFA2(J)**2*EGAMA(J)))/
-        (24.*EAlan*EALFA1(J)**2*EALFA2(J)**2*
-         EBETA3(J)**2*EElas**2*Er))
        return
        end
        SUBROUTINE TETAFONK(ibsay,iksay,EALFA1,EALFA2,EBETA1,EBETA2,EBETA3
@                       ,EGAMA,EK1,EK2,EK3,EK4,EElas,EG,EEJ
@                      ,EPx,EPy,EWx,EWy,Edx,Edy,Er,EEIOw,EAlan,EH
@                            ,ED1,ED2,ED3,ED4,ETETA,ETET,J,jm,EG1,EG2)
        implicit real*8 (A-H,K-Z)
        dimension ETETA(iksay),ETET(iksay),EG1(ibsay),EG2(ibsay)
@                  ,ED1(ibsay),ED2(ibsay),ED3(ibsay),ED4(ibsay)
@         ,EALFA1(ibsay),EALFA2(ibsay),EGAMA(ibsay)
@         ,EBETA1(ibsay),EBETA2(ibsay),EBETA3(ibsay)
 ETETA(jm)=
-     ETET(jm)*EG1(J)+EG2(J)-(EALFA1(J)**2*
-     EALFA2(J)**2*ETET(jm)**2*
-    (6*EAlan*EBETA3(J)*
-    (2*EEJ*EG*EGAMA(J)*(EK3*EWx+EK4*EWy)+
-     EBETA3(J)*EElas*EH*
-    (2*EK3*EPx+2*EK4*EPy+EH*EK3*EWx+
-     EH*EK4*EWy))-
-     6*(2*EBETA2(J)*EEJ*EG*(EK3*EWx+EK4*EWy)+
-     EBETA3(J)*(EEJ*EG*EH*
-    (2*EK3*EPx+2*EK4*EPy+EH*EK3*EWx+
-     EH*EK4*EWy)-2*EElas*
-    (EEIOw*EK3*EWx-Edy*Er*EWx+EK1*Er*EWx+
-     EEIOw*EK4*EWy+Edx*Er*EWy-EK2*Er*EWy)))
-     -4*EBETA3(J)*(EAlan*EBETA3(J)*EElas-EEJ*EG)*
-    (EK3*(EPx+EH*EWx)+EK4*(EPy+EH*EWy))*ETET(jm)+
-     EBETA3(J)*(EAlan*EBETA3(J)*EElas-EEJ*EG)*
-    (EK3*EWx+EK4*EWy)*ETET(jm)**2)+
-     24*EALFA2(J)**2*EBETA3(J)**2*ED2(J)*EElas*
-    (-1+EAlan*EALFA1(J)**2*EGAMA(J))*
-     Cosh(EALFA1(J)*ETET(jm))+
-     24*EBETA3(J)**2*EElas*
-    (EALFA1(J)**2*ED4(J)*(-1+EAlan*EALFA2(J)**2*EGAMA(J))*
-     Cosh(EALFA2(J)*ETET(jm))+
-     EALFA2(J)**2*ED1(J)*(-1+EAlan*EALFA1(J)**2*EGAMA(J))*
```

```
-     Sinh(EALFA1(J)*ETET(jm))+
-     EALFA1(J)**2*ED3(J)*(-1+EAlan*EALFA2(J)**2*EGAMA(J))*
-     Sinh(EALFA2(J)*ETET(jm))))/
-    (24.*EAlan*EALFA1(J)**2*EALFA2(J)**2*
-     EBETA3(J)**2*EElas**2*Er)
      return
      end
      SUBROUTINE COEF1U(ibsay,EALFA1,EALFA2,EBETA1,EBETA2,EBETA3
@               ,EZ,EGAMA,EG,EEJ,EK1,EK2,EK3,EK4,EH,EDELTA
@              ,EPx,EPy,EWx,EWy,Edx,Edy,Er,EEIOw,EAlan,EEIx,EEIxy
@                                     ,EElas,ED1,ED2,ED3,ED4,REK1,REKB1,J)
      implicit real*8 (A-H,K-Z)
      dimension REK1(4),EBETA1(ibsay),EBETA2(ibsay),EBETA3(ibsay)
@               ,EALFA1(ibsay),EALFA2(ibsay),EGAMA(ibsay)
@               ,ED1(ibsay),ED2(ibsay),ED3(ibsay),ED4(ibsay)
 REK1(1)=1
      REK1(2)=0
      REK1(3)=-1
      REK1(4)=0
      REKB1= -((EALFA1(J)**2*EALFA2(J)**2*EZ**2*
-     (EDELTA*(-4*EBETA3(J)*
-          (EAlan*EBETA3(J)*EElas*EK1 - EEJ*EG*EK1 +
-            EAlan*EEJ*EG*EK3*Er)*
-          (EK3*(EPx + EH*EWx) + EK4*(EPy + EH*EWy)) +
-         2*EBETA3(J)*
-          (EAlan*EBETA3(J)*EElas*EK1 - EEJ*EG*EK1 +
-            EAlan*EEJ*EG*EK3*Er)*(EK3*EWx + EK4*EWy)*EZ)
-        + EAlan*EBETA3(J)**2*EElas*Er*
-        (EEIx*(4*(EPx + EH*EWx) - 2*EWx*EZ) +
-         EEIxy*(-4*(EPy + EH*EWy) + 2*EWy*EZ))) +
-    2*EALFA1(J)**2*EALFA2(J)**2*EZ*
-     (EDELTA*(12*EAlan*EBETA2(J)*EEJ*EG*EK3*Er*
-          (EK3*EWx + EK4*EWy) +
-         6*EAlan*EBETA3(J)**2*EElas*EH*EK1*
-          (2*EK3*EPx + 2*EK4*EPy + EH*EK3*EWx +
-            EH*EK4*EWy) -
-         12*EAlan*EBETA3(J)*EElas*EK3*Er*
-          (Er*(-(Edy*EWx) + EK1*EWx + Edx*EWy -
-               EK2*EWy) + EEIOw*(EK3*EWx + EK4*EWy)) +
-         6*EAlan*EBETA3(J)*EEJ*EG*
-          (2*EH*EK3*(EK3*EPx + EK4*EPy)*Er +
-            2*EGAMA(J)*EK1*(EK3*EWx + EK4*EWy) +
-            EH**2*EK3*Er*(EK3*EWx + EK4*EWy)) -
-         6*EK1*(2*EBETA2(J)*EEJ*EG*(EK3*EWx + EK4*EWy) +
-            EBETA3(J)*
-             (EEJ*EG*EH*
-                (2*EK3*EPx + 2*EK4*EPy + EH*EK3*EWx +
-                  EH*EK4*EWy) -
-               2*EElas*
-                (EEIOw*EK3*EWx - Edy*Er*EWx +
-                  EK1*Er*EWx + EEIOw*EK4*EWy +
-                  Edx*Er*EWy - EK2*Er*EWy))) -
-         4*EBETA3(J)*
-          (EAlan*EBETA3(J)*EElas*EK1 - EEJ*EG*EK1 +
-            EAlan*EEJ*EG*EK3*Er)*
```

```
-          (EK3*(EPx + EH*EWx) + EK4*(EPy + EH*EWy))*EZ +
-         EBETA3(J)*(EAlan*EBETA3(J)*EElas*EK1 - EEJ*EG*EK1 +
-            EAlan*EEJ*EG*EK3*Er)*(EK3*EWx + EK4*EWy)*
-          EZ**2) +
-       EAlan*EBETA3(J)**2*EElas*Er*
-        (EEIx*(-6*EH*(2*EPx + EH*EWx) +
-            4*(EPx + EH*EWx)*EZ - EWx*EZ**2) +
-         EEIxy*(6*EH*(2*EPy + EH*EWy) -
-            4*(EPy + EH*EWy)*EZ + EWy*EZ**2))) -
-    24*EDELTA*EBETA3(J)**2*EElas*
-     (EALFA1(J)*EALFA2(J)**2*ED1(J)*
-        (EK1 - EAlan*EALFA1(J)**2*EGAMA(J)*EK1 -
-          EAlan*EK3*Er)*Cosh(EALFA1(J)*EZ) +
-       EALFA1(J)*EALFA2(J)**2*ED2(J)*
-        (EK1 - EAlan*EALFA1(J)**2*EGAMA(J)*EK1 -
-          EAlan*EK3*Er)*Sinh(EALFA1(J)*EZ) -
-       EALFA1(J)**2*((-1 + EAlan*EALFA2(J)**2*EGAMA(J))*EK1 +
-          EAlan*EK3*Er)*
-        (EALFA2(J)*ED3(J)*Cosh(EALFA2(J)*EZ) +
-          EALFA2(J)*ED4(J)*Sinh(EALFA2(J)*EZ))))/
-  (24.*EDELTA*EAlan*EALFA1(J)**2*EALFA2(J)**2*EBETA3(J)**2*
-    EElas**2*Er) + (-(EALFA1(J-1)**2*EALFA2(J-1)**2*EZ**2*
-       (EDELTA*(-4*EBETA3(J-1)*
-            (EAlan*EBETA3(J-1)*EElas*EK1 - EEJ*EG*EK1 +
-              EAlan*EEJ*EG*EK3*Er)*
-            (EK3*(EPx + EH*EWx) + EK4*(EPy + EH*EWy)) +
-           2*EBETA3(J-1)*
-            (EAlan*EBETA3(J-1)*EElas*EK1 - EEJ*EG*EK1 +
-              EAlan*EEJ*EG*EK3*Er)*(EK3*EWx + EK4*EWy)*EZ
-           ) + EAlan*EBETA3(J-1)**2*EElas*Er*
-         (EEIx*(4*(EPx + EH*EWx) - 2*EWx*EZ) +
-           EEIxy*(-4*(EPy + EH*EWy) + 2*EWy*EZ)))) -
-    2*EALFA1(J-1)**2*EALFA2(J-1)**2*EZ*
-     (EDELTA*(12*EAlan*EBETA2(J-1)*EEJ*EG*EK3*Er*
-          (EK3*EWx + EK4*EWy) +
-         6*EAlan*EBETA3(J-1)**2*EElas*EH*EK1*
-          (2*EK3*EPx + 2*EK4*EPy + EH*EK3*EWx +
-            EH*EK4*EWy) -
-         12*EAlan*EBETA3(J-1)*EElas*EK3*Er*
-          (Er*(-(Edy*EWx) + EK1*EWx + Edx*EWy -
-               EK2*EWy) + EEIOw*(EK3*EWx + EK4*EWy)) +
-         6*EAlan*EBETA3(J-1)*EEJ*EG*
-          (2*EH*EK3*(EK3*EPx + EK4*EPy)*Er +
-            2*EGAMA(J-1)*EK1*(EK3*EWx + EK4*EWy) +
-            EH**2*EK3*Er*(EK3*EWx + EK4*EWy)) -
-         6*EK1*(2*EBETA2(J-1)*EEJ*EG*(EK3*EWx + EK4*EWy) +
-            EBETA3(J-1)*
-             (EEJ*EG*EH*
-                (2*EK3*EPx + 2*EK4*EPy + EH*EK3*EWx +
-                  EH*EK4*EWy) -
-               2*EElas*
-                (EEIOw*EK3*EWx - Edy*Er*EWx +
-                  EK1*Er*EWx + EEIOw*EK4*EWy +
-                  Edx*Er*EWy - EK2*Er*EWy))) -
-         4*EBETA3(J-1)*
```

```
-          (EAlan*EBETA3(J-1)*EElas*EK1 - EEJ*EG*EK1 +
-            EAlan*EEJ*EG*EK3*Er)*
-          (EK3*(EPx + EH*EWx) + EK4*(EPy + EH*EWy))*EZ +
-         EBETA3(J-1)*(EAlan*EBETA3(J-1)*EElas*EK1 -
-            EEJ*EG*EK1 + EAlan*EEJ*EG*EK3*Er)*
-          (EK3*EWx + EK4*EWy)*EZ**2) +
-      EAlan*EBETA3(J-1)**2*EElas*Er*
-       (EEIx*(-6*EH*(2*EPx + EH*EWx) +
-            4*(EPx + EH*EWx)*EZ - EWx*EZ**2) +
-         EEIxy*(6*EH*(2*EPy + EH*EWy) -
-            4*(EPy + EH*EWy)*EZ + EWy*EZ**2))) +
-    24*EDELTA*EBETA3(J-1)**2*EElas*
-     (EALFA1(J-1)*EALFA2(J-1)**2*ED1(J-1)*
-       (EK1 - EAlan*EALFA1(J-1)**2*EGAMA(J-1)*EK1 -
-         EAlan*EK3*Er)*Cosh(EALFA1(J-1)*EZ) +
-      EALFA1(J-1)*EALFA2(J-1)**2*ED2(J-1)*
-       (EK1 - EAlan*EALFA1(J-1)**2*EGAMA(J-1)*EK1 -
-         EAlan*EK3*Er)*Sinh(EALFA1(J-1)*EZ) -
-      EALFA1(J-1)**2*((-1 + EAlan*EALFA2(J-1)**2*EGAMA(J-1))*
-          EK1 + EAlan*EK3*Er)*
-       (EALFA2(J-1)*ED3(J-1)*Cosh(EALFA2(J-1)*EZ) +
-         EALFA2(J-1)*ED4(J-1)*Sinh(EALFA2(J-1)*EZ))))/
-   (24.*EDELTA*EAlan*EALFA1(J-1)**2*EALFA2(J-1)**2*EBETA3(J-1)**2*
-    EElas**2*Er))
 return
        end
        SUBROUTINE COEF2U(ibsay,EALFA1,EALFA2,EBETA1,EBETA2,EBETA3
@               ,EZ,EGAMA,EG,EEJ,EK1,EK2,EK3,EK4,EH,EDELTA
@              ,EPx,EPy,EWx,EWy,Edx,Edy,Er,EEIOw,EAlan,EEIx,EEIxy
@                                   ,EElas,ED1,ED2,ED3,ED4,REK2,REKB2,J)
        implicit real*8 (A-H,K-Z)
        dimension REK2(4),EBETA1(ibsay),EBETA2(ibsay),EBETA3(ibsay)
@              ,EALFA1(ibsay),EALFA2(ibsay),EGAMA(ibsay)
@              ,ED1(ibsay),ED2(ibsay),ED3(ibsay),ED4(ibsay)
 REK2(1)=EZ
        REK2(2)=1
        REK2(3)=-EZ
        REK2(4)=-1
        REKB2= -((EALFA1(J)**2*EALFA2(J)**2*EZ**2*
-     (EDELTA*(12*EAlan*EBETA2(J)*EEJ*EG*EK3*Er*
-          (EK3*EWx + EK4*EWy) +
-         6*EAlan*EBETA3(J)**2*EElas*EH*EK1*
-          (2*EK3*EPx + 2*EK4*EPy + EH*EK3*EWx +
-            EH*EK4*EWy) -
-         12*EAlan*EBETA3(J)*EElas*EK3*Er*
-          (Er*(-(Edy*EWx) + EK1*EWx + Edx*EWy -
-               EK2*EWy) + EEIOw*(EK3*EWx + EK4*EWy)) +
-         6*EAlan*EBETA3(J)*EEJ*EG*
-          (2*EH*EK3*(EK3*EPx + EK4*EPy)*Er +
-            2*EGAMA(J)*EK1*(EK3*EWx + EK4*EWy) +
-            EH**2*EK3*Er*(EK3*EWx + EK4*EWy)) -
-         6*EK1*(2*EBETA2(J)*EEJ*EG*(EK3*EWx + EK4*EWy) +
-            EBETA3(J)*
-             (EEJ*EG*EH*
-               (2*EK3*EPx + 2*EK4*EPy + EH*EK3*EWx +
```

```
-                  EH*EK4*EWy) -
-               2*EElas*
-                (EEIOw*EK3*EWx - Edy*Er*EWx +
-                  EK1*Er*EWx + EEIOw*EK4*EWy +
-                  Edx*Er*EWy - EK2*Er*EWy))) -
-          4*EBETA3(J)*
-           (EAlan*EBETA3(J)*EElas*EK1 - EEJ*EG*EK1 +
-             EAlan*EEJ*EG*EK3*Er)*
-           (EK3*(EPx + EH*EWx) + EK4*(EPy + EH*EWy))*EZ +
-          EBETA3(J)*(EAlan*EBETA3(J)*EElas*EK1 - EEJ*EG*EK1 +
-             EAlan*EEJ*EG*EK3*Er)*(EK3*EWx + EK4*EWy)*
-           EZ**2) +
-       EAlan*EBETA3(J)**2*EElas*Er*
-        (EEIx*(-6*EH*(2*EPx + EH*EWx) +
-             4*(EPx + EH*EWx)*EZ - EWx*EZ**2) +
-          EEIxy*(6*EH*(2*EPy + EH*EWy) -
-             4*(EPy + EH*EWy)*EZ + EWy*EZ**2))) -
-    24*EDELTA*EBETA3(J)**2*EElas*
-     (EALFA2(J)**2*ED2(J)*
-        (EK1 - EAlan*EALFA1(J)**2*EGAMA(J)*EK1 -
-          EAlan*EK3*Er)*Cosh(EALFA1(J)*EZ) +
-       EALFA2(J)**2*ED1(J)*
-        (EK1 - EAlan*EALFA1(J)**2*EGAMA(J)*EK1 -
-          EAlan*EK3*Er)*Sinh(EALFA1(J)*EZ) -
-       EALFA1(J)**2*((-1 + EAlan*EALFA2(J)**2*EGAMA(J))*EK1 +
-          EAlan*EK3*Er)*
-      (ED4(J)*Cosh(EALFA2(J)*EZ) + ED3(J)*Sinh(EALFA2(J)*EZ))))/
-  (24.*EDELTA*EAlan*EALFA1(J)**2*EALFA2(J)**2*EBETA3(J)**2*
-    EElas**2*Er) + (-(EALFA1(J-1)**2*EALFA2(J-1)**2*EZ**2*
-       (EDELTA*(12*EAlan*EBETA2(J-1)*EEJ*EG*EK3*Er*
-             (EK3*EWx + EK4*EWy) +
-            6*EAlan*EBETA3(J-1)**2*EElas*EH*EK1*
-             (2*EK3*EPx + 2*EK4*EPy + EH*EK3*EWx +
-               EH*EK4*EWy) -
-            12*EAlan*EBETA3(J-1)*EElas*EK3*Er*
-             (Er*(-(Edy*EWx) + EK1*EWx + Edx*EWy -
-                  EK2*EWy) + EEIOw*(EK3*EWx + EK4*EWy)) +
-            6*EAlan*EBETA3(J-1)*EEJ*EG*
-             (2*EH*EK3*(EK3*EPx + EK4*EPy)*Er +
-               2*EGAMA(J-1)*EK1*(EK3*EWx + EK4*EWy) +
-               EH**2*EK3*Er*(EK3*EWx + EK4*EWy)) -
-            6*EK1*(2*EBETA2(J-1)*EEJ*EG*
-                (EK3*EWx + EK4*EWy) +
-               EBETA3(J-1)*
-                (EEJ*EG*EH*
-                   (2*EK3*EPx + 2*EK4*EPy + EH*EK3*EWx +
-                     EH*EK4*EWy) -
-                  2*EElas*
-                   (EEIOw*EK3*EWx - Edy*Er*EWx +
-                     EK1*Er*EWx + EEIOw*EK4*EWy +
-                     Edx*Er*EWy - EK2*Er*EWy))) -
-            4*EBETA3(J-1)*
-             (EAlan*EBETA3(J-1)*EElas*EK1 - EEJ*EG*EK1 +
-               EAlan*EEJ*EG*EK3*Er)*
-             (EK3*(EPx + EH*EWx) + EK4*(EPy + EH*EWy))*EZ
```

```
-            + EBETA3(J-1)*
-            (EAlan*EBETA3(J-1)*EElas*EK1 - EEJ*EG*EK1 +
-              EAlan*EEJ*EG*EK3*Er)*(EK3*EWx + EK4*EWy)*
-            EZ**2) +
-        EAlan*EBETA3(J-1)**2*EElas*Er*
-         (EEIx*(-6*EH*(2*EPx + EH*EWx) +
-              4*(EPx + EH*EWx)*EZ - EWx*EZ**2) +
-           EEIxy*(6*EH*(2*EPy + EH*EWy) -
-              4*(EPy + EH*EWy)*EZ + EWy*EZ**2)))) +
-    24*EDELTA*EBETA3(J-1)**2*EElas*
-     (EALFA2(J-1)**2*ED2(J-1)*
-        (EK1 - EAlan*EALFA1(J-1)**2*EGAMA(J-1)*EK1 -
-          EAlan*EK3*Er)*Cosh(EALFA1(J-1)*EZ) +
-       EALFA2(J-1)**2*ED1(J-1)*
-        (EK1 - EAlan*EALFA1(J-1)**2*EGAMA(J-1)*EK1 -
-          EAlan*EK3*Er)*Sinh(EALFA1(J-1)*EZ) -
-       EALFA1(J-1)**2*((-1 + EAlan*EALFA2(J-1)**2*EGAMA(J-1))*
-           EK1 + EAlan*EK3*Er)*
-        (ED4(J-1)*Cosh(EALFA2(J-1)*EZ) +
-          ED3(J-1)*Sinh(EALFA2(J-1)*EZ))))/
-   (24.*EDELTA*EAlan*EALFA1(J-1)**2*EALFA2(J-1)**2*EBETA3(J-1)**2*
-    EElas**2*Er))

       return
       end
       SUBROUTINE COEF3U(ibsay,EALFA1,EALFA2,EBETA1,EBETA2,EBETA3
@              ,EZ,EGAMA,EG,EEJ,EK1,EK2,EK3,EK4,EH,EDELTA
@             ,EPx,EPy,EWx,EWy,Edx,Edy,Er,EEIOw,EAlan,EEIx,EEIxy
@                                   ,EElas,ED1,ED2,ED3,ED4,REK1,REKB1,J)
       implicit real*8 (A-H,K-Z)
       dimension REK1(4),EBETA1(ibsay),EBETA2(ibsay),EBETA3(ibsay)
@             ,EALFA1(ibsay),EALFA2(ibsay),EGAMA(ibsay)
@             ,ED1(ibsay),ED2(ibsay),ED3(ibsay),ED4(ibsay)
 REK1(1)=1
       REK1(2)=0
       REKB1= -((EALFA1(J)*EALFA2(J)**2*ED1(J)*
-    (EK1 - EAlan*EALFA1(J)**2*EGAMA(J)*EK1 - EAlan*EK3*Er) -
-   EALFA1(J)**2*EALFA2(J)*ED3(J)*
-    ((-1 + EAlan*EALFA2(J)**2*EGAMA(J))*EK1 + EAlan*EK3*Er))/
-  (EAlan*EALFA1(J)**2*EALFA2(J)**2*EElas*Er))
       return
       end
       SUBROUTINE COEF4U(ibsay,EALFA1,EALFA2,EBETA1,EBETA2,EBETA3
@              ,EZ,EGAMA,EG,EEJ,EK1,EK2,EK3,EK4,EH,EDELTA
@             ,EPx,EPy,EWx,EWy,Edx,Edy,Er,EEIOw,EAlan,EEIx,EEIxy
@                                   ,EElas,ED1,ED2,ED3,ED4,REK2,REKB2,J)
       implicit real*8 (A-H,K-Z)
       dimension REK2(4),EBETA1(ibsay),EBETA2(ibsay),EBETA3(ibsay)
@             ,EALFA1(ibsay),EALFA2(ibsay),EGAMA(ibsay)
@             ,ED1(ibsay),ED2(ibsay),ED3(ibsay),ED4(ibsay)
 REK2(1)=0
       REK2(2)=1
       REKB2=  -((EALFA2(J)**2*ED2(J)*(EK1 - EAlan*
-        EALFA1(J)**2*EGAMA(J)*EK1 -
-      EAlan*EK3*Er) -
```

```
-   EALFA1(J)**2*ED4(J)*((-1 + EAlan*EALFA2(J)**2*EGAMA(J))*EK1+
-      EAlan*EK3*Er))/
-  (EAlan*EALFA1(J)**2*EALFA2(J)**2*EElas*Er))
        return
        end

        SUBROUTINE UFONK(ibsay,iksay,EALFA1,EALFA2,EBETA1,EBETA2,EBETA3
@                      ,EGAMA,EK1,EK2,EK3,EK4,EElas,EG,EEJ,EDELTA
@                     ,EPx,EPy,EWx,EWy,Edx,Edy,Er,EEIOw,EAlan,EH
@                           ,EEIx,EEIxy,ED1,ED2,ED3,ED4,EU,EKAT,J,jm
@                     ,EF1,EF2)
        implicit real*8 (A-H,K-Z)
        dimension EU(iksay),EKAT(iksay),EF1(ibsay),EF2(ibsay)
@                   ,ED1(ibsay),ED2(ibsay),ED3(ibsay),ED4(ibsay)
@         ,EALFA1(ibsay),EALFA2(ibsay),EGAMA(ibsay)
@         ,EBETA1(ibsay),EBETA2(ibsay),EBETA3(ibsay)
  EU(jm)=   EKAT(jm)*EF1(J) + EF2(J) + ( -(EALFA1(J)**2*
-         EALFA2(J)**2*EKAT(jm)**2*
-       (EDELTA*(12*EAlan*EBETA2(J)*EEJ*EG*EK3*Er*
-            (EK3*EWx + EK4*EWy) +
-           6*EAlan*EBETA3(J)**2*EElas*EH*EK1*
-            (2*EK3*EPx + 2*EK4*EPy + EH*EK3*EWx +
-              EH*EK4*EWy) -
-           12*EAlan*EBETA3(J)*EElas*EK3*Er*
-            (Er*(-(Edy*EWx) + EK1*EWx + Edx*EWy -
-                 EK2*EWy) + EEIOw*(EK3*EWx + EK4*EWy)) +
-           6*EAlan*EBETA3(J)*EEJ*EG*
-            (2*EH*EK3*(EK3*EPx + EK4*EPy)*Er +
-              2*EGAMA(J)*EK1*(EK3*EWx + EK4*EWy) +
-              EH**2*EK3*Er*(EK3*EWx + EK4*EWy)) -
-           6*EK1*(2*EBETA2(J)*EEJ*EG*(EK3*EWx + EK4*EWy) +
-              EBETA3(J)*
-               (EEJ*EG*EH*
-                  (2*EK3*EPx + 2*EK4*EPy + EH*EK3*EWx +
-                    EH*EK4*EWy) -
-                 2*EElas*
-                  (EEIOw*EK3*EWx - Edy*Er*EWx +
-                    EK1*Er*EWx + EEIOw*EK4*EWy +
-                    Edx*Er*EWy - EK2*Er*EWy))) -
-           4*EBETA3(J)*
-            (EAlan*EBETA3(J)*EElas*EK1 - EEJ*EG*EK1 +
-              EAlan*EEJ*EG*EK3*Er)*
-            (EK3*(EPx + EH*EWx) + EK4*(EPy + EH*EWy))*EKAT(jm)
-            + EBETA3(J)*
-            (EAlan*EBETA3(J)*EElas*EK1 - EEJ*EG*EK1 +
-              EAlan*EEJ*EG*EK3*Er)*(EK3*EWx + EK4*EWy)*
-            EKAT(jm)**2) +
-         EAlan*EBETA3(J)**2*EElas*Er*
-          (EEIx*(-6*EH*(2*EPx + EH*EWx) +
-              4*(EPx + EH*EWx)*EKAT(jm) - EWx*EKAT(jm)**2) +
-           EEIxy*(6*EH*(2*EPy + EH*EWy) -
-              4*(EPy + EH*EWy)*EKAT(jm) + EWy*EKAT(jm)**2))))+
-    24*EDELTA*EBETA3(J)**2*EElas*
-     (EALFA2(J)**2*ED2(J)*
-        (EK1 - EAlan*EALFA1(J)**2*EGAMA(J)*EK1 -
```

```
-          EAlan*EK3*Er)*Cosh(EALFA1(J)*EKAT(jm)) +
-       EALFA2(J)**2*ED1(J)*
-        (EK1 - EAlan*EALFA1(J)**2*EGAMA(J)*EK1 -
-          EAlan*EK3*Er)*Sinh(EALFA1(J)*EKAT(jm)) -
-       EALFA1(J)**2*((-1 + EAlan*EALFA2(J)**2*EGAMA(J))*EK1 +
-          EAlan*EK3*Er)*
-     (ED4(J)*Cosh(EALFA2(J)*EKAT(jm)) +
-       ED3(J)*Sinh(EALFA2(J)*EKAT(jm)))))/
-   (24.*EDELTA*EAlan*EALFA1(J)**2*EALFA2(J)**2*EBETA3(J)**2*
-    EElas**2*Er)
       return
       end

       SUBROUTINE COEF1V(ibsay,EALFA1,EALFA2,EBETA1,EBETA2,EBETA3
@                ,EZ,EGAMA,EG,EEJ,EK1,EK2,EK3,EK4,EH,EDELTA
@              ,EPx,EPy,EWx,EWy,Edx,Edy,Er,EEIOw,EAlan,EEIy,EEIxy
@                                     ,EElas,ED1,ED2,ED3,ED4,REK1,REKB1,J)

       implicit real*8 (A-H,K-Z)
       dimension REK1(4),EBETA1(ibsay),EBETA2(ibsay),EBETA3(ibsay)
@               ,EALFA1(ibsay),EALFA2(ibsay),EGAMA(ibsay)
@               ,ED1(ibsay),ED2(ibsay),ED3(ibsay),ED4(ibsay)
 REK1(1)=1
       REK1(2)=0
       REK1(3)=-1
       REK1(4)=0
       REKB1= -((-(EALFA1(J)**2*EALFA2(J)**2*EZ**2*
-       (EDELTA*(4*EBETA3(J)*
-           (-(EAlan*EBETA3(J)*EElas*EK2) + EEJ*EG*EK2 +
-             EAlan*EEJ*EG*EK4*Er)*
-           (EK3*(EPx + EH*EWx) + EK4*(EPy + EH*EWy)) +
-          2*EBETA3(J)*
-           (EAlan*EBETA3(J)*EElas*EK2 - EEJ*EG*EK2 -
-             EAlan*EEJ*EG*EK4*Er)*(EK3*EWx + EK4*EWy)*EZ
-          ) + EAlan*EBETA3(J)**2*EElas*Er*
-         (EEIxy*(4*(EPx + EH*EWx) - 2*EWx*EZ) +
-          EEIy*(-4*(EPy + EH*EWy) + 2*EWy*EZ)))) -
-    2*EALFA1(J)**2*EALFA2(J)**2*EZ*
-     (EDELTA*(-12*EAlan*EBETA2(J)*EEJ*EG*EK4*Er*
-         (EK3*EWx + EK4*EWy) +
-        6*EAlan*EBETA3(J)**2*EElas*EH*EK2*
-         (2*EK3*EPx + 2*EK4*EPy + EH*EK3*EWx +
-           EH*EK4*EWy) +
-        12*EAlan*EBETA3(J)*EElas*EK4*Er*
-         (Er*(-(Edy*EWx) + EK1*EWx + Edx*EWy -
-             EK2*EWy) + EEIOw*(EK3*EWx + EK4*EWy)) -
-        6*EAlan*EBETA3(J)*EEJ*EG*
-         (2*EH*EK4*(EK3*EPx + EK4*EPy)*Er -
-           2*EGAMA(J)*EK2*(EK3*EWx + EK4*EWy) +
-           EH**2*EK4*Er*(EK3*EWx + EK4*EWy)) -
-        6*EK2*(2*EBETA2(J)*EEJ*EG*(EK3*EWx + EK4*EWy) +
-           EBETA3(J)*
-            (EEJ*EG*EH*
-               (2*EK3*EPx + 2*EK4*EPy + EH*EK3*EWx +
-                 EH*EK4*EWy) -
```

```
-              2*EElas*
-               (EEIOw*EK3*EWx - Edy*Er*EWx +
-                 EK1*Er*EWx + EEIOw*EK4*EWy +
-                 Edx*Er*EWy - EK2*Er*EWy))) +
-          4*EBETA3(J)*
-           (-(EAlan*EBETA3(J)*EElas*EK2) + EEJ*EG*EK2 +
-             EAlan*EEJ*EG*EK4*Er)*
-           (EK3*(EPx + EH*EWx) + EK4*(EPy + EH*EWy))*EZ +
-          EBETA3(J)*(EAlan*EBETA3(J)*EElas*EK2 - EEJ*EG*EK2 -
-             EAlan*EEJ*EG*EK4*Er)*(EK3*EWx + EK4*EWy)*
-           EZ**2) +
-       EAlan*EBETA3(J)**2*EElas*Er*
-        (EEIxy*(-6*EH*(2*EPx + EH*EWx) +
-             4*(EPx + EH*EWx)*EZ - EWx*EZ**2) +
-          EEIy*(6*EH*(2*EPy + EH*EWy) -
-             4*(EPy + EH*EWy)*EZ + EWy*EZ**2))) -
-    24*EDELTA*EBETA3(J)**2*EElas*
-     (EALFA1(J)*EALFA2(J)**2*ED1(J)*
-        ((-1 + EAlan*EALFA1(J)**2*EGAMA(J))*EK2 -
-          EAlan*EK4*Er)*Cosh(EALFA1(J)*EZ) +
-       EALFA1(J)*EALFA2(J)**2*ED2(J)*
-        ((-1 + EAlan*EALFA1(J)**2*EGAMA(J))*EK2 -
-          EAlan*EK4*Er)*Sinh(EALFA1(J)*EZ) +
-       EALFA1(J)**2*((-1 + EAlan*EALFA2(J)**2*EGAMA(J))*EK2 -
-          EAlan*EK4*Er)*
-        (EALFA2(J)*ED3(J)*Cosh(EALFA2(J)*EZ) +
-          EALFA2(J)*ED4(J)*Sinh(EALFA2(J)*EZ))))/
-  (24.*EDELTA*EAlan*EALFA1(J)**2*EALFA2(J)**2*EBETA3(J)**2*
-    EElas**2*Er) + (EALFA1(J-1)**2*EALFA2(J-1)**2*EZ**2*
-     (EDELTA*(4*EBETA3(J-1)*
-           (-(EAlan*EBETA3(J-1)*EElas*EK2) + EEJ*EG*EK2 +
-             EAlan*EEJ*EG*EK4*Er)*
-           (EK3*(EPx + EH*EWx) + EK4*(EPy + EH*EWy)) +
-          2*EBETA3(J-1)*
-           (EAlan*EBETA3(J-1)*EElas*EK2 - EEJ*EG*EK2 -
-             EAlan*EEJ*EG*EK4*Er)*(EK3*EWx + EK4*EWy)*EZ)
-        + EAlan*EBETA3(J-1)**2*EElas*Er*
-        (EEIxy*(4*(EPx + EH*EWx) - 2*EWx*EZ) +
-          EEIy*(-4*(EPy + EH*EWy) + 2*EWy*EZ))) +
-    2*EALFA1(J-1)**2*EALFA2(J-1)**2*EZ*
-     (EDELTA*(-12*EAlan*EBETA2(J-1)*EEJ*EG*EK4*Er*
-           (EK3*EWx + EK4*EWy) +
-          6*EAlan*EBETA3(J-1)**2*EElas*EH*EK2*
-           (2*EK3*EPx + 2*EK4*EPy + EH*EK3*EWx +
-             EH*EK4*EWy) +
-          12*EAlan*EBETA3(J-1)*EElas*EK4*Er*
-           (Er*(-(Edy*EWx) + EK1*EWx + Edx*EWy -
-                EK2*EWy) + EEIOw*(EK3*EWx + EK4*EWy)) -
-          6*EAlan*EBETA3(J-1)*EEJ*EG*
-           (2*EH*EK4*(EK3*EPx + EK4*EPy)*Er -
-             2*EGAMA(J-1)*EK2*(EK3*EWx + EK4*EWy) +
-             EH**2*EK4*Er*(EK3*EWx + EK4*EWy)) -
-          6*EK2*(2*EBETA2(J-1)*EEJ*EG*(EK3*EWx + EK4*EWy) +
-             EBETA3(J-1)*
-              (EEJ*EG*EH*
```

```
-                (2*EK3*EPx + 2*EK4*EPy + EH*EK3*EWx +
-                  EH*EK4*EWy) -
-               2*EElas*
-                (EEIOw*EK3*EWx - Edy*Er*EWx +
-                  EK1*Er*EWx + EEIOw*EK4*EWy +
-                  Edx*Er*EWy - EK2*Er*EWy))) +
-          4*EBETA3(J-1)*
-           (-(EAlan*EBETA3(J-1)*EElas*EK2) + EEJ*EG*EK2 +
-             EAlan*EEJ*EG*EK4*Er)*
-           (EK3*(EPx + EH*EWx) + EK4*(EPy + EH*EWy))*EZ +
-          EBETA3(J-1)*(EAlan*EBETA3(J-1)*EElas*EK2 -
-             EEJ*EG*EK2 - EAlan*EEJ*EG*EK4*Er)*
-           (EK3*EWx + EK4*EWy)*EZ**2) +
-       EAlan*EBETA3(J-1)**2*EElas*Er*
-        (EEIxy*(-6*EH*(2*EPx + EH*EWx) +
-             4*(EPx + EH*EWx)*EZ - EWx*EZ**2) +
-          EEIy*(6*EH*(2*EPy + EH*EWy) -
-             4*(EPy + EH*EWy)*EZ + EWy*EZ**2))) +
-    24*EDELTA*EBETA3(J-1)**2*EElas*
-     (EALFA1(J-1)*EALFA2(J-1)**2*ED1(J-1)*
-        ((-1 + EAlan*EALFA1(J-1)**2*EGAMA(J-1))*EK2 -
-          EAlan*EK4*Er)*Cosh(EALFA1(J-1)*EZ) +
-       EALFA1(J-1)*EALFA2(J-1)**2*ED2(J-1)*
-        ((-1 + EAlan*EALFA1(J-1)**2*EGAMA(J-1))*EK2 -
-          EAlan*EK4*Er)*Sinh(EALFA1(J-1)*EZ) +
-       EALFA1(J-1)**2*((-1 + EAlan*EALFA2(J-1)**2*EGAMA(J-1))*
-           EK2 - EAlan*EK4*Er)*
-        (EALFA2(J-1)*ED3(J-1)*Cosh(EALFA2(J-1)*EZ) +
-          EALFA2(J-1)*ED4(J-1)*Sinh(EALFA2(J-1)*EZ))))/
-   (24.*EDELTA*EAlan*EALFA1(J-1)**2*EALFA2(J-1)**2*EBETA3(J-1)**2*
-    EElas**2*Er))

      return
end

         SUBROUTINE COEF2V(ibsay,EALFA1,EALFA2,EBETA1,EBETA2,EBETA3
    @              ,EZ,EGAMA,EG,EEJ,EK1,EK2,EK3,EK4,EH,EDELTA
    @              ,EPx,EPy,EWx,EWy,Edx,Edy,Er,EEIOw,EAlan,EEIy,EEIxy
    @                                  ,EElas,ED1,ED2,ED3,ED4,REK2,REKB2,J)

         implicit real*8 (A-H,K-Z)
         dimension REK2(4),EBETA1(ibsay),EBETA2(ibsay),EBETA3(ibsay)
    @              ,EALFA1(ibsay),EALFA2(ibsay),EGAMA(ibsay)
    @              ,ED1(ibsay),ED2(ibsay),ED3(ibsay),ED4(ibsay)

      REK2(1)=EZ
         REK2(2)=1
         REK2(3)=-EZ
         REK2(4)=-1
         REKB2= -((-(EALFA1(J)**2*EALFA2(J)**2*EZ**2*
-        (EDELTA*(-12*EAlan*EBETA2(J)*EEJ*EG*EK4*Er*
-             (EK3*EWx + EK4*EWy) +
-            6*EAlan*EBETA3(J)**2*EElas*EH*EK2*
-             (2*EK3*EPx + 2*EK4*EPy + EH*EK3*EWx +
-               EH*EK4*EWy) +
```

```
-           12*EAlan*EBETA3(J)*EElas*EK4*Er*
-            (Er*(-(Edy*EWx) + EK1*EWx + Edx*EWy -
-                 EK2*EWy) + EEIOw*(EK3*EWx + EK4*EWy))  -
-           6*EAlan*EBETA3(J)*EEJ*EG*
-            (2*EH*EK4*(EK3*EPx + EK4*EPy)*Er  -
-              2*EGAMA(J)*EK2*(EK3*EWx + EK4*EWy) +
-              EH**2*EK4*Er*(EK3*EWx + EK4*EWy))  -
-           6*EK2*(2*EBETA2(J)*EEJ*EG*(EK3*EWx +  EK4*EWy) +
-              EBETA3(J)*
-               (EEJ*EG*EH*
-                  (2*EK3*EPx + 2*EK4*EPy + EH*EK3*EWx +
-                    EH*EK4*EWy)  -
-                 2*EElas*
-                  (EEIOw*EK3*EWx - Edy*Er*EWx +
-                    EK1*Er*EWx + EEIOw*EK4*EWy +
-                    Edx*Er*EWy - EK2*Er*EWy))) +
-           4*EBETA3(J)*
-            (-(EAlan*EBETA3(J)*EElas*EK2) + EEJ*EG*EK2 +
-              EAlan*EEJ*EG*EK4*Er)*
-            (EK3*(EPx + EH*EWx) + EK4*(EPy + EH*EWy))*EZ
-            + EBETA3(J)*
-            (EAlan*EBETA3(J)*EElas*EK2  - EEJ*EG*EK2  -
-              EAlan*EEJ*EG*EK4*Er)*(EK3*EWx + EK4*EWy)*
-            EZ**2) +
-        EAlan*EBETA3(J)**2*EElas*Er*
-         (EEIxy*(-6*EH*(2*EPx + EH*EWx) +
-              4*(EPx + EH*EWx)*EZ - EWx*EZ**2) +
-           EEIy*(6*EH*(2*EPy + EH*EWy)  -
-              4*(EPy + EH*EWy)*EZ + EWy*EZ**2)))) -
-   24*EDELTA*EBETA3(J)**2*EElas*
-    (EALFA2(J)**2*ED2(J)*
-       ((-1 + EAlan*EALFA1(J)**2*EGAMA(J))*EK2  -
-         EAlan*EK4*Er)*Cosh(EALFA1(J)*EZ) +
-      EALFA2(J)**2*ED1(J)*
-       ((-1 + EAlan*EALFA1(J)**2*EGAMA(J))*EK2  -
-         EAlan*EK4*Er)*Sinh(EALFA1(J)*EZ) +
-      EALFA1(J)**2*((-1 + EAlan*EALFA2(J)**2*EGAMA(J))*EK2  -
-         EAlan*EK4*Er)*
-     (ED4(J)*Cosh(EALFA2(J)*EZ) + ED3(J)*Sinh(EALFA2(J)*EZ))))/
-  (24.*EDELTA*EAlan*EALFA1(J)**2*EALFA2(J)**2*EBETA3(J)**2*
-   EElas**2*Er) + (EALFA1(J-1)**2*EALFA2(J-1)**2*EZ**2*
-    (EDELTA*(-12*EAlan*EBETA2(J-1)*EEJ*EG*EK4*Er*
-          (EK3*EWx + EK4*EWy) +
-         6*EAlan*EBETA3(J-1)**2*EElas*EH*EK2*
-          (2*EK3*EPx + 2*EK4*EPy + EH*EK3*EWx +
-            EH*EK4*EWy) +
-         12*EAlan*EBETA3(J-1)*EElas*EK4*Er*
-          (Er*(-(Edy*EWx) + EK1*EWx + Edx*EWy -
-               EK2*EWy) + EEIOw*(EK3*EWx + EK4*EWy))  -
-         6*EAlan*EBETA3(J-1)*EEJ*EG*
-          (2*EH*EK4*(EK3*EPx + EK4*EPy)*Er  -
-            2*EGAMA(J-1)*EK2*(EK3*EWx + EK4*EWy) +
-            EH**2*EK4*Er*(EK3*EWx + EK4*EWy)) -
-         6*EK2*(2*EBETA2(J-1)*EEJ*EG*(EK3*EWx + EK4*EWy) +
-            EBETA3(J-1)*
```

```
-             (EEJ*EG*EH*
-               (2*EK3*EPx + 2*EK4*EPy + EH*EK3*EWx +
-                 EH*EK4*EWy) -
-              2*EElas*
-               (EEIOw*EK3*EWx - Edy*Er*EWx +
-                 EK1*Er*EWx + EEIOw*EK4*EWy +
-                 Edx*Er*EWy - EK2*Er*EWy))) +
-         4*EBETA3(J-1)*
-          (-(EAlan*EBETA3(J-1)*EElas*EK2) + EEJ*EG*EK2 +
-            EAlan*EEJ*EG*EK4*Er)*
-          (EK3*(EPx + EH*EWx) + EK4*(EPy + EH*EWy))*EZ +
-         EBETA3(J-1)*(EAlan*EBETA3(J-1)*EElas*EK2 -
-            EEJ*EG*EK2 - EAlan*EEJ*EG*EK4*Er)*
-          (EK3*EWx + EK4*EWy)*EZ**2) +
-       EAlan*EBETA3(J-1)**2*EElas*Er*
-        (EEIxy*(-6*EH*(2*EPx + EH*EWx) +
-            4*(EPx + EH*EWx)*EZ - EWx*EZ**2) +
-         EEIy*(6*EH*(2*EPy + EH*EWy) -
-            4*(EPy + EH*EWy)*EZ + EWy*EZ**2))) +
-    24*EDELTA*EBETA3(J-1)**2*EElas*
-     (EALFA2(J-1)**2*ED2(J-1)*
-        ((-1 + EAlan*EALFA1(J-1)**2*EGAMA(J-1))*EK2 -
-         EAlan*EK4*Er)*Cosh(EALFA1(J-1)*EZ) +
-       EALFA2(J-1)**2*ED1(J-1)*
-        ((-1 + EAlan*EALFA1(J-1)**2*EGAMA(J-1))*EK2 -
-         EAlan*EK4*Er)*Sinh(EALFA1(J-1)*EZ) +
-       EALFA1(J-1)**2*((-1 + EAlan*EALFA2(J-1)**2*EGAMA(J-1))*
-          EK2 - EAlan*EK4*Er)*
-        (ED4(J-1)*Cosh(EALFA2(J-1)*EZ) +
-         ED3(J-1)*Sinh(EALFA2(J-1)*EZ))))/
-   (24.*EDELTA*EAlan*EALFA1(J-1)**2*EALFA2(J-1)**2*EBETA3(J-1)**2*
-    EElas**2*Er))

       return
       end

       SUBROUTINE COEF3V(ibsay,EALFA1,EALFA2,EBETA1,EBETA2,EBETA3
@                ,EZ,EGAMA,EG,EEJ,EK1,EK2,EK3,EK4,EH,EDELTA
@               ,EPx,EPy,EWx,EWy,Edx,Edy,Er,EEIOw,EAlan,EEIy,EEIxy
@                                     ,EElas,ED1,ED2,ED3,ED4,REK1,REKB1,J)

       implicit real*8 (A-H,K-Z)
       dimension REK1(4),EBETA1(ibsay),EBETA2(ibsay),EBETA3(ibsay)
@               ,EALFA1(ibsay),EALFA2(ibsay),EGAMA(ibsay)
@               ,ED1(ibsay),ED2(ibsay),ED3(ibsay),ED4(ibsay)

 REK1(1)=1
       REK1(2)=0
       REKB1= -((EALFA1(J)*EALFA2(J)**2*ED1(J)*
-    ((-1 + EAlan*EALFA1(J)**2*EGAMA(J))*EK2 - EAlan*EK4*Er) +
-   EALFA1(J)**2*EALFA2(J)*ED3(J)*
-    ((-1 + EAlan*EALFA2(J)**2*EGAMA(J))*EK2 - EAlan*EK4*Er))/
-  (EAlan*EALFA1(J)**2*EALFA2(J)**2*EElas*Er))

       return
```

```
        end

        SUBROUTINE COEF4V(ibsay,EALFA1,EALFA2,EBETA1,EBETA2,EBETA3
@             ,EZ,EGAMA,EG,EEJ,EK1,EK2,EK3,EK4,EH,EDELTA
@            ,EPx,EPy,EWx,EWy,Edx,Edy,Er,EEIOw,EAlan,EEIy,EEIxy
@                                  ,EElas,ED1,ED2,ED3,ED4,REK2,REKB2,J)

        implicit real*8 (A-H,K-Z)
        dimension REK2(4),EBETA1(ibsay),EBETA2(ibsay),EBETA3(ibsay)
@             ,EALFA1(ibsay),EALFA2(ibsay),EGAMA(ibsay)
@             ,ED1(ibsay),ED2(ibsay),ED3(ibsay),ED4(ibsay)

 REK2(1)=0
        REK2(2)=1
        REKB2= -((EALFA2(J)**2*ED2(J)*((-1 + EAlan*EALFA1(J)**2*
-      EGAMA(J))*EK2 - EAlan*EK4*Er) +
-   EALFA1(J)**2*ED4(J)*((-1 + EAlan*EALFA2(J)**2*EGAMA(J))*EK2 -
-      EAlan*EK4*Er))/
-  (EAlan*EALFA1(J)**2*EALFA2(J)**2*EElas*Er))

        return
        end

        SUBROUTINE VFONK(ibsay,iksay,EALFA1,EALFA2,EBETA1,EBETA2,EBETA3
@                    ,EGAMA,EK1,EK2,EK3,EK4,EElas,EG,EEJ,EDELTA
@                   ,EPx,EPy,EWx,EWy,Edx,Edy,Er,EEIOw,EAlan,EH
@                         ,EEIy,EEIxy,ED1,ED2,ED3,ED4,EV,EKAT,J,jm
@                   ,EP1,EP2)

        implicit real*8 (A-H,K-Z)
        dimension EV(iksay),EKAT(iksay),EP1(ibsay),EP2(ibsay)
@                  ,ED1(ibsay),ED2(ibsay),ED3(ibsay),ED4(ibsay)
@        ,EALFA1(ibsay),EALFA2(ibsay),EGAMA(ibsay)
@        ,EBETA1(ibsay),EBETA2(ibsay),EBETA3(ibsay)

 EV(jm)= EKAT(jm)*EP1(J) + EP2(J) + (EALFA1(J)**2*
-       EALFA2(J)**2*EKAT(jm)**2*
-     (EDELTA*(-12*EAlan*EBETA2(J)*EEJ*EG*EK4*Er*
-          (EK3*EWx + EK4*EWy) +
-         6*EAlan*EBETA3(J)**2*EElas*EH*EK2*
-          (2*EK3*EPx + 2*EK4*EPy + EH*EK3*EWx +
-            EH*EK4*EWy) +
-         12*EAlan*EBETA3(J)*EElas*EK4*Er*
-          (Er*(-(Edy*EWx) + EK1*EWx + Edx*EWy -
-              EK2*EWy) + EEIOw*(EK3*EWx + EK4*EWy)) -
-         6*EAlan*EBETA3(J)*EEJ*EG*
-          (2*EH*EK4*(EK3*EPx + EK4*EPy)*Er -
-            2*EGAMA(J)*EK2*(EK3*EWx + EK4*EWy) +
-            EH**2*EK4*Er*(EK3*EWx + EK4*EWy)) -
-         6*EK2*(2*EBETA2(J)*EEJ*EG*(EK3*EWx + EK4*EWy) +
-            EBETA3(J)*
-             (EEJ*EG*EH*
-                (2*EK3*EPx + 2*EK4*EPy + EH*EK3*EWx +
-                  EH*EK4*EWy) -
-              2*EElas*
```

```
-                 (EEIOw*EK3*EWx - Edy*Er*EWx +
-                   EK1*Er*EWx + EEIOw*EK4*EWy +
-                   Edx*Er*EWy - EK2*Er*EWy))) +
-          4*EBETA3(J)*
-           (-(EAlan*EBETA3(J)*EElas*EK2) + EEJ*EG*EK2 +
-             EAlan*EEJ*EG*EK4*Er)*
-           (EK3*(EPx + EH*EWx) + EK4*(EPy + EH*EWy))*EKAT(jm)+
-          EBETA3(J)*(EAlan*EBETA3(J)*EElas*EK2 - EEJ*EG*EK2 -
-             EAlan*EEJ*EG*EK4*Er)*(EK3*EWx + EK4*EWy)*
-           EKAT(jm)**2) +
-       EAlan*EBETA3(J)**2*EElas*Er*
-        (EEIxy*(-6*EH*(2*EPx + EH*EWx) +
-             4*(EPx + EH*EWx)*EKAT(jm) - EWx*EKAT(jm)**2) +
-          EEIy*(6*EH*(2*EPy + EH*EWy) -
-             4*(EPy + EH*EWy)*EKAT(jm) + EWy*EKAT(jm)**2))) +
-    24*EDELTA*EBETA3(J)**2*EElas*
-     (EALFA2(J)**2*ED2(J)*
-        ((-1 + EAlan*EALFA1(J)**2*EGAMA(J))*EK2 -
-          EAlan*EK4*Er)*Cosh(EALFA1(J)*EKAT(jm)) +
-       EALFA2(J)**2*ED1(J)*
-        ((-1 + EAlan*EALFA1(J)**2*EGAMA(J))*EK2 -
-          EAlan*EK4*Er)*Sinh(EALFA1(J)*EKAT(jm)) +
-       EALFA1(J)**2*((-1 + EAlan*EALFA2(J)**2*EGAMA(J))*EK2 -
-          EAlan*EK4*Er)*
-       (ED4(J)*Cosh(EALFA2(J)*EKAT(jm)) +
-        ED3(J)*Sinh(EALFA2(J)*EKAT(jm)))))/
-  (24.*EDELTA*EAlan*EALFA1(J)**2*EALFA2(J)**2*EBETA3(J)**2*
-    EElas**2*Er)

      return
      end

##################################################################
C    ####################################################################
C    #         GAUSS-ELIMINATION WITH  [AA]{XB}={B.X}             #
C    #            AND CALCULATION OF {XB} VECTOR                 #
C    ################################## ##############################
C    ####################################################################
      SUBROUTINE GAUSS(SS,N,EVT,EV2)
      IMPLICIT REAL*8(A-H,O-Z)
      PARAMETER(NE=50)
      REAL*8 SS(NE,NE),EVT(NE),EV2(NE),AA(NE,NE+1)
      M=N+1
C *** MATRIX FORMED (INCREASED) ***
      DO 3 I=1,N
      DO 3 J=1,N
      AA(I,J)=SS(I,J)
3     AA(I,M)=EVT(I)
      L=N-1
      DO 12 K=1,L
      JJ=K
      BIG=DABS(AA(K,K))
      KP1=K+1
      DO 7 I=KP1,N
      AB=DABS(AA(I,K))
```

```
      IF(BIG-AB)6,7,7
6     BIG=AB
      JJ=I
7     CONTINUE
      IF(JJ-K)8,10,8
8     DO 9 J=K,M
      TEMP=AA(JJ,J)
      AA(JJ,J)=AA(K,J)
9     AA(K,J)=TEMP
10    DO 11 I=KP1,N
      QUOT=AA(I,K)/AA(K,K)
      DO 11 J=KP1,M
11    AA(I,J)=AA(I,J)-QUOT*AA(K,J)
      DO 12 I=KP1,N
12    AA(I,K)=0.
C *** SONDAN YERINE KOYMA ***
      EV2(N)=AA(N,M)/AA(N,N)
      DO 14 NN=1,L
      SUM=0.
      I=N-NN
      IP1=I+1
      DO 13 J=IP1,N
13    SUM=SUM+AA(I,J)*EV2(J)
14    EV2(I)=(AA(I,M)-SUM)/AA(I,I)
      RETURN
      END

*****************************************************************
c
c              CALCULATION OF WARPING MOMENT OF INERTIA (Iw)
c
c ****************************************************************

          SUBROUTINE CAIw(JJ,CSAREA,PN,EN,SCN,Sx,Sy,P,DX,DY,
     -           EDI,EDJ,THICK,PRSECAREA,PRSA,SIW)

      PARAMETER (N=50)
          IMPLICIT REAL*8 (A-H,K-Z)
c     I and J variables

          dimension  DX(N),DY(N),THICK(N),DIS(N),PRSECAREA(N)
     @    ,EDI(N),EDJ(N),EKIX(N),EKIY(N),EKJX(N),EKJY(N)
     @    ,SECAREA1(N),PRSA(N,N),SCAR(N),SIW(N),CSAREA(N)

  910 FORMAT(A8)
  920 FORMAT(A50)
  922 FORMAT(1X,30F10.3)
  923 FORMAT(1X,30F10.2)
  925 FORMAT(1X,30F13.4)

      TOL1=0.9999999
          TOL2=1.0000001

          DO I=1,EN
          EKIX(I)=  DX(EDI(I))
```

```
          EKIY(I)=  DY(EDI(I))
          EKJX(I)=  DX(EDJ(I))
          EKJY(I)=  DY(EDJ(I))
          ENDDO
          WRITE(6,*) '      '
          DO I=1,EN
C    product of two vectors
      SCAR(I)=((EKIX(I)-Sx)*(EKJY(I)-Sy)-(EKJX(I)-Sx)*(EKIY(I)-Sy))
      WRITE(6,922) SCAR(I)
          ENDDO

      WRITE(6,*) '                              '
          WRITE(6,*) '  W PRIME (for initial radius)  '
          WRITE(6,*) '-------------------------------'

      SECAREA1(1)=0.0

C    1. method
      PNF=PN-1

      DO I=1,PNF
      fark=EDJ(I)-EDI(I)
          IF((fark.GT.TOL1).AND.(fark.LT.TOL2)) THEN
      SECAREA1(I+1)=SECAREA1(I)+SCAR(I)
      else
      SECAREA1(I+1)=SECAREA1(I+1-fark)+SCAR(I)
      ENDIF
          ENDDO

          WRITE(6,*) '          '
      DO I=1,PN
      WRITE(6,922) SECAREA1(I)
          ENDDO

C    2. method

C     DO I=2,PN
C     SECAREA1(I)=SECAREA1(EDI(I-1))+SCAR(I-1)
C         ENDDO
C         WRITE(6,*) '          '
C     DO I=1,PN
C     WRITE(6,922) SECAREA1(I)
C         ENDDO

      WRITE(6,*) '                    '
          WRITE(6,*) '  LENGTH OF ELEMENTS  '
          WRITE(6,*) '---------------------'

      DO I=1,EN
      DIS(I)=((DX(EDJ(I))-DX(EDI(I)))**2
     @              +(DY(EDJ(I))-DY(EDI(I)))**2)**(0.5)
      WRITE(6,922) DIS(I)
      ENDDO

      WRITE(6,*) '      '
```

```
        WRITE(6,*) '  SWS  '
        WRITE(6,*) '-------'

SWS=0.0

DO I=1,EN-1
SWS=SWS+(0.5)*THICK(I)*DIS(I)*(SECAREA1(EDI(I))+SECAREA1(EDJ(I)))
ENDDO

        WRITE(6,922) SWS

R=SWS/CSAREA(JJ)

WRITE(6,*) '      '
        WRITE(6,*) '  R   '
        WRITE(6,*) '------'
WRITE(6,922) R
WRITE(6,*) '         '
        WRITE(6,*) '  W PRI  '
        WRITE(6,*) '---------'

DO I=1,PN
PRSECAREA(I)=SECAREA1(I)-R
WRITE(6,922) PRSECAREA(I)
ENDDO

DO I=1,PN
PRSA(JJ,I)=PRSECAREA(I)
ENDDO

SSIW=0.0

DO I=1,EN-1
SSIW=SSIW+(1./3.)*DIS(I)*THICK(I)*((PRSECAREA(EDI(I)))**2.+
@                PRSECAREA(EDI(I))*PRSECAREA(EDJ(I))+
@               (PRSECAREA(EDJ(I)))**2.)
ENDDO

WRITE(6,*) '         '
        WRITE(6,*) '   Iw    '
        WRITE(6,*) '---------'

WRITE(6,922) SSIW

SIW(JJ)=SSIW

RETURN
END
```

APPENDIX 4. Computation Procedure for the Sectorial Area in an Open Section

The sectorial area of the cross-section of a thin-walled beam refers to the center line (contour line) of its outline. This property and the other related sectorial properties were defined in Chapter 3. In Fig. A4.1. an example is given for the calculation of the sectorial area of a section for an arbitrary chosen center of rotation (pole) R and an initial (trial) radius $\vec{RO_1}$.

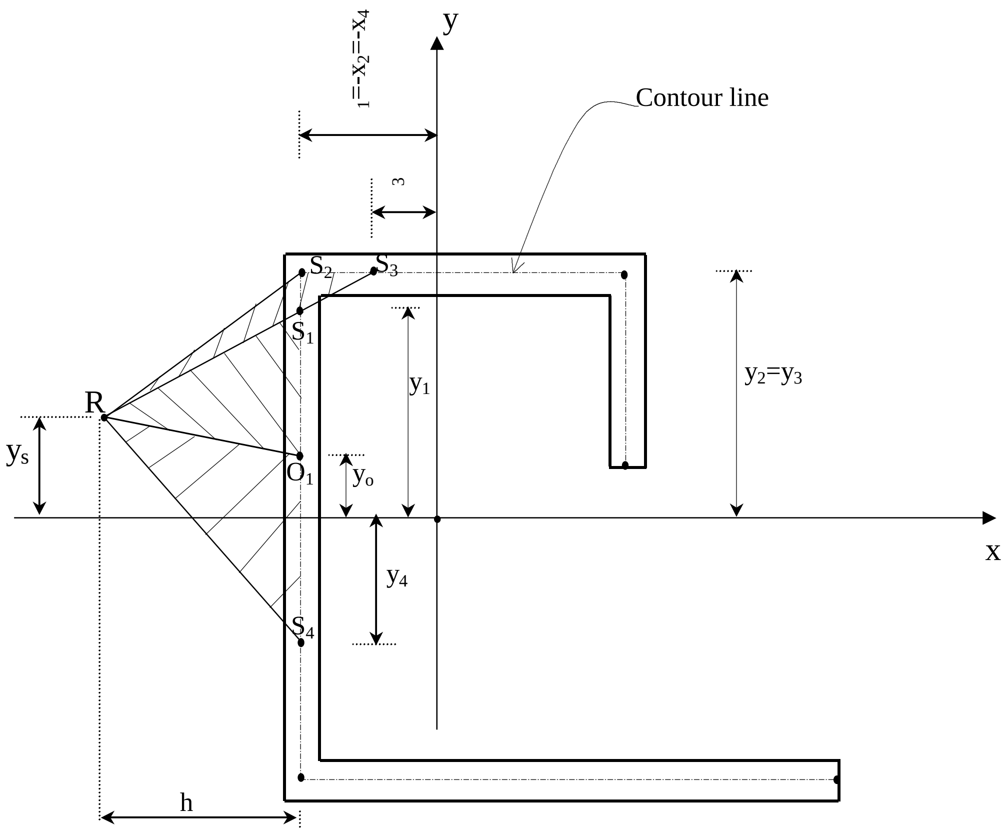

Figure A4.1. Part of the sectorial area diagram for the section

The angle $O_1\hat{R}S_4$ is measured from $\vec{RO_1}$ in the clockwise direction. Thus the sectorial area is negative. The absolute value of the sectorial area $\left|\omega_{RO_1S_4}\right|$ is equal to twice the area of the hatched triangle RO_1S_4. In other words $\omega_{RO_1S_4} = -h\left(\left|y_4\right| + y_0\right)$. The value of the sectorial area at point S_1 is positive and is equal to $\omega_{RO_1S_1} = h(y_1 - y_0)$. The value of the sectorial area at point S_2 can be obtained by adding, algebraically, twice the area of triangle RS_1S_2 to $\omega_{RO_1S_1}$, because the radius swept from pole R moving from point S_1 to S_2, rotates in an anti-clockwise direction. The sign of this additional area is also positive. In other words, $\omega_{RO_1S_2} = \omega_{RO_1S_1} + h(y_2 - y_1)$ or $\omega_{RO_1S_2} = h(y_2 - y_0)$.

From S_2 to S_3, the angle $O_1 \hat{R} S_2$ decreases and the radius $\overrightarrow{RO_1}$ rotates in the clockwise direction. Hence, this additional area (twice the area of the triangle S_3RS_2) is negative. Therefore, $\omega_{RO_1S_3} = \omega_{RO_1S_2} - (y_3 - y_s) \times |x_2 - x_3|$.

The method of computation of the sectorial area diagram of a section can best be explained by a numerical example. In Fig. A4.2 such an example is given for the calculation of the sectorial area diagram and the resulting warping moment of inertia. In Fig. A4.3 the contour of the section is given, with the origin at the centroid (to be calculated) of the section.

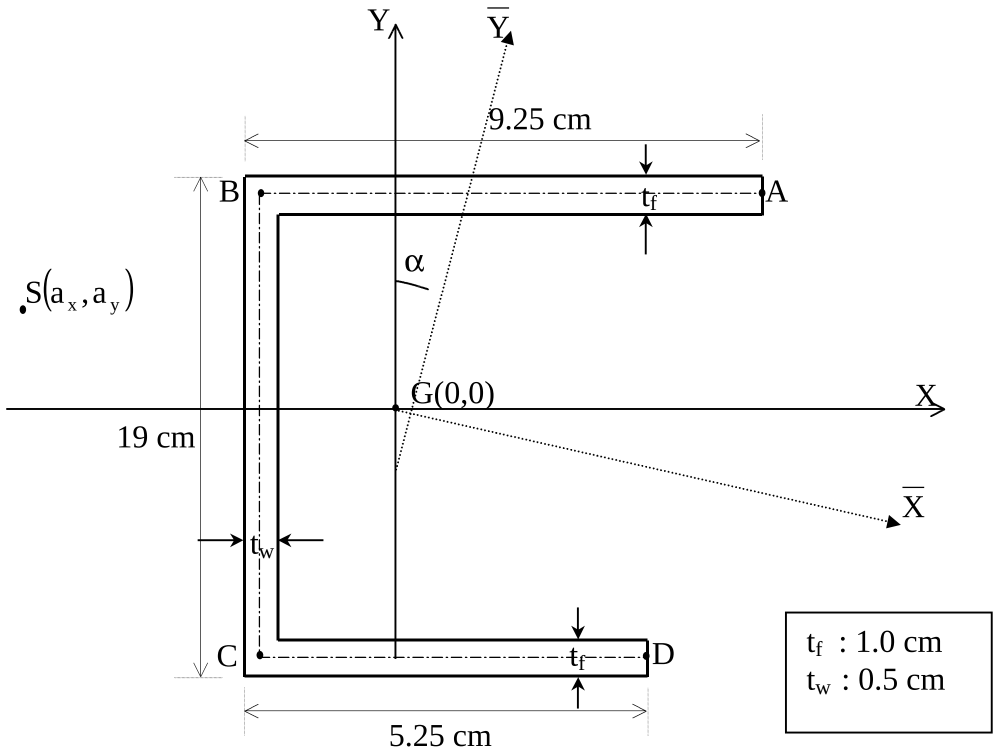

Figure A4.2. Plan of the section

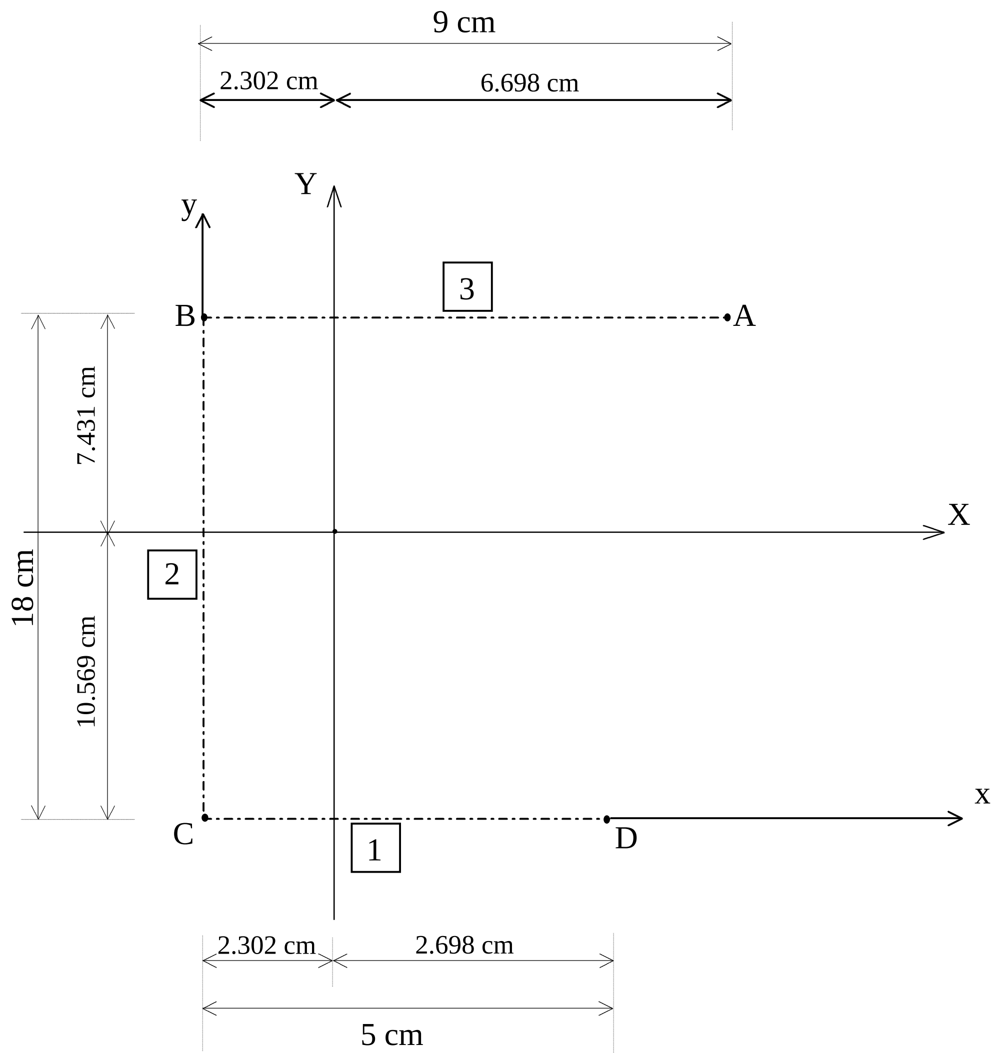

Figure A4.3. Contour of the section

The computation procedure for the sectorial properties is given below:

<u>Step:1</u> Find the position of the centre of gravity of the section.

The area of this section is,

$$A=1\times(8.75+4.75)+0.5\times19=23\,\text{cm}^2$$

The position of the centre of gravity is,

$$x=(8.75\times4.625+4.75\times2.625)/23=2.302\,\text{cm}$$

$$y=\quad(8.75\times18\times1+0.5\times19\times9)/23=10.569\text{cm}$$

Thus,

Coordinates of node A : (6.698,7.431)

Coordinates of node B : (-2.302,7.431)

Coordinates of node C : (-2.302,-10.569)

Coordinates of node D : (2.698,-10.569)

<u>Step:2</u> Calculate the values of I_X, I_Y and I_{XY} for the set of orthogonal axes X-Y with the origin at the centre of gravity.

I_{XY}=

$$\int_{-2.302}^{6.698} x \times (7.431) \times 1 \times dx + \int_{-10.569}^{7.431} (-2.302) \times y \times 0.5 \times dy + \int_{-2.302}^{6.698} (-10.569) \times x \times 1 \times dx = 168.03\,cm^4$$

$I_{XY} \neq 0$, in other words, given axes X and Y do not coincide with the principal axes of the section. Therefore, equations (3.18) and (3.19) can be used for the determination of the shear center.

I_X=1310 cm^4

I_Y=177 cm^4

Generally, the direction of the principal axes as shown in Fig. A4.2, can be determined from the well-known formula,

$$\tan 2\alpha = \frac{-2I_{xy}}{I_x - I_y}$$

Step:3 **Choose any trial position for the pole (R) and an initial radius (RO_1) for the sectorial area.**

The location of the trial pole and the initial radius can be chosen arbitrarily. For simplicity, the trial pole is chosen at corner C and the initial radius along web CB.

Step:4 **Calculate the values of the sectorial linear statical moments.**

The sectorial area $(\omega_s)_{BC}$ can be given as -18s. The sectorial statical moments are

$$\left(S_{\omega X}\right)_{CB} = \int_0^9 -18s\left(7.431\right)ds = -5417\,cm^5$$

and

$$\left(S_{\omega Y}\right)_{CB} = \int_0^9 -18s\left(6.698\right)ds = -2696\,cm^5$$

Step:5 **Find the coordinates (a_x,a_y) of the principal pole (shear center) S from expressions (3.18) and (3.19) since $I_{XY} \neq 0$.**

Substituting the values found from the previous step into expressions (3.18) and (3.19), a_x and a_y can be obtained as

$$a_x = -2.302 + \frac{-5417\times177-(168.03)\times-2696}{177\times1310-(168.03)^2} = -4.786\ \text{cm}$$

$$a_y = -10.569 - \frac{1310\times(-2696)-(168.03)\times-5417}{177\times1310-(168.03)^2} = 2.3048\ \text{cm}$$

<u>Step:6</u> Assume an arbitrary direction for the initial radius from the principal pole (shear center) and find the sectorial area values.

For finding the initial sectorial area diagram, the initial radius is chosen from the shear center S to point C (see Fig. A4.3)

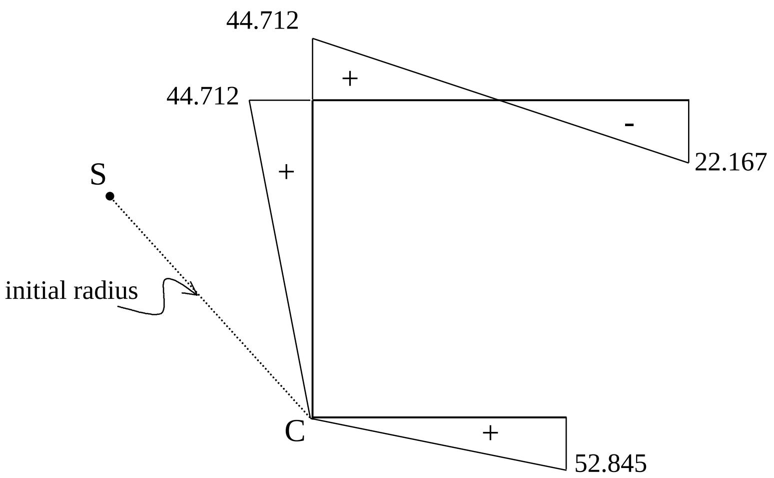

Figure A4.3. Initial sectorial area diagram ω'

The sectorial areas of points A, B, C and D are:

$$(\omega_D)_{SC} = 5 \times 10.569 = 52.845\,\text{cm}^2$$

$$(\omega_C)_{SC} = 0.0\,\text{cm}^2$$

$$(\omega_B)_{SC} = 18 \times 2.484 = 44.712\,\text{cm}^2$$

$$(\omega_A)_{SC} = 44.712 - 7.431 \times 9 = -22.167\,\text{cm}^2$$

<u>Step:7</u> Find the principal radius.

The principal radius is found using the following formula:

$$(\omega_O)_{SC} = \frac{1}{A}\int (\omega)_{SC}\, dA$$

This equation gives the actual sectorial area value for the end (C) of the second initial radius. The integral on the right side of equation (A4.2), which is equal to the sectorial statical moment of the section is found as follows:

$$\left(S_\omega\right)_{SC} = 1\times 5\times\frac{52.845}{2} + 0.5\times 18\times\frac{1}{2}\times 44.712 + 1\times 9\times\frac{1}{2}\times\left(44.712-22.167\right) = 434.769\,\text{cm}^4$$

The sectorial area of the point on the section contour line through which the actual principal radius SO passes, is

$$\left(\omega_O\right)_{SC} = \frac{434.769}{23} = 18.903\,\text{cm}^2$$

<u>Step:8</u> Find the principal sectorial area diagram of the section.

The principal sectorial area values for the points of the section can be found either by re-calculating them from the principal radius or from the following formula:

$$\left(\omega_{SO}\right)_S = \left(\omega_{SC}\right)_S - \left(\omega_{SC}\right)_O$$

Here, the latter method will be employed. Hence,

$$\left(\omega_D\right)_O = 52.845 - (18.903) = 33.942\,\text{cm}^2$$

$$\left(\omega_C\right)_O = 0.0 - (18.903) = -18.903\,\text{cm}^2$$

$$\left(\omega_B\right)_O = 44.712 - (18.903) = 25.809\,\text{cm}^2$$

$$\left(\omega_A\right)_O = -22.167 - (18.903) = -41.07\,\text{cm}^2$$

The principal sectorial area diagram is given in Fig. A4.4.

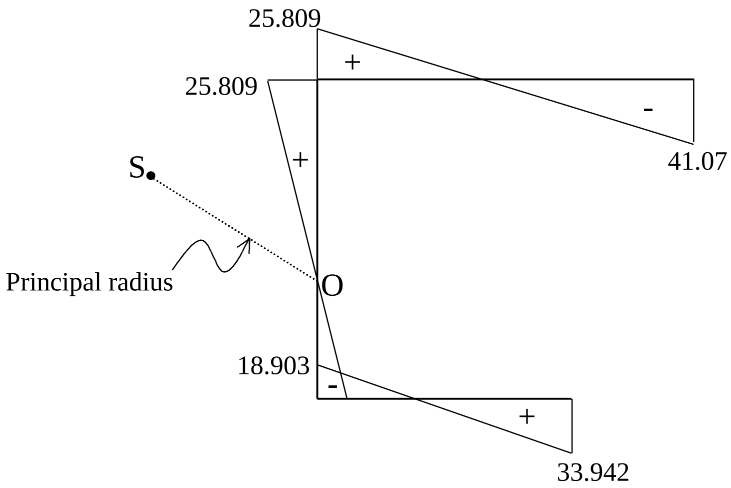

Figure A4.4. Principal sectorial area diagram

The equations for the parts of the principal sectorial area diagram can be written as follows:

Between points D and C:

$$(\omega_s)_{SO} = (\omega_D)_{SO} + \frac{(\omega_C)_{SO} - (\omega_D)_{SO}}{|DC|} \times s$$

$$(\omega_s)_{SO} = 33.942 + \frac{0.0 - 52.845}{5} \times s = 33.942 - 10.569s$$

Between points C and B:

$$(\omega_s)_{SO} = (\omega_C)_{SO} + \frac{(\omega_B)_{SO} - (\omega_C)_{SO}}{|CB|} \times s$$

$$(\omega_s)_{SO} = -18.903 + 2.484s$$

Between points B and A:

$$(\omega_s)_{SO} = (\omega_B)_{SO} + \frac{(\omega_A)_{SO} - (\omega_B)_{SO}}{|BA|} \times s$$

$$(\omega_s)_{SO} = 25.809 - 7.431s$$

<u>Step:9</u> Calculate the principal sectorial moment of inertia (warping moment of inertia) I_ω from the formula.

$$I_\omega = \int_A \left[(\omega_s)_{SO}\right]^2 dA$$

$$I_\omega = \int_0^5 (33.942 - 10.569s)^2 \times 1\ ds + \int_0^{18} 0.5 \times (-18.903 + 2.484s)^2\ ds +$$

$$\int_0^9 (25.809 - 7.431s)^2 \times 1\ ds$$

$$I_\omega = 8537.6671\ cm^6$$

APPENDIX 5. Derivation of the Formulas for the Position of a Shear Center

It was mentioned in Chapter 3 that there are some properties of cross-sections of thin-walled beams which are defined on the basis of sectorial area. For the analysis of internal stresses in thin-walled beams, these properties must be known to determine the location of the shear center through the use of the sectorial area. The procedure for the determination of the location of the shear center formulas based on the sectorial area is as follows:

The cross-section of a thin-walled beam is shown in Fig. A5.1. The coordinate axes x-y pass through the center of gravity of the cross-section, but they do not coincide with the principal axes of the cross-section.

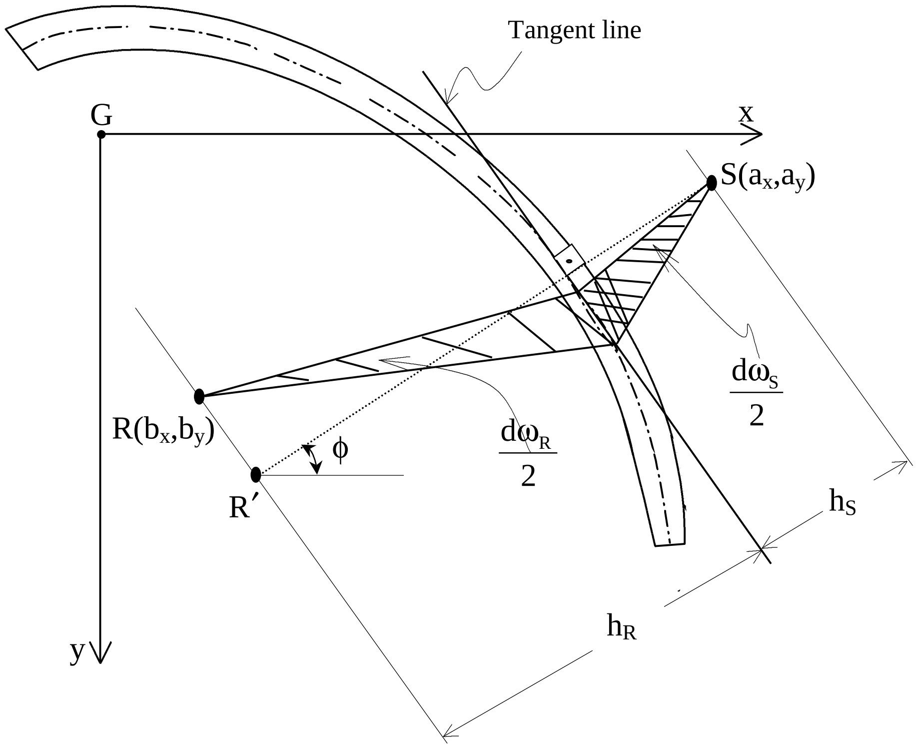

Figure A5.1. Cross-section of a thin-walled beam

The point S in this figure is located at the principal pole (shear center) of the cross-section. The point R represents an arbitrarily chosen pole (trial pole) of the sectorial diagram. The increments of the sectorial areas in these two systems over a distance ds are given respectively by the following equations:

$$d\omega_S = ds\, h_S \text{ (cross-hatched in Fig. A5.1)} \tag{A5.1}$$

$$d\omega_R = -ds\, h_R \tag{A5.2}$$

The distance between point S and R' is,

$$|SR'| = h_R + h_S \tag{A5.3}$$

and

$$d\omega_S = ds\left(|SR'| - h_R\right) = ds|SR'| + d\omega_R \tag{A5.4}$$

The distance $|SR'|$ can be given by the coordinates of the points S and R (see Fig. A5.2) as follows:

$$|SR'| = |R'R''| + |R''S| = (b_y - a_y)\mathrm{Cos}\phi + (a_x - b_x)\mathrm{Sin}\phi \tag{A5.5}$$

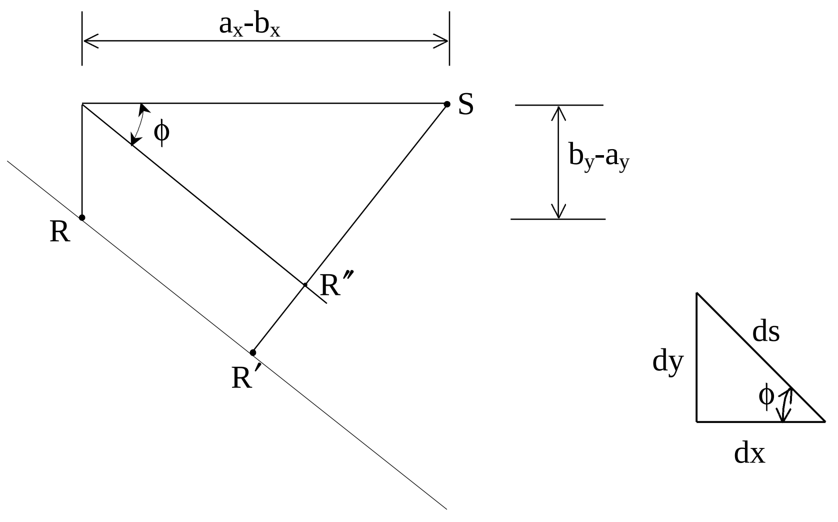

Figure A5.2. Geometric and trigonometric relations in a thin-walled beam

The trigonometrical function of an angle ϕ can be replaced by the derivatives as follows:

$$\mathrm{Cos}\,\phi = \frac{dx}{ds} \quad , \quad \mathrm{Sin}\phi = \frac{dy}{ds} \tag{A5.6}$$

Hence,

$$\left|SR'\right| = (b_y - a_y)\frac{dx}{ds} + (a_x - b_x)\frac{dy}{ds} \tag{A5.7}$$

Substituting (A5.7) into (A5.4),

$$d\omega_S = \left(a_y - b_y\right)dx - \left(a_x - b_x\right)dy + d\omega_R \tag{A5.8}$$

Integration of equation (A5.8) yields,

$$\omega_S = \omega_R + \left(a_y - b_y\right)x - \left(a_x - b_x\right)y + C \tag{A5.9}$$

where C is a constant of integration, depending on the choice of initial radii of both systems of sectorial areas. It is known from section 3.2.5. that, the principal pole (shear center) of a section can be defined by the two conditions that the sectorial statical moments about x and y axes, must be equal to zero,

$$S_{\omega y} = \int_A x\,\omega_s\,dA = 0 \tag{A5.10}$$

and

$$S_{\omega x} = \int_A y\,\omega_s\, dA = 0 \tag{A5.11}$$

Hence, multiplying equation (A5.9) by x and y and substituting into (A5.10) and (A5.11), respectively,

$$\int_A \omega_R\, x\, dA + \left(a_y - b_y\right)\int_A x^2 dA - \left(a_x - b_x\right)\int_A xy\, dA + C\int_A x\, dA = 0 \tag{A5.12}$$

and

$$\int_A \omega_R\, y\, dA + \left(a_y - b_y\right)\int_A xy\, dA - \left(a_x - b_x\right)\int_A y^2\, dA + C\int_A y\, dA = 0 \tag{A5.13}$$

Since the axes x-y pass through the center of gravity of the cross-section,

$$\int_A x\, dA = \int_A y\, dA = 0 \tag{A5.14}$$

Because of this, the coordinates of the shear center are independent of the choice of the initial radius of the system ω_R .

Here the following definitions apply:

$$\int_A x^2 dA = I_y \tag{A5.15}$$

$$\int_A y^2 dA = I_x \tag{A5.16}$$

$$\int_A xy\, dA = I_{xy} \tag{A5.17}$$

$$\int_A \omega_R \, x \, dA = S_{R\omega x} \tag{A5.18}$$

$$\int_A \omega_R \, y \, dA = S_{R\omega y} \tag{A5.19}$$

With the definitions (A5.15-19), (A5.12-13) are put into the following forms:

$$\begin{aligned} &(a_y - b_y)I_y - (a_x - b_x)I_{xy} + S_{R\omega x} = 0 \\ &(a_y - b_y)I_{xy} - (a_x - b_x)I_y + S_{R\omega y} = 0 \end{aligned} \tag{A5.20}$$

The solutions of these two simultaneous equations for a_x and a_y yield expressions (3.18) and (3.19). These expressions are used when the given axes x and y do not coincide with the principal axes of a section ($I_{xy} \neq 0$), but pass through the center of gravity. If the axes x and y coincide with the principal axes of a cross-section ($I_{xy}=0$), the formulas are simplified to the forms (3.16) and (3.17) in section 3.2.5.2.